Generalizations of Total Positivity

A DISSERTATION
SUBMITTED TO THE FACULTY OF THE GRADUATE SCHOOL
OF THE UNIVERSITY OF MINNESOTA
BY

Sunita Chepuri

IN PARTIAL FULFILLMENT OF THE REQUIREMENTS
FOR THE DEGREE OF
DOCTOR OF PHILOSOPHY

Pavlo Pylyavskyy

July, 2020

Acknowledgements

I would first like to thank my advisor Pasha Pylyavskyy for all of his mentorship. From suggesting problems to helping me develop my research process, his guidance has been invaluable.

I also want to thank the rest of the combinatorics/combinatorics-adjacent faculty at UMN: Vic Reiner, Dennis Stanton, Gregg Musiker, Ben Brubaker, and Christine Berkesch. I have learned a lot from all of them in classes they've taught, in seminar, through suggestions they've had for my work, and while mentoring the REU together. I appreciate all the work they put in to make the UMN combinatorics community vibrant and welcoming.

I would not have come to grad school without the encouragement of the Bowdoin Math Department, in particular Jen Taback, Thom Pietraho, Manny Reyes, and Michael King.

I am grateful for all the combinatorics students and postdocs I have overlapped with at the University of Minnesota, especially Becky Patrias, Al Garver, Emily Gunawan, Theo Douvropoulos, Elise DelMas, Galen Dorpalen-Berry, Elizabeth Kelley, Eric Stucky, Esther Banian, Sarah Brauner, Kayla Wright, Joel Lewis, Chris Fraser, and Sam Hopkins. Their advice (on life and math) was extremely helpful throughout my graduate career. I have enjoyed traveling to conferences and attending classes and seminars with them and I look forward to seeing the great things they will do in the future.

I want to thank all my co-authors (Yulia Alexandr, Anna Brosowsky, B Burks, Patty Commins, CJ Dowd, Andy Hardt, Neeraja Kulkarni, Alex Mason, Greg Michel, Melissa Sherman-Bennett, Joe Suk, Ewin Tang, Sylvester Zhang, and Valerie Zhang) for their hard work. I would have far fewer and weaker results without their substantial contributions.

Every milestone in my graduate career (Svitlana's real analysis class, prelims, finding an advisor, taking my oral exam, applying for jobs) was made easier because I was going through it along with the other students in my cohort. I can't thank them enough for the hours spent working, venting, and, when called for, celebrating together.

I feel incredibly lucky to have had such amazing officemates while in grad school. Thank you to Becky Patrias, Darío Valdebenito Castillo, Cora Brown, Harini Chandramouli, Carolynn Johnson, Olivia Cannon, Emily Tibor, and Montie Avery (honorarily) for making work a place I enjoyed going.

I am grateful for the Minnesota-located branches of my family and for the Bader family for helping me with my transition to Minnesota and for providing chances for me to escape from my school-centric life.

I want to thank Brian Barthel, Jimmy Broomfield, Therese Broomfield, Rachel Johnson, Zach Levonian, Mac Marti, Greg Michel, Tony Tran and the many other friends that have made the Twin Cities home for me for the past 6 years. I am also forever appreciative of my college and childhood friends, especially Monica Das, Kate Kearns, Matt Leiwant, Ben Ash, Berit Elvejord, Martha Muldowney, and Dylan Pickus, for their continued love and support.

My parents instilled in me a high regard for education from a young age and they have always worked to make sure I had access to the best possible opportunities. I would not be here were it not for their tireless efforts and I want to thank them as well as my brother for their encouragement.

I thank Cora Brown for being my first friend in grad school, my officemate from day 1 to the end, and my cookie dough-eating, Bachelor-watching, Royal Diaries-reading, Winter Storm Stella-braving partner-in-crime.

And lastly, my greatest thanks go to Harini Chandramouli. She has been with me through everything for the last 6 years: school-related stresses, life crises, quarantine, protests, and anything else that has come our way. She has been the best person I could possibly imagine going through grad school with and I don't know how I will manage without her next year.

Dedication

To my grandparents: Shanta Chepuri, Chary Chepuri, Ruth Field, and Lawrence Field

Abstract

The theory of total positivity was classically concerned with totally nonnegative matrices (matrices with all nonnegative minors). These matrices appear in many varied areas of mathematics including probability, asymptotic representation theory, algebraic and enumerative combinatorics, and linear algebra. However, motivated by surprising positivity properties of Lusztig's canonical bases for quantum groups, the field of total positivity has more recently grown to include other totally nonnegative varieties.

We first discuss results regarding immanants on the space of k-positive matrices (matrices where all minors of size up to k are positive). Immanants are functions on square matrices generalizing the determinant and permanent. Kazhdan–Lustzig immanants, defined by Rhoades and Skandera, are of particular interest, as elements of the dual canonical basis of the coordinate ring of $GL_n(\mathbb{C})$ can be expressed as Kazhdan–Lustzig immanants. Results of Stembridge, Haiman, and Rhoades–Skandera show that Kazhdan–Lustzig immanants are nonnegative on totally nonnegative matrices. Here, we give conditions on $v \in S_n$ so that the Kazhdan-Lusztig immanant corresponding to v is positive on k-positive matrices.

We then consider a space that arises from the study of totally nonnegative Grassmannians. Postnikov's plabic graphs in a disk are used to parametrize these spaces. In recent years plabic graphs have found numerous applications in math and physics. One of the key features of the theory is the fact that if a plabic graph is reduced, the face weights can be uniquely recovered from boundary measurements. On surfaces more complicated than a disk this property is lost. In this thesis, we undertake a comprehensive study of a certain semi-local transformation of weights for plabic networks on a cylinder that preserve boundary measurements. We call this a plabic R-matrix. We show that plabic R-matrices have underlying cluster algebra structure, generalizing work of Inoue–Lam–Pylyavskyy. Special cases of transformations we consider include geometric R-matrices appearing in Berenstein–Kazhdan theory of geometric crystals, and also certain transformations appearing in a recent work of Goncharov–Shen.

Contents

Acknowledgements **i**

Dedication **iii**

Abstract **iv**

List of Figures **viii**

1 Introduction **1**

1.1 Totally Positive Matrices 1

1.2 Totally Nonnegative Varieties 2

1.3 Overview 3

1.4 Main Results 4

2 k-Positivity of Kazhdan-Lusztig Immanants **6**

2.1 k-Positive Matrices 6

2.2 Kazhdan-Lusztig Immanants 8

2.3 Question and Motivation 9

2.4 Main Theorem 10

2.5 Formula for 1324- and 2143-avoiding Permutations 11

2.6 Dodgson Condensation 14

2.6.1 Young diagrams 15

2.6.2 General case 17

2.7 Proof of Proposition 2.6.12 26

2.8 Proof of Proposition 2.6.14 36

2.9 Pattern Avoidance Conditions 42
2.10 Future Directions 44

3 Cluster Algebras and k-Positivity **45**
3.1 Cluster Algebra Background 45
3.2 Double Rim Hook Cluster Algebras 47
3.3 Applications to Kazhdan-Lusztig Immanants 55
3.4 Cluster Algebras and k-Positivity Tests 58
3.5 Double Rim Hook Cluster Algebras and 2-Positivity 67

4 Total Positivity and Networks **73**
4.1 Totally Nonnegative Matrices and Planar Directed Networks 73
4.2 Totally Nonnegative Grassmannians and Planar Directed Networks . . . 75
4.3 Planar Directed Networks to Plabic Networks 78
4.4 Moves and Reductions 83
4.5 Postnikov Diagrams 85

5 Plabic Networks on the Cylinder **87**
5.1 Planar Directed Networks on a Cylinder 87
5.2 Face Weights on the Cylinder 91
5.3 Changing Orientation on the Cylinder 94

6 Plabic R-matrix **98**
6.1 Cylindric k-loop Plabic Graphs 98
6.2 Edge-weighted Plabic R-matrix 100
6.3 Face-weighted Plabic R-matrix 108
6.4 Postnikov Diagram Proofs 114
6.4.1 Proof of Theorem 6.1.2 114
6.4.2 Proof of Theorem 6.1.5 115
6.5 Proof of Theorems 6.2.5 and 6.3.3 121

7 Spider Web Quivers **135**
7.1 Spider Web Quivers and a Mutation Sequence τ 135
7.2 x-dynamics 140

7.3 y-dynamics 144

8 Plabic R-matrix, Revisited **152**

References **156**

List of Figures

2.1 An illustration of Lemma 2.5.4 with $\Gamma[v, w_0]$ for $v = 14253$. 13
2.2 An example where $\Gamma[v, w_0]$ is block-antidiagonal. 18
2.3 Bounding boxes for $\Gamma[v, w_0]$, with $v = 6\ 10\ 4\ 7\ 8\ 9\ 3\ 1\ 2$. 19
2.4 An illustration of Proposition 2.6.14. 22
2.5 An illustration of (2) in the proof of Theorem 2.6.15. 23
2.6 An example of the bijection from Proposition 2.7.12. 30
3.1 The NNEE-DRH and the ENEN-DRH. 47
3.2 A choice of correspondence and the resulting diagram. 48
3.3 The initial NNEE-DRH seed and the initial ENEN-DRH seed. 51
3.4 The standardization of NNEE and ENEN. 52
3.5 The initial minors seed for $n = 4$. 59
3.6 A double wiring diagram. 60
3.7 A 2-seed coming from the initial minors seed. 61
3.8 The components of a 2-positivity test graph. 63
3.9 Bridges between the two largest components for $n = 3$, $k = 2$. 65
4.1 A path P with $wind(P) = -1$. 76
4.2 A planar directed network in a disk transformed into a perfect network. 79
4.3 A face with $y_f = x_1 x_2^{-1} x_3^{-1} x_4^{-1} x_5 x_6^{-1} x_5^{-1} = \frac{x_1}{x_2 x_3 x_4 x_6}$. 81
4.4 A plabic graph and its Postnikov diagram. 86
5.1 A cylinder, as we will represent them in this paper. 87
5.2 Turning a cylinder into an annulus. 89
6.1 A cylindric 2-loop plabic graph and its Postnikov diagram. 100
6.2 A 1-expanded directed plabic network. 102
6.3 An illustration of Lemma 6.3.1. 110

6.4 Adding edges p, $-p$ to a cylindric 2-loop directed plabic network. 122
6.5 A square move used to push the edge p around the cylinder. 123
6.6 A face of a network with added edges p, $-p$, q, $-q$, r, and $-r$. 130
7.1 Two spider web quivers. 136

Chapter 1

Introduction

The work presented in this thesis lies in the area of total positivity. Classically, the field of total positivity was concerned with the study of totally positive and totally nonnegative matrices. This introduction will define these objects and give a brief background on the classical field of total positivity. It will then explain how the field has more recently grown to include other totally nonnegative varieties before giving an overview of the rest of this thesis and a summary of our main results.

1.1 Totally Positive Matrices

Definition 1.1.1. Given an $m \times n$ matrix M, a *minor* of M is $\Delta(M)_{I,J}$ where $I \subseteq [m]$, $J \subseteq [n]$, and $\Delta(M)_{I,J}$ is defined to be the determinant of the submatrix of M obtained by taking only the rows indexed by I and columns indexed by J. Note that $\Delta(M)_{I,J}$ is only defined if $|I| = |J|$.

A matrix is said to be *totally positive* if all of its minors are positive and *totally nonnegative* if all of its minors are nonnegative.

We will usually be considering totally positive $n \times n$ matrices, which we will denote as $GL_n(\mathbb{R})_{>0}$, and totally nonnegative $n \times n$ matrices, which we will denote as $GL_n(\mathbb{R})_{\geq 0}$.

Example 1.1.2. Since any square submatrix of the matrix

$$A = \begin{bmatrix} 13 & 4 & 2 & 1 \\ 6 & 4 & 3 & 2 \\ 6 & 5 & 4 & 3 \\ 7 & 6 & 5 & 6 \end{bmatrix}$$

is positive, $A \in GL_4(\mathbb{R})_{>0}$.

Since any square submatrix of the matrix

$$B = \begin{bmatrix} 4 & 4 & 2 & 1 \\ 4 & 4 & 3 & 2 \\ 5 & 5 & 4 & 3 \\ 6 & 6 & 5 & 6 \end{bmatrix}$$

is nonnegative, $B \in GL_4(\mathbb{R})_{\geq 0}$.

Totally positive and totally nonnegative matrices have been studied since the 1930's. The first known reference to these matrices was in work of Schoenberg [Sch30]. Schoenberg was interested variation-diminishing linear transformations, that is, matrices M where multiplication by M does not increase the number of sign changes in any vector. He found that totally nonnegative matrices have this property. Totally positive matrices also appeared separately in work of Gantmacher and Krein [GK37], who showed that matrices in $GL_n(\mathbb{R})_{>0}$ have n distinct positive eigenvalues.

Since their introduction, totally positive and totally nonnegative matrices have appeared in many varied areas of mathematics, including classical mechanics [GK60], electrical networks [CIM98, KW09, KW11], probability [Kar68, GM96], representation theory of the infinite symmetric group [Edr52, Tho64], and algebraic and enumerative combinatorics [Lin73, GV85, GV89, Sta89, Ste91].

1.2 Totally Nonnegative Varieties

One of the most important results in total positivity is the Loewner-Whitney Theorem [Whi52, Loe55]. This theorem states that the set of nonsingular totally nonnegative matrices is generated (multiplicatively) by the set of *elementary Jacobi matrices* with nonnegative matrix entries. Elementary Jacobi matrices are invertible matrices that differ from the identity by one entry on the diagonal, subdiagonal, or superdiagonal. While this theorem is useful for understanding the structure and combinatorial properties of $GL_n(\mathbb{R})_{\geq 0}$, it is most notable for us in that it led to the definition of totally positivity for other Lie groups.

In [Lus94], Lusztig observed that the elementary Jacobi matrices that have a positive entry on the superdiagonal are the *Chevalley generators* for the Lie group of upper unitriangular matrices. This allowed Lustzig to introduce a notion of total positivity for other Lie groups G by defining the totally nonnegative part of G, $G_{\geq 0}$, to be the subset of G generated by Chevalley generators. He then showed that $G_{\geq 0}$ was exactly the subset of G where all elements of the dual canonical basis were nonnegative.

The concept of total positivity can be extended further to algebraic varieties. If X is an algebraic variety, we can determine a set of important functionals on X and define $X_{\geq 0}$ to be the subset of X where all of the specified functionals take nonnegative values. We will be particularly interested in the totally nonnegative Grassmanian, $Gr_{k,n}(\mathbb{R})_{\geq 0}$, defined in Chapter 4. This object arises naturally, as $Gr_{k,n}(\mathbb{R})$ can be considered as a quotient of $GL_n(\mathbb{R})$. The combinatorial properties [Pos06] and topology [Pos06, GKL17] of $Gr_{k,n}(\mathbb{R})_{\geq 0}$ make it an interesting object of study.

1.3 Overview

In this thesis, we will be concerned with generalizations of the notion of total positivity. Chapters 2 and 3 will be concerned with k-positive matrices, a generalization of totally positive matrices. The rest of the thesis will consider a generalization of plabic networks, combinatorial objects intimately connected to the totally nonnegative Grassmannian.

In Chapter 2, we first introduce our central objects: k-positive matrices and Kazhdan–Lusztig immanants. We provide motivation for our line of study and then state our main theorem. The rest of the chapter is dedicated to proving that theorem, our main proof technique being Dodgson condensation.

One promising tool for tackling the questions left unresolved in Chapter 2 is cluster algebras. Chapter 3 gives an introduction to cluster algebras and explains how they may be useful in answering the open questions from Chapter 2.

Chapter 4 explores the combinatorial relationship between total positivity and networks. We begin by discussing planar directed networks and totally nonnegative matrices and then move on to discussing plabic networks and the totally nonnegative Grassmannian. We also introduce Postnikov diagrams as tools for studying plabic networks.

We then define plabic networks on the cylinder in Chapter 5. In this chapter, we investigate which aspects of Postnikov's theory of plabic networks can be transferred to plabic networks on the cylinder.

In Chapter 6, we introduce the plabic R-matrix, a semi-local transformation on plabic networks on a cylinder. We give both an edge-weighted and face-weighted version of this transformation and prove several properties. In particular, we show that applying the plabic R-matrix to a plabic network on the cylinder preserves the network's image under the boundary measurement map.

Chapter 7 discusses mutation dynamics of a certain class of quivers. We first give a brief introduction to cluster algebras. Then we introduce spider web quivers, the family we will be studying, and define a mutation sequence τ on these quivers. We prove that τ is an involution on spider web quivers and compute how it changes the associated x- and y-variables.

Chapter 8 ties Chapters 6 and 7 together. Given a plabic network on the cylinder where we can apply the plabic R-matrix, the dual quiver is a spider web quiver. We show that the y-variables obtained by applying τ are exactly the same as the face variables obtained by applying the plabic R-matrix.

1.4 Main Results

- Theorem 2.4.4 characterizes permutations $v \in S_n$ such that $\mathrm{Imm}_v(M)$ is positive if M is k-positive.
- Corollary 2.9.3 gives a pattern avoidance criteria for permutations $v \in S_n$ such that $\mathrm{Imm}_v(M)$ is positive if M is 2-positive.
- Section 3.3 reproves Corollary 2.9.3 using cluster algebras.

- Theorem 3.5.1 identifies the DRH matrices studied in [CJS15] as being a special case of the k-positivity cluster algebras studied in [BCM20].
- Definition 5.2.3 gives a formula for computing weights of paths in a plabic network on a cylinder with face and trail weights.
- Given an involution of weights for a directed plabic network on the cylinder N, Theorem 5.3.3 gives a canonical way to define an involution of weights for N' where N' is the same as N up to path and cycle reversal.
- Definition 6.1.1 defines Postnikov diagrams on a surface with boundary and Theorem 6.1.2 states that Postnikov diagrams on a cylinder are in bijection with leafless reduced plabic graphs on a cylinder with no unicolored edges.
- Definition 6.2.4 gives formulas for the edge-weighted plabic R-matrix and Definition 6.3.2 gives formulas for the face-weighted plabic R-matrix. Theorems 6.2.5 and 6.3.3 state several properties of the transformation.
- Example 6.2.6, shows how the plabic R-matrix recovers the geometric R-matrix.
- Theorem 7.2.1 gives formulas for the x-variables of spider web quivers under τ
- Theorem 7.2.5 states that τ gives an involution on the x-variables and Theorem 7.2.6 states that τ satisfies the braid relation for x-variables.
- Theorem 7.3.1 gives formulas for the y-variables of spider web quivers under τ.
- Theorem 7.3.11 states that τ gives an involution on the y-variables spider web quivers and Theorem 7.3.12 states that τ satisfies the braid relation for y-variables.
- Given a plabic network on the cylinder where we can apply the plabic R-matrix, Theorem 8.0.3 states that the y-variables obtained by applying τ to the dual quiver of the network are exactly the same as the face variables obtained by applying the plabic R-matrix to the network.

Chapter 2

k-Positivity of Kazhdan-Lusztig Immanants

The work presented in this chapter is joint work with Melissa Sherman-Bennett and can be found in [CSB20].

We will first introduce the main players in this chapter: k-positive matrices (Section 2.1) and Kazhdan-Lusztig immanants (Section 2.2). In Section 2.3 we lay out our main question and the motivation behind it. We then present our main theorem in Section 2.4. Section 2.5 gives a simplified formula for Kazhdan-Lusztig immanants in our case that allows us to prove the main theorem in Section 2.6. Two technical lemmas used in the proof are proven in Sections 2.7 and 2.8. We consider ways of reformulating our theorem in Section 2.9. Finally, in Section 2.10 we provide some further questions in this area and address alternative methods for working on problems of this type.

2.1 k-Positive Matrices

Definition 2.1.1. A matrix M is *k-positive* if all minors of M of size k and smaller are positive. The matrix is *k-nonnegative* if all minors of size k and smaller are nonnegative.

Example 2.1.2. The matrix

$$\begin{bmatrix} 11 & 9 & 3 \\ 8 & 7 & 3 \\ 2 & 2 & 1 \end{bmatrix}$$

has all positive entries and 2-minors, so it is 2-positive. However, this matrix has a negative determinant, so it is not totally positive.

Notice that an $n \times n$ matrix that is n-positive (respectively, n-nonnegative) is totally positive (respectively, totally nonnegative). This makes k-positivity a very natural generalization of total positivity.

It is natural to ask to what extent k-positive and k-nonnegative matrices inherit the properties of totally positive and totally nonnegative matrices. One nice property of $n \times n$ k-nonnegative matrices is that they, like totally nonnegative matrices, form a multiplicative semigroup. This means we can determine a set of generators that form a basis for the semigroup. In the case of totally nonnegative matrices, the answer is elementary Jacobi matrices, as discussed in Section 1.2. This question is answered for certain other cases in [CKST17].

Another property of totally nonnegative matrices that extends partially to k-nonnegative matrices is their nice topology. Fomin and Zelevinsky [FZ99] showed that there is a cell decomposition for the semigroup of invertible totally nonnegative matrices based on their factorizations into elementary Jacobi matrices. In the case of upper unitriangular matrices, these cells form a regular CW-complex with a closure poset isomorphic to the Bruhat poset on words corresponding to factorizations of matrices. In the cases studied in [CKST17], the semigroup of k-nonnegative matrices has an analogous cell decomposition that behaved well with respect to closure. In the upper unitriangular case considered, the cells form a CW-complex, although it is not regular.

One more area of study for k-positive matrices is their relationship to cluster algebras (see Section 3.4). Totally positive matrices have an underlying cluster structure; in fact, they were a main motivator for the discovery of cluster algebras [Fom10]. Part of this structure applies to k-positive matrices as well [BCM20]. Rather than having one cluster algebra associated to them, k-positive matrices correspond to a family of cluster algebras, each a sub-cluster algebra of the total positivity cluster algebra. We can move between these sub-cluster algebras by doing an operation called a *bridge*.

2.2 Kazhdan-Lusztig Immanants

Definition 2.2.1. Given a function $f : S_n \to \mathbb{C}$, the *immanant* associated to f, $\mathrm{Imm}_f : \mathrm{Mat}_{n\times n}(\mathbb{C}) \to \mathbb{C}$, is the function

$$\mathrm{Imm}_f(M) := \sum_{w\in S_n} f(w)\; m_{1,w(1)} \cdots m_{n,w(n)}.$$

Well-studied examples include the determinant, where $f(w) = (-1)^{\ell(w)}$, the permanent, where $f(w) = 1$, and more generally *character immanants*, where f is an irreducible character of S_n.

The positivity properties of immanants have been of interest since the early 1990s. In [GJ92], Goulden and Jackson conjectured (and Greene [Gre92] later proved) that character immanants of Jacobi-Trudi matrices are polynomials with nonnegative coefficients. This was followed by a number of positivity conjectures by Stembridge [Ste91], including two that were proved shortly thereafter: Haiman showed that character immanants of generalized Jacobi-Trudi matrices are Schur-positive [Hai93] and Stembridge showed that character immanants of totally nonnegative matrices are nonnegative [Ste92].

In [Ste92], Stembridge also asks if certain immanants are nonnegative on k-nonnegative matrices. More generally, it is natural to ask what one can say about the signs of immanants on k-nonnegative matrices. Stembridge's proof in [Ste91] does not extend to k-nonnegative matrices, as it relies on the existence of a certain factorization for totally nonnegative matrices which does not exist for all k-nonnegative matrices.

We will focus on the signs of *Kazhdan-Lusztig immanants*, which were defined by Rhoades and Skandera [RS06].

Definition 2.2.2. Let $v \in S_n$. The *Kazhdan-Lusztig immanant* $\mathrm{Imm}_v : \mathrm{Mat}_{n\times n}(\mathbb{C}) \to \mathbb{C}$ is given by

$$\mathrm{Imm}_v(M) := \sum_{w\in S_n} (-1)^{\ell(w)-\ell(v)} P_{w_0 w, w_0 v}(1)\; m_{1,w(1)} \cdots m_{n,w(n)} \tag{2.1}$$

where $P_{x,y}(q)$ is the Kazhdan-Lusztig polynomial associated to $x, y \in S_n$ and $w_0 \in S_n$ is the longest permutation. (For the definition of $P_{x,y}(q)$ and their basic properties, see e.g. [BB06].)

For example, $\mathrm{Imm}_e(M) = \det M$ and $\mathrm{Imm}_{w_0}(M) = m_{n,1}m_{n-1,2}\cdots m_{1,n}$.

Using results of [Ste91, Hai93], Rhoades and Skandera [RS06] show that Kazhdan-Lusztig immanants are nonnegative on totally nonnegative matrices, and are Schur-positive on generalized Jacobi-Trudi matrices. Further, they show that character immanants are nonnegative linear combinations of Kazhdan-Lusztig immanants, so from the perspective of positivity, Kazhdan-Lusztig immanants are the more fundamental object to study.

2.3 Question and Motivation

We will call an immanant *k-positive* if it is positive on all k-positive matrices. We are interested in the following question.

Question 2.3.1. Let $0 < k < n$ be an integer. For which $v \in S_n$ is $\mathrm{Imm}_v(M)$ k-positive?

Notice that $\mathrm{Imm}_e(M) = \det M$ is k-positive only for $k = n$. On the other hand, $\mathrm{Imm}_{w_0}(M)$ is k-positive for all k, since it is positive as long as the entries (i.e.the 1×1 minors) of M are positive. So, the answer to Question 2.3.1 is a nonempty proper subset of S_n.

The motivation for Question 2.3.1 comes from the connection between total positivity and the dual canonical basis discussed in Section 1.2. Fomin and Zelevinsky [FZ00b] showed that for semisimple groups, $G_{>0}$ is characterized by the positivity of generalized minors, which are dual canonical basis elements corresponding to the fundamental weights of G and their images under Weyl group action. Note that the generalized minors are a finite subset of the (infinite) dual canonical basis, but their positivity guarantees the positivity of all other elements of the basis. In the case we are considering, $G = GL_n(\mathbb{C})$, $G_{>0}$ consists of the totally positive matrices and generalized minors are just ordinary minors. Skandera [Ska08] showed that Kazhdan-Lusztig immanants are part of the dual canonical basis of $\mathcal{O}(GL_n(\mathbb{C}))$, which gives another perspective on their positivity properties. (In fact, Skandera proved that every dual canonical basis element is the projection of a Kazhdan-Lusztig immanant evaluated on matrices with repeated rows and columns.) In light of these facts, Question 2.3.1 becomes a question of the following kind.

Question 2.3.2. Suppose some finite subset S of the dual canonical basis is positive on $M \in G$. Which other elements of the dual canonical basis are positive on M? In particular, what if S consists of the generalized minors corresponding to the first k fundamental weights and their images under the Weyl group action?

2.4 Main Theorem

Pylyavskyy [Pyl18] conjectured that there is a link between $\mathrm{Imm}_v(M)$ being k-positive and v avoiding certain patterns.

Definition 2.4.1. Let $v \in S_n$, and let $w \in S_m$. Suppose $v = v_1 \cdots v_n$ and $w = w_1 \cdots w_m$ in one-line notation. The pattern $w_1 \cdots w_m$ *occurs* in v if there exists $1 \leq i_1 < \cdots < i_m \leq n$ such that $v_{i_1} \cdots v_{i_m}$ are in the same relative order as $w_1 \cdots w_m$. Additionally, v *avoids* the pattern $w_1 \cdots w_m$ if it does not occur in v.

More precisely, Pylyavskyy conjectured the following.

Conjecture 2.4.2 ([Pyl18])**.** *Let $0 < k < n$ be an integer and let $v \in S_n$ avoid $12 \cdots (k+1)$. Then $\mathrm{Imm}_v(M)$ is k-positive.*

Our main result is a description of some k-positive Kazhdan-Lusztig immanants, in the spirit of Pylyavskyy's conjecture.

Definition 2.4.3. For $v, w \in S_n$ with $v \leq w$ in the Bruhat order, the graph of the interval $[v, w]$ is $\Gamma[v, w] := \{(i, u_i) : u = u_1 \ldots u_n \in [v, w], i = 1, \ldots, n\}$. We denote the graph of v by $\Gamma(v)$.

Theorem 2.4.4. *Let $v \in S_n$ be 1324-, 2143-avoiding and suppose the largest square region contained in $\Gamma[v, w_0]$ has size $k \times k$. Then $\mathrm{Imm}_v(M)$ is k-positive.*

Example 2.4.5. Consider $v = 2413$ in S_4. We have $[v, w_0] = \{2413, 4213, 3412, 2431, 4312, 4231, 3421\}$, and so $\Gamma[v, w_0]$ is as follows:

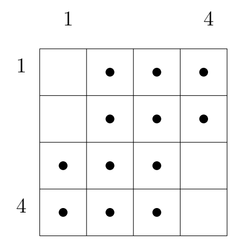

Notice that v avoids the patterns 1324 and 2143. In addition, we can see that the largest square region in $\Gamma[v, w_0]$ is 2×2.

So, Theorem 2.4.4 guarantees that

$$\begin{aligned}\mathrm{Imm}_v(M) = {} & m_{12}m_{24}m_{31}m_{43} - m_{14}m_{22}m_{31}m_{43} - m_{13}m_{24}m_{31}m_{42} + m_{14}m_{23}m_{31}m_{42} \\ & - m_{12}m_{24}m_{33}m_{41} + m_{14}m_{22}m_{33}m_{41} + m_{13}m_{24}m_{32}m_{41} - m_{14}m_{23}m_{32}m_{41}\end{aligned}$$

is positive on all 2-positive 4×4 matrices.

Note that Theorem 2.4.4 supports Conjecture 2.4.2, as detailed in Section 2.9.

2.5 Formula for 1324- and 2143-avoiding Permutations

We first introduce some notation that we will use for the rest of this chapter. For integers $i \leq j$, let $[i, j] := \{i, i+1, \ldots, j-1, j\}$. We abbreviate $[1, n]$ as $[n]$. For $v \in S_n$, we write v_i or $v(i)$ for the image of i under v. For $v \leq w$, we think of an element $(i, j) \in \Gamma[v, w]$ as a point in row i and column j of an $n \times n$ grid, indexed so that row indices increase going down and column indices increase going right. To discuss an inversion or non-inversion of a permutation v, we'll write $\langle i, j \rangle$ to avoid confusion with a matrix index or point in the plane. In the notation $\langle i, j \rangle$, we always assume $i < j$.

We first note that (2.1) has a much simpler form when v is 1324- and 2143-avoiding. By [Kaz80], $P_{x,y}(q)$ is the Poincaré polynomial of the local intersection cohomology of the Schubert variety indexed by y at any point in the Schubert variety indexed by x; by [LS90], the Schubert variety indexed by y is smooth precisely when y avoids 4231 and 3412. These results imply that $P_{x,y}(q) = 1$ for y avoiding 4231 and 3412. Together with the fact that $P_{x,y}(q) = 0$ for $x \not\leq y$ in the Bruhat order, this gives the following lemma.

Lemma 2.5.1. *Let $v \in S_n$ be 1324- and 2143-avoiding. Then*

$$\operatorname{Imm}_v(M) = (-1)^{\ell(v)} \sum_{w \geq v} (-1)^{\ell(w)} \; m_{1,w(1)} \cdots m_{n,w(n)}. \tag{2.2}$$

The coefficients in the formula in Lemma 2.5.1 suggest a strategy for analyzing $\operatorname{Imm}_v(M)$ for $v \in S_n$ avoiding 1324 and 2143: find some matrix N such that $\det(N) = \pm \operatorname{Imm}_v(M)$. If such a matrix N exists, the sign of $\operatorname{Imm}_v(M)$ is the sign of some determinant, which we have tools (e.g. Lewis Carroll's identity) to analyze. The most straightforward candidate for N is a matrix obtained from M by replacing some entries with 0.

Definition 2.5.2. Let $Q \subseteq [n]^2$ and let $M = (m_{ij})$ be in $\operatorname{Mat}_{n \times n}(\mathbb{C})$. The *restriction of M to Q*, denoted $M|_Q$, is the matrix with entries

$$n_{ij} = \begin{cases} m_{ij} & \text{if } (i,j) \in Q \\ 0 & \text{else.} \end{cases}$$

For a fixed $v \in S_n$ that avoids 1324 and 2143, suppose there exists $Q \subseteq [n]^2$ such that $\operatorname{Imm}_v(M) = \pm \det M|_Q$. Given the terms appearing in (2.2), Q must contain $\Gamma(w)$ for all w in $[v, w_0]$, and so must contain $\Gamma[v, w_0]$. In fact, the minimal choice of Q suffices. Before proving this, we give a characterization of $\Gamma[v, w_0]$ as a subset of $[n]^2$.

Definition 2.5.3. Let $v \in S_n$ and $(i,j) \in [n]^2 \setminus \Gamma(v)$. Then (i,j) is *sandwiched* by a non-inversion $\langle k,l \rangle$ if $k \leq i \leq l$ and $v_k \leq j \leq v_l$ or $v_k \geq j \geq v_l$. We also say $\langle k,l \rangle$ *sandwiches* (i,j).

That is to say, (i,j) is sandwiched $\langle k,l \rangle$ if and only if, in the plane, it lies inside the rectangle with opposite corners (k, v_k) and (l, v_l).

Lemma 2.5.4. *Let $v \in S_n$. Then $\Gamma[v, w_0] = \Gamma(v) \cup \{(i,j) : (i,j)$ is sandwiched by a non-inversion of $v\}$.*

An example of this lemma is shown in Figure 2.1. We can see that $\Gamma[v, w_0]$ is the union of rectangles defined by crosses in the upper-left and lower-right corners.

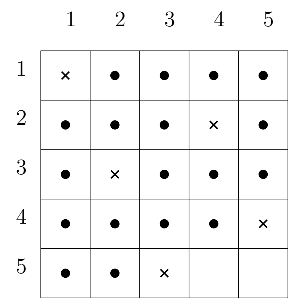

Figure 2.1: An illustration of Lemma 2.5.4 with $\Gamma[v, w_0]$ for $v = 14253$. Crosses mark the positions (i, v_i), and dots mark all other elements of $\Gamma[v, w_0]$.

Proof. Clearly $(i, v_i) \in \Gamma[v, w_0]$ for all i, so suppose (i, j) is sandwiched by a non-inversion $\langle k, l\rangle$ of v. We will produce a permutation $w > v$ sending i to j, which shows that $(i, j) \in \Gamma[v, w_0]$. Let $a = v^{-1}(j)$. If a, i form a non-inversion of v, then $v \cdot (a\ i) > v$ (where $(a\ i)$ is the transposition sending a to i and vice versa) and $v(a\ i)$ sends i to j. If a, i is an inversion, then $v \cdot (i\ k) \cdot (i\ a) > v$ if $i < a$ and $v \cdot (i\ l) \cdot (i\ a) > v$ if $i > a$. These permutations send i to j, so we are done.

To show that the above description gives all elements of $\Gamma[v, w_0]$, suppose that $\langle a, b\rangle$ is a non-inversion of v such that $\ell(v(a\ b)) = \ell(v) + 1$. The graph of $v \cdot (a\ b)$ can be obtained from $\Gamma(v)$ by applying the following move: look at the rectangle bounded by (a, v_a) and (b, v_b), and replace (a, v_a) and (b, v_b) with the other corners of the rectangle, (a, v_b) and (b, v_a). Notice that (a, v_b) and (b, v_a) are sandwiched by the non-inversion $\langle a, b\rangle$. Further, if (i, j) is sandwiched by a non-inversion of $v \cdot (a\ b)$, then it is also sandwiched by a non-inversion of v. Thus repeating this move produces graphs whose points are sandwiched by some non-inversion of v. Since for arbitrary $u > v$, the graph of u can be obtained from that of v by a sequence of these moves, we are done. □

We are now ready to prove the following proposition, which follows from work of Sjöstrand [Sjö07].

Proposition 2.5.5. *Let $v \in S_n$ avoid 1324, 24153, 31524, and 426153, and let $M \in Mat_{n\times n}(\mathbb{C})$. Then*

$$\det(M|_{\Gamma[v,w_0]}) = \sum_{w \geq v} (-1)^{\ell(w)}\ m_{1,w(1)} \cdots m_{n,w(n)}.$$

Proof. Notice that by definition,

$$\det(M|_{\Gamma[v,w_0]}) = \sum_{\substack{w \in S_n \\ \Gamma(w) \subseteq \Gamma[v,w_0]}} (-1)^{\ell(w)}\ m_{1,w(1)} \cdots m_{n,w(n)}. \tag{2.3}$$

We would like to show that for permutations v avoiding the appropriate patterns, $[v, w_0] = \{w \in S_n : \Gamma(w) \subseteq \Gamma[v, w_0]\}$.

Lemma 2.5.4 shows that for arbitrary $v \in S_n$, $\Gamma[v, w_0]$ is equal to what Sjöstrand calls the "left convex hull" of v. [Sjö07, Theorem 4] establishes that the left convex hull of v contains $\Gamma(w)$ for $w \notin [v, w_0]$ if and only if 1324, 24153, 31524, or 426153 occurs in v. Thus, if v avoids these 4 patterns, then $\{w \in S_n : \Gamma(w) \subseteq \Gamma[v, w_0]\} = [v, w_0]$, and the proposition follows. □

Combining Lemma 2.5.1 and Proposition 2.5.5, we obtain an expression for certain immanants as determinants (up to sign).

Corollary 2.5.6. *Let $v \in S_n$ avoid 1324 and 2143. Then*

$$\mathrm{Imm}_v(M) = (-1)^{\ell(v)} \det(M|_{\Gamma[v,w_0]}). \tag{2.4}$$

We will use Lewis Carroll's identity to determine the sign of (2.4) in Section 2.6, using some results on the structure of $\Gamma[v, w_0]$.

2.6 Dodgson Condensation

We are now ready to prove Theorem 2.4.4. Our main proof technique will be application of the following:

Proposition 2.6.1 (Lewis Carroll's Identity)**.** *If M is an $n \times n$ square matrix and M_A^B is M with the rows indexed by A and columns indexed by B removed, then*

$$\det(M)\det(M_{a,a'}^{b,b'}) = \det(M_a^b)\det(M_{a'}^{b'}) - \det(M_a^{b'})\det(M_{a'}^{b}),$$

where $1 \le a < a' \le n$ and $1 \le b < b' \le n$.

2.6.1 Young diagrams

We begin by considering the cases where $\Gamma[v, w_0]$ is a Young diagram or the complement of a Young diagram (using English notation). Recall that the *Durfee square* of a Young diagram λ is the largest square contained in λ.

Proposition 2.6.2. *Let $\lambda \subseteq n^n$ be a Young diagram with Durfee square of size k and $\mu := n^n/\lambda$. Let M be an $n \times n$ k-positive matrix. Then*

$$(-1)^{|\mu|} \det(M|_\lambda) \geq 0$$

and equality holds only if $(n, n-1, \ldots, 1) \not\subseteq \lambda$.

Proof. Let $A = M|_\lambda = \{a_{ij}\}$. For $\sigma \in S_n$, let $a_\sigma := a_{1,\sigma(1)} \cdots a_{n,\sigma(n)}$. Note that if $\lambda_{n-j+1} < j$, then the last j rows of λ are contained in a $j \times (j-1)$ rectangle. There is no way to choose j boxes in the last j rows of λ so that each box is in a different column and row. This means at least one of the matrix entries in a_σ is zero. So $\det A = 0$ if $(n, n-1, \ldots, 1) \not\subseteq \lambda$.

Now, assume that $(n, n-1, \ldots, 1) \subseteq \lambda$. We proceed by induction on n to show that $\det(A)$ has sign $(-1)^{|\mu|}$. The base cases for $n = 1, 2$ are clear.

We would like to apply Lewis Carroll's identity to find the sign of $\det(A)$. Let λ_I^J denote the Young diagram obtained from λ by removing rows indexed by I and columns indexed by J. Note that $A_I^J = M_I^J|_{\lambda_I^J}$. The submatrices M_I^J are k-positive and the Durfee square of λ_I^J is no bigger than the Durfee square of λ, so by the inductive hypothesis, we know the signs of $\det A_I^J$ for $|I| = |J| \geq 1$.

We will analyze the following Lewis Carroll identity:

$$\det(A)\det(A_{1,n}^{1,n}) = \det(A_1^1)\det(A_n^n) - \det(A_1^n)\det(A_n^1). \tag{2.5}$$

Note that $\lambda_{1,n}^{1,n}$ contains $(n-2, n-3, \ldots, 1)$ and $\lambda_n^n, \lambda_1^n, \lambda_n^1$ contain $(n-1, n-2, \ldots, 1)$, so the determinants of $A_{1,n}^{1,n}$, A_n^n, A_1^n, and A_n^1 are nonzero.

Suppose the last row of μ contains r boxes and the last column contains c (so that the union of the last column and row contains $r + c - 1$ boxes). Note that $r, c < n$. Then $\det(A_{1,n}^{1,n})$ and $\det(A_n^n)$ have sign $(-1)^{|\mu|-(r+c-1)}$, $\det(A_1^n)$ has sign $(-1)^{|\mu|-c}$, and $\det(A_n^1)$ has sign $(-1)^{|\mu|-r}$. Notice that $\det(A_1^1)$ is either zero or it has sign $(-1)^{|\mu|}$, since $\mu_1^1 = \mu$. In both of these cases, the right hand side of (2.5) is nonzero and has sign $(-1)^{2|\mu|-r-c+1}$; the left hand side has sign $\operatorname{sgn}(\det(A)) \cdot (-1)^{|\mu|-r-c+1}$, which gives the proposition.

□

Corollary 2.6.3. *Let $\mu \subseteq n^n$ be a Young diagram and let $\lambda := n^n/\mu$. Suppose λ has Durfee square of size k, and M is a k-positive $n \times n$ matrix. Then*

$$(-1)^{|\mu|} \det(M|_\lambda) \geq 0$$

and equality holds if and only if $(n^n/(n-1, n-2, \ldots, 1, 0)) \subseteq \lambda$ (or equivalently, $\mu \subseteq (n-1, n-2, \ldots, 1, 0)$).

Proof. If you transpose $M|_\lambda$ across the antidiagonal, you obtain the scenario of Proposition 2.6.2. Transposition across the antidiagonal is the same as reversing columns, taking transpose, and reversing columns again, which doesn't effect the sign of minors. □

Proposition 2.6.2 and Corollary 2.6.3 give us the following results about immanants.

Corollary 2.6.4. *Let $v \in S_n$ avoid 1324 and 2143. Suppose $\Gamma[v, w_0]$ is a Young diagram λ with Durfee square of size k. Then $\operatorname{Imm}_v(M)$ is k-positive.*

Proof. Suppose M is k-positive. Note that $\Gamma(w_0) \subseteq \Gamma[v, w_0]$ implies λ contains the partition $(n, n-1, \ldots, 1)$. If $\mu = n^n/\lambda$ then we know that $(-1)^{|\mu|} \det M|_{\Gamma[v,w_0]} > 0$ by Proposition 2.6.2.

In fact, there is a bijection between boxes of μ and inversions of v. If a box of μ is in row r and column c, then $v(r) < c$ and $v^{-1}(c) < r$; otherwise, that box would be in $\Gamma[v, w_0]$. This means exactly that $(v^{-1}(c), r)$ is an inversion. If (a, b) was an inversion of v and the box in row b and column $v(a)$ was not in μ, then for some j, the box in row j and column $v(j)$ is southeast of the box in row b and column $v(a)$. But then $1\ v(a)\ v(b)\ v(j)$ would be an occurrence of the pattern 1324, a contradiction.

So, we know $(-1)^{|\mu|} \det M|_{\Gamma[v,w_0]} = (-1)^{\ell(v)} \det M|_{\Gamma[v,w_0]} > 0$. By Corollary 2.5.6, this means $\operatorname{Imm}_v(M) > 0$. □

Corollary 2.6.5. *Let $v \in S_n$ avoid 1324 and 2143. Suppose $\Gamma[v, w_0]$ is $\lambda = n^n/\mu$ for some partition μ and the largest square in λ is of size k. Then $\operatorname{Imm}_v(M)$ is k-positive.*

Proof. Suppose M is k-positive. Note that $\Gamma(w_0) \subseteq \Gamma[v, w_0]$ implies λ contains the partition $(n^n/(n-1, n-2, \ldots, 1, 0))$. By Corollary 2.6.3, we know that $(-1)^{|\mu|} \det M|_{\Gamma[v,w_0]} > 0$.

As in the proof of Corollary 2.6.4, there is a bijection between boxes of μ and inversions of v. So, we know $(-1)^{|\mu|} \det M|_{\Gamma[v,w_0]} = (-1)^{\ell(v)} \det M|_{\Gamma[v,w_0]} > 0$. By Corollary 2.5.6, this means $\mathrm{Imm}_v(M) > 0$. □

2.6.2 General case

To prove Theorem 2.4.4, we need to show that if v avoids 1324 and 2143, then $\det M|_{\Gamma[v,w_0]}$ has sign $(-1)^{\ell(v)}$ for M satisfying positivity assumptions.

We first reduce to the case when $w_0 v$ is not in any parabolic subgroup of S_n.

Lemma 2.6.6. *Let $v \in S_n$. Suppose $w_0 v$ is contained in a maximal parabolic subgroup $S_j \times S_{n-j}$ of S_n. Then $\Gamma[v, w_0]$ is block-antidiagonal, with upper-right block of size $j \times j$ and lower-left block of size $(n-j) \times (n-j)$.*

Further, let $w_{(j)}$ denote the longest element of S_j. Let $v_1 \in S_j$ and $v_2 \in S_{n-j}$ be permutations such that upper-right antidiagonal block of $\Gamma[v, w_0]$ is equal to $\Gamma[v_1, w_{(j)}]$ and the other antidiagonal block is equal to $\Gamma[v_2, w_{(n-j)}]$ (up to translation; see Figure 2.2). If M is an $n \times n$ matrix, then

$$(-1)^{\ell(v)} \det M|_{\Gamma[v,w_0]} = (-1)^{\ell(v_1)} \det M_1|_{\Gamma[v_1,w_{(j)}]} \cdot (-1)^{\ell(v_2)} \det M_2|_{\Gamma[v_2,w_{(n-j)}]}$$

where M_1 (resp. M_2) is the square submatrix of M using columns $n-j+1$ through n and rows 1 through j (resp. columns 1 through $n-j$ and rows $j+1$ through n).

Proof. Notice that v is the permutation

$$v : i \mapsto \begin{cases} v_1(i) + n - j & \text{if } 1 \leq i \leq j \\ v_2(i-j) & \text{if } j < i \leq n. \end{cases}$$

So all elements of $\Gamma(v)$ are contained in $([j] \times [n-j, n]) \cup ([j+1, n] \times [n-j])$. If $\langle i, k \rangle$ is a non-inversion of v, then either $i, k \leq j$ or $i, k > j$, so by Lemma 2.5.4, $\Gamma[v, w_0]$ is contained in the same set. In other words, $\Gamma[v, w_0]$ block-antidiagonal.

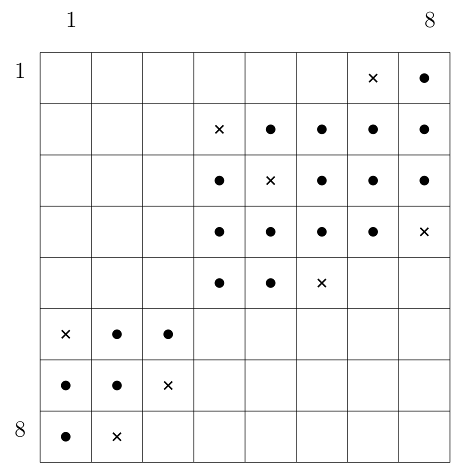

Figure 2.2: An example where $\Gamma[v, w_0]$ is block-antidiagonal. Here, $v = 74586132$. In the notation of Lemma 2.6.6, $j = 3$, $v_1 = 41253$, and $v_2 = 132$.

For a block-antidiagonal matrix A with blocks A_1, A_2 of size j and $n-j$, respectively, we have

$$\begin{aligned}
\det(A) &= (-1)^{\ell(w_0)} \det(Aw_0) \\
&= (-1)^{\ell(w_0)} \det(A_1 w_{(j)}) \ \det(A_2 w_{(n-j)}) \\
&= (-1)^{\ell(w_0)+\ell(w_{(j)})+\ell(w_{(n-j)}} \det(A_1)\det(A_2) \\
&= (-1)^{\binom{n}{2}+\binom{j}{2}+\binom{n-j}{2}} \det(A_1)\det(A_2).
\end{aligned}$$

From the above description of v, $\ell(v) = j(n-j) + \ell(v_1) + \ell(v_2)$. This, together with the fact that $\binom{n}{2} = \binom{j}{2} + \binom{n-j}{2} + j(n-j)$ and the formula for the determinant of a block-antidiagonal matrix, gives the desired equality. □

We have the following immediate corollary.

Lemma 2.6.7. *Let $v \in S_n$ avoid 1324 and 2143, let M be an $n \times n$ matrix, and let v_i, and M_i be as in Lemma 2.6.6. Then*

$$\mathrm{Imm}_v(M) = \mathrm{Imm}_{v_1}(M_1)\,\mathrm{Imm}_{v_2}(M_2).$$

We now introduce two propositions we will need for the proof of the general case.

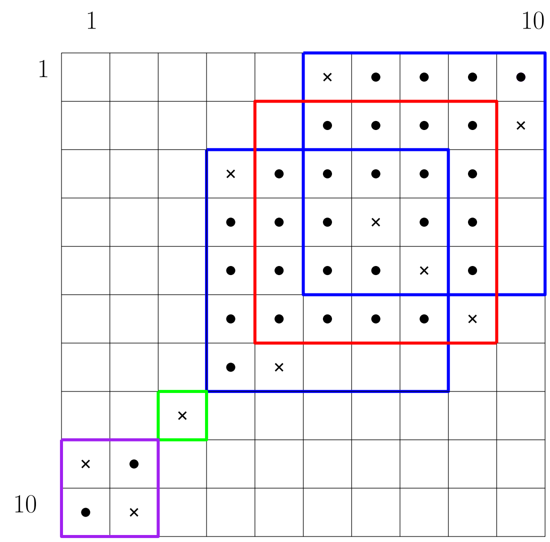

Figure 2.3: An example of $\Gamma[v, w_0]$, with $v = 6\ 10\ 4\ 7\ 8\ 9\ 3\ 1\ 2$. The bounding boxes are shown in the appropriate color. The spanning corners of $\Gamma[v, w_0]$ are $(1,6)$, $(3,4)$, $(6,9)$, $(8,3)$, $(9,1)$, and $(10,2)$.

Definition 2.6.8. Let $v \in S_n$. Define $\mathbf{B}_{i,v_i}$ to be the square region of $[n]^2$ with corners (i, v_i), $(i, n-i+1)$, $(n-v_i+1, v_i)$ and $(n-v_i+1, n-i+1)$. In other words, $\mathbf{B}_{i,v_i}$ is the the square region of $[n]^2$ on the antidiagonal with a corner at (i, v_i). We say $\mathbf{B}_{i,v_i}$ is a *bounding box* of $\Gamma[v, w_0]$ if there does not exist some j such that $\mathbf{B}_{i,v_i} \subsetneq \mathbf{B}_{j,v_j}$. If $\mathbf{B}_{i,v_i}$ is a bounding box of $\Gamma[v, w_0]$, we call (i, v_i) a *spanning corner* of $\Gamma[v, w_0]$. We denote the set of spanning corners of $\Gamma[v, w_0]$ by S. (See Figure 2.3 for an example.)

Remark 2.6.9. To justify the name "spanning corners," notice that if (i, v_i) not sandwiched by any non-inversion of v, then (i, v_i) is a corner of $\Gamma[v, w_0]$ (i.e. there are either no elements of $\Gamma[v, w_0]$ weakly northwest of (i, v_i) or no elements of $\Gamma[v, w_0]$ weakly southeast of (i, v_i)). Conversely, if (i, v_i) is sandwiched by a non-inversion $\langle k, l \rangle$ of v, then (i, v_i) is in the interior of $\Gamma[v, w_0]$, and $\mathbf{B}_{i,v_i} \subseteq \mathbf{B}_{k,v_k}$. So all elements of S are corners of $\Gamma[v, w_0]$.

The name "bounding boxes" comes from the following lemma.

Lemma 2.6.10. *Let $v \in S_n$. Then*

$$\Gamma[v, w_0] \subseteq \bigcup_{(i,v_i) \in S} \mathbf{B}_{i,v_i}.$$

Proof. Let $R_{k,l}$ denote the rectangle with corners $(k, v_k), (l, v_l), (k, v_l)$, and (l, v_k). If $\langle k, l \rangle$ is a non-inversion of v, then $R_{k,l}$ consists exactly of the points sandwiched by $\langle k, l \rangle$. So by Lemma 2.5.4, we have that

$$\Gamma[v, w_0] = \bigcup_{\langle k,l \rangle \text{ non-inversion of } v} R_{k,l}.$$

Notice that if (i, w_i) is sandwiched by $\langle k, l \rangle$, then $R_{i,l}$ and $R_{k,i}$ are contained in $R_{k,l}$. So to show the desired containment, it suffices to show that $R_{k,l}$ is contained in $\bigcup_{(i,v_i) \in S} \mathbf{B}_{i,v_i}$ for all non-inversions $\langle k, l \rangle$ such that (k, v_k) and (l, v_l) are both corners of $\Gamma[v, w_0]$.

So consider a non-inversion $\langle k, l \rangle$ where $(k, v_k), (l, v_l)$ are corners. Working through the possible relative orders of k, l, v_k, v_l, one can see that $R_{k,l} \subseteq \mathbf{B}_{k,v_k} \cup \mathbf{B}_{l,v_l}$. Since S consists of spanning corners, we have $(a, v_a), (b, v_b) \in S$ such that $\mathbf{B}_{a,v_a}$ and $\mathbf{B}_{b,v_b}$ contain $\mathbf{B}_{k,w_k}$ and $\mathbf{B}_{l,w_l}$, respectively. So $R_{k,l} \subseteq \mathbf{B}_{a,w_a} \cup \mathbf{B}_{b,w_b}$, as desired. □

We also color the bounding boxes.

Definition 2.6.11. A bounding box $\mathbf{B}_{i,v_i}$ is said to be *red* if (i, v_i) is below the antidiagonal, *green* if (i, v_i) is on the antidiagonal, and *blue* if (i, v_i) is above the antidiagonal. In the case where $\mathbf{B}_{i,v_i}$ is a bounding box and $\mathbf{B}_{n-v_i+1,n-i+1}$ is also a bounding box, then $\mathbf{B}_{i,v_i} = \mathbf{B}_{n-v_i+1,n-i+1}$ is both red and blue, in which case we call it *purple.* (See Figure 2.3 for an example.)

Proposition 2.6.12. *Suppose $v \in S_n$ avoids 2143 and $w_0 v$ is not contained in a maximal parabolic subgroup of S_n. Order the bounding boxes of $\Gamma[v, w_0]$ by the row of the northwest corner. If $\Gamma[v, w_0]$ has more than one bounding box, then they alternate between blue and red and there are no purple bounding boxes.*

Example 2.6.13. If $v = 371456$, then $\Gamma[v, w_0]$ is the same as the upper right antidiagonal block of Figure 2.3. The bounding boxes of v, in the order of Proposition 2.6.12, are $\mathbf{B}_{1,3}$, $\mathbf{B}_{6,5}$, and $\mathbf{B}_{3,1}$. The colors are blue, red, and blue, respectively.

For the next proposition, we need some additional notation.

Define $\delta_i : [n] \setminus \{i\} \to [n-1]$ as

$$\delta_i(j) = \begin{cases} j, & j < i; \\ j-1, & j > i. \end{cases}$$

For $i, k \in [n]$ and $P \subseteq [n]^2$, let $P_i^k \subseteq [n-1] \times [n-1]$ be P with row i and column k deleted. That is, $P_i^k = \{(\delta_i(r), \delta_k(c)) : (r, c) \in P\}$.

Proposition 2.6.14. *Let $v \in S_n$ be 2143- and 1324-avoiding, and choose $i \in [n]$. Let $x \in S_{n-1}$ be the permutation $x : \delta_i(j) \mapsto \delta_{v_i}(v_j)$ (that is, x is obtained from v by deleting v_i from v in one-line notation and shifting the remaining numbers appropriately). Then*

$$\det(M|_{\Gamma[x,w_0]}) = \det(M|_{\Gamma[v,w_0]_i^{v_i}}). \tag{2.6}$$

See Figure 2.4 for an example of Proposition 2.6.14.

The proofs of Propositions 2.6.12 and 2.6.14 are quite technical and appear below in Sections 2.7 and 2.8 respectively.

Theorem 2.6.15. *Let $v \in S_n$ avoid 1324 and 2143 and let k be the size of the largest square in $\Gamma[v, w_0]$. For M k-positive, $(-1)^{\ell(v)} \det M|_{\Gamma[v,w_0]} > 0$.*

Proof. We proceed by induction on n; the base case $n = 2$ is clear.

Now, let $n > 2$. If $\Gamma[v, w_0]$ is a partition or a complement of a partition (that is, it has a single bounding box), we are done by Corollary 2.6.4 or Corollary 2.6.5. If it is block-antidiagonal (that is, $w_0 v$ is contained in some parabolic subgroup), then we are done by Lemma 2.6.7. So we may assume that v has at least 2 bounding boxes and that adjacent bounding boxes have nonempty intersection (where bounding boxes are ordered as usual by the row of their northeast corner). Indeed, if adjacent bounding boxes have empty intersection, then the fact that $\Gamma[v, w_0]$ is contained in the union of bounding boxes (Lemma 2.6.10) implies that $\Gamma[v, w_0]$ is block-antidiagonal.

Because v avoids 1324 and 2143, the final two bounding boxes of $\Gamma[v, w_0]$ are of opposite color by Proposition 2.6.12. Without loss of generality, we assume the final box is red and the second to last box is blue. (Otherwise, we can consider the antidiagonal transpose of M restricted to $\Gamma[w_0 v^{-1} w_0, w_0]$, which has the same determinant.)

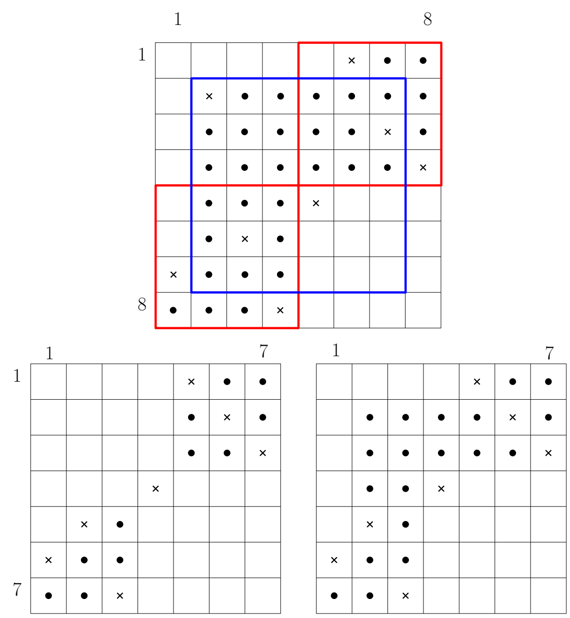

Figure 2.4: At the top, $\Gamma[v, w_0]$ for $v = 62785314$. On the bottom left, the region $\Gamma[x, w_0]$, where $x = 5674213$ is the permutation obtained by deleting 2 from the one-line notation of v and shifting remaining numbers appropriately. On the bottom right, the region $\Gamma[v, w_0]_3^2$. The determinant of $M|_{\Gamma[x,w_0]}$ is the same as the determinant of $M|_{\Gamma[v,w_0]_3^2}$ for all 7×7 matrices M, illustrating Proposition 2.6.14.

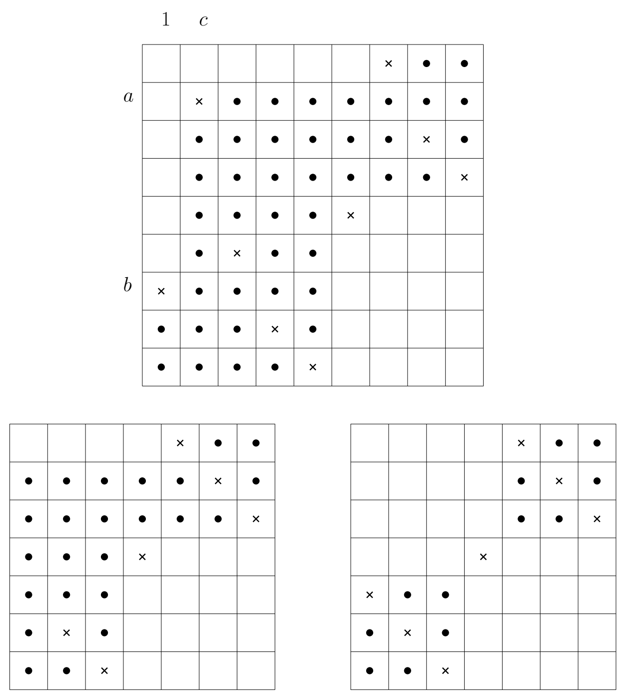

Figure 2.5: An illustration of (2) in the proof of Theorem 2.6.15. Let $v = 62785314$; $\Gamma[v, w_0]$ is shown with bounding boxes at the top of Figure 2.4. In this case, $a = c = 2$, $b = 7$, $w = 728963145$ and $y = 5674123$. On the top is $\Gamma[w, w_0]$. On the bottom left is $\Gamma[v, w_0]^1_a$, which is equal to $\Gamma[w, w_0]^{1,c}_{a,b}$. On the bottom right is $\Gamma[y, w_0]$.

This means the final box is $\mathbf{B}_{n,v_n}$, and the second to last box is $\mathbf{B}_{a,v_a}$ for some $a < n$ with $1 < v_a < v_n$. We analyze the sign of $\det M|_{\Gamma[v,w_0]}$ using Lewis Carroll's identity on rows $a, b := v^{-1}(1)$ and columns $1, c := v_a$. Note that $a < b$ and $1 < c$.

We will consider the determinants appearing in Lewis Carroll's identity one by one, and show that they are of the form $\det(N|_{\Gamma[u,w_0]})$ for some permutation u. Note that $(M|_{\Gamma[v,w_0]})^i_j = M^i_j|_{\Gamma[v,w_0]^i_j}$.

(1) Consider $(M|_{\Gamma[v,w_0]})^{1,c}_{a,b}$. The determinant of this matrix is equal to $\det(M^{1,c}_{a,b}|_{\Gamma[x,w_0]})$ where x is the permutation obtained from v by deleting 1 and v_a from v in one-line notation and shifting remaining values to obtain a permutation of $[n-2]$. Indeed, $(b, 1)$ is a corner of $\Gamma[v, w_0]$ but not a spanning corner. Combining the proof of Proposition 2.8.1 with Lemma 2.7.1, we have that $\Gamma[v, w_0]^1_b = \Gamma[u, w_0]$, where u is obtained from v by deleting 1 from v in one-line notation and shifting appropriately. So we have

$$\begin{aligned}(M|_{\Gamma[v,w_0]})^{1,c}_{a,b} &= ((M|_{\Gamma[v,w_0]})^1_b)^{c-1}_a \\ &= (M^1_b|_{\Gamma[u,w_0]})^{c-1}_a \\ &= M^{1,c}_{a,b}|_{\Gamma[u,w_0]^{c-1}_a}.\end{aligned}$$

Note that $u_a = c - 1$ and deleting $c - 1$ from the one-line notation of u gives x. So taking determinants and applying Proposition 2.6.14 gives the desired equality.

Note that $\ell(x) = \ell(v) - a - b - c + 4$. Indeed, 1 is involved in exactly $b-1$ inversions of v. Because there are no (j, v_j) northwest of (a, c), a is involved in exactly $a+c-2$ inversions of v: each of the $c - 1$ columns to the left of column c contains a dot (j, v_j) southwest of (a, c), and each of the $a - 1$ rows above (a, c) contains a dot (j, v_j) northeast of (a, c). We have counted the inversion $\langle 1, a\rangle$ twice, so deleting 1 and c from v deletes $(b - 1) + (a + c - 2) - 1$ inversions.

(2) Consider $(M|_{\Gamma[v,w_0]})^1_a$. The determinant of this matrix is equal to the determinant of $M^1_a|_{\Gamma[y,w_0]}$, where y is obtained from v by adding v_n+1 to the end of v in one-line notation and shifting appropriately to get w, then deleting 1 and v_a from w and shifting values to obtain a permutation of $[n-1]$.

To see this, first note that there are no pairs (i, v_i) with $n > i > b$ and $v_i > v_n$; such a pair would mean that $v_a 1 v_i v_n$ form a 2143 pattern, which is impossible. There are also no pairs (i, v_i) with $i < a$ and $v_i < v_n$. Indeed, because (a, v_a) is a corner, we would have to have $v_a < v_i < v_n$. This means we would have a red bounding box $\mathbf{B}_{j,v_j}$ following $\mathbf{B}_{a,v_a}$ with $a < j$ and $v_n < v_j$. Then $v_i v_a v_b v_n$ would form a 2143 pattern. This implies that the number of elements of $\Gamma[v, w_0]$ in row b and in row n are the same. Similarly, the number of elements of $\Gamma[v, w_0]$ in column c and column v_n are the same. So to obtain $\Gamma[w, w_0]$ from $\Gamma[v, w_0]$, add a copy of row b of $\Gamma[v, w_0]$ below the last row, a copy of column c to the right of the v_nth row, and a dot in position $(n+1, v_{n+1})$. It follows that $\Gamma[w, w_0]_{a,b}^{1,c} = \Gamma[v, w_0]_a^1$.

One can check that w (and thus y) avoid 2143 and 1324. A similar argument to (1) shows that the determinant of $M|_{\Gamma[w,w_0]_{a,b}^{1,c}}$ is equal to the determinant of $M_{a,b}^{1,c}|_{\Gamma[y,w_0]}$. See Figure 2.5 for an example.

Note that $\ell(y) = \ell(v) - a - b - c + 4 + n - v_n$.

(3) Consider $(M|_{\Gamma[v,w_0]})_b^c$. The determinant of this matrix is equal to the determinant of $M_b^c|_{\Gamma[z,w_0]}$, where z is obtained from v by deleting v_n from v in one-line notation and shifting as necessary. This follows from the fact that $\Gamma[v, w_0]$ has the same number of dots in rows b and n, and in columns c and v_n (proved in *(2)*). So $\Gamma[v, w_0]_b^c = \Gamma[v, w_0]_n^{v_n}$. The claim follows from Proposition 2.6.14 applied to $M|_{\Gamma[v,w_0]_n^{v_n}}$.

Note that $\ell(z) = \ell(v) - (n - v_n)$.

(4) Consider $(M|_{\Gamma[v,w_0]})_b^1$. By Proposition 2.6.14, the determinant of this matrix is equal to the determinant of $M_b^1|_{\Gamma[p,w_0]}$, where p is obtained from v by deleting 1 from v in one-line notation and shifting appropriately.

Note that $\ell(p) = \ell(v) - b + 1$.

(5) Consider $(M|_{\Gamma[v,w_0]})_a^c$. By Proposition 2.6.14, the determinant of this matrix is equal to the determinant of $M_a^c|_{\Gamma[q,w_0]}$, where q is obtained from v by deleting v_a from v in one-line notation and shifting appropriately.

Note that $\ell(q) = \ell(v) - c - a + 2$.

Notice that the permutations x, y, z, p, q listed above avoid 2143 and 1324. By induction, the determinant of $M_I^J|_{\Gamma[u,w_0]}$ has sign $\ell(u)$, and, in particular, is nonzero, so we know the signs of each determinant involved in Lewis Carroll's identity besides $\det M$. Dividing both sides of Lewis Carroll's identity by $\det(M|_{\Gamma[v,w_0]})_{a,b}^{1,c}$, we see that both terms on the right-hand side have sign $\ell(v)$. Thus, the right-hand side is nonzero and has sign $\ell(v)$, which completes the proof.

□

2.7 Proof of Proposition 2.6.12

In order to simplify the proofs in the next two sections, we will consider the graphs of lower intervals $[e,w]$ rather than upper intervals $[v,w_0]$. As the next lemma shows, the two are closely related.

Lemma 2.7.1. *Let $v \in S_n$. Then $\Gamma[v,w_0] = \{(i,w_0(j)) : (i,j) \in \Gamma[e,w_0v]\}$. In other words, $\Gamma[v,w_0]$ can be obtained from $\Gamma[e,w_0v]$ by reversing the columns of the $n \times n$ grid.*

Proof. This follows immediately from the fact that left multiplication by w_0 is an anti-automorphism of the Bruhat order. □

Since left-multiplication by w_0 takes non-inversions to inversions, we have an analogue of Lemma 2.5.4 for $\Gamma[e,w]$.

Lemma 2.7.2. *Let $w \in S_n$. Then $\Gamma[e,w] = \Gamma(w) \cup \{(i,j) \in [n]^2 : (i,j)$ is sandwiched by an inversion of $w\}$.*

Left-multiplication by w_0 takes the anti-diagonal to the diagonal, so we also have an analogue of bounding boxes and Lemma 2.6.10.

Definition 2.7.3. Let $w \in S_n$. Define $B_{i,w_i} \subseteq [n]^2$ to be the square region with corners (i,i), (i,w_i), (w_i,i), (w_i,w_i). We call B_{i,w_i} a *bounding box* of $\Gamma[e,w]$ if it is not properly contained in any B_{j,w_j}. In this situation, we call (i,w_i) a *spanning corner* of $\Gamma[e,w]$. We denote the set of spanning corners of $\Gamma[e,w]$ by $\overline{S}$.

Lemma 2.7.4. *Let $w \in S_n$. Then*

$$\Gamma[e,w] \subseteq \bigcup_{(i,w_i)\in\overline{S}} B_{i,w_i}.$$

Definition 2.7.5. A bounding box B_{i,w_i} is colored *red* if $i > w_i$, *green* if $i = w_i$, and *blue* if $i < w_i$. If $w^{-1}(i) = w_i$ (so that both (i, w_i) and (w_i, i) are spanning corners), then the bounding box $B_{i,w_i} = B_{w_i,i}$ is both red and blue. If a bounding box is both red and blue, we also call it *purple*.

Remark 2.7.6. Note that if $w = w_0 v$, then $\mathbf{B}_{i,v_i}$ is a bounding box of $\Gamma[v, w_0]$ if and only if B_{i,w_i} is a bounding box of $\Gamma[e, w]$. Further, $\mathbf{B}_{i,v_i} = \{(r, w_0(c)) : (r, c) \in B_{i,w_i}\}$ and $\mathbf{B}_{i,v_i}$ has the same color as B_{i,w_i}.

We introduce one new piece of terminology.

Definition 2.7.7. Let $w \in S_n$. The *span* of (i, w_i), denoted by $\sigma(i, w_i)$, is $[i, w_i]$ if $i \leq w_i$ and is $[w_i, i]$ otherwise. We say (i, w_i) *spans* (j, w_j) if $\sigma(i, w_i)$ contains $\sigma(j, w_j)$ (equivalently, if B_{i,w_i} contains B_{j,w_j}).

Rather than proving Proposition 2.6.12 directly, we instead prove the following:

Proposition 2.7.8. *Suppose $w \in S_n$ avoids 3412 and is not contained in a maximal parabolic subgroup of S_n. Order the bounding boxes of $\Gamma[e, w]$ by the row of the northwest corner. If $\Gamma[e, w]$ has more than one bounding box, then they alternate between blue and red and there are no purple bounding boxes.*

The first step to proving this is analyzing the bounding boxes of $\Gamma[e, w]$ when w is a 321- and 3412-avoiding permutation. We'll need the following result of [Ten07] and a lemma.

Proposition 2.7.9. *[Ten07, Theorem 5.3] Let $w \in S_n$. Then w avoids 321 and 3412 if and only if for all $a \in [n-1]$, s_a appears at most once in every (equivalently, any) reduced expression for w.*

Lemma 2.7.10. *Suppose $w \in S_n$ avoids 321 and 3412. If for some $i \in [n]$, $w^{-1}(i) = w_i$, then $|i - w_i| = 1$.*

Proof. Suppose $w^{-1}(i) = w_i$, and let t be the transposition sending i to w_i, w_i to i, and fixing everything else. We can assume that $i < w_i$. We compare w and t in the Bruhat order by comparing $w[j]$ and $t[j]$ for $j \in [n]$.

For two subsets $I = \{i_1 < \cdots < i_r\}$, $K = \{k_1 < \cdots < k_r\}$, we say $I \leq J$ if $i_j \leq k_j$ for all $j \in [r]$. For two permutations $v, w \in S_n$, we have $v \leq w$ if and only if for all $j \in [n]$, $v[j] \leq w[j]$.

For $j < i$ and $j \geq w_i$, $t[j] = [1, j]$, and so clearly $t[j] \leq w[j]$. For $i \leq j < w_i$, $t[j] = [1, i-1] \cup [i+1, j] \cup \{w_i\}$. Let $t[j] = \{a_1 < a_2 < \cdots < a_j\}$ and $w[j] = \{b_1 < b_2 < \cdots < b_j\}$. Notice that $a_j = w_i$ and $w_i \in w[j]$, so we definitely have that $a_j \leq b_j$. For the other inequalities, suppose $w[j] \cap [1, i] = \{b_1, \ldots, b_r\}$. Since i is not in $w[j]$, $r \leq i - 1$. This implies that $b_k \leq a_k$ for $k \leq r$. It also implies that $a_{r+k} \leq i + k$ and $b_{r+k} \geq i + k$ for $r + k < j$, which establishes the remaining inequalities. Thus, $w \geq t$.

Since $w \geq t$, every reduced expression for w has a reduced expression for t as a subexpression. Thus, Proposition 2.7.9 implies t must have a reduced expression in which each simple transposition appears once.

Now, t has a reduced expression which is a palindrome; it is length $2c + 1$ and contains at most $c + 1$ simple transpositions. Every reduced expression of t has the same length and contains the same set of simple transpositions. So if $c > 0$, in each reduced expression, some simple transposition appears twice. We conclude that $\ell(t) = 1$ and $|i - w_i| = 1$.

□

Proposition 2.7.11. *Suppose $w \in S_n$ avoids 321 and 3412 and is not contained in any maximal parabolic subgroup. Order the bounding boxes of $\Gamma[e, w]$ by the row of their northwest corner. Then no bounding boxes of $\Gamma[e, w]$ are green or purple, and they alternate between red and blue.*

Proof. If a bounding box B_{i,w_i} is green, then by definition $i = w_i$. The corner (i, i) has maximal span, which implies there are no (j, w_j) with $j < i$ and $w_j > i$. In other words, $w[i-1] = [i-1]$, which would contradict the assumption that w is not contained in a maximal parabolic subgroup.

There are also no spanning corners of the form $(i, i+1)$. Indeed, if $(i, i+1)$ were a spanning corner, then there are no (j, w_j) with $j \leq i - 1$ and $w_j > i + 1$ or with $j \geq i + 1$ and $w_j \leq i - 1$. The latter implies that $w_{i+1} = i$, which, together with the first inequality, implies $w[i-1] = [i-1]$, a contradiction. By Lemma 2.7.10, if a bounding box B_{i,w_i} is purple, then $|i - w_i| = 1$. This implies a spanning chord of the form $(k, k+1)$, which is impossible, so there are no purple bounding boxes.

So all bounding boxes are either blue or red. Suppose the bounding box B_{i,w_i} is followed by B_{j,w_j} in the ordering specified in the proposition. We suppose for the sake of contradiction that they are the same color. Without loss of generality, we may assume that they are blue, so $i < w_i$ and $j < w_j$. Otherwise, we consider w^{-1} instead of w. (By Proposition 2.7.9, w^{-1} is also 321- and 3412-avoiding. The span of (i, w_i) and $(w_i, w^{-1}(w_i))$ are the same, so the bounding boxes of $\Gamma[e, w^{-1}]$ are the same as the bounding boxes of $\Gamma[e, w]$, but with opposite color.)

Since B_{j,w_j} follows B_{i,w_i}, there are no pairs (k, w_k) with $k < j$ and $w_i < w_k$. Indeed, such a pair is spanned by neither (i, w_i) nor (j, w_j), so its existence would imply the existence of a bounding box between B_{i,w_i} and B_{j,w_j} or enclosing one of them, both of which are contradictions. In other words, $w[j-1] \subseteq [w_i]$, so we must have $j - 1 \leq w_i$. If $j = w_i + 1$, then $w[w_i] \subseteq [w_i]$, a contradiction. So we have $i < j \leq w_i < w_j$.

Now, consider the reduced expression for w obtained by starting at the identity, moving w_1 to position 1 using right multiplication by s_a's, then moving w_2 to position 2 (if it is not already there) using right multiplication, etc. Note that when w_k is moved to position k, no numbers greater than w_k have moved. Also, once w_k is in position k, it never moves again. Suppose w_{i-1} has just moved to position $i-1$. Because (i, w_i) is a spanning corner, we have not moved any numbers larger than w_i. In other words, k is currently in position k for $k \geq w_i$; in particular, w_i is in position w_i. Now, to move w_i to position i, we must use the transpositions $s_{w_i-1}, s_{w_i-2}, \ldots, s_{i+1}, s_i$ in that order. By Proposition 2.7.9, each simple transposition can only be used once in this reduced expression for w. Thus, these simple transpositions have not been used before we move w_i to position i, so in fact k is in position k for $k > i$ before we move w_i to position i.

Now we move w_i to position i. Since $s_{w_i-1}, \ldots, s_i$ will never be used again in the expression for w, we conclude that $w_{i+1}, \ldots, w_{w_i-1}$ are already in positions $i+1, \ldots, w_i-1$. Note also that the number currently in position w_i is $w_i - 1$, since $|i - w_i| > 1$.

Since $w_j > w_i$, w_j is not yet in position j. This implies that $j \geq w_i$. We already had that $j \leq w_i$, so in fact they are equal. So after w_i has moved to position i, w_j is the next number not yet in the correct position. Recall that for $k > w_i$, k is still in position k. So to move w_j to position w_i, we use $s_{w_j}, s_{w_j-1}, \ldots, s_j$ in that order (since $|j - w_j| > 1$, s_{j+1} is on this list of transpositions). Notice that the number in position

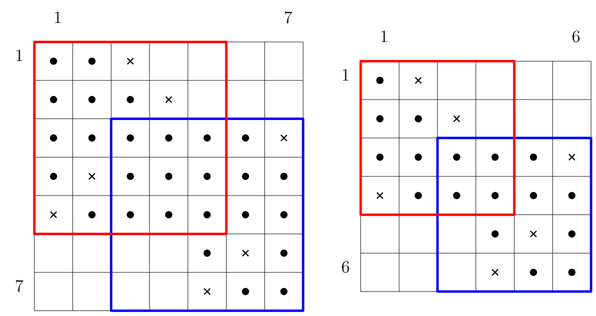

Figure 2.6: On the left, $\Gamma[e, w]$, where $w = 3472165$. On the right, $\Gamma[e, u]$, where $u = 236154$. The permutation u is obtained from w by deleting 2 from the one-line notation of w and shifting the other numbers appropriately. As Proposition 2.7.12 asserts, the spanning corners and bounding boxes of $\Gamma[e, w]$ are in bijection with the spanning corners and bounding boxes of $\Gamma[e, u]$, respectively, and this bijection is color-preserving.

j, which is $w_i - 1$, moves to position $j+1$. We cannot use s_j or s_{j+1} again, so $w_i - 1$ must be w_{j+1}. However, the pair $(j+1, w_i - 1)$ satisfies $j+1 > j$ and $w_i - 1 < w_i$, so it is spanned by neither (i, w_i) nor (j, w_j). Say $(j+1, w_i - 1)$ is spanned by the spanning corner (a, w_a). Then (a, w_a) spans neither of $(i, w_i), (j, w_j)$, which implies $i < \min(a, w_a) < j < \max(a, w_a) < w_j$. This means exactly that the bounding box order is $B_{i,w_i}, B_{a,w_a}, B_{j,w_j}$, a contradiction. □

We can in fact extend Proposition 2.7.11 to all permutations avoiding 3412.

Recall that $\delta_i : [n] \setminus \{i\} \to [n-1]$ is defined as

$$\delta_i(j) = \begin{cases} j & j < i \\ j-1 & j > i. \end{cases}$$

Proposition 2.7.12. *Suppose $w \in S_n$ avoids 3412 and let (i, w_i) be a non-corner of $\Gamma[e, w]$. Let $u \in S_{n-1}$ be the permutation $\delta_i(j) \mapsto \delta_{w_i}(w_j)$. Let $\overline{S}_w$ and $\overline{S}_u$ denote the spanning corners of $\Gamma[e, w]$ and $\Gamma[e, u]$, respectively.*

1. *The pair $(j, w_j) \in \overline{S}_w$ if and only if $(\delta_i(j), \delta_{w_i}(w_j)) \in \overline{S}_u$.*

2. *The map $\beta : \{B_{j,w_j} : (j, w_j) \in \overline{S}_w\} \to \{B_{k,u_k} : (k, u_k) \in \overline{S}_u\}$ defined by $B_{j,w_j} \mapsto B_{\delta_i(j),\delta_{w_i}(w_j)}$ is a color-preserving bijection.*

3. *Order the bounding boxes of* $\Gamma[e,w]$ *according to the row of their northwest corner. Then* β *also preserves this ordering.*

Proof. Let α_a denote the inverse of δ_a, so that w sends $\alpha_i(j)$ to $\alpha_{u_i}(w_j)$ (since (i, w_i) is a non-corner, $i, w_i \neq n$ and this is well-defined). Note that δ_a and α_a are order-preserving. Let $\delta := \delta_i \times \delta_{w_i}$ and $\alpha := \alpha_i \times \alpha_{w_i}$.

We first show that δ is a bijection from the non-corner pairs (j, w_j) of $\Gamma[e,w]$ with $j \neq i$ to the non-corner pairs (k, u_k) of $\Gamma[e,u]$. Recall that (j, w_j) is a non-corner of $\Gamma[e,w]$ if and only if (j, w_j) is sandwiched by an inversion of w. Moreover, every non-corner pair (j, w_j) is sandwiched by an inversion $\langle k, l\rangle$ where (k, w_k) and (l, w_l) are corners of $\Gamma[e,w]$. Indeed, choose the smallest k such that $\langle k, j\rangle$ is an inversion and the largest l such that $\langle j, l\rangle$ is an inversion. Then (k, w_k) and (l, w_l) are both corners.

Let $j \neq i$ and suppose (j, w_j) is sandwiched by an inversion $\langle k, l\rangle$ of w. We can choose k, l so that (k, w_k) and (l, w_l) are corners of $\Gamma[e,w]$; in particular, neither is equal to i. Because δ_a is order-preserving, $\langle \delta_i(k), \delta_i(l)\rangle$ is an inversion of u and sandwiches $\delta(j, w_j)$. Similarly, if (j, u_j) is sandwiched by an inversion $\langle k, l\rangle$ of u, then $\alpha(j, u_j)$ is sandwiched by the inversion $\langle \alpha_i(k), \alpha_i(l)\rangle$ of w. As δ and α are inverses, we are done.

This also implies that δ is a bijection from the corner pairs (j, w_j) of $\Gamma[e,w]$ to the corner pairs (k, u_k) of $\Gamma[e,u]$.

Next, we show that δ respects containment of spans for corner pairs of w.

Suppose $\sigma(k, w_k)$ is contained in $\sigma(j, w_j)$ and both pairs are corners of $\Gamma[e,w]$. We may assume that $k \neq j$ (otherwise, δ clearly respects containment of spans) and that $j < w_j$ (otherwise, we can consider instead w^{-1}, which avoids 3412 also, and u^{-1}). By assumption, $k, w_k \in [j, w_j]$, so $\delta_i(k)$ and $\delta_{w_i}(w_k)$ are in $[j-1, w_j]$. We have

$$\sigma(\delta_i(j), \delta_{w_i}(w_j)) = \begin{cases} [j, w_j] & \text{if } j < i, w_j < w_i \qquad \text{(Case I)} \\ [j, w_j - 1] & \text{if } j < i, w_j > w_i \qquad \text{(Case II)} \\ [j-1, w_j] & \text{if } j > i, w_j < w_i \qquad \text{(Case III)} \\ [j-1, w_j-1] & \text{if } j > i, w_j > w_i. \qquad \text{(Case IV)} \end{cases}$$

Case I: The only way $\sigma(\delta(j, w_j))$ could fail to contain $\sigma(\delta(k, w_k))$ here is if $j - 1 \in \{\delta_i(k), \delta_{w_i}(w_k)\}$. If $j - 1 = \delta_i(k)$, then $k = j$, a contradiction. If $j - 1 = \delta_{w_i}(w_k)$, then $w_k = j$ and $w_k > w_i$. But $w_k < w_j$ and $w_j < w_i$ by assumption, so we reach a contradiction.

Case II: The only way $\sigma(\delta(j, w_j))$ could fail to contain $\sigma(\delta(k, w_k))$ here is if $j-1$ or w_j is in $\{\delta_i(k), \delta_{w_i}(w_k)\}$. We will show that w_j is not in $\{\delta_i(k), \delta_{w_i}(w_k)\}$ by contradiction; the other case is similar.

Suppose $w_j \in \{\delta_i(k), \delta_{w_i}(w_k)\}$. Since $w_k < w_j$, we must have $w_j = \delta_i(k)$, which means $k = w_j$ and $k < i$. Notice that $\langle j, k\rangle$ is an inversion of w, as is $\langle j, i\rangle$. Since (k, w_k) is not sandwiched by any inversions of w, we must have $w_k < w_i$. To summarize, $j < k < i$ and $w_k < w_i < w_j$. This means $w_j w_k w_i$ form a 312 pattern in w.

Note that w cannot have any inversions $\langle a, j\rangle$ or $\langle k, a\rangle$, since this would result in (j, w_j) or (k, w_k), respectively, being sandwiched by an inversion. We further claim that if a forms an inversion with k and i, then it must also form an inversion with j. Indeed, if a forms an inversion with k and i, then $a < k < i$ and $w_a > w_i > w_k$. If $j < a$ and $w_j < w_a$, then $w_j w_a w_k w_i$ form a 3412 pattern; similarly if $j > a$ and $w_j > w_a$.

Consider $a < j$. From above, we know that $\langle a, j\rangle$ is not an inversion. If $w_a > w_i$, then $\langle a, i\rangle$ and $\langle a, k\rangle$ are both inversions. This combination is impossible, so $w[j-1] \subseteq [w_i-1]$. Also, any $a \in [j+1, k-1]$ with $w_a > k$ forms an inversion with k and i but not j, which is impossible. So $w[j+1, k-1] \subseteq [k]$. Since $w_j = k$ and $w_k < w_i < k$, we conclude $w[k] = [k]$. But $i > k$ and $w_i < k$, a contradiction.

Case III: The span of $\delta(k, w_k)$ is contained in $[j-1, w_j]$ by assumption.

Case IV: The only way $\sigma(\delta(j, w_j))$ could fail to contain $\sigma(\delta(k, w_k))$ here is if $w_j \in \{\delta_i(k), \delta_{w_i}(w_k)\}$. The argument that this cannot happen is similar to Case I; we leave it to the reader.

Finally, we will show that α respects span containment for corner pairs of u. This completes the proof of *(1)*: suppose that (j, w_j) is a spanning corner of $\Gamma[e, w]$ and $\sigma(\delta(j, w_j)) \subseteq \sigma((a, u_a))$ for a spanning corner (a, u_a). Note that $\delta(j, w_j)$ is a corner. Since α respects span containment for corners, $\sigma(j, w_j) \subseteq \sigma(\alpha(a, u_a))$. By maximality of $\sigma(j, w_j)$, we have $\sigma(j, w_j) = \sigma(\alpha(a, u_a))$. In particular, $\sigma(\alpha(a, u_a)) \subseteq \sigma(j, w_j)$, so since δ preserves span containment for corners, the span of (a, u_a) is contained in the span of $\delta(j, w_j)$. So $\delta(j, w_j)$ is a spanning corner of $\Gamma[e, u]$. Reversing the roles of w and u in the above argument shows that $\alpha(j, u_j)$ is a spanning corner of $\Gamma[e, w]$ if (j, u_j) is a spanning corner of $\Gamma[e, u]$. So δ is a bijection between the spanning corners of $\Gamma[e, w]$

and the spanning corners of $\Gamma[e,u]$.

Suppose $\sigma(k,u_k)$ is contained in $\sigma(j,u_j)$ and both pairs are corners of $\Gamma[e,u]$. Again, we may assume that $k \neq j$ (otherwise, δ clearly respects containment of spans) and that $j < u_j$ (otherwise, consider instead w^{-1}, which avoids 3412, and u^{-1}). By assumption, $k, u_k \in [j, u_j]$, so $\alpha_i(k)$ and $\alpha_{w_i}(u_k)$ are in $[j, u_j+1]$. We have

$$\sigma(\alpha_i(j), \alpha_{w_i}(u_j)) = \begin{cases} [j, u_j] & \text{if } j < i, u_j < w_i & \text{(Case I')} \\ [j, u_j+1] & \text{if } j < i, u_j \geq w_i & \text{(Case II')} \\ [j+1, u_j] & \text{if } j \geq i, u_j < w_i & \text{(Case III')} \\ [j+1, u_j+1] & \text{if } j \geq i, u_j \geq w_i. & \text{(Case IV')} \end{cases}$$

Case I': The only way $\sigma(\alpha(k,u_k))$ could fail to be contained in $\sigma(\alpha(j,u_j))$ is if $u_j + 1 \in \{\alpha_i(k), \alpha_{w_i}(u_k)\}$. Suppose that this occurs. Since $u_k < u_j$, we must have $k = u_j$ and $k \geq i$. Also, $u_k < u_j < w_i$. So $\alpha(k,u_k) = (k+1, u_k)$ and $\alpha(j,u_j) = (j,u_j)$. To summarize, we have $j < i < k+1$ and $w_{k+1} < w_j < w_i$. So $w_j w_i w_{k+1}$ form a 231 pattern.

Because $(k+1, w_k)$ and (j, w_j) are corners and are not sandwiched by any inversions, w has no inversions of the form $\langle a, j\rangle$ or $\langle k+1, a\rangle$. Also, any a forming an inversion with i and $k+1$ but not j would give rise to a 3412 pattern, so no such a exist.

Consider $a > k+1$. If $w_a < w_j$, then a would either form an inversion with $k+1$, which is impossible, or a would form an inversion with both i and j but not $k+1$, which is also impossible. So $w[k+2,n] \subseteq [w_j, n]$. Since $j < k+2$ and $w_j = k$, in fact $w[k+2,n] \subseteq [k+1,n]$. Notice that $w_i \geq k+1$ and $i < k+1$, so we can refine this further to $w[k+2,n] = [k+1,n] \setminus \{w_i\}$. But (i, w_i) is sandwiched be some inversion $\langle a, b\rangle$, so $a < i < k+1$ and $w_a > w_i \geq k+1$. This is clearly a contradiction.

Case II': By assumption, $\sigma(\alpha(k,u_k)) \subseteq [j, u_j+1]$, so the claim is true.

Case III': The only way $\sigma(\alpha(k,u_k))$ could fail to be contained in $\sigma(\alpha(j,u_j))$ is if j or u_j+1 were in $\{\alpha_i(k), \alpha_{w_i}(u_k)\}$. Suppose that $j \in \{\alpha_i(k), \alpha_{w_i}(u_k)\}$. Since $k > j$, this means $u_k = j = \alpha_{w_i}(u_k)$ and $w_i > u_k$. So $\alpha(k,u_k) = (k+1, u_k)$ and we have $i < j+1 < k+1$ and $w_{k+1} < w_{j+1} < w_i$. This means that $(j+1, w_{j+1})$ is sandwiched by the inversion $\langle i, k+1\rangle$, a contradiction. The other case is similar.

Case IV': The only way $\sigma(\alpha(k, u_k))$ could fail to be contained in $\sigma(\alpha(j, u_j))$ is if $j \in \{\alpha_i(k), \alpha_{w_i}(u_k)\}$. This is similar to Case I', so we leave it to the reader.

For *(2)*: The map

$$\beta : \{B_{j,w_j} : (j, w_j) \in \overline{S}_w\} \to \{B_{k,u_k} : k = 1, \ldots, n\}$$
$$B_{j,w_j} \mapsto B_{\delta_i(j),\delta_{w_i}(w_j)}$$

is well-defined and injective because α and δ preserve span containment (for corners) and thus also preserve equality of spans (for corners). So $B_{\delta_i(j),\delta_{w_i}(w_j)} = B_{\delta_i(k),\delta_{w_i}(w_k)}$ if and only if $B_{j,w_j} = B_{k,w_k}$. Its image is the bounding boxes of $\Gamma[e, u]$, since δ is a bijection between spanning corners of $\Gamma[e, w]$ and spanning corners of $\Gamma[e, u]$.

We will show β preserves the colors of the boxes by contradiction. Suppose the color of $\beta(B_{j,w_j})$ differs from the color of B_{j,w_j}. This situation means that the relative order of j, w_j must be different from that of $\delta_i(j), \delta_{w_i}(w_j)$. This can only happen if $\min(j, w_j)$ is not shifted down by δ_a (for the appropriate $a \in \{i, w_i\}$), $\max(j, w_j)$ is shifted down by δ_b (for $b \in \{i, w_i\} \setminus \{a\}$) and $|j - w_j| \leq 1$. That is, $\min(j, w_j) < a$ and $\max(j, w_j) > b$. If $j = w_j$, this implies (j, w_j) is spanned by (i, w_i), a contradiction. Otherwise, this implies (i, w_i) is spanned by (j, w_j). Because $|j - w_j| = 1$, the only possibility for this is that $i = w_j$ and $w_i = j$, so the spans are equal. But (j, w_j) is a corner and (i, w_i) is not, a contradiction.

This means β sends green bounding boxes to green bounding boxes, blue to blue, and red to red. It also sends purple to purple: suppose (j, w_j) is a spanning corner and B_{j,w_j} is purple. Then (w_j, j) is also a spanning corner of $\Gamma[e, w]$ and is not equal to (j, w_j). Since the span of (j, w_j) and (w_j, j) are the same, the span of $\delta(j, w_j)$ and $\delta(w_j, j)$ are the same; since δ is a bijection on spanning corners, $\delta(j, w_j) \neq \delta(w_j, j)$. So $B_{\delta(j,w_j)} = B_{\delta(w_j,j)}$ and this bounding box is both red and blue.

For *(3)*: Suppose B_{j,w_j} and B_{k,w_k} are two bounding boxes of $\Gamma[e, w]$ and B_{j,w_j} precedes B_{k,w_k} in the order given. That is, $\min(j, w_j) < \min(k, w_k)$. Suppose for the sake of contradiction that $\min(\delta_i(j), \delta_{w_i}(j)) \geq \min(\delta_i(k), \delta_{w_i}(k))$. In fact, because δ_a shifts numbers by at most 1, the only possibility is that $\min(\delta_i(j), \delta_{w_i}(j)) = \min(\delta_i(k), \delta_{w_i}(k))$.

Since $\delta(j, w_j)$ and $\delta(k, w_k)$ are both spanning corners of $\Gamma[e, u]$ and thus have maximal span, this implies that the span of $\delta(j, w_j)$ is equal to the span of $\delta(k, w_k)$. So $B_{\delta(j,w_j)} = B_{\delta(k,w_k)}$. Since β is a bijection, this implies $B_{j,w_j} = B_{k,w_k}$, a contradiction. □

Proposition 2.7.8 follows as a corollary.

Proof. (of Proposition 2.7.8) Note that no bounding boxes of $\Gamma[e, w]$ are green, since this would imply w is contained in some maximal parabolic subgroup.

Repeatedly apply the operation of Proposition 2.7.12 to w until you arrive at a permutation u with no non-corner pairs.

The permutation u will avoid 3412. Indeed, tne-line notation for u can be obtained from w by repeatedly deleting some number a and applying δ_a to the remaining numbers. Since δ_a preserves order, any occurrence of 3412 in u would imply an occurrence of 3412 in w. It will also avoid 321, since if $u_i u_j u_k$ form a 321 pattern, (j, w_j) is sandwiched by the inversion $\langle i, k\rangle$ and thus is a non-corner pair.

By Proposition 2.7.11, no bounding boxes of $\Gamma[e, u]$ are purple and they alternate between red and blue (when ordered by the row of the northwest corner). Proposition 2.7.12 implies that the bounding boxes of $\Gamma[e, w]$ are in bijection with the bounding boxes of $\Gamma[e, u]$ and that this bijection preserves the coloring and ordering of the bounding boxes. So no bounding boxes of $\Gamma[e, w]$ are purple, and they alternate between red and blue. □

We now are ready to prove Proposition 2.6.12.

Proof. (of Proposition 2.6.12) Since v avoids 2143, $w_0 v$ avoids 3412. By assumption, $w_0 v$ is not contained in a maximal parabolic subgroup, so by Proposition 2.7.8, the bounding boxes of $\Gamma[e, w_0 v]$ alternate in color between red and blue (and none are purple) when ordered by the row of their northeast corner. By Remark 2.7.6, reversing the columns of these bounding boxes gives the bounding boxes of $\Gamma[v, w_0]$, now ordered according to the row of their northwest color. Since the bounding boxes of $\Gamma[v, w_0]$ have the same color as the corresponding bounding boxes of $\Gamma[e, w_0 v]$, the proposition follows. □

2.8 Proof of Proposition 2.6.14

We apply a similar technique as in the above section. Rather than proving Proposition 2.6.14 directly, we instead prove the following:

Proposition 2.8.1. *Let $w \in S_n$ be 4231- and 3412-avoiding, and choose $i \in [n]$. Let $u \in S_{n-1}$ be the permutation obtained from w by deleting w_i from w in one-line notation and shifting appropriately (that is, $u : \delta_i(j) \mapsto \delta_{w_i}(w_j)$). Then*

$$\det(M|_{\Gamma[e,u]}) = \det(M|_{\Gamma[e,w]_i^{w_i}}). \tag{2.7}$$

We prove this using a sequence of lemmas.

Lemma 2.8.2. *Let $w \in S_n$ be 3412-avoiding. Let (i, w_i) be a spanning corner, and let $q = \min(i, w_i)$. Let $N := \{j \in [n] : j, i$ form an inversion of $w\} \cup \{i\}$. Say $N = \{k_1, \ldots, k_m\}$ and let $\rho : w(N) \to [m]$ be the unique order-preserving bijection between the two sets. Let u be the permutation of $[m]$ whose one line notation is $\rho(w_{k_1})\rho(w_{k_2}) \cdots \rho(w_{k_m})$. Then $B_{i,w_i} \cap \Gamma[e, w] = \{(r, c) : (r, c) - (q - 1, q - 1) \in \Gamma[e, u]\}$.*

Example 2.8.3. Let $w = 3472165$ (see Figure 2.6 for a picture of $\Gamma[e, w]$). Choose the spanning wire $(3, 7)$. Then $N = \{3, 4, 5, 6, 7\}$ and $u = 52143$. The graph $\Gamma[e, u]$ is pictured below.

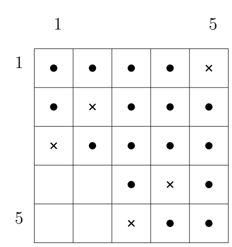

The part of $\Gamma[e, w]$ that lies in $B_{3,7}$ is identical to $\Gamma[e, u]$ (up to translation along the diagonal).

Proof. (of Lemma 2.8.2) We may assume $i < w_i$, so B_{i,w_i} is blue; otherwise, we can consider w^{-1}, which will still avoid 3412, u^{-1}, which can be obtained from w^{-1} by the same procedure as u is obtained from w, and the bounding box $B_{w_i,i}$, which is blue. The intersection $\Gamma[e, w^{-1}] \cap B_{w_i,i}$ is simply the transpose of $B_{i,w_i} \cap \Gamma[e, w]$.

We may also assume that w is not contained in a maximal parabolic subgroup of S_n. (If it were, we could consider just the block of $\Gamma[e,w]$ containing (i,w_i) and argue just about that block.) We may further assume that $\Gamma[e,w]$ has more than one bounding box. By Proposition 2.7.8, the bounding boxes of $\Gamma[e,w]$ alternate between blue and red, and none are green or purple.

Notice that N is contained in $[i,n]$, since if $\langle j,i\rangle$ were an inversion of w, (j,w_j) would span (i,w_i). So $k_1 = i$, and $u_1 = \rho(w_i)$. Because ρ is order preserving, $\langle 1,k\rangle$ is an inversion of u for all $k \in [m]$, which implies $\rho(w_i) = m$.

We have $j \in N$ precisely when (j,w_j) lies southwest of (i,w_i) in the plane, since there are no (j,w_j) to the northeast. To obtain $\Gamma(u)$ from $\Gamma(w)$, delete all rows and columns of the $n \times n$ grid which have a cross to the north or east of B_{i,w_i} (that is, a cross (j,w_j) with $j < i$ or $w_j > w_i$) and renumber remaining rows and columns with $[m]$. Note that $|i-w_i| = |1-m|$ because for every row above i that is deleted, a column to the left of w_i is deleted. So B_{i,w_i} is an $m \times m$ square, which we can identify with the $m \times m$ square containing $\Gamma[e,u]$ by relabeling rows and columns. Also, these deletions take the corners (resp. non-corners) of $\Gamma[e,w]$ with $j \in N$ to corners (resp. non-corners) of $\Gamma[e,u]$.

Thus, it suffices to check the following: if $(r,c) \in B_{i,w_i}$ is sandwiched by an inversion $\langle i,j\rangle$, where (j,w_j) is a corner of $\Gamma[e,w]$, then the corresponding square of $\Gamma[e,u]$ is sandwiched by an inversion of u.

First, let B_{a,w_a} and B_{b,w_b} be the red bounding boxes immediately preceding and following B_{i,w_i}, respectively, in the usual order on bounding boxes. If $\langle i,j\rangle$ is an inversion of w, then $(j,w_j) \in B_{a,w_a} \cup B_{i,w_i} \cup B_{b,w_b}$. Indeed, suppose (j,w_j) is a corner such that $\langle i,j\rangle$ is an inversion, and $(j,w_j) \notin B_{a,w_a} \cup B_{i,w_i} \cup B_{b,w_b}$. Then either $w_j < w_a$ or $j > b$; otherwise (j,w_j) would not be in the union of bounding boxes for w, a contradiction of Lemma 2.7.4. If $j > b$, then there is a blue bounding box B_{d,w_d} immediately following B_{b,w_b} in the usual order of bounding boxes. One can check that $i < d < b < j$ and $w_i w_d w_b w_j$ forms a 3412 pattern. If $w_j < w_a$, there is a blue bounding box B_{d,w_d} immediately preceding B_{a,w_a}, and one can check that $d < i < j < a$ and $w_d w_i w_j w_a$ forms a 3412 pattern. If (j,w_j) is not a corner but $\langle i,j\rangle$ is an inversion, then (j,w_j) is sandwiched by an inversion $\langle i,k\rangle$ where k is a corner, so (j,w_j) is also in the union of the three bounding boxes.

This implies that if $\langle i,j\rangle$ is an inversion of w such that (j,w_j) is a corner, then either $(j,w_j)\in B_{i,w_i}$ or $j\in\{a,b\}$. So either $w_i\geq j$ or $i\leq w_j$.

Suppose $w_i\geq j$ (so (j,w_j) is either in B_{i,w_i} or $j=a$). We claim no rows between i and j are deleted. Indeed, a row between i and j is deleted only if there is a dot (k,w_k) to the east of B_{i,w_i} with $i<k<j$. Necessarily, $w_k>w_i$. If there is a dot to the east of B_{i,w_i}, then B_{i,w_i} is not the last bounding box. By Proposition 2.7.8, the following bounding box B_{s,w_s} is red. One can check that $w_iw_kw_jw_s$ is a 3412 pattern, a contradiction. By a similar argument, if (j,w_j) is a corner such that $\langle i,j\rangle$ is an inversion of w, and $i\leq w_j$ (so (j,w_j) is either in B_{i,w_i} or $j=b$), then no column between w_j and w_i is deleted.

Now, if a corner (j,w_j) is in B_{i,w_i}, then $i\leq w_j$ and $w_i\geq j$, so the relative position of (i,w_i) and (j,w_j) is the same as the relative position of the images of (i,w_i) and (j,w_j) after deletion. So if $(a,b)\in B_{i,w_i}$ is sandwiched by $\langle i,j\rangle$, the corresponding square in $\Gamma[e,u]$ is sandwiched by the image of $\langle i,j\rangle$.

If $j=a$ (resp. $j=b$), then $\rho(w_j)=1$ (resp. $j=k_m$). That is, the image of (j,w_j) after deletion is $(j,1)$ (resp. (m,w_j)). This is because (j,w_j) is the west-most (resp. south-most) cross forming an inversion with (i,w_i). So if $(a,b)\in B_{i,w_i}$ is sandwiched by $\langle i,j\rangle$, the corresponding square in $\Gamma[e,u]$ is sandwiched by the image of $\langle i,j\rangle$.

□

From Lemma 2.8.2, we can derive the following.

Lemma 2.8.4. *Let $w\in S_n$ be 3412-avoiding, and let (i,w_i) be a spanning corner. Suppose $(r,c)\notin B_{i,w_i}$ is sandwiched by an inversion involving i. Then (r,c) is also sandwiched by some inversion $\langle a,b\rangle$ where neither (a,w_a) nor (b,w_b) are in B_{i,w_i}.*

Proof. We will assume that B_{i,w_i} is blue; otherwise, we consider w^{-1} instead. We also assume that $w\in S_n$ is not contained in any parabolic subgroup; if it were, $\Gamma[e,w]$ is block-diagonal and we can argue for each block individually. The lemma is vacuously true if $\Gamma[e,w]$ has a single box, so we may assume it does not. By Proposition 2.7.8, the bounding boxes of $\Gamma[e,w]$ alternate between red and blue, and none are purple.

Suppose B_{a,w_a} and B_{b,w_b} are the (red) bounding boxes immediately preceding and following B_{i,w_i}, respectively. As in Lemma 2.8.2, if j forms an inversion with i, then $(j,w_j)\in B_{a,w_a}\cup B_{i,w_i}\cup B_{b,w_b}$.

This implies that the positions (r, c) satisfying the conditions of the lemma are contained $B_{a,w_a} \cup B_{b,w_b}$. The positions $(r, c) \subseteq B_{a,w_a}$ satisfying the conditions of the lemma are exactly those with $w_a \leq c < i$ and $i \leq r \leq a$. By Lemma 2.8.2, $\Gamma[e, w] \cap B_{a,w_a}$ is the graph of another interval $[e, u]$ where $u \in S_m$; since B_{a,w_a} is red, u sends m to 1. This means that u is greater than the permutation $23 \cdots m1$. In particular, this means that positions $(q, q + 1)$ for $q = 1, \ldots, m - 1$ are in $\Gamma[e, u]$, so the upper off-diagonal of B_{a,w_a} is in $\Gamma[e, w]$. Thus, $(i - 1, i)$ is sandwiched by some inversion of w, implying there is a dot (j, w_j) northeast of $(i - 1, i)$. This dot is necessarily not in B_{i,w_i}, and the inversion (j, a) sandwiches all of the positions $(r, c) \subseteq B_{a,w_a}$ satisfying the conditions of the lemma.

The argument for the positions $(r, c) \subseteq B_{b,w_b}$ satisfying the conditions of the lemma is essentially the same. □

We can now prove Proposition 2.8.1.

Proof of Proposition 2.8.1. Let $D = \Gamma[e, w]_i^{w_i}$.

Consider $\Gamma[e, w]$ drawn in an $n \times n$ grid with the positions (j, w_j) marked with crosses and all others marked with dots. Recall that D is the collection of crosses and dots obtained from $\Gamma[e, w]$ by deleting row i and column w_i and renumbering rows by δ_i and columns by δ_{w_i}. Note that the crosses of D are in positions (j, u_j).

If (i, w_i) was an internal dot of $\Gamma[e, w]$, then all dots in D are sandwiched by an inversion of u, so $D = \Gamma[e, u]$. In this case, $M|_D = M|_{\Gamma[e,u]}$, so the determinants are equal.

If (i, w_i) is a corner but not a spanning corner of $\Gamma[e, w]$, we claim we again have $D = \Gamma[e, u]$. Suppose (i, w_i) is contained in a blue bounding box B_{k,w_k} (if it is only contained in a red bounding box, we can consider w^{-1} and the transpose of M instead). Notice that since (i, w_i) is a corner, we only have inversions $\langle r, i\rangle$ with $r < i$. Further, there are no inversions $\langle r, i\rangle$ where $r < k$ or $w_r > w_k$; otherwise, we can find an occurrence of 3412. For example, if there were an inversion $\langle r, i\rangle$ with $r < k$, then there must be a red bounding box B_{a,w_a} immediately preceding B_{k,w_k} which overlaps with it. One can check that $r < k < a < i$ and $w_r w_k w_a w_i$ is an occurrence of 3412. A similar argument works for the $w_r > w_k$ case. Thus, if $\langle r, i\rangle$ is an inversion, $\langle k, r\rangle$ is an inversion as well, so every dot sandwiched by an inversion (r, i) is also sandwiched by the inversion (k,i).

In particular, there are no crosses above or to the right of the rectangle with corners (k,w_k) and (i,w_i), since any such cross would be inversions $\langle r,i\rangle$ where $\langle k,r\rangle$ is not an inversion. There are also no crosses northeast of (k,w_k), since such a cross would span (k,w_k). This means there are no dots above or to the right of the rectangle with corners (k,w_k) and (i,w_i). So in fact it suffices to show that all dots in the rectangle with corners (k,w_k) and $(i-1,w_i+1)$ are sandwiched by an inversion of v that does not involve i; that inversion will correspond to an inversion in u. If $w_{i-1} < w_i$ or if $w^{-1}(w_i+1) > i$, this is true. Otherwise, we have that $(i-1,w_{i-1})$ and $(w^{-1}(w_i+1),w_i+1)$ both lie in the rectangle with corners (k,w_k) and $(i-1,w_i+1)$. If these points are distinct, then $w_{i-1} > w_i+1$, so $w_k\ w_i+1\ w_{i-1}\ w_i$ form a 4231 pattern, which is impossible. So we must have $w_{i-1}w_i+1$, which means all points in the rectangle with corners $(k,w_k),(i-1,w_i+1)$ are sandwiched by the inversion $\langle k,i-1\rangle$.

Now, suppose (i,w_i) is a spanning strand and B_{i,w_i} is blue (if it is red, we can consider w^{-1} and the transpose of M instead). If $w_{i+1} = w_i - 1$, we again have $A = B$. If not, then the D is not equal to $\Gamma[e,u]$; $D = \Gamma[e,u] \sqcup \{(r,c) : (r,c)$ sandwiched only by inversions involving $i\}$. We will show that if (r,c) is sandwiched only by inversions involving i, then $m_{r,c}$ will not appear in $\det(M|_D)$. This will imply that $\det(M|_D)$ agrees with $\det(M|_{\Gamma[e,u]})$ for all $(n-1)\times(n-1)$ matrices M.

Let $I := \{(r,c) : (r,c)$ sandwiched only by inversions involving $i\}$. By Lemma 2.8.4, $I \subseteq B_{i,w_i}$. We would like to show that D is block-upper triangular, and that all $(r,c) \in I$ are in blocks that are not on the main diagonal. This would imply that $\det(M|_D)$, as claimed, does not contain $m_{r,c}$, as it is the product of the determinants of the blocks on the diagonal. To verify this, we just need to show that $D \cap B_{i,w_i}$ is block-upper triangular and for all $(r,c) \in I \cap B_{i,w_i}$, (r,c) is in a block that is not on the main diagonal. By Lemma 2.8.2, $\Gamma[e,w] \cap B_{i,w_i}$ is another $\Gamma[e,x]$. So $D \cap B_{i,w_i}$ is simply $\Gamma[e,x]$ with the first row and last column removed. Thus, it suffices to prove the following lemma.

Lemma 2.8.5. *Let $x \in S_m$ be 4231 avoiding. Suppose $x_1 = m$ and $x_2 \neq m-1$. Let Q be the region obtained by removing the first row and last column of $\Gamma[e,x]$. Then Q is block-upper triangular, and for all positions (r,c) sandwiched only by inversions involving 1, (r,c) is in a block not on the main diagonal.*

Proof. First, recall that $\Gamma[e, x]$ contains the lower off-diagonal $\{(j, j-1) : j = 2, \ldots, m\}$, since $x > m123 \cdots (m-1)$.

Call a dot (i, x_i) *leading* if it is not southwest of any (j, x_j) besides $(1, m)$. (For example, in Example 2.8.3, the leading dots of $\Gamma[e, u]$ are $(2, 2)$ and $(4, 4)$.) We claim that for each leading dot (i, x_i), position $(x_i + 2, x_i)$ is not sandwiched by an inversion of x.

We show this first for the northmost leading dot $(2, w_2)$. Notice that there cannot be any (j, x_j) with $2 < j \leq x_2 + 1$ and $x_j > x_2$; in this case, avoiding 4231 would imply that (j, x_2) is not sandwiched by any inversion, which would in turn imply that $(x_2 + 1, x_2)$ is not sandwiched by any inversion. But the lower off-diagonal is contained in $\Gamma[e, x]$, so this is a contradiction. This means that for all $2 < j \leq x_2 + 1$, (j, x_j) is contained in the square with opposing corners $(2, 1)$ and $(x_2 + 1, x_2)$. In particular, there is a dot (j, x_j) in every row and every column of this square. So for $j > x_2 + 1$, we have $x_j > x_2$, which implies $(x_2 + 2, x_2)$ is not sandwiched by an inversion of x. In other words, there are no elements of $\Gamma[e, x]$ in columns $1, \ldots, x_2$ and rows $x_2 + 2, \ldots, m$. This implies that Q is block-upper triangular, and the first diagonal block has northwest corner $(2, w_2)$.

Note that the next leading dot is in row $i_2 := x_2 + 2$. We can repeat the above argument with this dot to reach the analogous conclusion: the second block of Q has northwest corner (i_2, x_{i_2}). We can continue with the remaining leading dots to see that Q is block-upper triangular with northwest corners of each diagonal block given by the leading dots.

Notice that the union of the diagonal blocks contains every position (r, c) sandwiched by an inversion not involving 1. Thus, the complement of the union of diagonal blocks in Q is exactly the positions (r, c) which are sandwiched only by an inversion involving 1. This finishes the proof of the lemma. □

□

Finally, we can prove Proposition 2.6.14.

Proof. (of Proposition 2.6.14) Let $w := w_0 v$ and $u := w_0 x$. Notice that $u : \delta_i(j) \mapsto \delta_{w_i}(w_j)$ and that w avoids 3412 and 4231.

It follows from Lemma 2.7.1 that restricting M to $\Gamma[x, w_0]$ is the same as reversing the columns of M, restricting to $\Gamma[e, u]$, and then reversing the columns again. That is

$$M|_{\Gamma[x,w_0]} = (M\overline{w_0}|_{\Gamma[e,u]})\overline{w_0}.$$

Also, note that reversing the columns of $\Gamma[v,w_0]_i^{v_i}$ gives $\Gamma[e,w]_i^{w_i}$. This means that

$$M|_{\Gamma[v,w_0]_i^{v_i}} = [(M\overline{w_0})|_{\Gamma[e,w]_i^{w_i}}]\overline{w_0}.$$

Thus, the proposition follows from taking determinants of both sides of (2.6) and applying Proposition 2.8.1. □

2.9 Pattern Avoidance Conditions

In this section, we investigate restating Theorem 2.4.4 fully in terms of pattern avoidance. That is, we consider pattern avoidance conditions for a permutation v that are equivalent to the condition that $\Gamma[v,w_0]$ has no square of size $k+1$.

Proposition 2.9.1. *If $v \in S_n$ and $\Gamma[v,w_0]$ has no square of size $k+1$, then v avoids* $12...(k+1)$.

Proof. Suppose $i_1 < i_2 < ... < i_{k+1}$ and $v_{i_1} < v_{i_2} < ... < v_{i_{k+1}}$. In other words, $v_{i_1}, v_{i_2}, ..., v_{i_{k+1}}$ is an occurrence of the pattern $12...(k+1)$. Let R be the rectangle with corners at (i_1, v_{i_1}), $(i_1, v_{i_{k+1}})$, $(i_{k+1}, v_{i_{k+1}})$, and (i_{k+1}, v_{i_1}). Notice that R is at least of size $(k+1)\times(k+1)$. For all $(r,c) \in R$, (r,c) is sandwiched by $\langle i_1, i_{k+1}\rangle$, a non-inversion. By Lemma 2.5.4, this means (r,c) is in $\Gamma[v,w_0]$. So, all of R is is in $\Gamma[v,w_0]$ and there is a square of size $k+1$ in $\Gamma[v,w_0]$. □

Notice that this proposition tells us that Theorem 2.4.4 supports Conjecture 2.4.2.

Proposition 2.9.2. *Let $v \in S_n$ avoid 2143. Then $\Gamma[v,w_0]$ has no square of size* 3 *if and only if v avoids* 123*,* 1432*, and* 3214*.*

Proof. We have shown in Proposition 2.9.1 that if v contains 123, then $\Gamma[v,w_0]$ contains a square of size 3. An analogous argument to the proof of Proposition 2.9.1 shows that if v contains 1432 or 3214, then $\Gamma[v,w_0]$ contains a square of size 3.

Now, we assume that $\Gamma[v, w_0]$ contains a square of size 3 and show that v must contain a pattern 123, 1432, or 3214. Let a square of size 3 be located in rows i, $i+1$, $i+2$ and columns j, $j+1$, $j+2$. By Lemma 2.5.4, we know that either (i, j) is in $\Gamma[v, w_0]$ or is sandwiched by $\langle a, b\rangle$, a non-inversion of v. If the former, let $\alpha = i$. If the latter, let $\alpha = a$ (this choice may not be unique). We also know that either $(i+2, j+2)$ is in $\Gamma[v, w_0]$ or is sandwiched by $\langle c, d\rangle$, a non-inversion of v. If the former, let $\beta = i+2$. If the latter, let $\beta = d$ (this choice may also not be unique). Since $\alpha \leq i$ and $\beta \geq j+2$, we have that for any (r, c) in our square, $\alpha \leq r \leq \beta$. Also, since $v_\alpha \leq j$ and $v_\beta \geq j+2$, we know $v_\alpha \leq c \leq v_\beta$. So, every (r, c) in our square is sandwiched by the non-inversion $\langle \alpha, \beta\rangle$.

Consider v_{i+1} and $\ell := v^{-1}(j+1)$. If $v_\alpha < v_{i+1} < v_\beta$, then v has a 123 pattern. Similarly, if $\alpha < \ell < \beta$, then v has a 123 pattern. If $v_{i+1} < v_\alpha < v_\beta$ and $\ell < \alpha < \beta$, then v has a 3214 pattern. If $v_\alpha < v_\beta < v_{i+1}$ and $\alpha < \beta < \ell$, then v has a 1432 pattern. If $v_{i+1} < v_\alpha < v_\beta$ and $\alpha < \beta < \ell$ or if $v_\alpha < v_\beta < v_{i+1}$ and $\ell < \alpha < \beta$, then v has a 2143 pattern, which can't happen. □

We get the following immediate corollary from the above proposition and Theorem 2.4.4:

Corollary 2.9.3. *Let $v \in S_n$ avoid 123, 2143, 1432, and 3214. Then* $\mathrm{Imm}_v(M)$ *is 2-positive.*

However, analogous statements for $k > 2$ are difficult to state. The larger k is, the more patterns need to be avoided in order to mandate hat $\Gamma[v, w_0]$ has no square of size $k+1$. We illustrate with the following example.

Example 2.9.4. In order to guarantee that $\Gamma[v, w_0]$ does not have a square of size 4, v must avoid the following patterns: 1234, 15243, 15342, 12543, 13542, 32415, 42315, 32145, 42135, 165432, 543216.

Due the number of patterns to be avoided, statements analogous to Corollary 2.9.3 for larger k seem unlikely to be useful.

2.10 Future Directions

There are many avenues of further study in this area. Conjecture 2.4.2 is still unresolved. While this conjecture is difficult in the general case, it may be easier to show for the $k = 2$ case. In particular, a formula by Billey-Warrington [BW01] for Kazhdan-Lusztig polynomials for 123-hex-avoiding permutations could prove useful in studying this case.

Our work also suggests that it may be interesting to investigate the signs of determinants of matrices where some rows or columns are duplicated and then certain entries of the matrix are replaced with 0's. As previously mentioned, Skandera [Ska08] showed that all elements of the dual canonical canonical basis of $\mathcal{O}(GL_n(\mathbb{C}))$ can be written as immanants evaluated on matrices with repeated rows and columns. Our Corollary 2.5.6 shows that in the case of 1324- and 2143-avoiding permutations v, $\mathrm{Imm}_v(M)$ can be written as a signed determinant of M with some entries replaced with 0's. If N is a k-positive (or totally positive) matrix and M is obtained from N by repeating some of the rows and columns, then understanding the signs of $\det(M')$, where M' is M with certain entries replaced with 0's, gives information regarding Question 2.3.2.

Another potential tool for tackling this problem is cluster algebras. This will be investigated more fully in Chapter 3.

Chapter 3

Cluster Algebras and k-Positivity

In this section we discuss the relationship between cluster algebras and k-positive matrices. In particular, we look at how these constructions and work done by Chmutov–Jiradilok–Stevens [CJS15] can be applied to determine the positivity of Kazhdan-Lusztig immanants on 2-positive matrices. This gives an alternate proof of Corollary 2.9.3.

3.1 Cluster Algebra Background

Definition 3.1.1. A *quiver* Q is a directed graph with vertices labeled $1, ..., n$ and no loops or 2-cycles.

Definition 3.1.2. If k is a vertex in a quiver Q, a *quiver mutation* at k, $\mu_k(Q)$ is defined from Q as follows:

(1) for each pair of edges $i \to k$ and $k \to j$, add a new edge $i \to j$,

(2) reverse any edges incident to k,

(3) remove any 2-cycles.

We may specify some vertices of a quiver to be *frozen*, meaning we do not allow mutation at those vertices. The other vertices are called *mutable*.

Definition 3.1.3. A *seed* is a pair $(Q, \mathbf{x})$ where Q is a quiver and $\mathbf{x} = (x_1, ..., x_n)$ an n-tuple of algebraically independent expressions with n the number of vertices of Q. In any seed, the n-tuple of variables is called a *cluster* and the elements $x_1, \ldots, x_n$ are the *cluster variables.*

Definition 3.1.4. If k is a mutable vertex in Q, we can define a *seed mutation* of $(Q, \mathbf{x})$ at k, $\mu_k(Q, \mathbf{x}) = (Q', \mathbf{x}')$ by $Q' = \mu_k(Q)$ and $\mathbf{x}' = (x'_1, ..., x'_n)$ where

$$x'_i = \begin{cases} x_i & i \neq k, \\ \prod_{j=1}^n x_j^{\#\{\text{edges } k \to j \text{ in } Q\}} + \prod_{j=1}^n x_j^{\#\{\text{edges } j \to k \text{ in } Q\}} & i = k. \end{cases}$$

Recall that Q has no 2-cycles, so x_j shows up in at most one of the products in the formula for x'_k.

An important property of this mutation relation is that it is subtraction free. This means that if a cluster has all positive cluster variables, then any other cluster variable we get through mutation is also positive.

Definition 3.1.5. If two quivers or two seeds are related by a sequence of mutations, we say they are *mutation equivalent.* For some initial seed $(Q, \mathbf{x})$, let χ be the union of all cluster variables over seeds which are mutation equivalent to $(Q, \mathbf{x})$. Then the *cluster algebra* of rank n over $\mathbb{C}$ associated to this initial seed is $\mathcal{A} = \mathbb{C}[\chi]$.

In this chapter, we will only use the definitions above relating to quivers and x-dynamics. However, we include some definitions regarding y-dynamics here as well as they will be necessary in Chapter 7.

Definition 3.1.6. A *seed with coefficients* is a triple $(Q, \mathbf{x}, \mathbf{y})$ where Q is a quiver, $\mathbf{x} = (x_1, ..., x_n)$, and $\mathbf{y} = (y_1, ..., y_n)$ with n the number of vertices of Q.

Definition 3.1.7. If k is a vertex in Q, we can define a *seed mutation* of $(Q, \mathbf{x}, \mathbf{y})$ at k, $\mu_k(Q, \mathbf{x}, \mathbf{y}) = (Q', \mathbf{x}', \mathbf{y}')$ by $Q' = \mu_k(Q), \mathbf{x}' = (x'_1, ..., x'_n)$, and $\mathbf{y}' = (y'_1, ..., y'_n)$ where

$$x'_i = \begin{cases} x_i & i \neq k, \\ \prod_{j=1}^n x_j^{\#\{\text{edges } k \to j \text{ in } Q\}} + \prod_{j=1}^n x_j^{\#\{\text{edges } j \to k \text{ in } Q\}} & i = k, \end{cases}$$

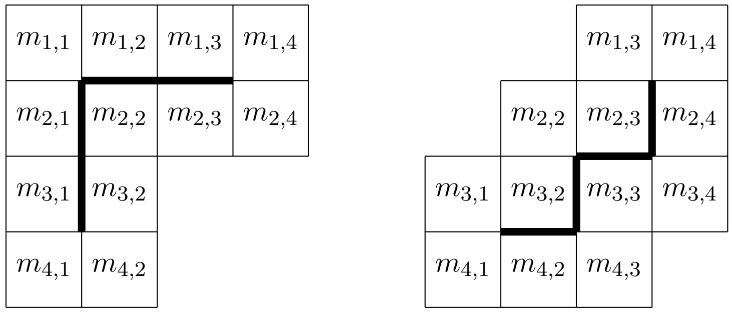

Figure 3.1: The NNEE-DRH (left) and the ENEN-DRH (right).

$$y_i' = \begin{cases} y_k^{-1} & i = k \\ y_i(1+y_k^{-1})^{-\#\{\text{edges } k\to i \text{ in } Q\}} & i \neq k, \#\{\text{edges } k \to i \text{ in } Q\} \geq 0, \\ y_i(1+y_k)^{\#\{\text{edges } i\to k \text{ in } Q\}} & i \neq k, \#\{\text{edges } i \to k \text{ in } Q\} \geq 0. \end{cases}$$

Definition 3.1.8. A *y-seed*, $(Q, \mathbf{y})$ and its mutations are defined as above, but without the $\mathbf{x}$ variables.

Frequently the y-dynamics above will be defined over a semifield that may have a different addition. However, for our purposes, we will use these less general definitions.

3.2 Double Rim Hook Cluster Algebras

In [CJS15], Chmutov, Jiradilok, and Stevens study *double rim hook algebras* as a way to better understand the coordinate ring of the open double Bruhat cell G^{w_0,w_0} of $GL_n(\mathbb{C})$. They give a formula for all cluster variables in a certain subclusteralgebra of this cluster algebra. Their work can be used to partially answer Question 2.3.1 when $k = 2$. We review their formula here.

Definition 3.2.1. Let λ be a finite lattice path in an infinite grid made up of north and east steps. The *λ-array* is the union of all 2×2 squares in the infinite grid with centers at a point on λ. We label the rows and columns of the λ-array in the usual way and then assign the square in row i, column j the value $m_{i,j}$. This is the *λ-DRH* (see Figure 3.1).

We will construct a seed from an λ-DRH. To do this, let the *initial worm* be the path of length $\ell(\lambda)+1$ defined as follows. Begin in the square directly above the farthest

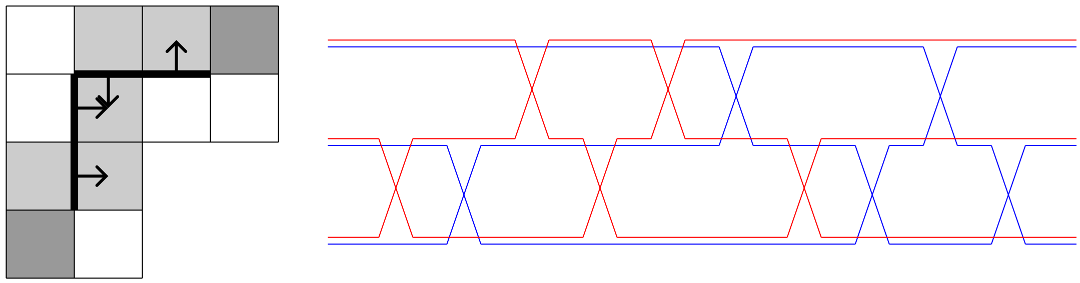

Figure 3.2: A choice of correspondence for the NNEE-DRH and the resulting diagram.

southwest square. Proceed to the right as far as possible, then up as far as possible, then right again, and so on until reaching a square adjacent to the farthest northeast square.

To define the quiver we construct the following diagram. We begin with three pairs of red and blue lines. The area between the bottom and middle pair will be called the *first track* and the area between the top and middle pair will be called the *second track*. First extend the initial worm to the farthest southwest and northeast cells. Define a map ε from steps in λ to cells in the initial worm such that for any step s, $\varepsilon(s)$ is adjacent to s. This map is called a *choice of correspondence*. Travel along the extended initial worm beginning with the farthest southwest cell. At each cell c, if there is a step s in λ such that $\varepsilon(s) = c$, add a crossing in the second track. The crossing should be between red lines if s is a north step and blue lines if s is an east step. If there are multiple steps in λ that map to c under ε, put the crossings for these steps in the order in which the steps occur in λ. Move to the next cell c' in the initial worm. If c' is to the north of c, then add a red crossing in the first track and if c' is to the east of c, add a blue crossing in the first track. Add crossings to the second track based on the steps that map to c' under w and continue this process until reaching the end of the extended initial worm. See Figure 3.2 for an example. These diagrams are very similar to *double wiring diagrams*, which will be introduced in Section 3.4, but in this case wires are allowed to intersect multiple times.

The areas in each track between crossings or at the edge of the diagram are called *chambers*. The chambers will become the vertices of our quiver. Arrows of the quiver are given by the following rules (see Definition 2.4.1 of [FWZ16]): Let c and c' be two chambers, at least one of which is bounded by crossings on both sides. Then there is an arrow $c \to c'$ in the associated quiver if and only if one of the following conditions is met:

(1) the right (resp., left) boundary of c is blue (resp., red), and coincides with the left (resp., right) boundary of c'.

(2) the left boundary of c' is red, the right boundary of c' is blue, and the entire chamber c' lies directly above or directly below c.

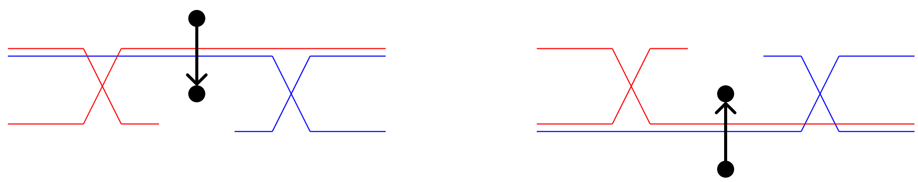

(3) the left boundary of c is blue, the right boundary of c is red, and the entire chamber c lies directly above or directly below c'.

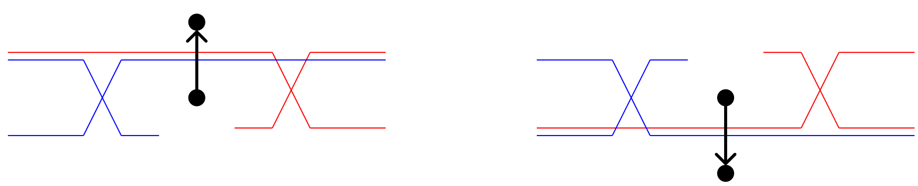

(4) the left (resp., right) boundary of c' is above c and the right (resp., left) boundary of c is below c' and both boundaries are red (resp., blue).

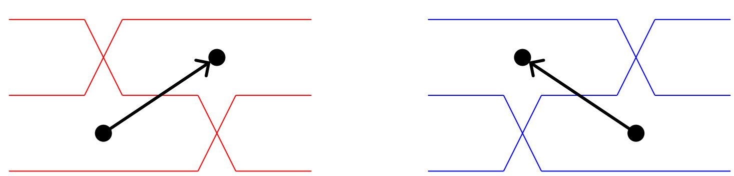

(5) the left (resp., right) boundary of c is above c' and the right (resp., left) boundary of c' is below c and both boundaries are blue (resp., red).

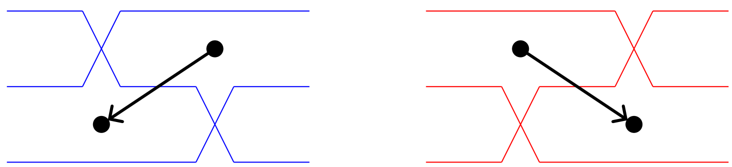

The cluster variables corresponding to the vertices in the first track are given by the variables in the boxes along the extended worm, in order from southwest to northeast. The cluster variables for the vertices in the second track are the the determinants of the connected 2×2 squares in the initial λ-DRH, in order from southwest to northeast. Vertices corresponding to variables in boxes along the (not extended) initial worm are mutable, the rest are frozen. See Figure 3.3 for examples.

Remark 3.2.2. The choice of correspondence is not always unique. However, the process outlined above does uniquely define a quiver. If a step of λ borders both c and c' in a worm, then either the step of λ is a north step and c, c' are side-by-side, or λ is an east step and c, c' are stacked on top of each other. In the first case, changing which cell λ corresponds to slides a red crossing in the second track past a blue crossing in the first track. In the second case, it slides a blue crossing in the second track past a red crossing in the first track. The diagrams obtained from doing these slides do not change the underlying quiver.

In [CJS15], Chmutov, Jiradilok, and Stevens give a formula for all cluster variables in the cluster algebra defined by an initial λ-DRH seed. To state this, we first need some definitions.

Let b_1 be the 2×2 block of the λ-DRH that appears at the first bend of λ, b_2 the 2×2 block that appears at the second bend of λ, and so on. Let f be the 1×2 matrix that appears at the top of the λ-DRH if the last step of λ is N or the 2×1 matrix that appears at the right of the λ-DRH if the last step of λ is E.

Suppose the first step of λ is N. Then let s be 1×2 matrix that appears at the bottom of the initial λ-DRH. Define $sb_1b_2...b_kf$ to be the concatenation of the blocks where b_1 is attached to the top of s, then b_2 is attached to the right of b_1, and the rest of the blocks are alternately added on top and to the right.

Suppose the first step of λ is E. Then let s be 2×1 matrix that appears at the left of the initial λ-DRH. Define $sb_1b_2...b_kf$ to be the concatenation of the blocks where b_1

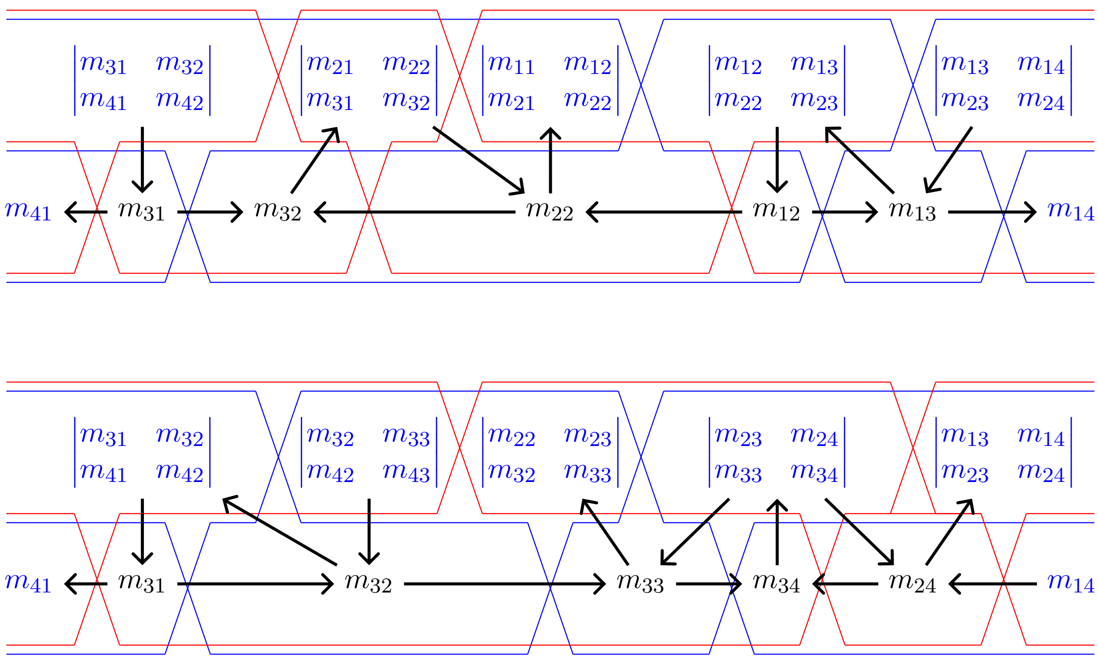

Figure 3.3: The initial NNEE-DRH seed (top) and the initial ENEN-DRH seed (bottom). The seeds are drawn inside the diagrams for clarity. Frozen vertices appear in blue and arrows between them have been removed, as they don't affect the cluster algebra.

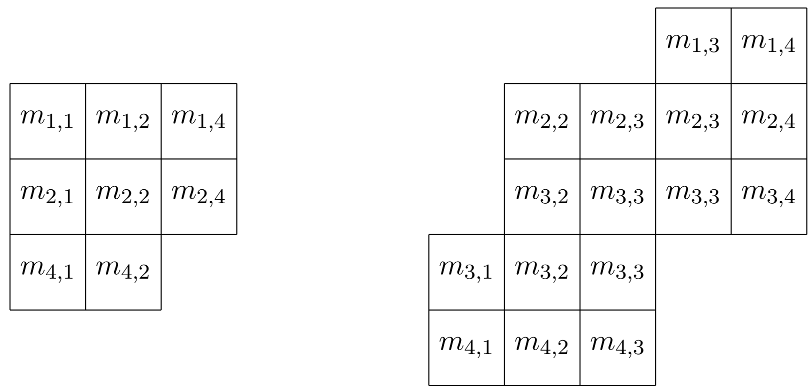

Figure 3.4: The standardization of NNEE (left) and ENEN (right).

is attached to the right of s, then b_2 is attached to the top of b_1, and the rest of the blocks are alternately added to the right and on top.

Definition 3.2.3. Then the standardization of λ is $\mathrm{Std}(\lambda) := sb_1b_2...b_kf$, where $sb_1b_2...b_kf$ is defined as above depending on the first step of λ (see Figure 3.4).

In order to state the main theorem, it is important to note that $\mathrm{Std}(\lambda)$ always has the same number of rows as columns. Because of this, we can think of it as a square matrix where all entries not belonging to the shape $\mathrm{Std}(\lambda)$ are 0. Abusing notation, we will call this matrix $\mathrm{Std}(\lambda)$.

Theorem 3.2.4 ([CJS15])**.** *Consider an initial λ-DRH seed. The mutable cluster variables are all variables inside a cell of the λ-DRH (except for the two that are frozen variables) and all expressions*

$$(-1)^{\frac{(\eta-1)(\eta-2)}{2}} \det(\mathrm{Std}(\mu))$$

where μ ranges over all nonempty connected subwords of λ and $\mathrm{Std}(\mu)$ is an $\eta\times\eta$ matrix.

Example 3.2.5. Let λ be NNEE. We will label the steps $\mathrm{N}^1\mathrm{N}^2\mathrm{E}^3\mathrm{E}^4$ in order to better keep track of the subskeleta. The mutable cluster variables in the cluster algebra generated from the initial λ-DRH seed are as follows:

From N^1: $\begin{vmatrix} m_{2,1} & m_{2,2} \\ m_{4,1} & m_{4,2} \end{vmatrix}$

From N^2: $\begin{vmatrix} m_{1,1} & m_{1,2} \\ m_{3,1} & m_{3,2} \end{vmatrix}$

From E^3: $\begin{vmatrix} m_{1,1} & m_{1,3} \\ m_{2,3} & m_{2,3} \end{vmatrix}$

From E^4: $\begin{vmatrix} m_{1,2} & m_{1,4} \\ m_{2,2} & m_{2,4} \end{vmatrix}$

From N^1N^2: $\begin{vmatrix} m_{1,1} & m_{1,2} \\ m_{4,1} & m_{4,2} \end{vmatrix}$

From N^2E^3: $-\begin{vmatrix} m_{1,1} & m_{1,2} & m_{1,3} \\ m_{2,1} & m_{2,2} & m_{2,3} \\ m_{3,1} & m_{3,2} & 0 \end{vmatrix}$

From E^3E^4: $\begin{vmatrix} m_{1,1} & m_{1,4} \\ m_{2,1} & m_{2,4} \end{vmatrix}$

From $N^1N^2E^3$: $-\begin{vmatrix} m_{1,1} & m_{1,2} & m_{1,3} \\ m_{2,1} & m_{2,2} & m_{2,3} \\ m_{4,1} & m_{4,2} & 0 \end{vmatrix}$

From $N^2E^3E^4$: $-\begin{vmatrix} m_{1,1} & m_{1,2} & m_{1,4} \\ m_{2,1} & m_{2,2} & m_{2,4} \\ m_{3,1} & m_{3,2} & 0 \end{vmatrix}$

From $N^1N^2E^3E^4$: $-\begin{vmatrix} m_{1,1} & m_{1,2} & m_{1,4} \\ m_{2,1} & m_{2,2} & m_{2,4} \\ m_{4,1} & m_{4,2} & 0 \end{vmatrix}$

As well as $m_{1,1}$, $m_{1,2}$, $m_{1,3}$, $m_{2,1}$, $m_{2,2}$, $m_{2,3}$, $m_{2,4}$, $m_{3,1}$, $m_{3,2}$, and $m_{4,2}$.

Example 3.2.6. Let λ be ENEN. We will label the steps $E^1N^2E^3N^4$ in order to better keep track of the subskeleta. The mutable cluster variables in the cluster algebra generated from the initial λ-DRH seed are as follows:

From E^1: $\begin{vmatrix} m_{3,1} & m_{3,3} \\ m_{4,1} & m_{4,3} \end{vmatrix}$

From N^2: $\begin{vmatrix} m_{2,2} & m_{2,3} \\ m_{4,2} & m_{4,3} \end{vmatrix}$

From E^3: $\begin{vmatrix} m_{2,2} & m_{2,4} \\ m_{3,2} & m_{3,4} \end{vmatrix}$

From N^4: $\begin{vmatrix} m_{1,3} & m_{1,4} \\ m_{3,3} & m_{3,4} \end{vmatrix}$

From E^{1}N^2: $-\begin{vmatrix} 0 & m_{2,2} & m_{2,3} \\ m_{3,1} & m_{3,2} & m_{3,3} \\ m_{4,1} & m_{4,2} & m_{4,3} \end{vmatrix}$

From N^{2}E^3: $-\begin{vmatrix} m_{2,2} & m_{2,3} & m_{2,4} \\ m_{3,2} & m_{3,3} & m_{3,4} \\ m_{4,2} & m_{4,3} & 0 \end{vmatrix}$

From E^{3}N^4: $-\begin{vmatrix} 0 & m_{1,3} & m_{1,4} \\ m_{2,2} & m_{2,3} & m_{2,4} \\ m_{3,2} & m_{3,3} & m_{3,4} \end{vmatrix}$

From E^{1}N^{2}E^3: $-\begin{vmatrix} 0 & m_{2,2} & m_{2,3} & m_{2,4} \\ 0 & m_{3,2} & m_{3,3} & m_{3,4} \\ m_{3,1} & m_{3,2} & m_{3,3} & 0 \\ m_{4,1} & m_{4,2} & m_{4,3} & 0 \end{vmatrix}$

From N^{2}E^{3}N^4: $-\begin{vmatrix} 0 & 0 & m_{1,3} & m_{1,4} \\ m_{2,2} & m_{2,3} & m_{2,3} & m_{2,4} \\ m_{3,2} & m_{3,3} & m_{3,3} & m_{3,4} \\ m_{4,2} & m_{4,3} & 0 & 0 \end{vmatrix}$

From E^{1}N^{2}E^{3}N^4: $\begin{vmatrix} 0 & 0 & 0 & m_{1,3} & m_{1,4} \\ 0 & m_{2,2} & m_{2,3} & m_{2,3} & m_{2,4} \\ 0 & m_{3,2} & m_{3,3} & m_{3,3} & m_{3,4} \\ m_{3,1} & m_{3,2} & m_{3,3} & 0 & 0 \\ m_{4,1} & m_{4,2} & m_{4,3} & 0 & 0 \end{vmatrix}$

As well as $m_{1,3},\ m_{2,2},\ m_{2,3},\ m_{2,4},\ m_{3,1},\ m_{3,2},\ m_{3,3},\ m_{3,4},\ m_{4,2}$, and $m_{4,3}$.

3.3 Applications to Kazhdan-Lusztig Immanants

Since all cluster variables in an initial λ-DRH seed are matrix entries or 2×2 minors, we can use Chmutov, Jiradilok, and Stevens' cluster variable formulas to learn about 2-positivity of Kazhdan–Lusztig immanants. In particular, if a Kazhdan–Lusztig immanant has the form of a DRH cluster variable, then we know it is 2-positive.

Definition 3.3.1. We will say the lattice path λ is *standard* if $\mathrm{Std}(\lambda)$ is exactly the λ-DRH.

A standard lattice path λ can constructed by alternately concatenating the paths EN and NE, starting and ending with either. That is, λ can have one of four forms:

(1) ENNEENNE...EN

(2) ENNEENNE...NE

(3) NEENNEEN...EN

(4) NEENNEEN...NE

Proposition 3.3.2. *Let λ be standard and have length $2n-4$. Then $\mathrm{Std}(\lambda) = M|_{\Gamma[v,w_0]}$ where v is one of the following permutations in S_n:*

$$n-1, n-3, n, n-5, n-2, n-7, n-4, ..., 7, 2, 5, 1, 3 \qquad \textit{with } n \textit{ odd}$$

$$n-2, n, n-4, n-1, n-6, n-3, n-8, ..., 7, 2, 5, 1, 3 \qquad \textit{with } n \textit{ even}$$

$$n-1, n-3, n, n-5, n-2, n-7, n-4, ..., 3, 6, 1, 4, 2 \qquad \textit{with } n \textit{ even}$$

$$n-2, n, n-4, n-1, n-6, n-3, n-8, ..., 3, 6, 1, 4, 2 \qquad \textit{with } n \textit{ odd}$$

Proof. The first case corresponds to λ having the shape ENNEENNE...EN, the second to λ having the shape ENNEENNE...NE, the third to λ having the shape NEENNEEN...EN, and the fourth to λ having the shape NEENNEEN...NE. The permutations can be obtained easily from drawing out $\mathrm{Std}(\lambda)$. $\square$

Theorem 3.3.3. *The permutations $v \in S_n$ such that $M|_{\Gamma[v,w_0]} = \mathrm{Std}(\lambda)$ for some standard λ are exactly the permutations $v \in S_n$ such that v is 123-, 2143-, 1432-, and 3214-avoiding and w_0v does not belong to any parabolic subgroup of S_n.*

Proof. First we will assume we have a permutation v such that$M|_{\Gamma[v,w_0]} = \mathrm{Std}(\lambda)$ and prove that v is 123-, 2143-, 1432-, and 3214-avoiding and w_0v does not belong to any parabolic subgroup of S_n.

Since the nonzero entries of $\mathrm{Std}(\lambda)$ are given by a double rim hook, there are no elements of $\Gamma[v, w_0]$ that are completely surrounded by other elements of $\Gamma[v, w_0]$. If v contained any of 123, 2143, 1432, and 3214, then there would be an element of $\Gamma[v, w_0]$ that completely surrounded by other elements of $\Gamma[v, w_0]$. This is a contradiction, so v is 123-, 2143-, 1432-, and 3214-avoiding.

From the construction, it is easy to see that $\mathrm{Std}(\lambda)$ is not block antidiagonal matrix with multiple blocks. Thus, w_0v does not belong to any parabolic subgroup of S_n.

We will now show that for every $v \in S_n$ that avoids 123, 2143, 1432, and 3214 where w_0v is not in a parabolic subgroup of S_n, there is a standard λ such that $\mathrm{Std}(\lambda) = M|_{\Gamma[v,w_0]}$. We proceed by induction. The cases for $n = 3$ and $n = 4$ can be checked by hand.

Suppose our result holds for $k \leq n$. Then let $v \in S_{n+1}$ such that v is 123-, 2143-, 1432-, and 3214-avoiding and w_0v is not in a parabolic subgroup of S_{n+1}. Let $v = v_1...v_{n+1}$ and let $v_i = n + 1$. Then define $u \in S_n$ by $u = u_1...u_n$ where

$$u_j = \begin{cases} v_j & j < i, \\ v_{j+1} & j \geq i. \end{cases}$$

Notice that u is still 123-, 2143-, 1432-, and 3214-avoiding. So, if w_0u is not in a parabolic subgroup of S_n, then by induction $M|_{\Gamma[u,w_0]} = \mathrm{Std}(\lambda)$ for some standard λ. This means u is one of the four permutations listed in Proposition 3.3.2. Adding $n + 1$ to the beginning does not give us v, because w_0v is not in a parabolic subgroup of S_{n+1}. There are only two possible ways we can insert $n + 1$ after the end of u and still avoid the patterns 123, 2143, 1432, and 3214. These give us the following permutations:

$$n-1, n+1, n-3, n, n-5, n-2, n-7, n-4, ..., 7, 2, 5, 1, 3 \qquad \text{with } n \text{ odd}$$

$$n-1, n+1, n-3, n, n-5, n-2, n-7, n-4, ..., 3, 6, 1, 4, 2 \qquad \text{with } n \text{ even}$$

For both of these permutations, $M|_{\Gamma[v,w_0]} = \text{Std}(\lambda)$ for some standard λ.

Now suppose that w_0u does belong to a parabolic subgroup of S_n. Let m be the largest integer less than n such that $w_0u[m] = [m]$. Since v is 123-avoiding, we know $v_1 > v_2 > ... > v_{i-1}$. Since v is 3214-avoiding, we know $i \leq 3$. Since v is not block decomposable, $m < i - 1$. Therefore, $i = 3, m = 1$, and $u_2u_3...u_n$ is one of the four permutations listed in Proposition 3.3.2 (but for S_{n-1} rather than S_n).

Checking all the options for inserting $n + 1$ in a way that meets our criteria for v, we find v must be one of the following:

$$n, n-2, n+1, n-4, n-1, n-6, n-3, n-8, n-5, ..., 7, 2, 5, 1, 3 \qquad \text{with } n \text{ odd}$$

$$n, n-2, n+1, n-4, n-1, n-6, n-3, n-8, n-5, ..., 3, 6, 1, 4, 2 \qquad \text{with } n \text{ even}$$

For both of these permutations, $M|_{\Gamma[v,w_0]} = \text{Std}(\lambda)$ for some standard λ, so we have our result. □

We now can give a new proof of Corollary 2.9.3 using cluster algebra techniques.

Corollary 2.9.3. *Let $v \in S_n$ avoid 123, 2143, 1432, and 3214. Then* $\text{Imm}_v(M)$ *is 2-positive.*

Second proof. By Lemma 2.6.7, we can restrict to the case when w_0v is not in a parabolic subgroup of S_n. Then

$$\begin{aligned} \text{Imm}_v(M) &= M|_{\Gamma[v,w_0]} && \text{by Corollary 2.5.6} \\ &= \text{Std}(\lambda) \text{ for some standard } \lambda && \text{by Theorem 3.3.3} \end{aligned}$$

Theorem 3.2.4 tells us that this is a cluster variable in the cluster algebra generated by the initial λ-DRH seed. Since all cluster variables in the initial λ-DRH seed are positive on 2-positive minors and the cluster exchange relation is subtraction-free, all cluster variables are positive on 2-positive matrices. Thus, $\text{Imm}_v(M)$ is 2-positive. □

The fact that we were able to use cluster algebra techniques to reprove Corollary 2.9.3

provides evidence that cluster algebras may be a useful technique for further investigation into k-positivity of Kazhdan–Lusztig immanants. However, DRH cluster algebras can only provide information in the $k = 2$ case. In the next section, we will explore another family of cluster algebras that we may be able to use for larger k.

3.4 Cluster Algebras and k-Positivity Tests

The results in this section arose from joint work with Anna Brosowsky and Alex Mason at the 2017 University of Minnesota Combinatorics REU [BCM20]. The initial motivation for this project was to find efficient ways to test matrices for k-positivity, so this is the context in which this section will be framed. However, we will see in Section 3.5 that the objects defined here may have relevance to Question 2.3.1.

Definition 3.4.1. Let M be an $n \times n$ matrix. For each $(i, j) \in [n] \times [n]$, define $x_{i,j}$ as the minor corresponding to the largest sub matrix of M that has $m_{i,j}$ in the lower right corner. That is, $x_{i,j} = \left|M_{\{i-\min(i,j)\}+1, i-\min(i,j)\}+2,\ldots,i\},\{j-\min(i,j)\}+1,j-\min(i,j)\}+2,\ldots,j\}}\right|$. We define a quiver with vertices $\{(i, j)\}_{1\leq i,j\leq n}$ and edges as follows:

(1) $(i, j) \to (i + 1, j)$ for $1 \leq i < n$ and $j \in [n - 1]$,

(2) $(i, j) \to (i, j + 1$ for $i \in [n - 1]$ and $1 \leq j < n$,

(3) $(i, j) \to (i - 1, j - j)$ for $1 < i, j \leq n$.

The vertices $\{(i, j)\}_{1\leq i\leq n, j=n}$ and $\{(i, j)\}_{i=n,1\leq j\leq n}$ are frozen, all other vertices are mutable. This quiver and the associated variables $x_{i,j}$ give a seed for the *total positivity cluster algebra*. We call this seed the *initial minors seed*. See Figure 3.5 for an example.

An $n \times n$ matrix has $\binom{2n}{n} - 1$ minors, so it is generally inefficient to test whether a matrix is totally positive by testing all of its minors. However, a seed in the total positivity cluster algebra has only n^2 variables. Notice that all of the cluster variables in the initial minors seed are minors, and therefore positive if M is totally positive. As noted in Section 3.1, this means any cluster variables that arise in the total positivity cluster algebra are also positive. All minors appear as cluster variables in the total positivity cluster algebra [Fom10], so we know that any cluster in this cluster algebra

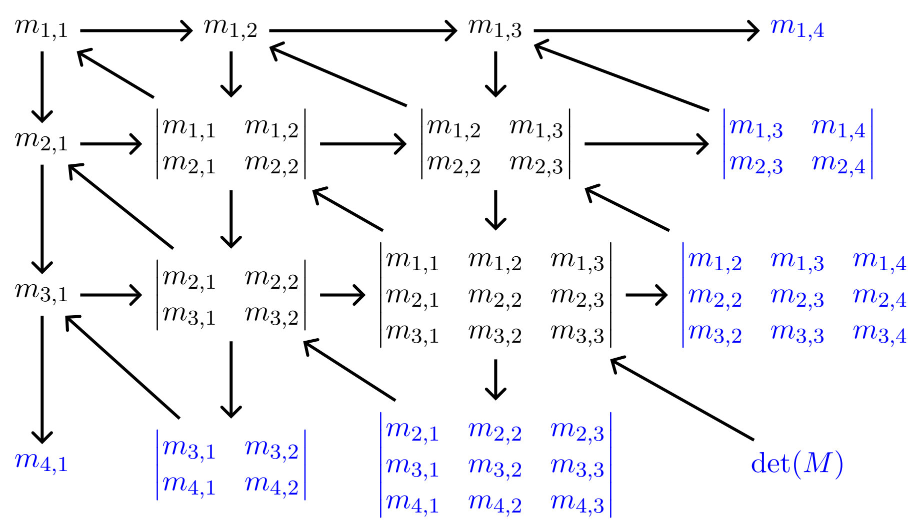

Figure 3.5: The initial minors seed for $n = 4$. Frozen vertices are in blue.

gives a total positivity test. In fact, work by Fomin and Zelevinsky shows that these are minimal total positivity tests [FZ00a].

Our ability to consider the total positivity cluster algebra as giving rise to a family of total positivity tests relies on the fact that we have a seed where we know all cluster variables are positive on totally positive matrices. We know some of these cluster variables are positive for k-positive matrices, but not all of them. If we want a similar object for k-positivity, we will need a seed where all cluster variables are positive on k-positive matrices. This leads us to define a set of subcluster algebras within the total positivity cluster algebra. To do this we introduce double wiring diagrams.

Definition 3.4.2. A *wiring diagram* consists of a family of n piecewise straight lines, all of the same color, such that each line intersects every other line exactly once. A *double wiring diagram* is two wiring diagrams of different colors which are overlaid. We will color our diagrams red and blue, and number the lines such that when reading from bottom to top, the left endpoints of the red lines are in decreasing order, and the left endpoints of the blue lines are in increasing order. Each diagram has n^2 *chambers*, see Figure 3.6. For double wiring diagrams (unlike the diagrams described in Section 3.2) the area on the top of the diagram is considered a chamber. A chamber is *bounded* if it is enclosed entirely by wires, and is called *unbounded* otherwise.

From each double wiring diagram, we obtain a seed in the total positivity cluster algebra [FZ99]. The chambers of the wiring diagram will correspond to vertices of the quiver. Bounded chambers will be mutable vertices in the quiver and unbounded chambers will be frozen. To find the variable associated to each vertex, we label each chamber by the tuple (r, b), where r is the subset of $[n]$ indexing all red strings passing below the chamber, and b is the subset of $[n]$ indexing all blue strings passing below the chamber (see Figure 3.6). Then the variable associated to the vertex for a chamber labelled (r, b) is the minor of the corresponding submatrix $|M_{r,b}|$. The rules for arrows in a quiver based on a double wiring diagram are exactly the rules listed in Section 3.2.

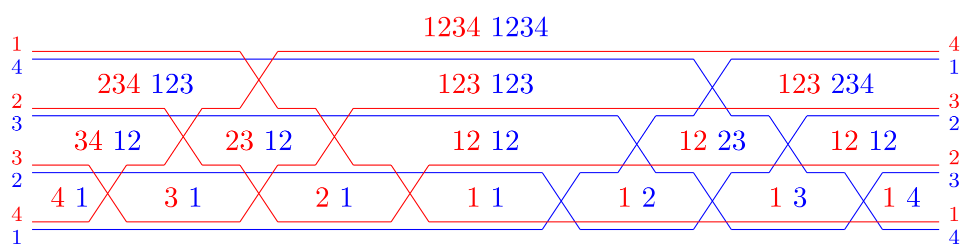

Figure 3.6: A double wiring diagram with wires and chambers labeled. This double wiring diagram gives us the initial minors seed for $n = 4$.

Definition 3.4.3. Let $(Q, \mathbf{x})$ be a seed in the total positivity cluster algebra. Denote all vertices corresponding to expressions that may be nonpositive in a k-positive matrix as *dead vertices* and freeze all vertices adjacent to a dead vertex. The seed we obtain from deleting all dead vertices is called a *k-seed*. See Figure 3.7 for an example.

Double wiring diagrams are useful for finding k-seeds because they give seeds in the total positivity cluster algebra comprised entirely of minors. We know exactly which cluster variables in the seed are required to be positive for all k-positive matrices are which are not. To obtain a k-seed from a double wiring diagram, we construct the seed as normal, but then freeze all vertices in the kth row (from the bottom) of the double wiring diagram and delete all vertices above the kth row.

We can see how the cluster algebra generated by a k-seed lives inside the total positivity cluster algebra by using exchange graphs.

Definition 3.4.4. We consider two clusters *equivalent* if they share the same variables, up to permutation. The *exchange graph* of a cluster algebra is a graph on vertices

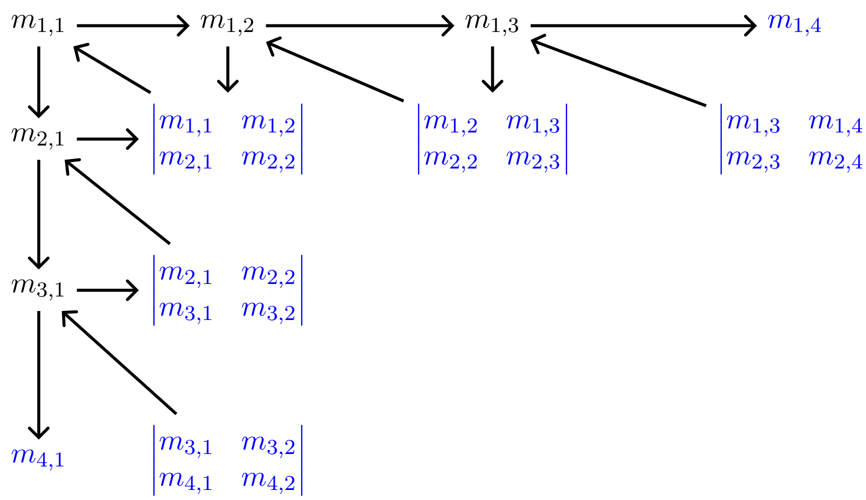

Figure 3.7: A 2-seed coming from the initial minors seed for the $n = 4$ total positivity cluster algebra.

indexed by equivalence classes of clusters, where there is an edge between two vertices if the clusters corresponding to the vertices are connected by a mutation.

Definition 3.4.5. Freezing or deleting a vertex in a seed in the total positivity cluster algebra corresponds to deleting all edges corresponding to mutation at that vertex in the exchange graph of the total positivity cluster algebra. The exchange graph for each sub-cluster algebra generated by a k-seed is thus a connected component of this new graph, and we will refer to these exchange graphs as *components*.

Definition 3.4.6. Freezing or deleting a vertex in a seed in the total positivity cluster algebra corresponds to deleting all edges corresponding to mutation at that vertex in the exchange graph of the total positivity cluster algebra. The exchange graph for each sub-cluster algebra generated by a k-seed is thus a connected component of this new graph, and we will refer to these exchange graphs as *components*.

Example 3.4.7. Consider the $n = 3, k = 2$ case. We will consider our 3×3 matrix to be as follows:

$$M = \begin{bmatrix} a & b & c \\ d & e & f \\ g & h & j \end{bmatrix}$$

This labelling allows us to refer to the 2×2 minors of M with uppercase letters: each uppercase letter will denote the 2×2 minor formed by the rows and columns that do not contain the corresponding lowercase letter. For example, A is the 2×2 minor obtained from the rows and columns that do not contain a, so $A := ej - fh$. In this case there are only two non-minor cluster variables in the total positivity cluster algebra. These are $K := aA - \det M$ and $L := jJ - \det M$ (see Exercise 1.4.4 of [FWZ16]).

For a matrix which is totally positive, K and L (our non-minor variables occurring in tests) must also be positive since they occur in clusters, and hence can be written as subtraction-free rational expressions in the initial minors. For a matrix which is 2-positive but has a nonpositive determinant, K and L are also positive as they are both a nonpositive term subtracted from a positive one. Thus, in any seed for the $n = 3$ total positivity cluster algebra, the only dead vertex is the determinant and we only freeze vertices adjacent to the determinant. The exchange graphs for the 8 sub-cluster algebras are depicted in Figure 3.8. The vertices in this figure are labeled by the cluster variables which are mutable in the total positivity cluster algebra, so that the extended cluster contains the listed variables plus c, g, C, and G.

Armed with our k-seeds, we can return to our initial motivations. While the size of a minimal k-positivity test is not known in general, it was conjectured in [BCM20] that for any k, a minimal k-positivity test consist of n^2 expressions. For $k < n$, each cluster in a k-seed has fewer than n^2 expressions. However, some of these clusters can be augmented by additional expressions to find a k-positivity test of size n^2.

Definition 3.4.8. A *test cluster* is a cluster from a k-seed with additional rational functions in the matrix entries appended to the cluster to give k-positivity test of size n^2. The variables that are in the test cluster and not the cluster are called *test variables*. These test variables along with the k-seed give a *test seed*.

Example 3.4.9. A *solid minor* is a minor with rows indexed by $I = [i, i + \ell - 1]$ and columns indexed by $J = [j, j + \ell - 1]$. An *initial minor* is a solid minor where $1 \in I \cup J$ (these are exactly the minors that appear in the initial minors seed for the total positivity cluster algebra). From Theorem 2.3 of [FJS17], we know that the set of all solid k-minors and all initial minors of size less than k gives a k-positivity test of size n^2. This is the *k-initial minors test*. The k-seed obtained from the initial minors

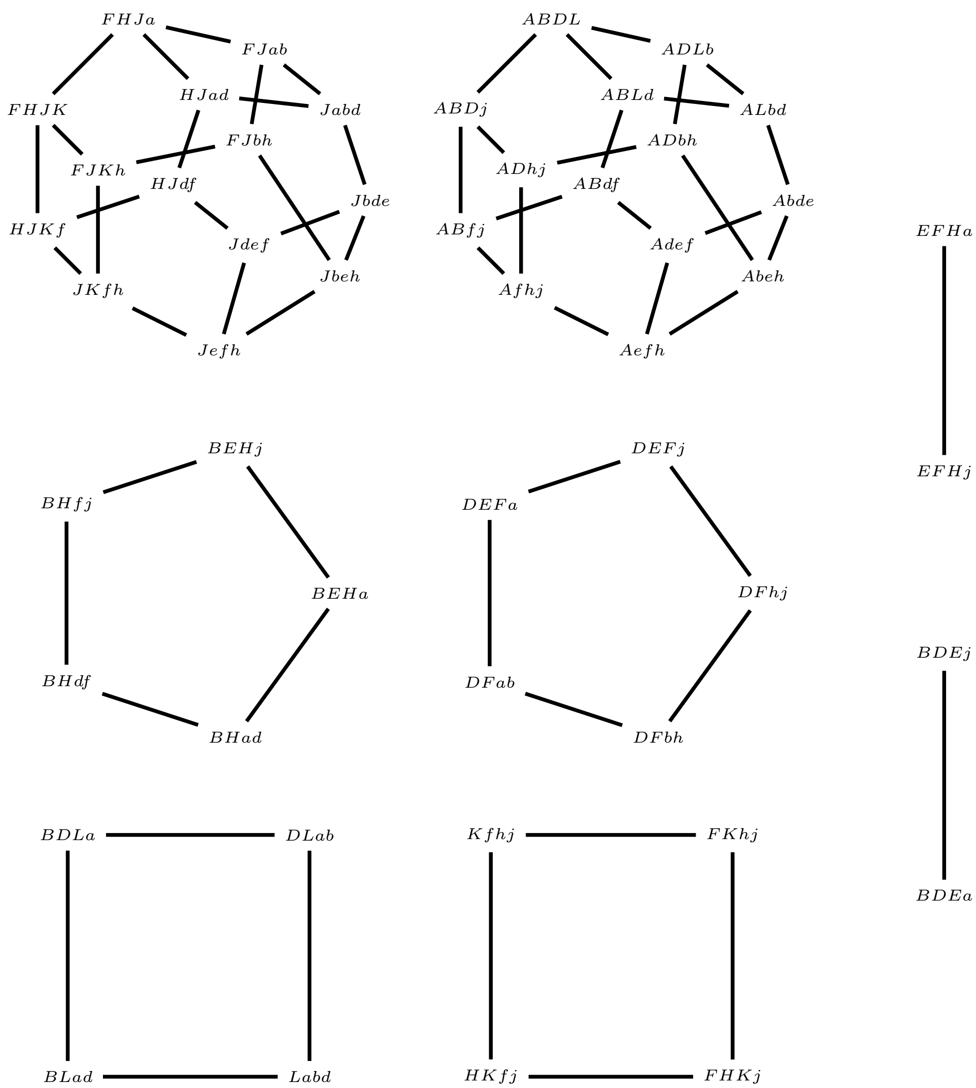

Figure 3.8: The components of a 2-positivity test graph derived from the 3×3 exchange graph.

seed includes exactly the initial minors of order $\leq k$ (such as in Figure 3.7). So, this cluster can be augmented to a test cluster by including all the missing solid k-minors as test variables.

Note that not all k-seeds can be extended to a test seed (see Examples 4.5 and 4.7 of [BCM20]).

A test seed in one component implies that the same test variables appended to any k-seed in the component is a test seed. This means that Example 3.4.9 gives us a family of test seeds. However, we would like to know how to find other test seeds. To do this, we need to have a way to move between components.

Definition 3.4.10. Two test seeds from different components have a *bridge* between them if they have the same test cluster and there is a quiver mutation connecting them which occurs at a vertex which is frozen in the k-quiver.

We can think of a bridge as swapping a cluster variable for a test variable. If one component provides k-positivity tests, then so do any components connected by a bridge. This is easy to see because the test cluster that both components share is a k-positivity test, which tells us that all test clusters in the second component are k-positivity tests.

Example 3.4.11. The two largest components in the $n = 3,\ k = 2$ case (see Figure 3.8) both generate 2-positivity tests. The left associahedron contains (J, a, b, d, c, g, C, G), and so appending the test variable A gives the k-initial minors test. The right associahedron contains the extended cluster (A, f, h, j, c, g, C, G), and so appending the test variable J gives the antidiagonal flip of the k-initial minors test. This is also a k-positivity test by Theorem 1.4.1 of [FJ11]. There are four bridges between these components, which we get by swapping the roles of A (a cluster variable on the left and test variable on the right) and J (a test variable on the left and cluster variable on the right) (see Figure 3.9).

Now that we have a way to move between components, we can identify many more test seeds. Below, we will use double wiring diagrams to describe a family of test seeds indexed by Young diagrams inside an $(n - 1) \times (n - 1)$ square.

To describe a double wiring diagram, it is sufficient to describe the relative positions of all of the crossings. We can think of a diagram as having n tracks numbered from

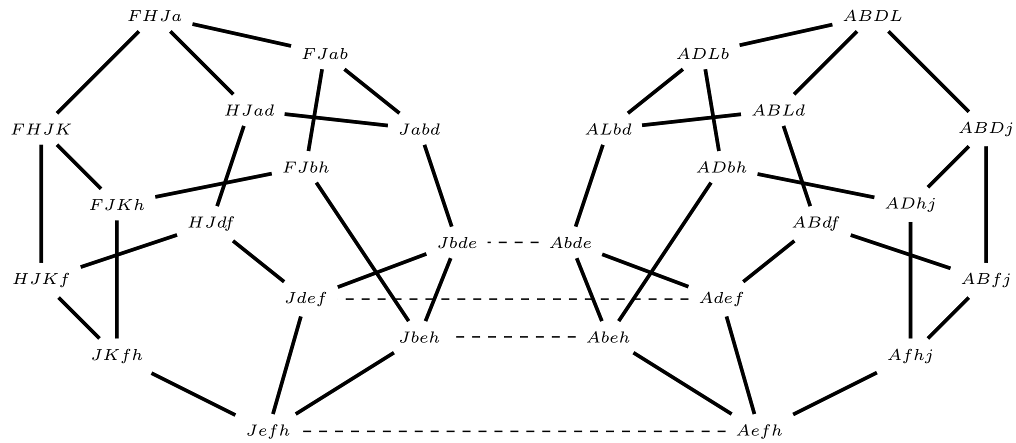

Figure 3.9: The bridges between the two largest components in the $n = 3$, $k = 2$ case. The left has test variable A and the right has test variable J. There are 4 bridges between these components, which we obtain by matching (J, d, e, f)-(A, d, e, f), (J, e, f, h)-(A, e, f, h), (J, b, e, h)-(A, b, e, h), and (J, b, d, e)-(A, b, d, e), i.e. those with the same test cluster (which also includes variables c, g, C, G in all cases).

bottom to top, where the chambers in track i have $|r| = |b| = i$ and each crossing occurs in one of the first $n-1$ tracks. We label a red crossing in the i^{th} track as e_i, and a blue crossing in the i^{th} track as f_i. With this notation, a sequence of crossings describing a double wiring diagram is a reduced word for the element (w_0, w_0) of the Coxeter group $S_n \times S_n$. We now define some useful groupings of crossings. Let $r_i = e_{n-i} \cdots e_2 e_1$ for $1 \leq i \leq n-1$, and let $b_i = f_1 f_2 \cdots f_{n-i}$ for $1 \leq i \leq n-1$. For convenience, when $i \notin [n-1]$ we define r_i and b_i to be empty, containing no crossings. Generally, r_i looks like a diagonal chain of red crossings going down and to the right, starting in the $(n-i)^{\text{th}}$ track and ending in the first track. Similarly, b_i looks like a a diagonal chain of blue crossings going up and to the right, starting in the first track and ending in the $(n-i)^{\text{th}}$ track.

Example 3.4.12. Suppose $n = 4$. Then the set of red crossings on the left is r_1 and the set of blue crossings on the right is b_2.

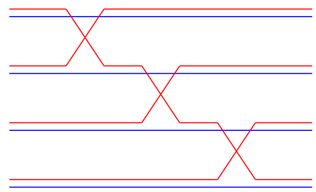 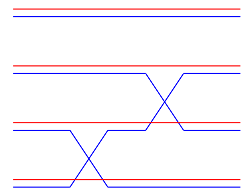

Example 3.4.13. The diagram $r_{n-1}...r_1b_1...b_{n-1}$ gives rise to the initial minors seed. The $n = 4$ case is depicted in Figures 3.5 and 3.6.

Definition 3.4.14. Let Y be a Young diagram inside an $(n-1) \times (n-1)$ square. Now construct the double wiring diagram $D(Y)$ as follows:

1. Start with the word $b_1b_2 \cdots b_{n-1}$.

2. Let ℓ_k be the number of boxes in the k^{th} row of Y.

3. For $k \in [n-1]$, insert r_k between b_{ℓ_k} and b_{ℓ_k+1}. If there are multiple r_s's between some b_t and b_{t+1}, arrange the r_s's in decreasing order from left to right.

The result is an interleaving of the words $b_1 \cdots b_{n-1}$ and $r_{n-1} \cdots r_1$.

Theorem 3.4.15 ([BCM20])**.** *Suppose Y is a Young diagram inside an $(n-1) \times (n-1)$ square. Construct the k-seed obtained from the double wiring diagram $D(Y)$ and let all solid k-minors not in the cluster be test variables. This gives a k-positivity test of size n^2.*

Proof (Sketch). The Young diagram $\emptyset$ gives the k-initial minors test. Adding a box to a Young diagram is the same as doing a sequence of mutations. The mutations required in the first $k-1$ tracks are mutations within the k-seed. If a box is being added inside the $(n-k) \times (n-k)$ square. there is a mutation in the kth track that is a valid bridge. Mutations above the first k tracks don't affect the test seed. □

As a consequence of the proof of Theorem 3.4.15, we can see that our test seeds lie in $(n-k)^2 + 1$ different components. Thus, we have constructed $(n-k)^2 + 1$ different sub-cluster algebras of the total positivity cluster algebra, each indexed by a Young diagram inside an $(n-k) \times (n-k)$ square.

3.5 Double Rim Hook Cluster Algebras and 2-Positivity

In Section 3.4, we constructed a family of cluster algebras indexed by Young diagrams inside an $(n-k)\times(n-k)$ square. In Section 3.2, we constructed a family of cluster algebras indexed by finite lattice paths of north and east steps. In this section, we will show that the cluster algebras from Section 3.4 when $k=2$ are exactly the cluster algebras from Section 3.2 when λ is a path with $n-2$ north steps and $n-2$ east steps.

Theorem 3.5.1. *If λ is a lattice path, with $n-2$ north steps and $n-2$ east steps, then consider λ inside an $(n-2)\times(n-2)$ square. Let Y by the Young diagram cut out by λ. Then the λ-DRH cluster algebra is the cluster algebra generated by the 2-seed obtained from $D(Y)$ as defined in Definition 3.4.14.*

To prove this theorem, we will first define a new way to construct a new seed for the λ-DRH cluster algebra.

Definition 3.5.2. Let a *worm* be any path of length $\ell(\lambda)+1$ in the λ-DRH that begins in a square adjacent to the farthest southwest square and ends in a square adjacent to the farthest northeast square. Note that any worm consists only of up and right steps. Let the *top worm* be the worm that is always to the northwest of λ.

We can define a cluster algebra from any worm in a λ-DRH as we did for the initial worm: Once we make a choice of correspondence, we can use this to construct a partial double wiring diagram in the same way as before. This double wiring diagram gives a seed for a cluster algebra. We will denote the seed we obtain from the worm w as the $w-\lambda$-DRH seed and in particular, we will call the seed we obtain from the top worm the *top λ-DRH seed.* Our first step is to show that every $w-\lambda$-DRH seed generates the same cluster algebra (that is, these seeds are all mutation equivalent).

Lemma 3.5.3. *Fix a worm in a λ-DRH. Let c be a cell that is at a bend in the worm. Then there exists a choice of correspondence map ε such that $\varepsilon^{-1}(c)$ is empty.*

Proof. There are six options for how λ can be arranged in the neighborhood of c:

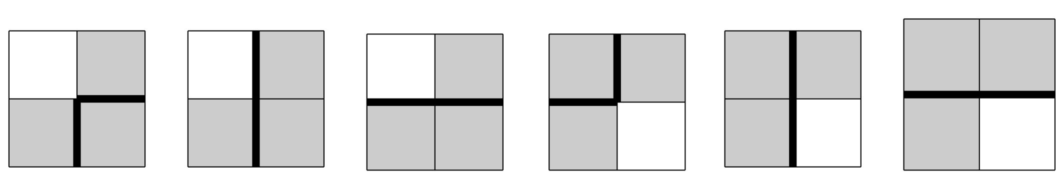

Consider the following choices of correspondence (shown by arrows):

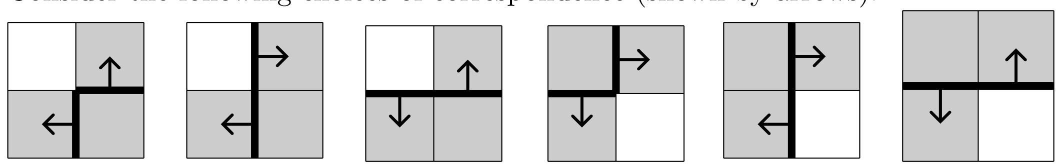

The above diagrams show that for each option, there is a choice of correspondence that doesn't have any steps of λ mapping to c. $\square$

Lemma 3.5.4. *Fix a worm w in a λ-DRH. Let c be a cell that is at a bend in the worm and $(Q, \boldsymbol{x})$ be the seed obtained from that worm. Denote the worm that is the same as the original but with c replaced by c' as w' and let $(Q', \boldsymbol{x}')$ be the seed obtained from w'. Then $(Q', \boldsymbol{x}') = \mu_c(Q, \boldsymbol{x})$, where μ_c denotes mutation at the vertex with cluster variable given by c.*

Proof. First note that there is exactly one way to replace c with another cell c', so w' is well-defined. Lemmas 5.4 and 5.5 of [CJS15] establish that μ_c changes the cluster variables as desired. So, we just need to check that the quiver also changes correctly.

By Lemma 3.5.3, there is a choice of correspondence ε for w such that $\varepsilon^{-1}(c)$ is empty. Use this choice of correspondence to create the diagram for w. Then the vertex that has cluster variable given by c comes from a chamber in the first track with a blue crossing on the right and a red crossing on the left. Using this same choice of correspondence, we can create a diagram for w'. These diagrams are related by swapping the blue and red crossings mentioned above. This move corresponds to quiver mutation in the quiver given by the double wiring diagram (Lemma 18 of [FZ00a]), so $(Q', \mathbf{x}') = \mu_c(Q, \mathbf{x})$. $\square$

We are now ready to prove Theorem 3.5.1.

Proof. (of Theorem 3.5.1). Since seeds for both cluster algebras are formed using double wiring diagram-type objects with the same rules for quiver arrows, we will show that the diagram we obtain from the λ-DRH with the top worm is the same as the bottom two tracks of $D(Y)$.

If s is a north step of λ, let $\varepsilon(s)$ be the cell to the left of s and if s is an east step, let $\varepsilon(s)$ be the cell above s. Notice that the top worm and λ have the same shape. This means that the pattern of crossings in the bottom track of the diagram associated to λ is the same as the pattern of crossings in the second track with an extra red crossing at the beginning (for the step from the farthest southwest cell to the first cell in the worm) and an extra blue crossing at the end (for the step from the last cell in the worm to the farthest northeast cell). Every red crossing in the second track will appear just before the corresponding red crossing in the first track and every blue crossing in the second track will appear just after the corresponding blue crossing in the first track.

For $i \in [n-1]$, let b_i^* be the crossings of b_i restricted to the bottom two tracks and r_i^* be the crossings of r_i restricted to the crossings in the bottom two tracks. This means b_{n-1}^* is one blue crossing in the bottom track and b_j^* is a blue crossing in the bottom track followed by a blue crossing in the second track for $j \in [n-2]$. Similarly, r_{n-1}^* is one red crossing in the bottom track and r_j^* is a red crossing in the second track followed by a red crossing in the first track for $j \in [n-2]$. With this notation, the partial double wiring diagram can be constructed in the following way:

1. Start with the word $b_1^* b_2^* \cdots b_{n-1}^*$. This encodes only the east steps of λ and the extended top worm.

2. Let ℓ_k be the number of boxes in the k^{th} row of Y.

3. For $k \in [n-1]$, insert r_k^* between $b_{\ell_k}^*$ and $b_{\ell_k+1}^*$ because this means the $n-k$th north step occurs between the ℓ_kth and ℓ_k+1st east step. If there are multiple r_s's between some b_t and b_{t+1}, arrange the r_s's in decreasing order from left to right (as a convention).

This construction exactly matches the construction of $D(Y)$, so we know that the quiver for the top λ-DRH seed and the 2-seed obtained from $D(Y)$ are the same.

Now we need to check the variables. Let's first check the variables in the first track. Using the formulas from Proposition 5.6 of [BCM20], the variables associated to the first track $D(Y)$ are, from left to right, $a_{i+y_{i-1},1+y_{i-1}}$ as i decreases from n to 2 and then $a_{1+y_{1-j},j+y_{1-j}}$ as j increases from 1 to n, where y_ℓ is the number of boxes on the ℓth diagonal of Y (the main diagonal is indexed as 0, the superdiagonal is indexed as 1, the subdiagonal is indexed as -1, and so on). We know that there can never be any boxes on the $n-1$st or $n-2$nd diagonal, so this sequence always starts as $a_{n,1}, a_{n-1,1}$. After that, until we get to the main diagonal, each north step doesn't affect the length of the diagonal and each east step increases the length of the diagonal by 1. Thus, using the formulas in terms of i, we find that every time we have a north step the first coordinate of the variable decreases by 1 (indicating moving a row up) and every time we have an east step the second coordinate increases by 1 (indicating moving a column right). Once we get to the main diagonal, the east steps stop affecting the length of the diagonals and the north steps decrease the length of the diagonals. Using the formulas in terms of j, we find it is still true that every time we have a north step the first coordinate of the variable decreases by 1 and every time we have an east step the second coordinate increases by 1. We have shown that the variables corresponding to the vertices in the bottom track are exactly the variables of the cells in the extended top worm, in order, so the cluster variables for these vertices match in both quivers.

For the variables in the second track, we can think of the variables in the top λ-DRH seed as being the determinants of the 2×2 blocks centered at each point in λ. They appear from left to right in the order that they appear when walking along λ. Using the formulas from Proposition 5.6 of [BCM20], the variables associated to the second track of $D(Y)$ are, from left to right, $|A_{\{i-1+y_{i-2}, i+y_{i-2}\},\{1+y_{i-2}, 2+y_{i-2}\}}|$ as i decreases from n to 3 and then $|A_{\{1+y_{2-j}, 2+y_{2-j}\},\{j-1+y_{2-j}, j+y_{2-j}\}}|$ as j increases from 2 to n. We know that there can never be any boxes on the $n-1$st or $n-2$nd diagonal, so this sequence always starts as $|A_{\{n-1,n\},\{1,2\}}|, |A_{\{n-2,n-1\},\{1,2\}}|$. The north and east steps act as described above with respect to the diagonals, which means that every time there is a north step in λ, the next variable is the determinant of the 2×2 box one row above the previous one and every time there is an east step in λ, the next variable is the determinant of the 2×2 box one column to the right of the previous one. This shows that the variables corresponding to the vertices in the second track the same in both quivers, which completes the proof. □

Example 3.5.5. Let λ be ENNENE. Then the λ-DRH with the top worm looks as follows:

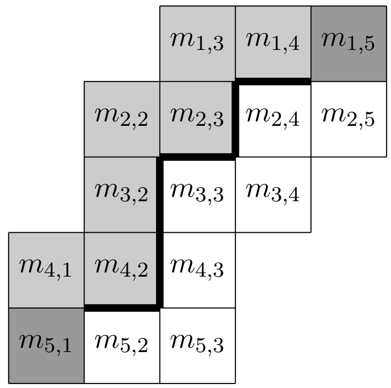

From this we obtain the top λ-DRH seed:

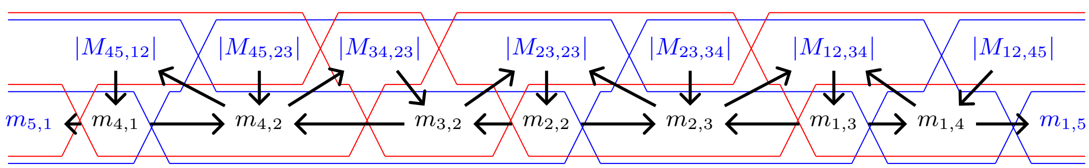

The Young diagram cut out by λ is (2,1,1):

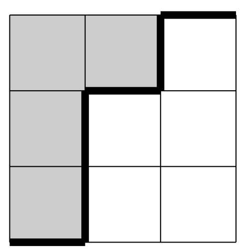

The double wiring diagram $D(Y)$ is given by the word $r_4b_1r_3r_2b_2r_1b_3b_4$. We can construct $D(Y)$ and the corresponding total positivity seed:

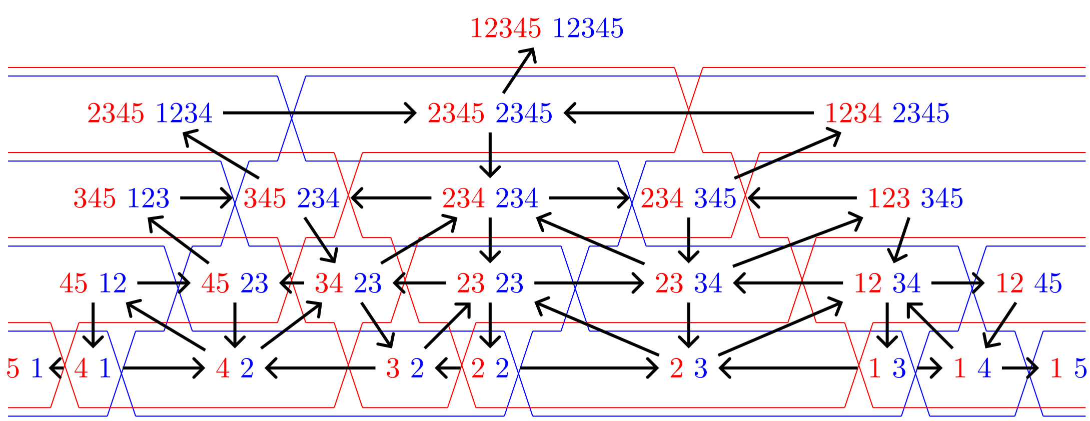

The 2-seed we get from $D(Y)$ is exactly the same as the top λ-DRH seed, which we can see by only looking at the bottom two tracks of the previous diagram.

This correspondence gives us hope for attacking Question 2.3.1 with cluster algebras. We could potentially look for immanants that show up as cluster variables in cluster algebras generated by k-seeds. This would prove those immanants were k-positive. However, k-positivity cluster algebras are not of finite type if $k > 2$, meaning it would be much harder to find a catalogue of cluster variables for these cluster algebras.

Chapter 4

Total Positivity and Networks

In this chapter, we give an overview of the relationship between total positivity and networks. Section 4.1 tells the classical story regarding totally nonnegative matrices. These results were generalized to the Grassmannian by Alex Postnikov [Pos06] in his groundbreaking 2006 paper. We highlight his main results in Sections 4.2, 4.3, and 4.4. In Section 4.5 we introduce a tool he uses in his work that we will rely on heavily in later chapters.

4.1 Totally Nonnegative Matrices and Planar Directed Networks

Our story starts with Lindström's Lemma. To state this theorem, we need to recall the definition of a minor from Section 1.1 as well as introducing some new definitions.

Definition 4.1.1. Let G be a directed, edge-weighted graph. If P is a (directed) path in G, then we say the *weight* of P is

$$\mathrm{wt}(P) := \sum_{e \in P} \mathrm{wt}(e),$$

where the sum is over all edges in P.

Definition 4.1.2. Let G be a directed, edge-weighted graph with n source vertices,

$\{s_i\}_{i=1}^n$, and m sink vertices, $\{t_i\}_{i=1}^m$. The *path matrix* of G is $M(G) = (m_{i,j})$ with

$$m_{i,j} = \sum_{\text{paths } P: s_i \to t_j} \mathrm{wt}(P),$$

where the sum is over all paths from s_i to t_j.

Example 4.1.3. Consider the following network:

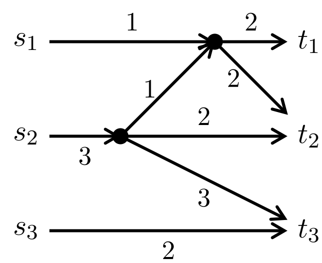

There are two paths that go from s_2 to t_2. The one that goes straight across has weight $(3)(2) = 6$. The one that goes up then back down has weight $(3)(1)(2) = 6$. So, $m_{2,2} = 6 + 6 = 12$. The full path matrix is as follows:

$$M(G) = \begin{bmatrix} 2 & 2 & 0 \\ 6 & 12 & 9 \\ 0 & 0 & 2 \end{bmatrix}$$

Theorem 4.1.4 (Lindström's Lemma, [Lin73, GV85])**.** *Let G be a planar, acyclic, directed, edge-weighted graph graph with n source vertices and n sink vertices such that the sources are all on the left (labeled s_1 to s_n from top to bottom) and the sinks are all on the right (labeled t_1 to t_n from top to bottom). Then for $I, J \subseteq [n]$ with $|I| = |J|$,*

$$\Delta(M(G))_{I,J} = \sum_{\substack{\textit{families of nonintersecting} \\ \textit{paths from sources indexed} \\ \textit{by } I \textit{ to sinks indexed by } J}} \left(\prod_{\substack{\textit{all paths } P \\ \textit{in a family}}} \mathrm{wt}(P) \right).$$

In particular $M(G)$ is a totally nonnegative matrix.

Example 4.1.5. We revisit the network from Example 4.1.3. Let $I = J = \{1, 2\}$. There are three families of paths from I to J:

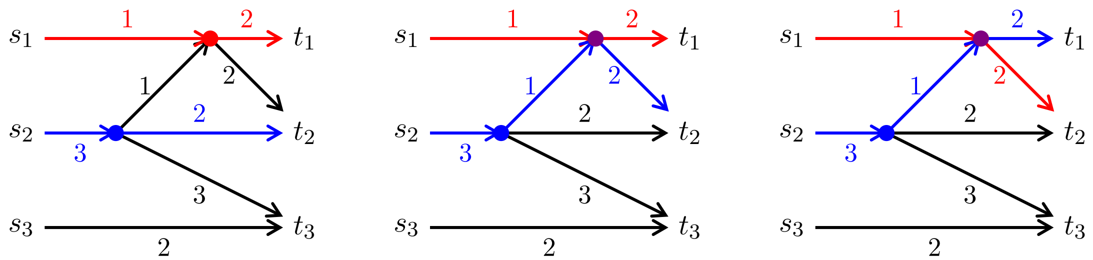

However, notice that the family of paths on the left is the only family where the paths don't intersect. So $\Delta(M(G))_{I,J} = [(1)(2)] * [(3)(2)] = 12$.

The converse of this theorem is also true.

Theorem 4.1.6 ([Bre95])**.** *Every nonnegative $n \times n$ matrix is the weight matrix of a planar, acyclic, directed, edge-weighted graph graph with n source vertices and n sink vertices such that the sources are all on the left (labeled s_1 to s_n from top to bottom) and the sinks are all on the right (labeled t_1 to t_n from top to bottom).*

4.2 Totally Nonnegative Grassmannians and Planar Directed Networks

While the relationship between planar directed networks and totally nonnegative matrices is beautiful, the networks we considered in the previous section are quite limited. In this section, we will consider planar, directed, edge-weighted networks that we allow to be cyclic, have different numbers of sources and sinks, and have the sources and sinks intertwined. The material in this section comes from Section 4 of [Pos06].

Definition 4.2.1. A *planar directed graph* in a disk, considered up to homotopy, has n vertices on the boundary labeled $b_1, ..., b_n$ in clockwise order. We will call these *boundary vertices*, and all other vertices *internal vertices*. Additionally, we will assume that all boundary vertices are sources or sinks. A *planar directed network* is a planar directed graph with a weight $x_e \in \mathbb{R}_{>0}$ assigned to each edge.

Definition 4.2.2. The *source set* of a planar directed graph or network is the set $I = \{i \in [n] \mid b_i \text{ is a source}\}$. The *sink set* is $\overline{I} = [n] \setminus I = \{j \in [n] \mid b_j \text{ is a sink}\}$.

Definition 4.2.3. For a path P in a planar directed graph or network in a disk from b_i to b_j, we define its *winding index*, $wind(P)$. First, we smooth any corners in P and make the tangent vector of P at b_j have the same direction as the tangent vector at b_i. Then $wind(P)$ is the full number of counterclockwise 360° turns the tangent vector makes from b_i to b_j, counting clockwise turns as negative. For C a closed curve, we can define $wind(C)$ similarly. See Lemma 4.2 in [Pos06] for a recursive formula for $wind(P)$ and $wind(C)$.

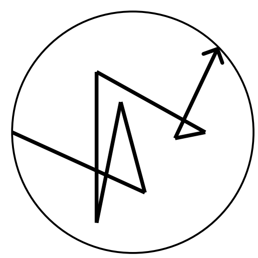

Figure 4.1: A path P with $wind(P) = -1$.

Definition 4.2.4. Let b_i be a source and b_j be a sink in a planar directed network in a disk with graph G. Let the edge weights be the formal variables x_e. Then the *formal boundary measurement* M_{ij}^{form} is the formal power series

$$M_{ij}^{\text{form}} := \sum_{\substack{\text{paths } P \text{ from} \\ b_i \text{ to } b_j}} (-1)^{wind(P)} \, \text{wt}(P).$$

Lemma 4.2.5. *The formal power series M_{ij}^{form} sum to subtraction-free rational expressions in the variables x_e. Thus, M_{ij}^{form} is well-defined function on $\mathbb{R}_{\geq 0}^{|E(G)|}$, where $E(G)$ is the set of edges in the graph G.*

Definition 4.2.6. The *boundary measurements* M_{ij} for a planar directed network in a disk are nonnegative real numbers obtained by writing the formal boundary measurements M_{ij}^{form} as subtraction-free rational expressions, and then specializing them by assigning x_e the real weight of the edge e.

Example 4.2.7. Suppose we have the following network:

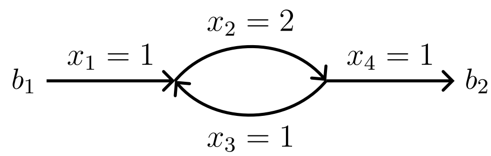

$$\begin{aligned} M_{12}^{\text{form}} &= x_1x_2x_4 - x_1x_2x_3x_2x_4 + x_1x_2x_3x_2x_3x_2x_4 - ... \\ &= x_1x_2x_4\sum_{i=0}^{\infty}(-x_2x_3)^i \\ &= \frac{x_1x_2x_4}{1+x_2x_3} \end{aligned}$$

Substituting our values for the x_e's, we find $M_{12} = \frac{2}{3}$.

Definition 4.2.8. For $0 \leq k \leq n$, the *Grassmannian* $Gr_{k,n}(\mathbb{R})$ is the manifold of k-dimensional subspaces of $\mathbb{R}^n$.

We can associate any full-rank real $k \times n$ matrix to a point in $Gr_{k,n}(\mathbb{R})$ by taking the span of its rows. Let $Mat^*_{k,n}(\mathbb{R})$ be the space of full-rank real $k \times n$ matrices. Since left-multiplying a matrix by an element of the general linear group is equivalent to performing row operations and row operations do not change the row-span of a matrix, we can think of $Gr_{k,n}(\mathbb{R})$ as the quotient $GL_k(\mathbb{R})\backslash Mat^*_{k,n}(\mathbb{R})$.

Definition 4.2.9. For a $k \times n$ matrix M, a *maximal minor* is $\Delta(M)_S$ where $S \subseteq [n]$ and $|S| = k$. $\Delta(M)_S$ is the determinant of the submatrix of M obtained by taking only the columns indexed by S.

Definition 4.2.10. If $Net_{k,n}$ is the set of planar directed networks in a disk with k boundary sources and $n-k$ boundary sinks, then we can define the *boundary measurement map* $Meas : Net_{k,n} \to Gr_{k,n}(\mathbb{R})$. $Meas(N)$ is the point in $Gr_{k,n}(\mathbb{R})$ represented by the matrix $A(N)$, which is defined as follows:

(1) $A(N)_I$, the submatrix of $A(N)$ containing only the columns in the source set, is the identity Id_k.

(2) For $I = \{i_1 < ... < i_k\}$, $r \in [k]$, and $b_j \in \overline{I}$, we define $a_{rj} = (-1)^s M_{i_r,j}$, where s is the number of elements of I strictly between i_r and j.

Note that the map $Meas$ is constructed so that $M_{ij} = \Delta(A(N))_{(I\setminus\{i\})\cup\{j\}}$.

Example 4.2.11. Consider the network from the previous example:

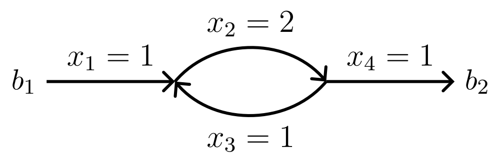

In this case $I = \{1\}$, so we put Id_1 in the first column of $A(N)$. We compute $a_{12} = (-1)^0 M_{12} = M_{12} = \frac{2}{3}$. So, we have $A(N) = \begin{bmatrix} 1 & \frac{2}{3} \end{bmatrix}$.

While a priori the image of the map $Meas$ is some subset of $Gr_{k,n}(\mathbb{R})$, Postnikov was able to prove an analogue of Lindström's Lemma and its converse:

Theorem 4.2.12. *The image of the boundary measurement map $Meas$ is exactly the totally nonnegative Grassmannian: $Meas(Net_{k,n}) = Gr_{k,n}(\mathbb{R})_{\geq 0}$.*

4.3 Planar Directed Networks to Plabic Networks

After proving Theorem 4.2.12 in [Pos06], Postnikov investigates the inverse problem for the boundary measurement map. Inverse problems deal with a map from a set X to a set Y. They ask, given a point $y \in Y$, what can information can be recovered about its preimage in X? In our case, we want to know about all networks that map to a point in $Gr_{k,n}(\mathbb{R})_{\geq 0}$. Postnikov's study of this problem led him to define plabic networks. The material in this section appears in sections 9, 10, and 11 of [Pos06].

To study the inverse boundary problem, Postnikov used perfect networks to identify certain families of networks that map to the same point in the Grassmannian.

Definition 4.3.1 (Definition 9.2 of [Pos06])**.** A *perfect network* is a planar directed network in which each boundary vertex has degree 1, and each internal vertex either has exactly one edge incoming (and all others outgoing) or exactly one edge outgoing (and all others incoming).

Proposition 4.3.2 (Proposition 9.3 of [Pos06])**.** *Any planar directed network in a disk can be transformed into a perfect network without changing the boundary measurements.*

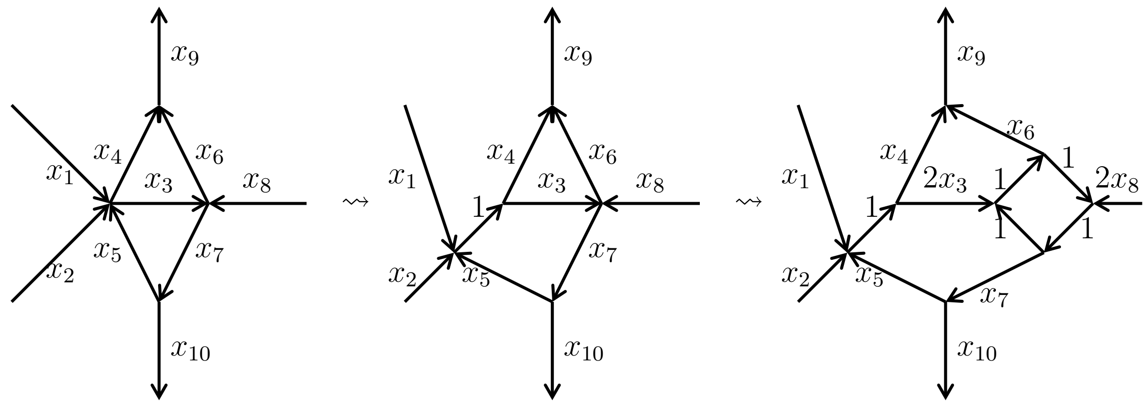

Figure 4.2: A planar directed network in a disk transformed into a perfect network.

Definition 4.3.3 (Section 9 of [Pos06])**.** For an internal vertex v in a perfect network, define the *color* of v, $col(v)$, to be black if v has exactly one outgoing edge and white if v has exactly one incoming edge.

Theorem 4.3.4. *Let N, N' be two perfect networks in a disk such that:*

(1) The underlying graphs G and G' are isomorphic as undirected graphs.

(2) Each internal vertex of degree $\neq 2$ has $col_N(v) = col_{N'}(v)$.

(3) If the undirected edge e is directed in the same way in N and N', then $x_e = x'_e$. If the edge e has opposite direction in N and N', then $x_e = (x'_e)^{-1}$.

Then $Meas(N) = Meas(N') \in Gr_{k,n}(\mathbb{R})$.

Example 4.3.5. Let N, N' be as below:

$N =$ 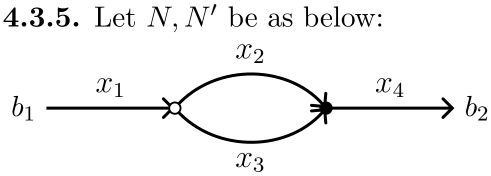

$$A(N) = \begin{bmatrix} 1 & x_1x_4(x_2+x_3) \end{bmatrix}$$

$N' =$ 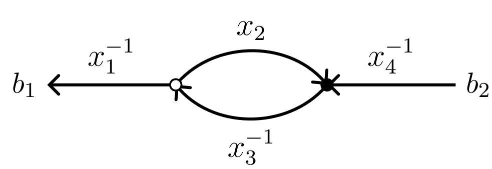

$$A(N') = \begin{bmatrix} \frac{(x_1x_3x_4)^{-1}}{1+x_2x_3^{-1}} & 1 \end{bmatrix} = \begin{bmatrix} \frac{1}{x_1x_4(x_2+x_3)} & 1 \end{bmatrix}$$

Since left multiplication of $A(N')$ by $[x_1x_4(x_2+x_3)] \in GL_1(\mathbb{R})$ gives $A(N)$, these two matrices represent the same point in the Grassmannian.

Notice that in our example, N' could be obtained from N by reversing a path from one boundary vertex to another. In fact, for any two networks N and N' satisfying the conditions of Theorem 4.3.4, N' can be obtained from N by reversing a set of paths between boundary vertices and a set of cycles. Thus, the theorem can be proven by showing that reversing paths between boundary vertices and reversing cycles preserve the boundary measurement map.

Another way to identify networks that map to the same point under $Meas$ is with gauge transformations.

Definition 4.3.6 (Section 4 of [Pos06])**.** A *gauge transformation* is a rescaling of edge weights in a planar directed network so that all incoming edges of a particular vertex are multiplied by a positive real number c and all outgoing edges of that vertex are divided by c.

It is clear that gauge transformations preserve the boundary measurements, as they preserve the weight of each path. This means that we can only ever hope to solve the inverse boundary problem up to gauge transformations. Postnikov eliminates gauge transformations by converting edge-weighted networks into face-weighted networks.

Definition 4.3.7 (Section 11 of [Pos06])**.** For a face in a planar directed network, define the *face weight* to be

$$y_f := \left(\prod_{e_i \in I_f^+} x_{e_i}\right)\left(\prod_{e_j \in I_f^-} x_{e_j}\right)$$

where I_f^+ is the set of edges on the outer boundary of f oriented clockwise and edges on the inner boundary (if f is not simply connected) oriented counterclockwise, and I_f^- is the set of edges on the outer boundary of f oriented counterclockwise and edges on the inner boundary (if f is not simply connected) oriented clockwise.

Notice that the product of weights of all the faces is 1, as each edge is counted once going clockwise and once going counterclockwise.

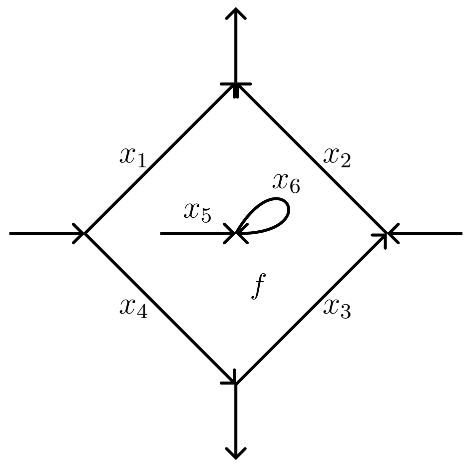

Figure 4.3: A face with $y_f = x_1 x_2^{-1} x_3^{-1} x_4^{-1} x_5 x_6^{-1} x_5^{-1} = \frac{x_1}{x_2 x_3 x_4 x_6}$.

It is clear that the map from edge weights to face weights is invariant under gauge transformations. Postnikov further showed that the space of face weighted networks was exactly the space of edge weighted networks modulo these transformations.

Lemma 4.3.8 (Lemma 11.2 of [Pos06])**.** *Let G be a planar directed graph with edge set E and face set F. We will denote the set of edge-weighted networks with underlying graph G as $\mathbb{R}^E$ and the set of face-weighted networks with underlying graph G and face weights multiplying to 1 as $\mathbb{R}^{F-1}$. Then*

$$\mathbb{R}^E / \{\textit{gauge transformations}\} \simeq \mathbb{R}^{F-1}$$

by the map $(x_e)_{e \in E} \mapsto (y_f)_{f \in F}$ given in Definition 4.3.7.

We can determine path weights, and therefore boundary measurements of a face weighted network in a manner that is consistent with those definitions for edge weighted networks.

Definition 4.3.9. Let Q be a non self-intersecting path in a face-weighted planar directed network in a disk and define $\text{wt}(Q, y)$ to be the product of the weights of faces to the right of the path. For a clockwise (resp. counterclockwise) cycle C, define $\text{wt}(Q, y)$ to be product of the weights of the faces inside (resp. outside) the cycle. A path P is made up of a non self-intersection path and a collection of cycles, so we define $\mathrm{wt}(P, y)$ to be the product of the weights of this path and these cycles.

Lemma 4.3.10 (Lemma 11.4 of [Pos06])**.** *Consider a planar directed network and define the face weights of the network as in Definition 4.3.7. Then* $\mathrm{wt}(P, y) = \mathrm{wt}(P)$*.*

Justified by the above lemma, we will refer to the weight of a path in a face-weighted planar directed network in a disk simply as $\mathrm{wt}(P)$, rather than $\mathrm{wt}(P, y)$, for the rest of this thesis.

We can see that reversing an edge and inverting its weight in an edge-weighted network does not affect the face weights of the network. That means converting to face weights plays nicely with reversing paths and cycles as in Theorem 4.3.4. Together, these lead us to the definition of plabic networks in a disk.

Definition 4.3.11 (Definition 11.5 of [Pos06])**.** A *planar bicolored graph*, or *plabic graph*, in a disk is a planar undirected graph such that each boundary vertex has degree 1 and each internal vertex is colored black or white. A *plabic network* in a disk is a plabic graph with a weight $y_f \in \mathbb{R}_{>0}$ assigned to each face such that the product of the weights is 1.

Plabic networks identify planar directed networks that are related by path and cycle reversal and by gauge transformations. Since these networks all mapped to the same point under $Meas$, we can define an induced map on those plabic networks that arise from planar directed networks.

Definition 4.3.12. A plabic graph is *perfectly orientable* if there exists an orientation of edges such that every black vertex has exactly 1 outgoing edge and every white vertex has exactly 1 incoming edge. A perfectly orientable plabic graph is of type (k, n) if it has n boundary vertices and some (equivalently, every) perfect orientation has k sources.

Definition 4.3.13. Let

$$\tilde{Meas} : \{\text{perfectly orientable plabic networks of type } (k, n)\} \to Gr_{k,n}(\mathbb{R})$$

be the map induced from $Meas : Net_{k,n} \to Gr_{k,n}(\mathbb{R})$.

4.4 Moves and Reductions

We will now consider the inverse boundary problem for $\tilde{Meas}$. While moving to the space of plabic networks rather than planar directed networks allows us to identify many networks that have the same image under $Meas$, we still don't have a one-to-one map. In Section 12 of [Pos06], Postnikov introduces a set of moves and reductions on plabic networks that preserve a network's image under the boundary measurement map $\tilde{Meas}$ (Theorem 12.1 of [Pos06]). These are as follows:

(M1) Square move.

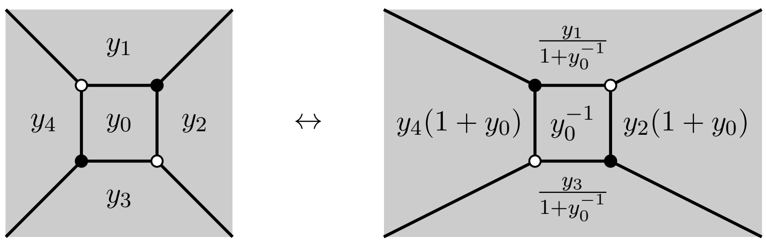

(M2) Unicolored edge contraction/uncontraction.

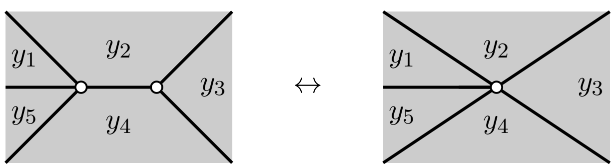

The unicolored edge may be white (as pictured) or black and there may be any number of edges on each of the vertices. All of the face weights remain unchanged.

(M3) Middle vertex insertion/removal

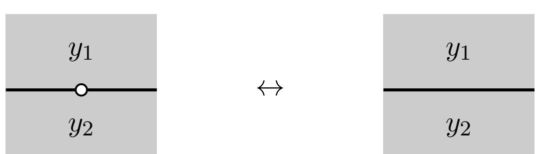

Vertex insertion/removal may be done with a vertex of either color.

(R1) Parallel edge reduction

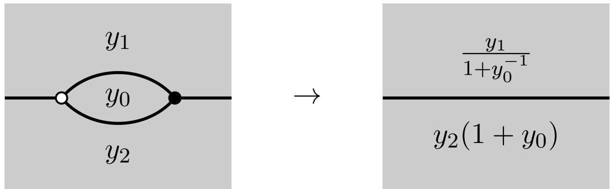

(R2) Leaf reduction

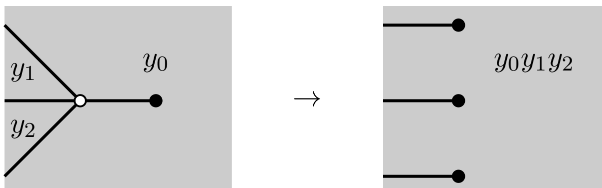

The vertex with degree 1, which we call a leaf, may be any color, and the vertex connected to the leaf (which is of the opposite color) may have any degree ≥ 2.

(R3) Dipole reduction

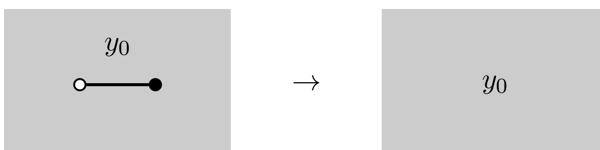

Definition 4.4.1. The transformations (M1) - (M3) are called *moves* and the transformations (R1) - (R3) are called *reductions.*

Definition 4.4.2. A plabic graph or network is *reduced* if it has no isolated connected components and it is not move-equivalent to any graph or network to which we can apply (R1) or (R2).

With these moves and reductions, Postnikov was able to show an amazing relationship between reduced plabic networks and the Grassmannian via $\widetilde{Meas}$.

Theorem 4.4.3 (Theorem 12.7 of [Pos06])**.** *If G is a reduced plabic graph in a disk of type (k,n), then $\widetilde{Meas}$ gives an injective map from valid assignments of face weights for G to $Gr_{k,n}(\mathbb{R})$. Further, for a fixed point $x \in Gr_{k,n}(\mathbb{R})$, all elements in the preimage of x under $\widetilde{Meas}$ are related to each other by a sequence of moves.*

One implication of this theorem that will be important later is the following: Assume $\tilde{Meas}(N) = x$. Then the information of x and the underlying graph of N is enough to uniquely recover the weights of N.

4.5 Postnikov Diagrams

In this section we introduce a particularly useful tool for studying reduced plabic graphs.

Definition 4.5.1. A *Postnikov diagram*, also known as an alternating strand diagram, in a disk is a set of directed curves, called *strands*, such that when we draw the strands on disk we have the following:

(1) Each strand begins and ends at a boundary vertex.

(2) There is exactly one strand that enters and one strand that leaves each boundary vertex.

(3) No three strands intersect at the same point.

(4) All intersections are transverse (the tangent vectors are independent).

(5) There is a finite number of intersection points.

(6) Along any strand, the strands that cross it alternate crossing from the left and crossing from the right.

(7) Strands do not have self-intersections, except in the case where a strand is a loop attached to a boundary vertex. Notice that this excludes the possibility of a closed cycle.

(8) If two strands intersect at u and v, then one strand is oriented from u to v and one strand is oriented from v to u.

Postnikov diagrams are considered up to homotopy. We can obtain a plabic graph from a Postnikov diagram as follows:

(1) Place a black vertex in every face oriented counterclockwise and a white vertex in every face oriented clockwise.

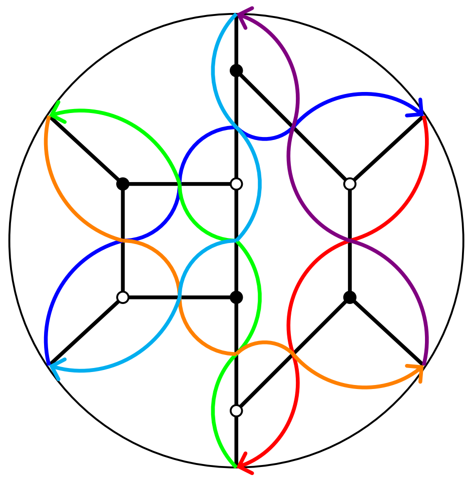

Figure 4.4: A plabic graph and its Postnikov diagram.

(2) If two oriented faces share a corner, connect the vertices in these two faces.

Theorem 4.5.2 (Corollary 14.2 of [Pos06])**.** *Postnikov diagrams in a disk are in bijection with reduced plabic graphs in a disk with no unicolored edges.*

Since (M2) is unicolored edge contraction/uncontraction, this theorem tells us that considering Postnikov diagrams allows us to consider every move-equivalence class of plabic graphs. This will be a very useful tool in Section 6.1.

Chapter 5

Plabic Networks on the Cylinder

Some constructions that arise in the study of planar directed networks and total positivity have been extended to other surfaces. In particular, the boundary measurement map for planar directed networks on surfaces with boundary have recently been a topic of interest [FGPW15, Mac18, Mac19].

We will focus on extending Postnikov's methods to the cylinder. This case was considered by Gekhtman, Shapiro, and Vainshtein [GSV08]. Below we summarize their definitions of the boundary measurement map and the space of face and trail weights. We further consider the usefulness of the plabic network structure in this space.

The work presented in this chapter, as well as Chapters 6 through 8 appear in [Che20].

5.1 Planar Directed Networks on a Cylinder

Throughout this paper, we will draw a cylinder as a fundamental domain of its universal cover such that it is a rectangle with boundary components on the left and right (see Figure 5.1).

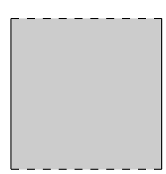

Figure 5.1: A cylinder, as we will represent them in this paper.

The constructions in this section may be found in [GSV08]. They are based on Postnikov's theory of planar directed networks in a disk [Pos06], as seen in Chapter 4.

For a planar directed graph or network on a cylinder, we will label the boundary vertices $b_1, ..., b_n$ from the top of the left boundary component to the bottom and then from the bottom of the right boundary component to the top.

Definition 5.1.1. A *cut* γ is an oriented non-self-intersecting curve from one boundary component to another, considered up to homotopy. The endpoints of the cut are *base points*. We will always assume the cut is disjoint from the set of vertices of the graph and that it corresponds to the top and bottom of our rectangle when we draw a cylinder. The cut is denoted by a directed dashed line.

Definition 5.1.2. For a path P, the *intersection number*, $int(P)$, is the number of times P crosses γ from the right minus the number where P crosses γ from the left.

Definition 5.1.3. If P is a path from b to b' where b, b' are on the same boundary component, then C_P is the closed loop created from following the path P and then going down along the boundary from b' to b. If P is a path from b to b' where b, b' are on the different boundary components, then C_P is the closed loop created from following the path P going down on the boundary from b' to the base point of the cut, following the cut (or its reverse), and then down on the boundary from base point of the cut to b.

Definition 5.1.4. We can glue together the top and bottom of our rectangle, which represents a cylinder, in the plane to form an annulus. Do this such that going up along the boundary of the rectangle corresponds to going clockwise around the boundary of the annulus (see Figure 5.2). Then for a path P, the *winding index* of P is defined to be $wind(C_P)$, when C_P is drawn on this annulus and $wind(C_P)$ is calculated as in Definition 4.2.3.

Example 5.1.5.

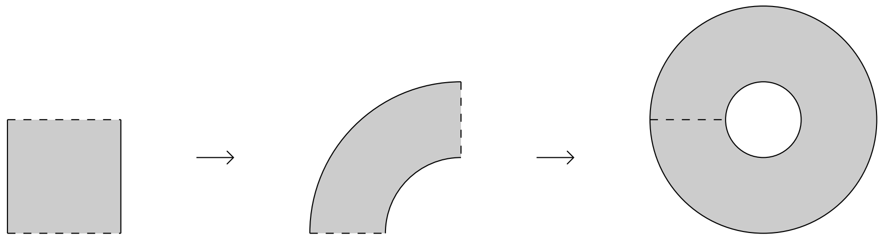

Figure 5.2: Turning a cylinder into an annulus.

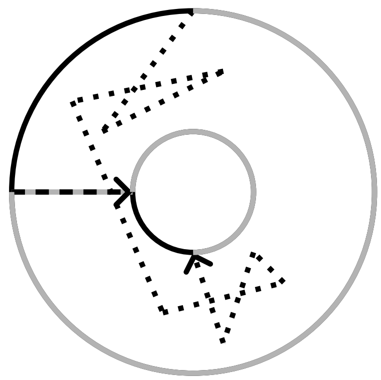

Here we have the cylinder depicted as an annulus. The dashed line is the cut. A path P is shown as a dotted line. P crosses the cut once from left to right, so $int(P) = -1$. The extension of P to C_P is shown in gray. We can see $wind(C_P) = -3$.

Definition 5.1.6. Let b_i be a source and b_j be a sink in a planar directed network on a cylinder with graph G. Let the edge weights be the formal variables x_e. Then the *formal boundary measurement* M_{ij}^{form} is the formal power series

$$M_{ij}^{\text{form}} := \sum_{\substack{\text{paths } P \text{ from} \\ b_i \text{ to } b_j}} (-1)^{wind(C_P)-1} \zeta^{int(P)} \, \text{wt}(P).$$

Lemma 5.1.7 (Corollary 2.3 of [GSV08]). *If N is a planar network on a cylinder, then the formal power series M_{ij}^{form} sum to rational expressions in the variables x_e and ζ.*

Definition 5.1.8. The *boundary measurements* M_{ij} for a planar directed network on a cylinder are rational functions in ζ obtained by writing the formal boundary measurements M_{ij}^{form} as rational expressions, and then specializing them by assigning x_e the real weight of the edge e.

Example 5.1.9. Suppose we have the following network:

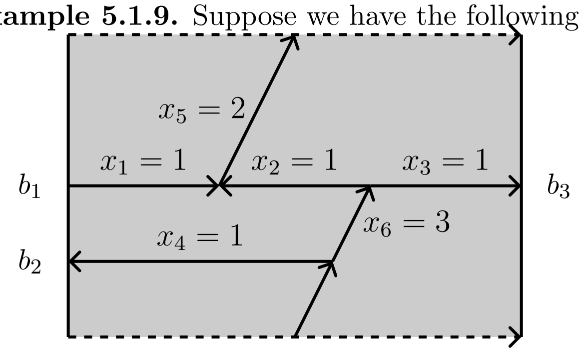

$$\begin{aligned} M_{12}^{\text{form}} &= x_1x_5x_4\zeta - x_1x_5x_6x_2x_5x_4\zeta^2 + x_1x_5x_6x_2x_5x_6x_2x_5x_4\zeta^3 ... \\ &= x_1x_5x_6\zeta \sum_{i=0}^{\infty}(-x_5x_6x_2\zeta)^i \\ &= \frac{x_1x_5x_6\zeta}{1+x_5x_6x_2\zeta} \\ M_{13}^{\text{form}} &= -x_1x_5x_6x_3\zeta + x_1x_5x_6x_2x_5x_6x_3\zeta^2 - x_1x_5x_6x_2x_5x_6x_2x_5x_6x_3\zeta^3 ... \\ &= -x_1x_5x_6x_3\zeta \sum_{i=0}^{\infty}(-x_5x_6x_2\zeta)^i \\ &= \frac{-x_1x_5x_6x_3\zeta}{1+x_5x_6x_2\zeta} \end{aligned}$$

Substituting our values for the x_e's, we find $M_{12} = \frac{2\zeta}{1+6\zeta}$ and $M_{13} = \frac{-6\zeta}{1+6\zeta}$.

Definition 5.1.10. The *space of Grassmannian loops*, $LGr_{k,n}(\mathbb{R})$ is the space of rational functions $X : \mathbb{R} \to Gr_{k,n}(\mathbb{R})$. Elements in $LGr_{k,n}(\mathbb{R})$ can be represented as a full-rank $k \times n$ matrix where the entries are functions of a parameter ζ.

Definition 5.1.11. If Net_{kn}^C is the set of planar directed networks on a cylinder with k boundary sources and $n-k$ boundary sinks, we can define the *boundary measurement map* as $Meas^C : Net_{k,n}^C \to LG_{k,n}(\mathbb{R})$ where $Meas^C(N)$ is represented by the matrix $A(N)$ such that:

(1) $A(N)_I$ is the identity Id_k.

(2) For $I = \{i_1 < ... < i_k\}, r \in [k]$, and $b_j \in \overline{I}$, we define $a_{rj} = (-1)^s M_{i_r,j}$, where s is the number of elements of I strictly between i_r and j.

Note that the map $Meas^C$ is constructed so that $M_{ij} = \Delta(A(N))_{(I\setminus\{i\})\cup\{j\}}$.

Example 5.1.12. Consider the network from the previous example:

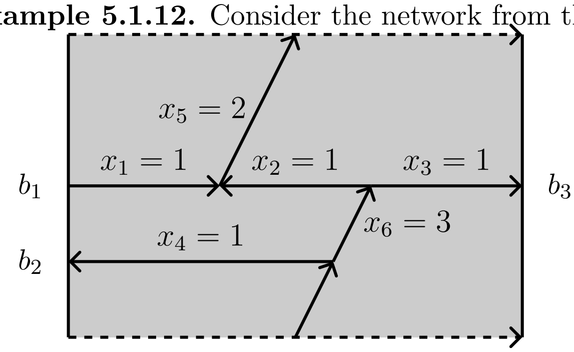

In this case $I = \{1\}$, so we put Id_1 in the first column of $A(N)$.
We compute $a_{12} = (-1)^0 M_{12} = \frac{2\zeta}{1+6\zeta}$ and $a_{13} = (-1)^0 M_{13} = \frac{-6\zeta}{1+6\zeta}$.
So, we have $A(N) = \begin{bmatrix} 1 & \frac{2\zeta}{1+6\zeta} & \frac{-6\zeta}{1+6\zeta} \end{bmatrix}$.

5.2 Face Weights on the Cylinder

Now that we've defined the boundary measurement map for planar directed networks on the cylinder, we can turn to the inverse boundary problem. Just as in the disk setting, gauge transformations don't affect the boundary measurements of our networks. To eliminate these, we will move from an edge-weighted setting to a face-weighted setting. We will define our face weights the same way we did in a disk (see Definition 4.3.7). However, in this case we will also need to include an additional parameter. We can see this must be true from a theoretical perspective because the Euler characteristic of a disk is 1, allowing the dimensions of $\mathbb{R}^E$ and $\mathbb{R}^{F-1}$ in 4.3.8 to match, but the Euler characteristic of a cylinder is 0. From a more experimental perspective, we can see that face weights alone would not give enough information to define the path weights as before.

Definition 5.2.1 (Section 2.3 of [GSV08])**.** A *trail* in a planar directed network on a cylinder N is a sequence of vertices $v_1, ..., v_{m+1}$ where v_1, v_{m+1} are boundary vertices on different boundary components and for each i, either (v_i, v_{i+1}) or (v_{i+1}, v_i) is an edge in N. The *weight* of a trail is

$$t = \left(\prod_{(v_i,v_{i+1}) \text{ an edge in } N} x_{(v_i,v_{i+1})} \right) \left(\prod_{(v_{i+1},v_i) \text{ an edge in } N} x^{-1}_{(v_{i+1},v_i)} \right).$$

Notice that a trail weight is invariant under gauge transformations.

Theorem 5.2.2 (Section 2.3 of [GSV08])**.** *For a planar directed graph G on a cylinder with edge set E and face set F,*

$$\mathbb{R}^E_{>0}/\{\textit{gauge transformations}\} = \begin{cases} \mathbb{R}^{F-1}_{>0} & \textit{if there is no trail,} \\ \mathbb{R}^{F-1}_{>0} \oplus \mathbb{R}_{>0} & \textit{otherwise,} \end{cases}$$

where $\mathbb{R}^{F-1}_{>0}$ is generated by the face weights under the relation that their product be equal to 1 and $\mathbb{R}_{>0}$ in the second case is generated by the weight of a trail.

Having a network that falls under the first case is equivalent to having a network in a disk. In this case, we recover Postnikov's face weight construction for planar directed networks in a disk.

Definition 5.2.3. We will define $\text{wt}(P, y, t)$ in three cases:

(1) For a path P that begins and ends on the same boundary component, draw enough copies of the fundamental domain that we can draw P as a connected curve. If P is path from b_i to b_j, then P along with a segment of the boundary between b_i and b_j form a closed shape P_b on the universal cover. When P_b is to the right of P, $\text{wt}(P, y, t)$ is the product of the weights of the faces in the interior of P_b. When P_b is to the left of P, $\text{wt}(P, y, t)$ is the inverse of this product.

(2) For a path P that begins on the same boundary component as the trail and ends on the other boundary component, draw enough copies of the fundamental domain we that we can draw P as a connected curve and that there is at least one copy of the trail that lies completely to the right of P. Then $\text{wt}(P, y, t)$ is the product of the weights of the faces that lie to the right of P and to the left of a copy of the trail that is completely to the right of P times the weight of the trail.

(3) For a path P that begins on the boundary component where the trail ends and ends on the other boundary component, draw enough copies of the fundamental domain we that we can draw P as a connected curve and that there is at least one copy of the trail that lies completely to the right of P. Then $\mathrm{wt}(P, y, t)$ is the product of the weights of the faces that lie to the right of P and to the right of a copy of the trail that is completely to the right of P times the inverse of the weight of the trail.

Example 5.2.4. Suppose we have the following network with face and trail weights:

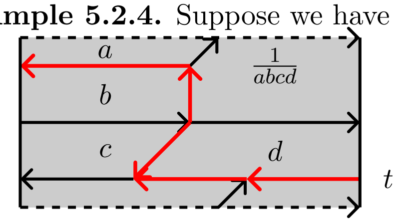

The trail appears in red, the trail weight is listed to the left of the network, and the trail is oriented from right to left.

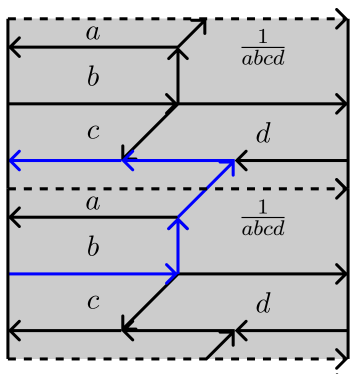

For the path P shown in blue, the interior of P_b is to the left of P. So, $\mathrm{wt}(P, y, t) = \frac{1}{ab}$.

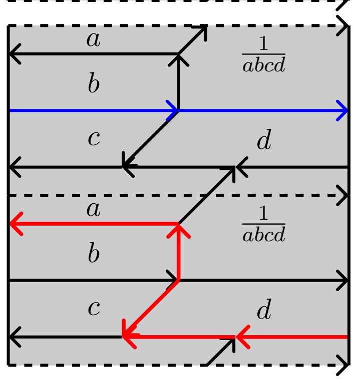

For the path P shown in blue, P is going in the opposite direction of the trail. So, $\mathrm{wt}(P, y, t) = \frac{d}{tb}$.

Remark 5.2.5. In Cases 2 and 3 of Definition 5.2.3, $\mathrm{wt}(P, y, t)$ is well-defined because if we choose two trails that lie completely to the right of P, the product of the weights of faces between the trails is 1.

Theorem 5.2.6. *For a path P in a planar directed network on a cylinder,*

$$\mathrm{wt}(P, y, t) = \mathrm{wt}(P).$$

Proof. We can see this by counting how many times the weight of an edge and its inverse are in the product $\mathrm{wt}(P, y, t)$ when the edge is in P, when it's is between P and the boundary component P that makes up part of P_b (in Case 1), and when it's between P and the trail (in Case 2 and 3). □

5.3 Changing Orientation on the Cylinder

In order to move from planar directed networks to plabic networks in a disk, we needed to be able to define the boundary measurement map for a face weighted network and we also needed to be able to reverse the orientation of paths and cycles in a network without affecting its image under the boundary measurement map. In the previous section, we showed how to do the first of these on the cylinder. However, Gekhtman, Shapiro, and Vainshtein [GSV08] showed that the second does not hold.

Theorem 5.3.1 (Theorem 4.1 of [GSV08])**.** *Let P be a path with no self-intersections from b_i to b_j in a planar directed network on a cylinder N such that $M_{ij} \not\equiv 0$ and P does not intersect the cut. Create N' from N by reversing the direction of all the edges in P and inverting their weights. Then*

$$(Meas^C(N'))(\zeta) = \begin{cases} (Meas^C(N))(\zeta) & b_i, b_j \text{ are on the same boundary component,} \\ (Meas^C(N))(-\zeta) & \text{otherwise.} \end{cases}$$

Since we cannot necessarily reverse paths that begin and end on different boundary components without changing the image of the network under the boundary measurement map, we cannot turn planar directed networks on a cylinder into plabic networks. In particular, we have to keep track of the orientation of the edges. However, as path reversal changes the boundary measurements in a predictable way, plabic networks will still prove useful to us (see Theorem 5.3.3).

Proposition 5.3.2 (Proposition 2.1 of [GSV08])**.** *Let N, N' be two networks with the* *same graph and weights, where N has cut γ and N' has cut γ' obtained by interchanging one of the base points with b, the first boundary vertex below the base point. Then*

$$(-1)^{wind(C'_P)-1}\zeta^{int(P')}\,\mathrm{wt}(P') = ((-1)^{\alpha(P)}\zeta)^{\beta(b,P)}(-1)^{wind(C_P)-1}\zeta^{int(P)}\,\mathrm{wt}(P),$$

and

$$\alpha(P) = \begin{cases} 0 & \textit{if the endpoints of } P \textit{ are on the same boundary component,} \\ 1 & \textit{otherwise,} \end{cases}$$

$$\beta(b,P) = \begin{cases} 1 & \textit{if } b \textit{ is the sink of } P, \\ -1 & \textit{if } b \textit{ is the source of } P, \\ 0 & \textit{otherwise.} \end{cases}$$

Theorem 5.3.3. *Let N, N' be two perfect networks on a cylinder such that:*

(1) The underlying graphs G and G' are isomorphic as undirected graphs.

(2) Each internal vertex of degree $\neq 2$ has $col_N(v) = col_{N'}(v)$.

(3) If the undirected edge e is directed in the same way in N and N', then $x_e = x'_e$. If the edge e has opposite direction in N and N', then $x_e = (x'_e)^{-1}$.

Given an involution on the edge weights of N that preserves the boundary measurement map, then there is a canonical way to define an involution of the edge weights of N'.

Proof. As with planar directed networks on a disk, we can always obtain N' from N by reversing a set of paths and cycles. Therefore, we only need to show the conclusion shows for N' equal to N with a cycle (with no self-intersections) reversed or N with a path (with no self-intersections) reversed.

First consider a cycle C with no self-intersections. If C is a contractible loop, then the proof that reversing cycles on a disk does not change the boundary measurements still holds (Lemma 10.5 of [Pos06]).

If C is not a contractible loop, a similar proof holds, except that the winding number is more complicated. We consider what happens for paths that have edges in C. First, for paths that begin and end on the same boundary component, the winding numbers behave the same as for networks on a disk. So, the boundary measurements for pairs of vertices on the same boundary component remain the same. Now consider paths that begin and end on different components. For vertices v_i and v_j in the cycle, going from v_i to v_j in one direction around the cycle, with as many loops as desired, crosses the cut the same number of times from each side and going from v_i to v_j in the other direction crosses the cut one more time from one side than from the other. Crossing the cut an additional time adds or removes a loop in C_P as we trace along the cut. So, we get an extra factor of -1 in the boundary measurements for pairs of vertices on different boundary components.

For any cycle in N' with no self-intersections, we can reverse the cycle, apply our involution, and reverse the cycle again. Any boundary measurements that change when we reverse the cycle change only by a factor of -1, and they change again by the same factor when we reverse the cycle a second time. So, for any cycle C, we have the following commutative diagram, where f is defined to be the map that makes this diagram commute:

$$\begin{array}{ccc} N & \xleftrightarrow{\text{cycle reversal}} & N' \\ {\scriptstyle \text{involution}}\updownarrow & & \downarrow {\scriptstyle f} \\ \widetilde{N} & \xleftrightarrow[\text{cycle reversal}]{} & \widetilde{N'} \end{array}$$

f is an involution that preserves the boundary measurements.

Now consider a path P with no self-intersections. If P does not intersect the cut, Theorem 5.3.1 says we can reverse P, possibly at the expense of replacing ζ with $-\zeta$. If P does intersect the cut, we can move the cut so that P no longer intersects it. Moving the cut changes the weight of each path by a power of ζ and a power of -1. These powers depend only on the source and sink of the path, so it changes the weight of each boundary measurement by a power of ζ and a power of -1. Then reversing the path, since it no longer intersects the cut, either keeps the boundary measurement map the same, or replaces ζ with $-\zeta$. Finally, we can move the cut back, which will cause each boundary measurement to again pick up a power of -1 and a power of ζ. This process gives us the following commutative diagram, where f is defined to be the map that makes the diagram commute and g is the composition of functions:

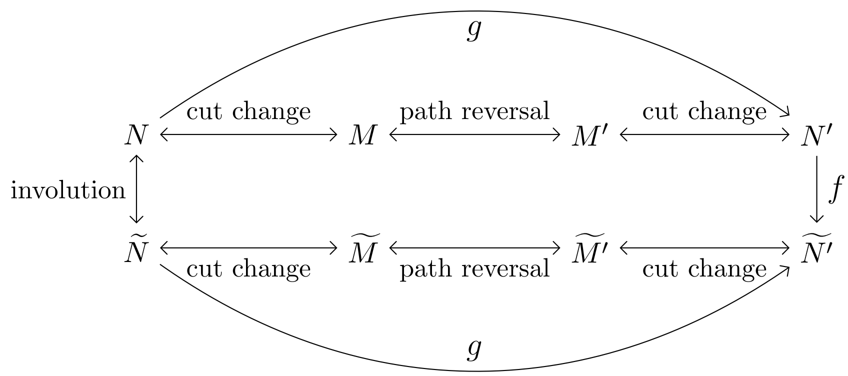

It is clear f is an involution, so we just need to check that $Meas^C(N') = Meas^C(\widetilde{N'})$. Given a matrix representing the image of a network under the boundary measurement map, g is equivalent to possibly switching ζ for $-\zeta$ and multiplying each entry by a power of -1 and a power of ζ. Since $Meas^C(N) = Meas^C(\widetilde{N})$, we can pick the same matrix representative for them, and we can see $Meas^C(g(N)) = Meas^C(g(\widetilde{N}))$ □

Since the plabic network structure is useful to us, but also we can't eliminate orientation, we will be working with directed plabic networks for the rest of this thesis.

Definition 5.3.4. A *directed plabic graph* on a cylinder is a planar directed graph on a cylinder such that each boundary vertex has degree 1 and each internal vertex is colored black of white. A *directed plabic network* on a cylinder is a directed plabic graph with a weight $y_f \in \mathbb{R}_{>0}$ assigned to each face and a specified trail with weight t.

Chapter 6

Plabic R-matrix

In this section we will explore a semi-local transformation of directed plabic networks on a cylinder that doesn't change the boundary measurements. We note that Postnikov's moves (see 4.4) still hold for plabic networks on a disk. In addition, these moves specialize to directed edge-weighted moves. For the rest of this section, we will be using these moves freely and considering (directed) plabic networks that differ by them to be equivalent.

6.1 Cylindric k-loop Plabic Graphs

We begin by revisiting Postnikov diagrams. The definition of a Postnikov diagram can easily be generalized for our setting.

Definition 6.1.1. A *Postnikov diagram*, also known as an alternating strand diagram, on a surface with boundary is a set of directed curves on the surface, called *strands*, such that when we draw the strands on the universal cover of the surface we have the following:

(1) Each strand begins and ends at a boundary vertex or is infinite.

(2) There is exactly one strand that enters and one strand that leaves each boundary vertex.

(3) No three strands intersect at the same point.

(4) All intersections are transverse (the tangent vectors are independent).

(5) There is a finite number of intersections in each fundamental domain.

(6) Along any strand, the strands that cross it alternate crossing from the left and crossing from the right.

(7) Strands do not have self-intersections, except in the case where a strand is a loop attached to a boundary vertex. Notice that this excludes the possibility of a closed cycle.

(8) If two strands intersect at u and v, then one strand is oriented from u to v and one strand is oriented from v to u.

Postnikov diagrams on a surface give rise to plabic networks by the same process as in a disk.

Theorem 6.1.2. *Postnikov diagrams on a cylinder are in bijection with leafless reduced plabic graphs on a cylinder with no unicolored edges.*

See Section 6.4.1 for proof.

Definition 6.1.3. A cylindric k-loop plabic graph is a plabic graph on a cylinder that arises from a Postnikov diagram where exactly k of the strands are loops around the cylinder with the same orientation.

Cylindric k-loop plabic graphs have k strings of vertices around the cylinder. Those strings alternate black and white vertices, and the black vertices only have additional edges on the left of the strand while the white vertices only have additional edges to the right of the strand (see Figure 6.1).

Definition 6.1.4. For a cylindric k-loop plabic graph, any vertices that are not on one of the strings of vertices defined by the k loops and lie between two of these strings are called *interior vertices.*

Theorem 6.1.5. *Any cylindric k-loop plabic graph can be transformed by moves to one that has no interior vertices.*

See Section 6.4.2 for proof.

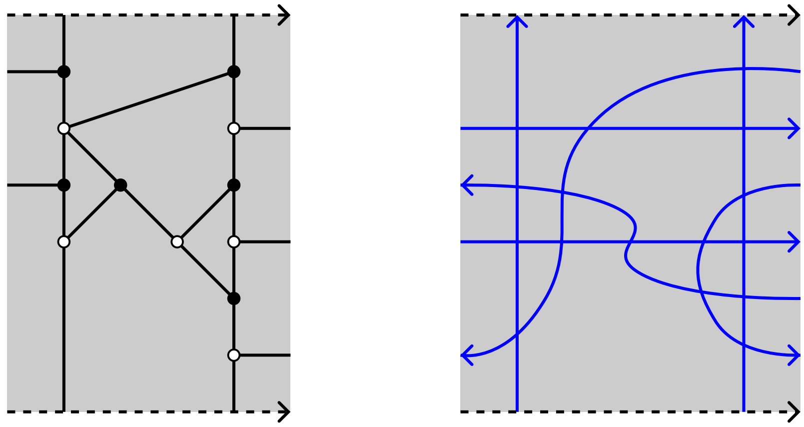

Figure 6.1: A cylindric 2-loop plabic graph and its Postnikov diagram.

6.2 Edge-weighted Plabic R-matrix

Consider a cylindric k-loop plabic graph. By Theorem 6.4.9, we can assume there are no interior vertices. We will be describing an involution on the edge weights of adjacent strings and the edges between them, so we'll ignore the rest of the graph. That is, we'll assume we have a cylindric k-loop plabic graph with no vertices other than those on the k strings. We label these strings 1 through k from left to right.

Definition 6.2.1. The *canonical orientation* of a cylindric k-loop plabic graph with no interior vertices is the orientation where the edges on the strings are oriented up and the other edges are oriented from left to right.

For the rest of this thesis, we will assume all directed cylindric k-loop plabic graphs have the canonical orientation. Let us choose the edges from white vertices to black vertices to be variables, and set all the other edges to have weight 1. We do this to have a canonical way to kill the gauge transformations on our network (notice the number of variables is the number of faces, or the dimension of $\mathbb{R}^E/\{\text{gauge transformations}\}$). In our diagrams, any edges that are not labeled are assumed to have weight 1. We now have a directed plabic network.

Definition 6.2.2. For $1 \leq \varkappa < k$, we can expand the directed plabic network by splitting each vertex in strings $\varkappa$ and $\varkappa+1$ that have multiple edges to the other string into that many vertices, and inserting vertices of the opposite color between them. Let any new edges created have weight 1. Thus, we have a new network that is equivalent to the old one, but all the faces between strings $\varkappa$ and $\varkappa+1$ are hexagons where the colors of the vertices alternate and where there are 2 white vertices on string $\varkappa$ and 2 black vertices on the string $\varkappa+1$. We'll call this the *$\varkappa$-expanded directed plabic network.*

Choose a white vertex on string $\varkappa$ of a $\varkappa$-expanded directed cylindric k-loop plabic network. Call the weight of the edge from this vertex to the black vertex above it on the string x_1. For the white vertex on string $\varkappa+1$ that is part of the same face as these two vertices, call the weight of the edge from this vertex to the black vertex above it on the string y_1. Call the weight of the edge that makes up the upper boundary of the face containing these vertices z_1. Moving up string $\varkappa$, give the next white to black edge the weight x_2, and so on. Do the same on string $\varkappa+1$. Moving in the same direction, label all the edges between the strings with weights z_2, z_3, etc. For a particular network, some of these values might be set to 1, because we created the edges when we expanded the network. Let $x = \{x_1, x_2, ..., x_n\}, y = \{y_1, y_2, ..., y_n\}, z = \{z_1, z_2, ..., z_n\}$. We will consider all of these indices to be modular. If $1 \leq i < j \leq n$, let $[i, j]$ denote the set $\{i, i+1, ..., j\}$. If $1 \leq j < i \leq n$ let $[i, j]$ denote the set $\{i, i+1, ..., n, 1, 2, ..., j\}$. For any set S, let $S + k := \{s + k \mid s \in S\}$. We'll define $\mathbf{x}_S := \prod_{i \in S} x_i$, and similarly for $\mathbf{y}_S$.

Consider the network on the universal cover of the cylinder. Choose a fundamental domain. Label all the edge weights in the fundamental domain with a superscript (1), so the weights on and between strings $\varkappa$ and $\varkappa+1$ are $x_1^{(1)}, y_1^{(1)}, z_1^{(1)}, x_2^{(1)}$, etc. Label all the edge weights in the copy of the fundamental domain that lies above with a superscript (2), and so on. Define $\lambda_i(x, y, z)$ to be the sum of the weights of paths from a to b, where a is a the highest vertex on string $\varkappa$ of the face between strings $\varkappa$ and $\varkappa+1$ that has an edge labeled $x_i^{(1)}$ and b is the lowest vertex on string $\varkappa+1$ of the face between strings $\varkappa$ and $\varkappa+1$ that has an edge labeled $x_i^{(2)}$. Define $\mathcal{X}_i := \{j \mid x_j = x_{j+1} = ... = x_{i-1} = 1\}$ and $\mathcal{Y}_i := \{j \mid y_j = y_{j-1} = ... = y_{i+1} = 1\}$.

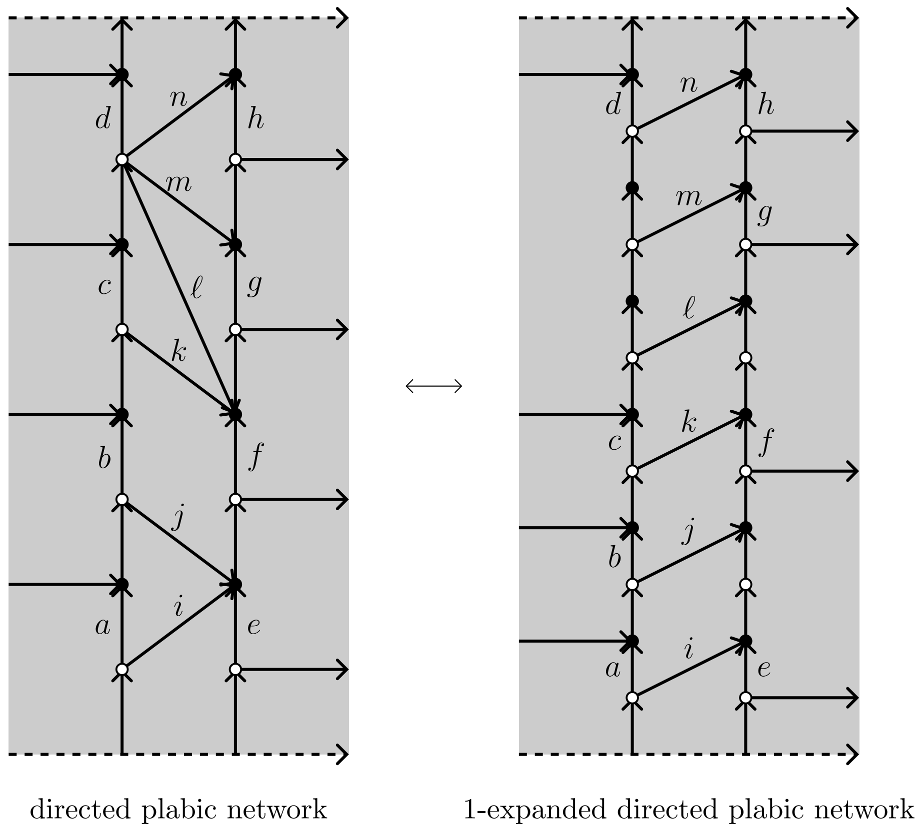

Figure 6.2: A directed plabic network and the corresponding 1-expanded directed plabic network.

Example 6.2.3. Consider the network below:

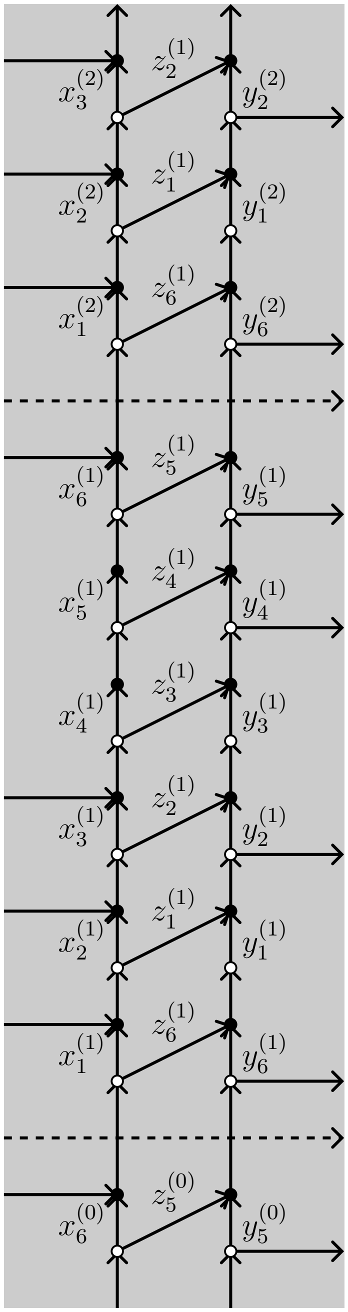

$\lambda_1(x,y,z)$ is the sum of weights of paths from the vertex at the bottom of $x_2^{(1)}$ to the vertex at the top of $y_6^{(2)}$, so $\lambda_1(x,y,z) = z_1\,\mathbf{y}_{[2,6]} + x_2 z_2\,\mathbf{y}_{[3,6]} + \mathbf{x}_{[2,3]}\,z_3\,\mathbf{y}_{[4,6]} + \mathbf{x}_{[2,4]}\,z_4\,\mathbf{y}_{[5,6]} + \mathbf{x}_{[2,5]}\,z_5 y_6 + \mathbf{x}_{[2,6]}\,z_6$.

$\mathcal{X}_1 = \emptyset$ because there are no weights directly below x_1 set to 1 from expanding the network.

$\mathcal{Y}_1 = \emptyset$ because there are no weights directly above y_1 set to 1 from expanding the network.

$\lambda_2(x,y,z) = z_2\,\mathbf{y}_{[3,1]} + x_3 z_3\,\mathbf{y}_{[4,1]} + \mathbf{x}_{[3,4]}\,z_4\,\mathbf{y}_{[5,1]} + \mathbf{x}_{[3,5]}\,z_5\,\mathbf{y}_{[6,1]} + \mathbf{x}_{[3,6]}\,z_6 y_1 + \mathbf{x}_{[3,1]}\,z_1$.

$\mathcal{X}_2 = \emptyset$ because there are no weights directly below x_2 set to 1 from expanding the network.

$\mathcal{Y}_2 = \{3\}$ because y_3, which is directly above y_2 is set to 1 from expanding the network, but y_4 is not set to 1.

Definition 6.2.4. Define $T_{\varkappa,e}$ to be the transformation on edge weights from (x, y, z) to (x', y', z') where

$$x'_i = \begin{cases} 1 & x_i \text{ set to } 1, \\ \dfrac{y_{i-1}\,\mathbf{y}_{\mathcal{X}_i-1}\,\lambda_{i-|\mathcal{X}_i|-1}(x,y,z)}{\lambda_i(x,y,z)} & \text{otherwise,} \end{cases}$$

$$y'_i = \begin{cases} 1 & y_i \text{ set to } 1, \\ \dfrac{x_{i+1}\,\mathbf{x}_{\mathcal{Y}_i+1}\,\lambda_{i+|\mathcal{Y}_i|+1}(x,y,z)}{\lambda_i(x,y,z)} & \text{otherwise,} \end{cases}$$

$$z'_i = \frac{\mathbf{x}_{\mathcal{Y}_i+1}\,\mathbf{y}_{\mathcal{X}_i-1}\,z_i\lambda_{i-|\mathcal{X}_i|-1}(x,y,z)\lambda_{i+|\mathcal{Y}_i|+1}(x,y,z)}{\lambda_{i-1}(x,y,z)\lambda_{i+1}(x,y,z)}.$$

We call $T_{\varkappa,e}$ the edge weighted *plabic R-matrix*.

Theorem 6.2.5. *$T_{\varkappa,e}$ has the following properties:*

1. *It preserves the boundary measurements.*

2. *It is an involution.*

3. *(x, y, z) and (x', y', z') are the only choices of weights on a fixed cylindric 2-loop plabic graph that preserve the boundary measurements.*

4. *It satisfies the braid relation. That is, for $1 \leq \varkappa < k-1$, $T_{\varkappa,e} \circ T_{\varkappa+1,e} \circ T_{\varkappa,e} = T_{\varkappa+1,e} \circ T_{\varkappa,e} \circ T_{\varkappa+1,e}$.*

See Section 6.5 for proof.

Example 6.2.6. Consider the network below:

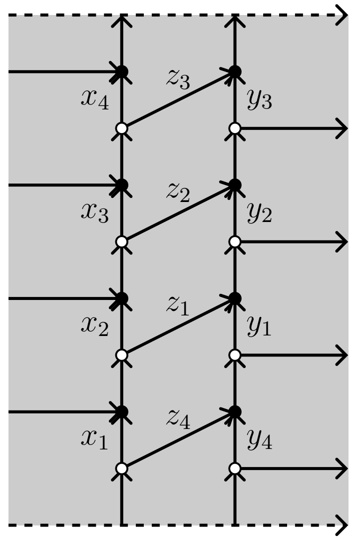

$T_{1,e}$ gives us the following values:

$$x'_1 = \frac{y_4\lambda_4(x,y,z)}{\lambda_1(x,y,z)} = \frac{\mathbf{x}_{[1,3]}\, y_4 z_3 + \mathbf{x}_{[1,2]}\,\mathbf{y}_{[3,4]}\, z_2 + x_1\,\mathbf{y}_{[2,3]}\, z_1 + \mathbf{y}_{[1,4]}\, z_4)}{\mathbf{x}_{[2,4]}\, z_4 + \mathbf{x}_{[2,3]}\, y_4 z_3 + x_2\,\mathbf{y}_{[3,4]}\, z_2 + \mathbf{y}_{[2,4]}\, z_1}$$

$$x'_2 = \frac{y_1\lambda_1(x,y,z)}{\lambda_2(x,y,z)} = \frac{\mathbf{x}_{[2,4]}\, y_1 z_4 + \mathbf{x}_{[2,3]}\,\mathbf{y}_{[4,1]}\, z_3 + x_2\,\mathbf{y}_{[3,1]}\, z_2 + \mathbf{y}_{[2,1]}\, z_1}{\mathbf{x}_{[3,1]}\, z_1 + \mathbf{x}_{[3,4]}\, y_1 z_4 + x_3\,\mathbf{y}_{[4,1]}\, z_3 + \mathbf{y}_{[3,1]}\, z_2}$$

$$x'_3 = \frac{y_2\lambda_2(x,y,z)}{\lambda_3(x,y,z)} = \frac{\mathbf{x}_{[3,1]}\, y_2 z_1 + \mathbf{x}_{[3,4]}\,\mathbf{y}_{[1,2]}\, z_4 + x_3\,\mathbf{y}_{[4,2]}\, z_3 + \mathbf{y}_{[3,2]}\, z_2}{\mathbf{x}_{[4,2]}\, z_2 + \mathbf{x}_{[4,1]}\, y_2 z_1 + x_4\,\mathbf{y}_{[1,2]}\, z_4 + \mathbf{y}_{[4,2]}\, z_3}$$

$$x'_4 = \frac{y_3\lambda_3(x,y,z)}{\lambda_4(x,y,z)} = \frac{\mathbf{x}_{[4,2]}\, y_3 z_2 + \mathbf{x}_{[4,1]}\,\mathbf{y}_{[2,3]}\, z_1 + x_4\,\mathbf{y}_{[1,3]}\, z_4 + \mathbf{y}_{[4,3]}\, z_3}{\mathbf{x}_{[1,3]}\, z_3 + \mathbf{x}_{[1,2]}\, y_3 z_2 + x_1\,\mathbf{y}_{[2,3]}\, z_1 + \mathbf{y}_{[1,3]}\, z_4}$$

$$y'_1 = \frac{x_2\lambda_2(x,y,z)}{\lambda_1(x,y,z)} = \frac{\mathbf{x}_{[2,1]}\, z_1 + \mathbf{x}_{[2,4]}\, y_1 z_4 + \mathbf{x}_{[2,3]}\,\mathbf{y}_{[4,1]}\, z_3 + x_2\,\mathbf{y}_{[3,1]}\, z_2}{\mathbf{x}_{[2,4]}\, z_4 + \mathbf{x}_{[2,3]}\, y_4 z_3 + x_2\,\mathbf{y}_{[3,4]}\, z_2 + \mathbf{y}_{[2,4]}\, z_1}$$

$$y'_2 = \frac{x_3\lambda_3(x,y,z)}{\lambda_2(x,y,z)} = \frac{\mathbf{x}_{[3,2]}\, z_2 + \mathbf{x}_{[3,1]}\, y_2 z_1 + \mathbf{x}_{[3,4]}\,\mathbf{y}_{[1,2]}\, z_4 + x_3\,\mathbf{y}_{[4,2]}\, z_3}{\mathbf{x}_{[3,1]}\, z_1 + \mathbf{x}_{[3,4]}\, y_1 z_4 + x_3\,\mathbf{y}_{[4,1]}\, z_3 + \mathbf{y}_{[3,1]}\, z_2}$$

$$y'_3 = \frac{x_4\lambda_4(x,y,z)}{\lambda_3(x,y,z)} = \frac{\mathbf{x}_{[4,3]}\, z_3 + \mathbf{x}_{[4,2]}\, y_3 z_2 + \mathbf{x}_{[4,1]}\,\mathbf{y}_{[2,3]}\, z_1 + x_4\,\mathbf{y}_{[1,3]}\, z_4}{\mathbf{x}_{[4,2]}\, z_2 + \mathbf{x}_{[4,1]}\, y_2 z_1 + x_4\,\mathbf{y}_{[1,2]}\, z_4 + \mathbf{y}_{[4,2]}\, z_3}$$

$$y'_3 = \frac{x_1\lambda_1(x,y,z)}{\lambda_4(x,y,z)} = \frac{\mathbf{x}_{[1,4]}\, z_4 + \mathbf{x}_{[1,3]}\, y_4 z_3 + \mathbf{x}_{[1,2]}\,\mathbf{y}_{[3,4]}\, z_2 + x_1\,\mathbf{y}_{[2,4]}\, z_1)}{\mathbf{x}_{[1,3]}\, z_3 + \mathbf{x}_{[1,2]}\, y_3 z_2 + x_1\,\mathbf{y}_{[2,3]}\, z_1 + \mathbf{y}_{[1,3]}\, z_4}$$

$$z'_1 = z_1$$

$$z'_2 = z_2$$

$$z'_3 = z_3$$

$$z'_4 = z_4$$

Notice that in this example, the directed plabic network is the same as the 1-expanded directed plabic network. These types of networks are of particular interest to us, both because of their simplicity and because they correspond to the simple-crossing networks studied in Section 6 of [LP12] where the horizontal wires are all in the same direction and either all the wire cycles are whirls or all the wire cycles are curls. Thus, if we let all of our z variables equal 1, we have recovered the whurl relation of [LP12], which is also the geometric R-matrix.

Example 6.2.7. Consider the network below:

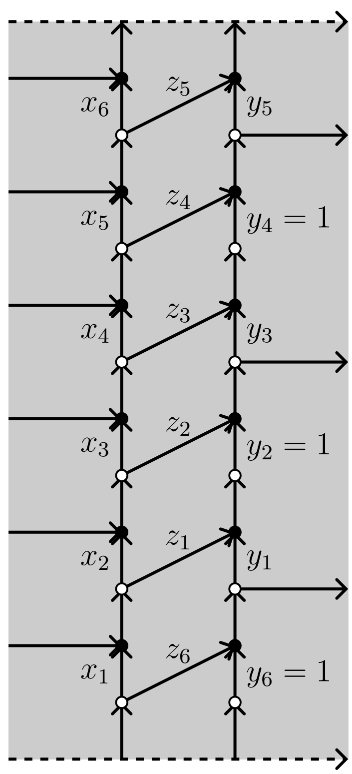

$T_{1,e}$ gives us the following values:

$$x_1' = \frac{y_6\lambda_6(x,y,z)}{\lambda_1(x,y,z)} = \frac{\mathbf{x}_{[1,5]}\,z_5 + \mathbf{x}_{[1,4]}\,y_5z_4 + \mathbf{x}_{[1,3]}\,y_5z_3 + \mathbf{x}_{[1,2]}\,\mathbf{y}_{3,5}\,z_2 + x_1\,\mathbf{y}_{3,5}\,z_1 + \mathbf{y}_{1,3,5}\,z_6}{\mathbf{x}_{[2,6]}\,z_6 + \mathbf{x}_{[2,5]}\,z_5 + \mathbf{x}_{[2,4]}\,y_5z_4 + \mathbf{x}_{[2,3]}\,y_5z_3 + x_2\,\mathbf{y}_{3,5}\,z_2 + \mathbf{y}_{3,5}\,z_1}$$

$$x_2' = \frac{y_1\lambda_1(x,y,z)}{\lambda_2(x,y,z)} = \frac{y_1(\mathbf{x}_{[2,6]}\,z_6 + \mathbf{x}_{[2,5]}\,z_5 + \mathbf{x}_{[2,4]}\,y_5z_4 + \mathbf{x}_{[2,3]}\,y_5z_3 + x_2\,\mathbf{y}_{3,5}\,z_2 + \mathbf{y}_{3,5}\,z_1)}{\mathbf{x}_{[3,1]}\,z_1 + \mathbf{x}_{[3,6]}\,y_1z_6 + \mathbf{x}_{[3,5]}\,y_1z_5 + \mathbf{x}_{[3,4]}\,\mathbf{y}_{1,5}\,z_4 + x_3\,\mathbf{y}_{1,5}\,z_3 + \mathbf{y}_{1,3,5}\,z_2}$$

$$x_3' = \frac{y_2\lambda_2(x,y,z)}{\lambda_3(x,y,z)} = \frac{\mathbf{x}_{[3,1]}\,z_1 + \mathbf{x}_{[3,6]}\,y_1z_6 + \mathbf{x}_{[3,5]}\,y_1z_5 + \mathbf{x}_{[2,4]}\,\mathbf{y}_{1,5}\,z_4 + x_3\,\mathbf{y}_{1,5}\,z_3 + \mathbf{y}_{1,3,5}\,z_2}{\mathbf{x}_{[4,2]}\,z_2 + \mathbf{x}_{[4,1]}\,z_1 + \mathbf{x}_{[4,6]}\,y_1z_6 + \mathbf{x}_{[4,5]}\,y_1z_5 + x_4\,\mathbf{y}_{1,5}\,z_4 + \mathbf{y}_{1,5}\,z_3}$$

$$x_4' = \frac{y_3\lambda_3(x,y,z)}{\lambda_4(x,y,z)} = \frac{y_3(\mathbf{x}_{[4,2]}\,z_2 + \mathbf{x}_{[4,1]}\,z_1 + \mathbf{x}_{[4,6]}\,y_1z_6 + \mathbf{x}_{[4,5]}\,y_1z_5 + x_4\,\mathbf{y}_{1,5}\,z_4 + \mathbf{y}_{1,5}\,z_3)}{\mathbf{x}_{[5,3]}\,z_3 + \mathbf{x}_{[5,2]}\,y_3z_2 + \mathbf{x}_{[5,1]}\,y_3z_1 + \mathbf{x}_{[5,6]}\,\mathbf{y}_{1,3}\,z_6 + x_5\,\mathbf{y}_{1,3}\,z_5 + \mathbf{y}_{1,3,5}\,z_4}$$

$$x_5' = \frac{y_4\lambda_4(x,y,z)}{\lambda_5(x,y,z)} = \frac{\mathbf{x}_{[5,3]}\,z_3 + \mathbf{x}_{[5,2]}\,y_3z_2 + \mathbf{x}_{[5,1]}\,y_3z_1 + \mathbf{x}_{[5,6]}\,\mathbf{y}_{1,3}\,z_6 + x_5\,\mathbf{y}_{1,3}\,z_5 + \mathbf{y}_{1,3,5}\,z_4}{\mathbf{x}_{[6,4]}\,z_4 + \mathbf{x}_{[6,3]}\,z_3 + \mathbf{x}_{[6,2]}\,y_3z_2 + \mathbf{x}_{[6,1]}\,y_3z_1 + x_6\,\mathbf{y}_{1,3}\,z_6 + \mathbf{y}_{1,3}\,z_5}$$

$$x_6' = \frac{y_5\lambda_5(x,y,z)}{\lambda_6(x,y,z)} = \frac{y_5(\mathbf{x}_{[6,4]}\,z_4 + \mathbf{x}_{[6,3]}\,z_3 + \mathbf{x}_{[6,2]}\,y_3z_2 + \mathbf{x}_{[6,1]}\,y_3z_1 + x_6\,\mathbf{y}_{1,3}\,z_6 + \mathbf{y}_{1,3}\,z_5)}{\mathbf{x}_{[1,5]}\,z_5 + \mathbf{x}_{[1,4]}\,y_5z_4 + \mathbf{x}_{[1,3]}\,y_5z_3 + \mathbf{x}_{[1,2]}\,\mathbf{y}_{3,5}\,z_2 + x_1\,\mathbf{y}_{3,5}\,z_1 + \mathbf{y}_{1,3,5}\,z_6}$$

$$y_1' = \frac{x_2x_3\lambda_3(x,y,z)}{\lambda_1(x,y,z)} = \frac{\mathbf{x}_{[2,3]}(\mathbf{x}_{[4,2]}\,z_2 + \mathbf{x}_{[4,1]}\,z_1 + \mathbf{x}_{[4,6]}\,y_1z_6 + \mathbf{x}_{[4,5]}\,y_1z_5 + x_4\,\mathbf{y}_{1,5}\,z_4 + \mathbf{y}_{1,5}\,z_3)}{\mathbf{x}_{[2,6]}\,z_6 + \mathbf{x}_{[2,5]}\,z_5 + \mathbf{x}_{[2,4]}\,y_5z_4 + \mathbf{x}_{[2,3]}\,y_5z_3 + x_2\,\mathbf{y}_{3,5}\,z_2 + \mathbf{y}_{3,5}\,z_1}$$

$$y_2' = 1$$

$$y_3' = \frac{x_4x_5\lambda_5(x,y,z)}{\lambda_3(x,y,z)} = \frac{\mathbf{x}_{[4,5]}(\mathbf{x}_{[6,4]}\,z_4 + \mathbf{x}_{[6,3]}\,z_3 + \mathbf{x}_{[6,2]}\,y_3z_2 + \mathbf{x}_{[6,1]}\,y_3z_1 + x_6\,\mathbf{y}_{1,3}\,z_6 + \mathbf{y}_{1,3}\,z_5)}{\mathbf{x}_{[4,2]}\,z_2 + \mathbf{x}_{[4,1]}\,z_1 + \mathbf{x}_{[4,6]}\,y_1z_6 + \mathbf{x}_{[4,5]}\,y_1z_5 + x_4\,\mathbf{y}_{1,5}\,z_4 + \mathbf{y}_{1,5}\,z_3}$$

$$y_4' = 1$$

$$y_5' = \frac{x_6x_1\lambda_1(x,y,z)}{\lambda_5(x,y,z)} = \frac{\mathbf{x}_{[6,1]}(\mathbf{x}_{[2,6]}\,z_6 + \mathbf{x}_{[2,5]}\,z_5 + \mathbf{x}_{[2,4]}\,y_5z_4 + \mathbf{x}_{[2,3]}\,y_5z_3 + x_2\,\mathbf{y}_{3,5}\,z_2 + \mathbf{y}_{3,5}\,z_1)}{\mathbf{x}_{[6,4]}\,z_4 + \mathbf{x}_{[6,3]}\,z_3 + \mathbf{x}_{[6,2]}\,y_3z_2 + \mathbf{x}_{[6,1]}\,y_3z_1 + x_6\,\mathbf{y}_{1,3}\,z_6 + \mathbf{y}_{1,3}\,z_5}$$

$$y_6' = 1$$

$$z_1' = \frac{x_3z_1\lambda_3(x,y,z)}{\lambda_2(x,y,z)} = \frac{x_3z_1(\mathbf{x}_{[4,2]}\,z_2 + \mathbf{x}_{[4,1]}\,z_1 + \mathbf{x}_{[4,6]}\,y_1z_6 + \mathbf{x}_{[4,5]}\,y_1z_5 + x_4\,\mathbf{y}_{1,5}\,z_4 + \mathbf{y}_{1,5}\,z_3)}{\mathbf{x}_{[3,1]}\,z_1 + \mathbf{x}_{[3,6]}\,y_1z_6 + \mathbf{x}_{[3,5]}\,y_1z_5 + \mathbf{x}_{[2,4]}\,\mathbf{y}_{1,5}\,z_4 + x_3\,\mathbf{y}_{1,5}\,z_3 + \mathbf{y}_{1,3,5}\,z_2}$$

$$z_2' = z_2$$

$$z_3' = \frac{x_5z_3\lambda_5(x,y,z)}{\lambda_4(x,y,z)} = \frac{x_5z_3(\mathbf{x}_{[6,4]}\,z_4 + \mathbf{x}_{[6,3]}\,z_3 + \mathbf{x}_{[6,2]}\,y_3z_2 + \mathbf{x}_{[6,1]}\,y_3z_1 + x_6\,\mathbf{y}_{1,3}\,z_6 + \mathbf{y}_{1,3}\,z_5)}{\mathbf{x}_{[5,3]}\,z_3 + \mathbf{x}_{[5,2]}\,y_3z_2 + \mathbf{x}_{[5,1]}\,y_3z_1 + \mathbf{x}_{[5,6]}\,\mathbf{y}_{1,3}\,z_6 + x_5\,\mathbf{y}_{1,3}\,z_5 + \mathbf{y}_{1,3,5}\,z_4}$$

$$z_4' = z_4$$

$$z_5' = \frac{x_1z_5\lambda_1(x,y,z)}{\lambda_6(x,y,z)} = \frac{x_1z_5(\mathbf{x}_{[2,6]}\,z_6 + \mathbf{x}_{[2,5]}\,z_5 + \mathbf{x}_{[2,4]}\,y_5z_4 + \mathbf{x}_{[2,3]}\,y_5z_3 + x_2\,\mathbf{y}_{3,5}\,z_2 + \mathbf{y}_{3,5}\,z_1)}{\mathbf{x}_{[1,5]}\,z_5 + \mathbf{x}_{[1,4]}\,y_5z_4 + \mathbf{x}_{[1,3]}\,y_5z_3 + \mathbf{x}_{[1,2]}\,\mathbf{y}_{3,5}\,z_2 + x_1\,\mathbf{y}_{3,5}\,z_1 + \mathbf{y}_{1,3,5}\,z_6}$$

$$z_6' = z_6$$

6.3 Face-weighted Plabic R-matrix

We will now rewrite $T_{\varkappa,e}$ in terms of face and trail weights. We begin with a $\varkappa$-expanded diredted cylindric k-loop plabic network with the canonical orientation. Choose an edge from string $\varkappa-1$ to string $\varkappa$ (or from the left boundary to string $\varkappa$ if $\varkappa=1$). Follow this edge, and then go up string $\varkappa$. At the first opportunity, make a right to cross to the string $\varkappa+1$. Follow the string $\varkappa+1$ up and at the first opportunity make a right to string $\varkappa+2$ (or to the right boundary if $\varkappa=k-1$). If there is more than one edge on string $\varkappa+1$ in this path, then the path passes a face between strings $\varkappa$ and $\varkappa+1$ that has no edge to the right. This face must have an edge to the left. Choose this edge to the left to begin with and repeat. Eventually, we obtain a directed path P with only 5 edges. Extend P to the left and right so it is a directed path from the left boundary to the right boundary. Let this path be our trail with trail weight t. Let the weights of the faces bordering string $\varkappa$ on the left and sharing a bicolored edge with the string be $a_1, a_2, ..., a_\ell$ starting above the trail and going up. In the same way, let the weights of the faces bordering string $\varkappa+1$ on the right and sharing a bicolored edge with the string be $b_1, b_2, ..., b_m$ and the weights of the faces between strings $\varkappa$ and $\varkappa+1$ be $c_1, c_2, ..., c_{n-1}, c_n = \frac{1}{a_1 a_2 ... a_\ell b_1 b_2 ... b_m c_1 c_2 ... c_{n-1}}$. We will consider all of these indices to be modular. For any set S we'll define $\mathbf{a}_S := \prod_{i\in S} a_i$, and similarly for $\mathbf{b}_S$ and $\mathbf{c}_S$. Let $d := \mathbf{a}_{[1,\ell]}\, \mathbf{b}_{[1,m]}$ for ease of notation.

We will say a_j is associated to i if the highest edge on string $\varkappa$ bordering the face labeled a_j also borders the face c_i. Similarly, b_j is associated to i if the lowest edge on string $\varkappa+1$ bordering the face labeled b_j also borders the face c_i. Let $\mathcal{A}_{[i,j]} := \{k \mid a_k \text{ is associated to } \ell \in [i,j]\}$ and $\mathcal{B}_{[i,j]} := \{k \mid b_k \text{ is associated to } \ell \in [i,j]\}$.

Lemma 6.3.1. *Suppose we have a $\varkappa$-expanded directed cylindric k-loop plabic network with the face and trail weights as above. We can turn this into an edge weighted network with the following edge weights:*

- *For a face weighted a_j, give the edge from a white vertex to a black vertex on string $\varkappa$ that is highest on the face the weight a_j^{-1}. If a_j is associated to i, this should be the edge that borders both the face labeled a_j and the face labeled c_i.*
- *For a face weighted b_j, give the edge from a white vertex to a black vertex on string*

$\varkappa+1$ that is lowest on the face the weight b_j. If b_j is associated to i, this should be the edge that borders both the face labeled b_j and the face labeled c_i.

- *Give all other edges on strings $\varkappa$ and $\varkappa+1$ weight 1.*
- *Give the edge between the strings $\varkappa$ and $\varkappa+1$ that is part of the trail the weight t.*
- *Give each edge between strings $\varkappa$ and $\varkappa+1$ the weight of the edge below it multiplied by the weight of the face in between and the weight of the edges of the face on the right string, and then divided by the weight of the edges of the face on the left string. That is, if an edge is between the faces labeled c_i and c_{i+1}, give it the weight $\mathbf{a}_{\mathcal{A}_{[1,i]}}\,\mathbf{b}_{\mathcal{B}_{[1,i]}}\,\mathbf{c}_{[1,i]}\,t$.*
- *Give all other edges in the network any weights that are consistent with the face weights for the network and the edge weights above.*

Proof. Clear by computation. □

Using this, we can define $\widehat{\lambda}_i(a,b,c)$ to be $\lambda_i(z,y,z)$, where x,y,z are defined from a,b,c as in Lemma 6.3.1 and we choose our indexing so that $y_1=b_1$.

Definition 6.3.2. Define $T_{\varkappa,f}$ to be the transformation on face weights from (a,b,c) to (a',b',c') where

$$a'_i=\frac{\widehat{\lambda}_j(a,b,c)}{\widehat{\lambda}_p(a,b,c)\,\mathbf{b}_{\mathcal{B}_{[p,j-1]}}}\quad\text{where } a_i \text{ is associated to } j, a_{i-1} \text{ is associated to } p$$

$$b'_i=\frac{\widehat{\lambda}_q(a,b,c)}{\widehat{\lambda}_j(a,b,c)\,\mathbf{a}_{\mathcal{A}_{[j+1,q]}}}\quad\text{where } b_i \text{ is associated to } j, b_{i+1} \text{ is associated to } q$$

$$c'_i=\frac{\mathbf{a}_{\mathcal{A}_{[i,i+1]}}\,\mathbf{b}_{\mathcal{B}_{[i-1,i]}}\,c_i\widehat{\lambda}_{i-1}(a,b,c)}{\widehat{\lambda}_{i+1}(a,b,c)}$$

We call $T_{\varkappa,f}$ the face weighted *plabic R-matrix.*

Theorem 6.3.3. *$T_{\varkappa,f}$ has the following properties:*

1. *It preserves the boundary measurements.*
2. *It is an involution.*

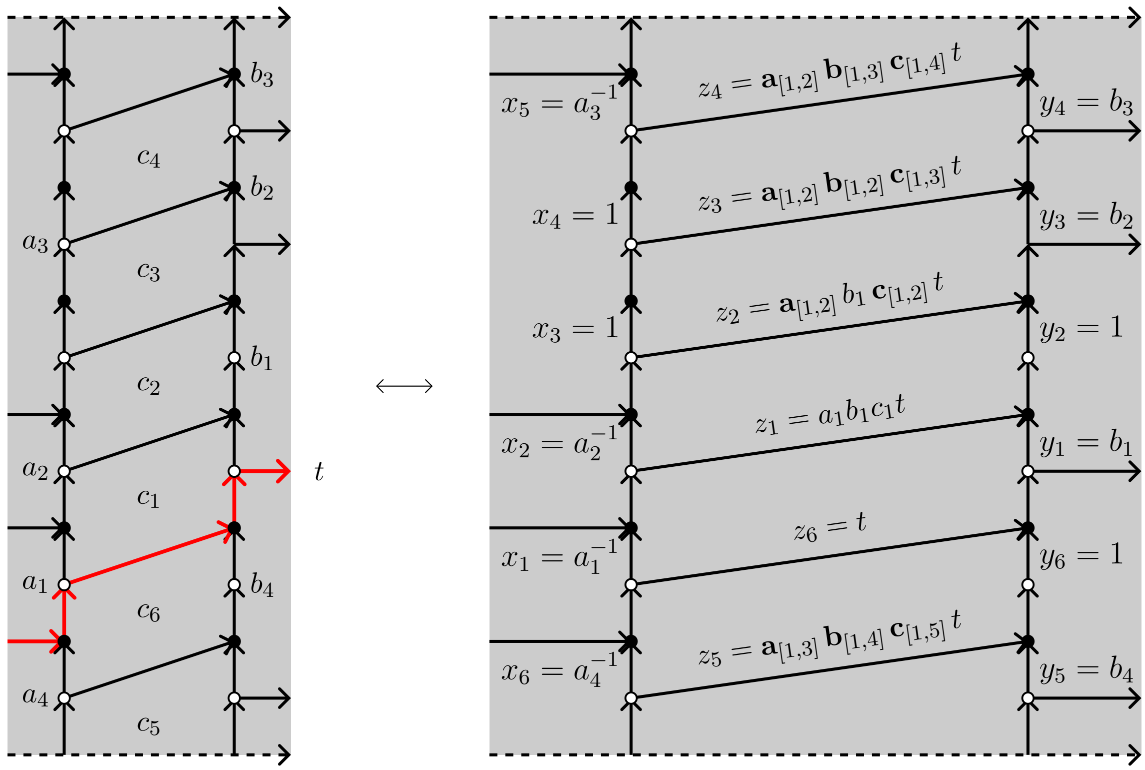

Figure 6.3: Changing a 1-expanded directed cylindric 2-loop plabic network with face and trail weights into one with edge weights as in Lemma 6.3.1.

3. *(a, b, c, t) and (a', b', c', t) are the only choices of face and trail weights on a fixed cylindric 2-loop plabic graph that preserve the boundary measurements.*

4. *It satisfies the braid relation. That is, for $1 \leq \varkappa < k-1$, $T_{\varkappa,f}T_{\varkappa+1,f}T_{\varkappa,f} = T_{\varkappa+1,f}T_{\varkappa,f}T_{\varkappa+1,f}$.*

See Section 6.5 for proof.

Example 6.3.4. We revisit Example 6.2.6, but with face variables this time.

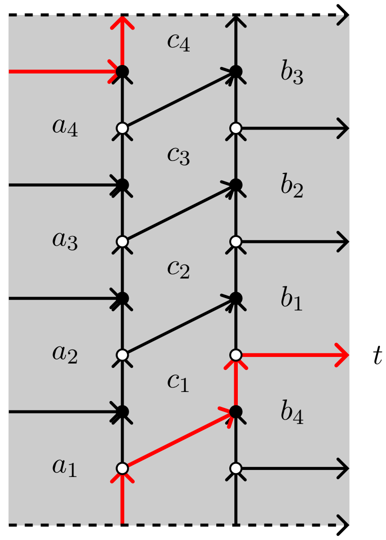

$T_{1,f}$ gives us the following values:

$$a_1' = \frac{\widehat{\lambda}_1(a,b,c)}{b_4\widehat{\lambda}_4(a,b,c)} = \frac{a_1(dc_1 + d\,\mathbf{c}_{[1,2]} + d\,\mathbf{c}_{[1,3]} + 1)}{d + dc_1 + d\,\mathbf{c}_{[1,2]} + d\,\mathbf{c}_{[1,3]}}$$

$$a_2' = \frac{\widehat{\lambda}_2(a,b,c)}{b_1\widehat{\lambda}_1(a,b,c)} = \frac{a_2(d\,\mathbf{c}_{[1,2]} + d\,\mathbf{c}_{[1,3]} + 1 + c_1)}{dc_1 + d\,\mathbf{c}_{[1,2]} + d\,\mathbf{c}_{[1,3]} + 1}$$

$$a_3' = \frac{\widehat{\lambda}_3(a,b,c)}{b_2\widehat{\lambda}_2(a,b,c)} = \frac{a_3(d\,\mathbf{c}_{[1,3]} + 1 + c_1 + \mathbf{c}_{[1,2]})}{d\,\mathbf{c}_{[1,2]} + d\,\mathbf{c}_{[1,3]} + 1 + c_1}$$

$$a_4' = \frac{\widehat{\lambda}_4(a,b,c)}{b_3\widehat{\lambda}_3(a,b,c)} = \frac{a_4(d + dc_1 + d\,\mathbf{c}_{[1,2]} + d\,\mathbf{c}_{[1,3]})}{d\,\mathbf{c}_{[1,3]} + 1 + c_1 + c_{[1,2]}}$$

$$b_1' = \frac{\widehat{\lambda}_2(a,b,c)}{a_2\widehat{\lambda}_1(a,b,c)} = \frac{b_1(d\,\mathbf{c}_{[1,2]} + d\,\mathbf{c}_{[1,3]} + 1 + c_1)}{dc_1 + d\,\mathbf{c}_{[1,2]} + d\,\mathbf{c}_{[1,3]} + 1}$$

$$b_2' = \frac{\widehat{\lambda}_3(a,b,c)}{a_3\widehat{\lambda}_2(a,b,c)} = \frac{b_2(d\,\mathbf{c}_{[1,3]} + 1 + c_1 + \mathbf{c}_{[1,2]})}{d\,\mathbf{c}_{[1,2]} + d\,\mathbf{c}_{[1,3]} + 1 + c_1}$$

$$b_3' = \frac{\widehat{\lambda}_4(a,b,c)}{a_4\widehat{\lambda}_3(a,b,c)} = \frac{b_3(1 + c_1 + \mathbf{c}_{[1,2]} + \mathbf{c}_{[1,3]})}{d\,\mathbf{c}_{[1,3]} + 1 + c_1 + \mathbf{c}_{[1,2]}}$$

$$b_4' = \frac{\widehat{\lambda}_1(a,b,c)}{a_1\widehat{\lambda}_4(a,b,c)} = \frac{dc_1 + d\,\mathbf{c}_{[1,2]} + d\,\mathbf{c}_{[1,3]} + 1}{d + dc_1 + d\,\mathbf{c}_{[1,2]} + d\,\mathbf{c}_{[1,3]}}$$

$$c_1' = \frac{a_1a_2b_1b_4c_1\widehat{\lambda}_4(a,b,c)}{\widehat{\lambda}_2(a,b,c)} = \frac{c_1(d + dc_1 + d\,\mathbf{c}_{[1,2]} + d\,\mathbf{c}_{[1,3]})}{d\,\mathbf{c}_{[1,2]} + d\,\mathbf{c}_{[1,3]} + 1 + c_1}$$

$$c_2' = \frac{a_2a_3b_1b_2c_2\widehat{\lambda}_1(a,b,c)}{\widehat{\lambda}_3(a,b,c)} = \frac{c_2(dc_1 + d\,\mathbf{c}_{[1,2]} + d\,\mathbf{c}_{[1,3]} + 1)}{d\,\mathbf{c}_{[1,3]} + 1 + c_1 + \mathbf{c}_{[1,2]}}$$

$$c_3' = \frac{a_3a_4b_2b_3c_3\widehat{\lambda}_2(a,b,c)}{\widehat{\lambda}_4(a,b,c)} = \frac{c_3(d\,\mathbf{c}_{[1,2]} + d\,\mathbf{c}_{[1,3]} + 1 + c_1)}{1 + c_1 + c_1c_2 + c_1c_2c_3}$$

$$c_4' = \frac{a_1a_4b_3b_4c_4\widehat{\lambda}_3(a,b,c)}{\widehat{\lambda}_1(a,b,c)} = \frac{dc_4(d\,\mathbf{c}_{[1,3]} + 1 + c_1 + c_1c_2)}{dc_1 + d\,\mathbf{c}_{[1,2]} + d\,\mathbf{c}_{[1,3]} + 1}$$

Example 6.3.5. We revisit Example 6.2.7, but with face variables this time.

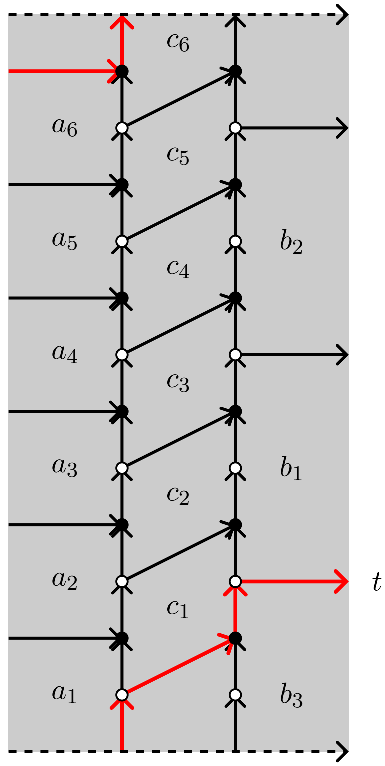

$T_{1,f}$ gives us the following values:

$$a_1' = \frac{\widehat{\lambda}_1(a,b,c)}{\widehat{\lambda}_6(a,b,c)} = \frac{a_1(dc_1 + d\,\mathbf{c}_{[1,2]} + d\,\mathbf{c}_{[1,3]} + d\,\mathbf{c}_{[1,4]} + d\,\mathbf{c}_{[1,5]} + 1)}{d(1 + c_1 + \mathbf{c}_{[1,2]} + \mathbf{c}_{[1,3]} + \mathbf{c}_{[1,4]} + \mathbf{c}_{[1,5]})}$$

$$a_2' = \frac{\widehat{\lambda}_2(a,b,c)}{b_1\widehat{\lambda}_1(a,b,c)} = \frac{a_2(d\,\mathbf{c}_{[1,2]} + d\,\mathbf{c}_{[1,3]} + d\,\mathbf{c}_{[1,4]} + d\,\mathbf{c}_{[1,5]} + 1 + c_1)}{dc_1 + d\,\mathbf{c}_{[1,2]} + d\,\mathbf{c}_{[1,3]} + d\,\mathbf{c}_{[1,4]} + d\,\mathbf{c}_{[1,5]} + 1}$$

$$a_3' = \frac{\widehat{\lambda}_3(a,b,c)}{\widehat{\lambda}_2(a,b,c)} = \frac{a_3(d\,\mathbf{c}_{[1,3]} + d\,\mathbf{c}_{[1,4]} + d\,\mathbf{c}_{[1,5]} + 1 + c_1 + \mathbf{c}_{[1,2]})}{d\,\mathbf{c}_{[1,2]} + d\,\mathbf{c}_{[1,3]} + d\,\mathbf{c}_{[1,4]} + d\,\mathbf{c}_{[1,5]} + 1 + c_1}$$

$$a_4' = \frac{\widehat{\lambda}_4(a,b,c)}{b_2\widehat{\lambda}_3(a,b,c)} = \frac{a_4(d\,\mathbf{c}_{[1,4]} + d\,\mathbf{c}_{[1,5]} + 1 + c_1 + \mathbf{c}_{[1,2]} + \mathbf{c}_{[1,3]})}{d\,\mathbf{c}_{[1,3]} + d\,\mathbf{c}_{[1,4]} + d\,\mathbf{c}_{[1,5]} + 1 + c_1 + \mathbf{c}_{[1,2]}}$$

$$a_5' = \frac{\widehat{\lambda}_5(a,b,c)}{\widehat{\lambda}_4(a,b,c)} = \frac{a_5(d\,\mathbf{c}_{[1,5]} + 1 + c_1 + \mathbf{c}_{[1,2]} + \mathbf{c}_{[1,3]} + \mathbf{c}_{[1,4]})}{d\,\mathbf{c}_{[1,4]} + d\,\mathbf{c}_{[1,5]} + 1 + c_1 + \mathbf{c}_{[1,2]} + \mathbf{c}_{[1,3]}}$$

$$a_6' = \frac{\widehat{\lambda}_6(a,b,c)}{b_3\widehat{\lambda}_5(a,b,c)} = \frac{a_6(1 + c_1 + \mathbf{c}_{[1,2]} + \mathbf{c}_{[1,3]} + \mathbf{c}_{[1,4]} + \mathbf{c}_{[1,5]})}{d\,\mathbf{c}_{[1,5]} + 1 + c_1 + \mathbf{c}_{[1,2]} + \mathbf{c}_{[1,3]} + \mathbf{c}_{[1,4]}}$$

$$b_1' = \frac{\widehat{\lambda}_3(a,b,c)}{a_2a_3\widehat{\lambda}_1(a,b,c)} = \frac{b_1(d\,\mathbf{c}_{[1,3]} + d\,\mathbf{c}_{[1,4]} + d\,\mathbf{c}_{[1,5]} + 1 + c_1 + \mathbf{c}_{[1,2]})}{dc_1 + d\,\mathbf{c}_{[1,2]} + d\,\mathbf{c}_{[1,3]} + d\,\mathbf{c}_{[1,4]} + d\,\mathbf{c}_{[1,5]} + 1}$$

$$b_2' = \frac{\widehat{\lambda}_5(a,b,c)}{a_4a_5\widehat{\lambda}_3(a,b,c)} = \frac{b_2(d\,\mathbf{c}_{[1,5]} + 1 + c_1 + \mathbf{c}_{[1,2]} + \mathbf{c}_{[1,3]} + \mathbf{c}_{[1,4]})}{d\,\mathbf{c}_{[1,3]} + d\,\mathbf{c}_{[1,4]} + d\,\mathbf{c}_{[1,5]} + 1 + c_1 + \mathbf{c}_{[1,2]}}$$
$$b_3' = \frac{\widehat{\lambda}_1(a,b,c)}{a_6a_1\widehat{\lambda}_5(a,b,c)} = \frac{b_3(dc_1 + d\,\mathbf{c}_{[1,2]} + d\,\mathbf{c}_{[1,3]} + d\,\mathbf{c}_{[1,4]} + d\,\mathbf{c}_{[1,5]} + 1)}{d(d\,\mathbf{c}_{[1,5]} + 1 + c_1 + \mathbf{c}_{[1,2]} + \mathbf{c}_{[1,3]} + \mathbf{c}_{[1,4]})}$$
$$c_1' = \frac{c_1a_1a_2b_1\widehat{\lambda}_6(a,b,c)}{\widehat{\lambda}_2(a,b,c)} = \frac{dc_1(1 + c_1 + \mathbf{c}_{[1,2]} + \mathbf{c}_{[1,3]} + \mathbf{c}_{[1,4]} + \mathbf{c}_{[1,5]})}{d\,\mathbf{c}_{[1,2]} + d\,\mathbf{c}_{[1,3]} + d\,\mathbf{c}_{[1,4]} + d\,\mathbf{c}_{[1,5]} + 1 + c_1}$$
$$c_2' = \frac{c_2a_2a_3b_1\widehat{\lambda}_1(a,b,c)}{\widehat{\lambda}_3(a,b,c)} = \frac{c_2(dc_1 + d\,\mathbf{c}_{[1,2]} + d\,\mathbf{c}_{[1,3]} + d\,\mathbf{c}_{[1,4]} + d\,\mathbf{c}_{[1,5]} + 1)}{d\,\mathbf{c}_{[1,3]} + d\,\mathbf{c}_{[1,4]} + d\,\mathbf{c}_{[1,5]} + 1 + c_1 + \mathbf{c}_{[1,2]}}$$
$$c_3' = \frac{c_3a_3a_4b_2\widehat{\lambda}_2(a,b,c)}{\widehat{\lambda}_4(a,b,c)} = \frac{c_3(d\,\mathbf{c}_{[1,2]} + d\,\mathbf{c}_{[1,3]} + d\,\mathbf{c}_{[1,4]} + d\,\mathbf{c}_{[1,5]} + 1 + c_1)}{d\,\mathbf{c}_{[1,4]} + d\,\mathbf{c}_{[1,5]} + 1 + c_1 + \mathbf{c}_{[1,2]} + \mathbf{c}_{[1,3]}}$$
$$c_4' = \frac{c_4a_4a_5b_2\widehat{\lambda}_3(a,b,c)}{\widehat{\lambda}_5(a,b,c)} = \frac{c_4(d\,\mathbf{c}_{[1,3]} + d\,\mathbf{c}_{[1,4]} + d\,\mathbf{c}_{[1,5]} + 1 + c_1 + \mathbf{c}_{[1,2]})}{d\,\mathbf{c}_{[1,5]} + 1 + c_1 + \mathbf{c}_{[1,2]} + \mathbf{c}_{[1,3]} + \mathbf{c}_{[1,4]}}$$
$$c_5' = \frac{c_5a_5a_6b_3\widehat{\lambda}_4(a,b,c)}{\widehat{\lambda}_6(a,b,c)} = \frac{c_5(d\,\mathbf{c}_{[1,4]} + d\,\mathbf{c}_{[1,5]} + 1 + c_1 + \mathbf{c}_{[1,2]} + \mathbf{c}_{[1,3]})}{1 + c_1 + \mathbf{c}_{[1,2]} + \mathbf{c}_{[1,3]} + \mathbf{c}_{[1,4]} + \mathbf{c}_{[1,5]}}$$
$$c_6' = \frac{c_6a_6a_1b_3\widehat{\lambda}_5(a,b,c)}{\widehat{\lambda}_1(a,b,c)} = \frac{dc_6(d\,\mathbf{c}_{[1,5]} + 1 + c_1 + \mathbf{c}_{[1,2]} + \mathbf{c}_{[1,3]} + \mathbf{c}_{[1,4]})}{dc_1 + d\,\mathbf{c}_{[1,2]} + d\,\mathbf{c}_{[1,3]} + d\,\mathbf{c}_{[1,4]} + d\,\mathbf{c}_{[1,5]} + 1}$$

6.4 Postnikov Diagram Proofs

6.4.1 Proof of Theorem 6.1.2

Definition 6.4.1 (Section 13 of [Pos06])**.** For a plabic graph G, a *trip* is a walk in G that turns right at each black vertex and left at each white vertex.

Definition 6.4.2 (Section 13 of [Pos06])**.** A trip in a plabic graph is a *round trip* if it is a closed cycle.

Definition 6.4.3 (Section 13 of [Pos06])**.** Two trips in a plabic graph have an *essential intersection* if there is an edge e with vertices of different colors such that the two trips pass through e in different directions. A trip in a plabic graph has an *essential self-intersection* if there is an edge e with vertices of different colors such that the trip passes through e in different directions.

Definition 6.4.4 (Section 13 of [Pos06])**.** Two trips in a plabic graph have an *bad double crossing* if they have essential intersections at edges e_1 and e_2 where both trips are directed from e_1 to e_2.

Theorem 6.4.5. *Let G be a leafless reduced plabic graph on a cylinder without isolated components. We will consider $\widetilde{G}$ to be G drawn on the universal cover of the cylinder. Then G is reduced if and only if the following are true:*

(1) There are no round trips in $\widetilde{G}$.

(2) $\widetilde{G}$ has no trips with essential self-intersections.

(3) There are no pairs of trips in $\widetilde{G}$ with a bad double crossing.

(4) If a trip begins and ends at the same boundary vertex, then either $\widetilde{G}$ has a boundary leaf at that vertex.

The above theorem is analogous to Theorem 13.2 of [Pos06].

Proof. Notice that G is reduced if and only if $\widetilde{G}$ is reduced. The proof for Theorem 13.2 of [Pos06] holds to show that $\widetilde{G}$ is reduced if and only if conditions (1) - (4) hold. □

Now we can prove Theorem 6.1.2.

Proof. Notice that the trips in a plabic graph follow the same paths as the strands in the associated Postnikov diagram. The conditions from Theorem 6.4.5 correspond exactly to the conditions we require in the definition of a Postnikov diagram. □

6.4.2 Proof of Theorem 6.1.5

Lemma 6.4.6. *Suppose a cylindric 2-loop plabic graph has an interior vertex that has one edge to a vertex on a string and one edge to a different vertex on the same string, such that there is only one vertex on the string between these two vertices, and the square formed by these four vertices is the boundary of a single face. Then, we can reduce the number of strand crossings in between the two loops in the associated Postnikov diagram using the square move.*

Proof. Without loss of generality, assume the interior vertex is black. Then we can apply transformations to our plabic graph as follows:

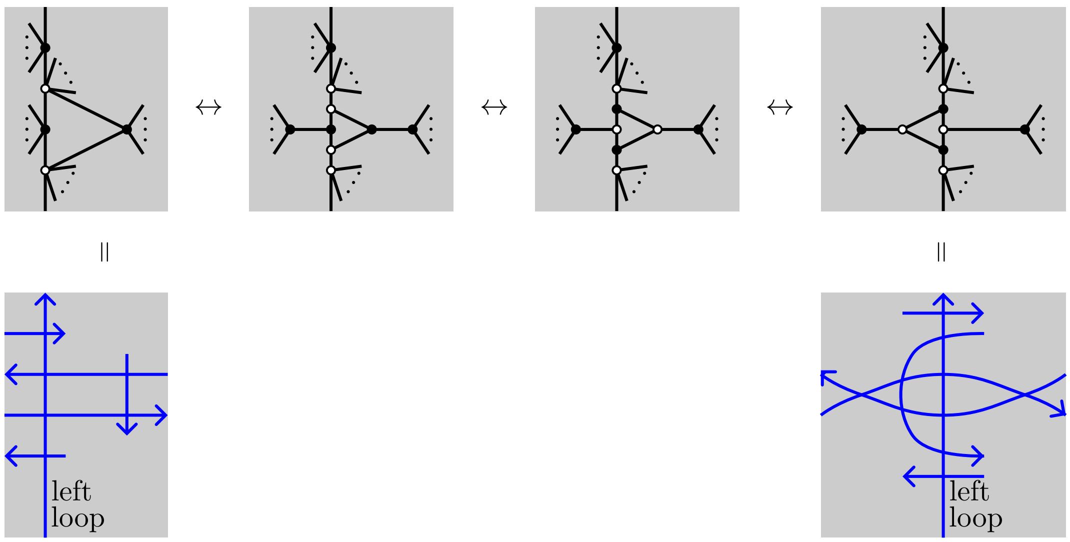

The Postnikov diagram on the left has two crossings between the left and the right loop, in addition to those we can't see in the picture. The Postnikov diagram on the right has one crossing between the left and the right loop, aside from those we can't see in the picture. So, we have reduced the number of crossings. □

Lemma 6.4.7. *Suppose a cylindric 2-loop plabic graph has at least one interior vertex. Assume no vertices in the plabic graph have degree two. Then at least one interior vertex must have multiple edges to vertices on a string.*

Proof. Note that only white vertices on the left string and black vertices on the right string can have edges to interior vertices. As the graph is bipartite, this means an interior vertex cannot have edges to vertices on both the left and right string.

Since there are interior vertices, there must be a vertex on a string attached to an interior vertex. Without loss of generality, assume there's such a vertex on the left string. Expand this vertex so that we have a vertex on the left string that is attached only to one interior vertex and two vertices on the left string. We allow some vertices of degree 2 to be created to keep the graph bipartite. Now we have an interior vertex must arise from a part of the alternating strand diagram that looks as follows:

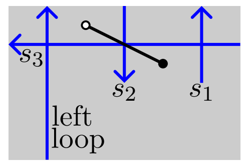

Call the strands s_1, s_2, and s_3, as denoted in the diagram. The black vertex in the diagram is not on the right string, so s_1 cannot be the right loop. Suppose s_1 starts and ends on the right boundary of the cylinder. If s_1 does not make a turn and head downward, then s_1 and the right loop would intersect in two places on the universal cover, and both would be oriented in the same direction (from one crossing to the other). So, s_1 must turn downwards at some point. If s_1 turns to the right to do this, it will have a self-crossing, which is not allowed. If s_1 turns to the left to do this, then $s_2 = s_1$. Then s_3 and s_1 intersect twice, and both are oriented from the crossing on the right to the crossing on the left. This is not allowed, so s_1 must cross the left loop.

Suppose s_1 crosses the left loop from left to right (the argument is very similar for s_1 crossing from right to left). There must be a strand oriented from right to left that crosses the left loop just above s_1. Call this strand s_4. Either s_4 must cross s_1 or $s_4 = s_2$. Suppose it's the former. The face above s_4 and to the right of the left loop corresponds to a white vertex on the left string, which must be connected to an interior vertex. Suppose there is another strand that crosses s_4 between the left loop and s_1 in the same direction as s_1. Since this strand did not cross s_3 in the same direction as s_1 between the left loop and s_1, it must cross s_1 somewhere above s_4. However, this strand would also have to cross s_1 below s_4, as nothing crosses the left loop between s_1 and s_4. This would introduce two crossings of s_1 and the additional upward pointing strand, and both of the strands would be oriented in the same direction. This cannot happen, so we have this section of the alternating strand diagram that looks as follows:

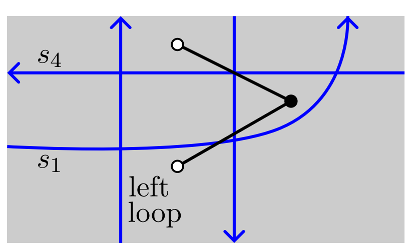

Now suppose we are in the second case: $s_4 = s_2$. We get a sequence of connected vertices beginning with the white vertex in the face bounded by s_2, s_3, and the left loop and ending with the white vertex in the face bounded by s_2 and the left loop such that vertices alternate being in faces to the left and right of s_2. This sequence and the section of the string bounded below by s_2 and above by s_3 form a closed cycle, where there may or may not be vertices shared by sequence zig-zagging across s_2 and the left string:

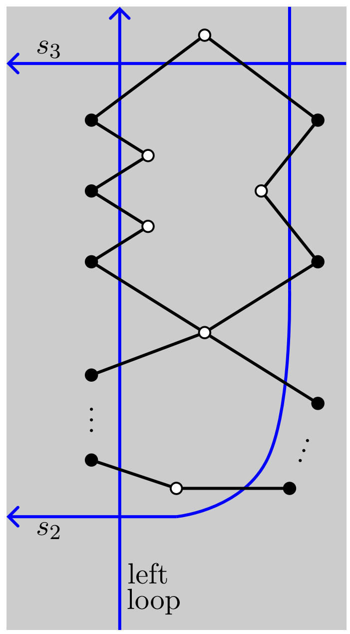

If there are no interior vertices inside this cycle, then we are done, as any black vertex in this cycle not on the left string, of which there is at least one, is adjacent to multiple vertices on the left string. Otherwise, we can repeat our process from the beginning, this time choosing an interior vertex that is inside the cycle. We will obtain an s_1', s_2', s_3', and s_4'. If $s_2' \neq s_4'$, then we get a contradiction, as above. Otherwise the cycle of vertices we obtain is inside the cycle we obtained from s_1, s_2 and s_3. Since the graph is finite, this process must eventually terminate, and we will have found an interior vertex with multiple non-parallel edges to vertices on the left string. □

Lemma 6.4.8. *Suppose a cylindric 2-loop plabic graph with no vertices of degree 2 has an interior vertex that has (at least) two edges to vertices on a string. If there are any other vertices of the same color on the string between these two vertices, they must also have edges to the same interior vertex.*

Proof. Assume for contradiction we have a plabic graph with an interior vertex that has (at least) two edges to vertices on a string and the vertices of the same color on the string between these two vertices do not have edges to the same interior vertex. Without loss of generality assume the interior vertex is a black vertex. We know this part of the Postnikov diagram looks as shown, where the interior of the darker box is unknown:

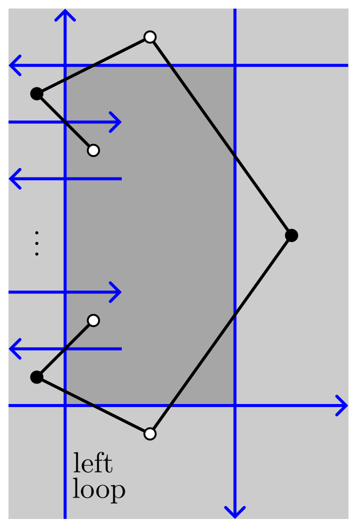

If any of the strands on the left exit the shaded face out the top or bottom and don't return, they'll disconnect the original edges from the interior vertex to the two vertices on the string. If they exit out the strand on the right and don't return, they'll split the one interior vertex into multiple. Thus, all the strands crossing the left loop from the left must also be the same strands that cross from the right. All strands like this must be oriented the opposite direction of the loop. The only way to pair up these strands in that way is for each strand going to the right is paired with the strand immediately below it. There is no way to do this without self-crossings and without creating vertices of degree 2. So, we have a contradiction. □

Theorem 6.4.9. *Any cylindric 2-loop plabic graph can be transformed by moves to one that has no interior vertices.*

Proof. If there are interior vertices, then by Lemmas 6.4.7 and 6.4.8, we are always in a situation where, by Lemma 6.4.6, we can reduce the number of edges until we get to a plabic graph where there are no interior vertices. □

Lemma 6.4.10. *If there are interior vertices in a cylindric 2-loop plabic graph, then there must be a black interior vertex that is adjacent to the left string.*

Proof. Assume for contradiction we have a cylindric 2-loop plabic graph with interior vertices, but no black interior vertex connected to the left string. Then each white vertex on the left string is connected only to two black vertices on left string and some positive number of black vertices on the right string. If we look at the area of the graph between two consecutive edges that connect the strands, we have three possibilities:

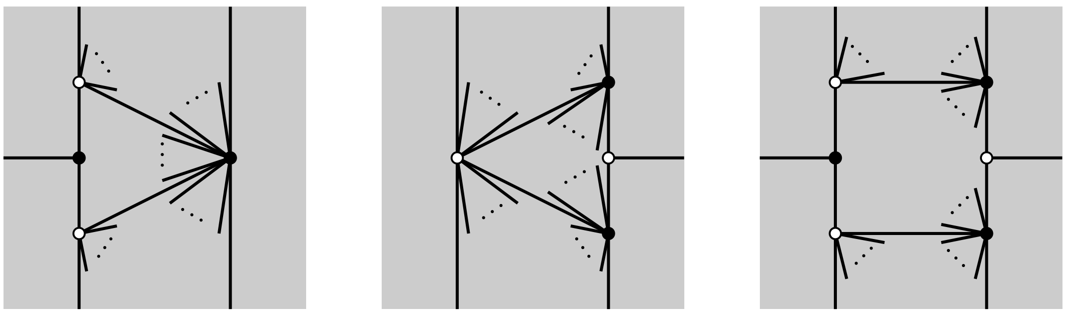

We can draw in parts of some strands based on what we know of the graph:

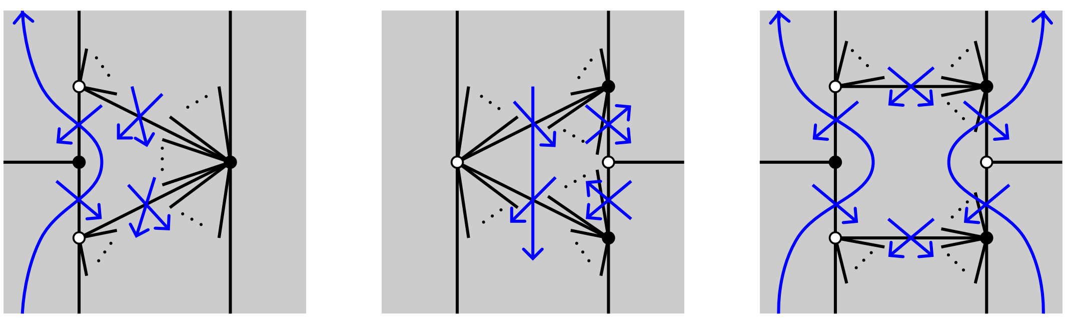

For each area enclosed by edges in these figures, the strands drawn above must be the only strands that enter or exit the area. If we test all the ways to connect the entering strands to the exiting strands, we find that in each case, there is only one way to do this while maintaining the rules of Postnikov diagrams and without creating additional edges between the vertices on the strands:

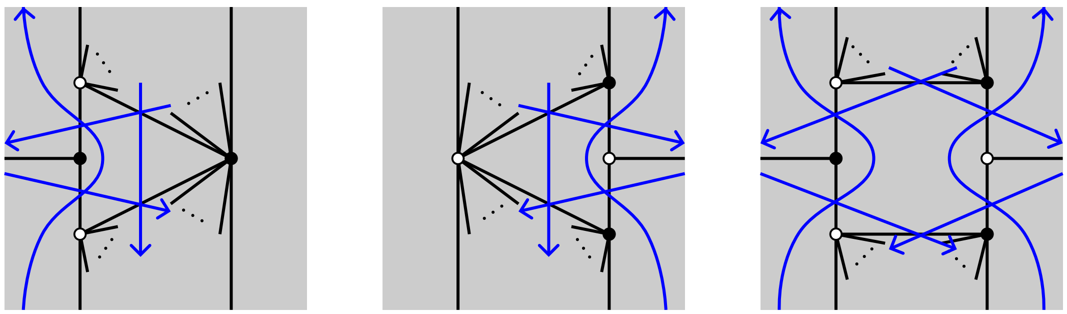

These Postnikov diagrams don't have any interior vertices, which is a contradiction. □

Now we are ready to prove Theorem 6.1.5.

Proof. First, we'll just consider the first and second farthest right loops. If there are interior vertices, then by Lemma 6.4.10, there must be a black interior vertex adjacent to the left string. The proof of Lemma 6.4.7 tells us that there must be a black vertex connected by multiple nonparallel edges to the left string. Then, by Lemmas 6.4.8 and 6.4.6, we can do a square move to reduce the number of crossings between the loops in the associated alternating strange diagram. Since we are doing this square move on a black vertex, we are pushing these crossings to the left (as pictured in the proof of Lemma 6.4.6). We can continue this process until there are no interior vertices between the first and second farthest right loops. Now we'll look at the second and third farthest right loops and, using the same method, remove all interior vertices here. Notice that we do not create any interior vertices between the first and second farthest right loops, as we are always pushing crossings to the left. Repeating this process with each pair of loops, going from right to left, removes all interior vertices. □

6.5 Proof of Theorems 6.2.5 and 6.3.3

Lemma 6.5.1. *We have the following relation between λ_j and λ_{j+1}:*

$$\lambda_{j+1}(x,y,z) = \frac{y_j\lambda_j(x,y,z) + z_j(\mathbf{x}_{[1,n]} - \mathbf{y}_{[1,n]})}{x_{j+1}}$$

Proof. If we take a path that gives a term in λ_j and does not start with z_j, we can add two additional edges at the end on the right string and remove two edges at the beginning on the left string, to get a path that gives a term in λ_{j+1}. This process gives us all the terms in λ_{j+1} except the one that comes from the path that stays on the left string and crosses over at the last moment on z_j. □

We can choose one black vertex on string $\varkappa$ of a $\varkappa$-expanded cylindric k-loop plabic network and the white vertex on string $\varkappa + 1$ that is part of the same face. Adding one edge of weight p and one edge of weight $-p$ from the white vertex to the black vertex does not change any of the boundary measurements, because every time there is a path that goes through the edge with weight p, there is another path exactly the same except it goes through the edge of weight $-p$. The weights of these paths will cancel out when computing the boundary measurements. We can expand these two vertices into 3 vertices each, as seen in Figure 6.4, where the top white vertex on the right and bottom black vertex on the left may have any number of edges, depending on the degree of the original white and black vertices.

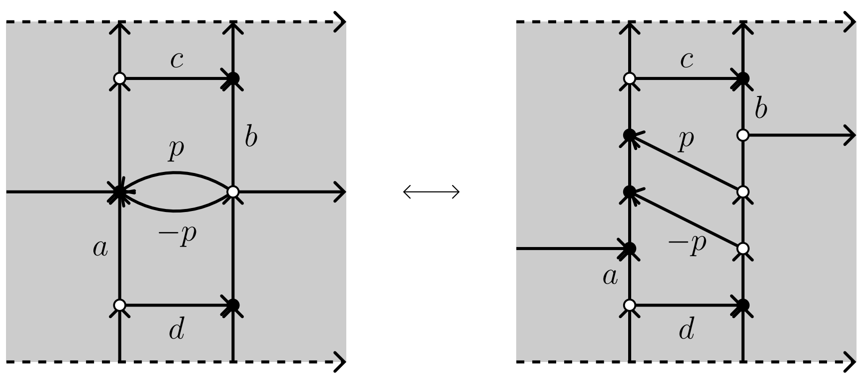

Figure 6.4: Adding the edges p and $-p$ to a cylindric 2-loop directed plabic network.

Notice that what was a hexagon is now a pentagon on top of a square on top of a pentagon. We can turn the upper pentagon into a square and perform the square move. This will allow us to perform the square move on the face above that, and so on. When we change original edge weights x_{i+1}, y_i, and z_i by a square move, we will denote the new weights by $\widetilde{x_{i+1}}, \widetilde{y_i}$, and $\widetilde{z_i}$, as in Figure 6.5. We can continue doing square moves in this way until we end up with a graph that looks the same as the one we started with. Now the edge weighted $-p$ will be the edge at the top of the square and the edge originally weighted p, which has a a new weight, has been pushed around the cylinder so that it is under the edge weighted $-p$. Notice that each original edge weight is changed by a square move exactly once, so ignoring the two edges oriented from right to left, we end up with a new graph with edge weights $\widetilde{x}, \widetilde{y}$, and $\widetilde{z}$.

Each square move looks as depicted in Figure 6.5. From the figure, we see that as we perform the sequence of square moves, there is always one edge, besides the fixed edge weighted $-p$, oriented from right to left.

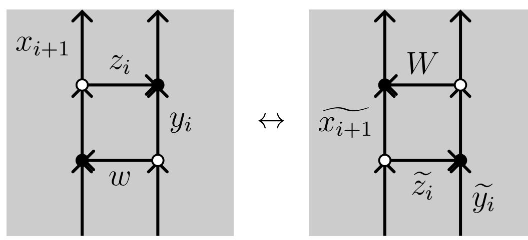

Figure 6.5: A square move in the sequence of moves that push the edge weighted p around the cylinder.

Lemma 6.5.2. *There is at most one value of p for which the weight of the bottom edge of the square in the network, after the square move has propagated all the way around the cylinder, is equal to p.*

Proof. If we are preforming the move where the edge oriented from right to left is pushed from between $\widetilde{z_{i-1}}$ and z_i to between $\widetilde{z}_i$ and z_{i+1}, then suppose this edge is weighted $w = \frac{ap}{bp+c}$ where a, b, c don't depend on p. Then the weight of the edge oriented from right to left after the square move is $\frac{x_{i+1}}{z_i(1+\frac{y_i}{z_i w})} = \frac{(ax_{i+1})p}{(az_i+by_i)p+cy_i}$. So, by induction, we find that the weight of the bottom edge of the square in the network, after the square move has propagated all the way around the cylinder, is a constant times p divided by a linear function of p. Setting this equal to p, we get a linear equation, so there is at most one solution. □

Theorem 6.5.3. *If we add the edges weighted by p and $-p$ such that the the face above edge p has the edge labeled y_j, and the face below edge $-p$ has the edge labeled x_j, then* *let* $p = p_j = \dfrac{\mathbf{x}_{[1,n]} - \mathbf{y}_{[1,n]}}{\lambda_j(x,y,z)}$ *and perform the sequence of square moves described above. Then when the edge directed from the right string to the left string that is not the edge weighted by* $-p$ *is just above the face with the edge labeled* $\widetilde{x_\ell}$*, the weight of this edge is* $p_\ell = \dfrac{\mathbf{x}_{[1,n]} - \mathbf{y}_{[1,n]}}{\lambda_\ell(x,y,z)}$*. After doing all the square moves, we have the following values of* $\widetilde{x_i}, \widetilde{y_i}$*, and* $\widetilde{z_i}$*:*

$$\widetilde{x_i} = \frac{y_{i-1}\lambda_{i-1}(x,y,z)}{\lambda_i(x,y,z)},$$

$$\widetilde{y_i} = \frac{x_{i+1}\lambda_{i+1}(x,y,z)}{\lambda_i(x,y,z)},$$

$$\widetilde{z_i} = z_i.$$

Proof. We only need to show this for one square move.

$$\widetilde{p_j} = \frac{x_{j+1}}{z_j\left(1 + \frac{y_j}{z_j p_j}\right)} = \frac{x_{j+1}(\mathbf{x}_{[1,n]} - \mathbf{y}_{[1,n]})}{z_j(\mathbf{x}_{[1,n]} - \mathbf{y}_{[1,n]}) + y_j\lambda_j(x,y,z)} = \frac{\mathbf{x}_{[1,n]} - \mathbf{y}_{[1,n]}}{\lambda_{j+1}(x,y,z)}$$

$$\widetilde{x_{j+1}} = \frac{x_{j+1}}{1 + \frac{z_j p_j}{y_j}} = \frac{x_{j+1}y_j\lambda_j(x,y,z)}{y_j\lambda_j(x,y,z) + z_j(\mathbf{x}_{[1,n]} - \mathbf{y}_{[1,n]})} = \frac{y_j\lambda_j(x,y,z)}{\lambda_{j+1}(x,y,z)}$$

$$\widetilde{y_j} = y_j\left(1 + \frac{z_j p_j}{y_j}\right) = \frac{y_j\lambda_j(x,y,z) + z_j(\mathbf{x}_{[1,n]} - \mathbf{y}_{[1,n]})}{\lambda_j(x,y,z)} = \frac{x_{j+1}\lambda_{j+1}(x,y,z)}{\lambda_j(x,y,z)}$$

$$\widetilde{z_j} = \frac{\widetilde{y_j}}{p_j\left(1 + \frac{y_j}{z_j p_j}\right)} = \frac{x_{j+1}z_j\lambda_{j+1}(x,y,z)}{z_j p_j\lambda_j(x,y,z) + y_j\lambda_j(x,y,z)} = \frac{x_{j+1}z_j\lambda_{j+1}(x,y,z)}{z_j(\mathbf{x}_{[1,n]} - \mathbf{y}_{[1,n]}) + y_j\lambda_j(x,y,z)} = z_j$$

The last equalities in each line are due to Lemma 6.5.1. □

Theorem 6.5.4. *After pushing the square move through every face, we can remove the edges weighted* p *and* $-p$*. Then we can use gauge transformations to force all the edge weights that were originally set to 1 equal to 1 again. We obtain the new edge weights*

x_i', y_i', z_i':

$$x_i' = \begin{cases} 1 & x_i \textit{ set to } 1, \\ \dfrac{y_{i-1}\,\mathbf{y}_{\mathcal{X}_i-1}\,\lambda_{i-|\mathcal{X}_i|-1}(x,y,z)}{\lambda_i(x,y,z)} & \textit{otherwise,} \end{cases}$$

$$y_i' = \begin{cases} 1 & y_i \textit{ set to } 1, \\ \dfrac{x_{i+1}\,\mathbf{x}_{\mathcal{Y}_i+1}\,\lambda_{i+|\mathcal{Y}_i|+1}(x,y,z)}{\lambda_i(x,y,z)} & \textit{otherwise,} \end{cases}$$

$$\begin{aligned} z_i' &= \widetilde{\mathbf{x}_{\mathcal{Y}_i}}\widetilde{\mathbf{y}_{\mathcal{X}_i}} z_i \\ &= \frac{\mathbf{x}_{\mathcal{Y}_i+1}\,\mathbf{y}_{\mathcal{X}_i-1}\,z_i\lambda_{i-|\mathcal{X}_i|-1}(x,y,z)\lambda_{i+|\mathcal{Y}_i|+1}(x,y,z)}{\lambda_{i-1}(x,y,z)\lambda_{i+1}(x,y,z)}. \end{aligned}$$

Proof. Clear by computation. Notice that the gauge transformations only occur at vertices on string $\varkappa$ that do not have edges to string $\varkappa - 1$ (or the left boundary if $\varkappa = 1$) and at vertices on string $\varkappa + 1$ that do not have edges to string $\varkappa + 2$ (or the right boundary if $\varkappa = k - 1$), so no other weights change. □

We can now prove the first part of Theorem 6.2.5.

Proof. $T_{\varkappa,e}$ is the transformation we obtain when we do the process from Theorem 6.5.3 and then Theorem 6.5.4. Since adding the p and $-p$ edges, applying square moves, removing the p and $-p$ edges, and applying gauge transformations all preserve the boundary measurements, $T_{\varkappa,e}$ preserves the boundary measurements. □

Lemma 6.5.5. *For any* $i, \lambda_i(x,y,z) = \lambda_i(\widetilde{x},\widetilde{y},\widetilde{z})$.

Proof. First suppose that we are in the case where $k = 2$ and the 1-expanded plabic network has no vertices of degree 2. Then $\lambda_i(x,y,z)$ is exactly the coefficient of a power of ζ in one of the boundary measurements. So $\lambda_i(x,y,z) = \lambda_i(x'y'z')$, as the transformation does not change the boundary measurements. But in this case, $(x'y'z') = (\widetilde{x},\widetilde{y},\widetilde{z})$, so $\lambda_i(x,y,z) = \lambda_i(\widetilde{x},\widetilde{y},\widetilde{z})$.

Now suppose $k = 2$ but there may be some vertices of degree 2 in the 1-expanded plabic network. The lack of a third edge on some vertices does not affect the square move in any way. The transformation from (x,y,z) to $(\widetilde{x},\widetilde{y},\widetilde{z})$ is the same as if all the vertices were degree 3, and thus, we still have that $\lambda_i(x,y,z) = \lambda_i(\widetilde{x},\widetilde{y},\widetilde{z})$.

Finally, suppose we are in the general case. The transformation from (x, y, z) to $(\widetilde{x}, \widetilde{y}, \widetilde{z})$ is the same as if we were in a cylindric 2-loop plabic network, so $\lambda_i(x, y, z) = \lambda_i(\widetilde{x}, \widetilde{y}, \widetilde{z})$ in this case as well. □

Since $\mathbf{x}_{[1,n]} = \widetilde{\mathbf{y}_{[1,n]}}$, $\mathbf{y}_{[1,n]} = \widetilde{\mathbf{x}_{[1,n]}}$, and $\lambda_i(x, y, z) = \lambda_i(\widetilde{x}, \widetilde{y}, \widetilde{z})$, we see that $-p_j$ from our original network is equal to p_j from the network with edge weights $(\widetilde{x}, \widetilde{y}, \widetilde{z})$. Thus, we can find $(\widetilde{\widetilde{x}}, \widetilde{\widetilde{y}}, \widetilde{\widetilde{z}})$ by taking our original network, moving the edge p_j around by square moves, and then moving the edge $-p_j$ around by square moves.

Lemma 6.5.6. *After applying the gauge transformations to the network to get from $(\widetilde{x}, \widetilde{y}, \widetilde{z})$ to (x', y', z'), the edges labeled by $p_j, -p_j$ in the $(\widetilde{x}, \widetilde{y}, \widetilde{z})$ network are replaced with $-p'_j$ and $p'_j = \dfrac{\mathbf{x}'_{[1,n]} - \mathbf{y}'_{[1,n]}}{\lambda_j(x', y', z')}$, respectively.*

Proof. In the network with edges $(\widetilde{x}, \widetilde{y}, \widetilde{z})$, consider $p_j \lambda_j(\widetilde{x}, \widetilde{y}, \widetilde{z}) = \mathbf{x}_{[1,n]} - \mathbf{y}_{[1,n]} =$ a sum of weights of some cycles beginning and ending at the vertex on the bottom right of the face between strings $\varkappa$ and $\varkappa + 1$ with edge $\widetilde{x}_j$. Since gauge transformations don't affect the weight of cycles, $p_j \lambda_j(\widetilde{x}, \widetilde{y}, \widetilde{z}) = -p'_j \lambda_j(x', y', z')$ where $-p'_j$ is the weight of the edge previously weighted p_j after applying gauge transformations to obtain the network with edge weights (x', y', z') from the one with edge weights $(\widetilde{x}, \widetilde{y}, \widetilde{z})$. So, $-p'_j$ must be $\dfrac{\mathbf{x}_{[1,n]} - \mathbf{y}_{[1,n]}}{\lambda_j(x', y', z')} = \dfrac{\mathbf{y}'_{[1,n]} - \mathbf{x}'_{[1,n]}}{\lambda_j(x', y', z')}$. A similar argument holds for p'_j. □

Lemma 6.5.7. *Gauge transformations commute with the square move.*

Proof. Since our formulas for the square move come from the face weighted square move, and gauge transformations don't affect face weights, gauge transformations commute with the square move. □

Theorem 6.5.8. *We have the following commutative diagram.*

$$
\begin{array}{ccccc}
(x,y,z) & \xrightarrow{\textit{square moves}} & (\widetilde{x},\widetilde{y},\widetilde{z}) & \xrightarrow{\textit{gauge trans.}} & (x',y',z') \\
 & & \Big\downarrow \scriptstyle{\textit{square moves}} & & \Big\downarrow \scriptstyle{\textit{square moves}} \\
 & & (\widetilde{\widetilde{x}},\widetilde{\widetilde{y}},\widetilde{\widetilde{z}}) & \xrightarrow{\textit{gauge trans.}} & (\widetilde{x'},\widetilde{y'},\widetilde{z'}) \\
 & & \searrow \scriptstyle{\textit{gauge trans.}} & & \swarrow \scriptstyle{\textit{gauge trans.}} \\
 & & & \left((\widetilde{x})',(\widetilde{y})',(\widetilde{z})'\right) = (x'',y'',z'') &
\end{array}
$$

Proof. By Lemma 6.5.6 we can get from (x',y',z') to $(\widetilde{x'},\widetilde{y'},\widetilde{z'})$ by square moves. By Lemma 6.5.5, we can find $(\widetilde{\widetilde{x}},\widetilde{\widetilde{y}},\widetilde{\widetilde{z}})$ from $(\widetilde{x},\widetilde{y},\widetilde{z})$ by doing square moves. Lemma 6.5.7 tells us we have the bottom arrow of the square in the diagram such that the square commutes. Both $\left((\widetilde{x})',(\widetilde{y})',(\widetilde{z})'\right)$ and (x'',y'',z'') can be obtained from $(\widetilde{\widetilde{x}},\widetilde{\widetilde{y}},\widetilde{\widetilde{z}})$ by gauge transformations. Since $\left((\widetilde{x})',(\widetilde{y})',(\widetilde{z})'\right)$ and (x'',y'',z'') both have the same edge weights set equal to 1 and the number of edge weights not set to be 1 is the same as the dimension of the space of face and trail weights, $\left((\widetilde{x})',(\widetilde{y})',(\widetilde{z})'\right) = (x'',y'',z'')$. $\square$

We can now prove the second part of Theorem 6.2.5.

Proof. This is a matter of checking that $(x'',y'',z'') = (x,y,z)$. We will to this using the left branch of our commutative diagram in Theorem 6.5.8.

Notice that rather than moving the edge p all the way around and then moving the edge $-p$ all the way around, we can do one square move with p and one square move with $-p$. Computations very similar to those in the proof of Theorem 6.5.3 show that $(\widetilde{\widetilde{x}},\widetilde{\widetilde{y}},\widetilde{\widetilde{z}}) = (x,y,z)$. This means we don't have to do any gauge transformations to get to (x'',y'',z'') and in fact $(x'',y'',z'') = (\widetilde{\widetilde{x}},\widetilde{\widetilde{y}},\widetilde{\widetilde{z}}) = (x,y,z)$. $\square$

Suppose we have a directed cylindric 2-loop plabic network with no interior vertices. Consider the 1-expanded network on its universal cover. Let y_i be a weight in the expanded network that has not been set to 1. Let j be minimal such that $j > i$ and x_j is not set to 1. Let k, ℓ be maximal such that $k \leq i, \ell < i$ and x_k, y_ℓ are not set to 1. Let a be the source below x_k, b be the source between x_j and x_k, c be the source above x_j, d be the sink between y_i and y_ℓ, and e be the sink below y_ℓ. Let $n(w) =$ the number of times the edge w crosses the cut from the right $-$ the number of times the edge w

crosses the cut from the left. Then we have the following relations:

$$M_{bd} = x_j(-\zeta)^{n(x_j)}M_{cd} + y_\ell(-\zeta)^{n(y_\ell)}M_{be} - x_jy_\ell(-\zeta)^{n(x_j)+n(y_\ell)}M_{ce}$$
$$M_{ad} = x_k(-\zeta)^{n(x_k)}M_{bd} + y_\ell(-\zeta)^{n(y_\ell)}M_{ae} - x_ky_\ell(-\zeta)^{n(x_k)+n(y_\ell)}M_{be}$$

Thus, we have relations between y_ℓ and x_j and between y_ℓ and x_k. In particular, we have:

$$x_j = \frac{M_{bd} - y_\ell(-\zeta)^{n(y_\ell)}M_{be}}{(-\zeta)^{n(x_j)}M_{cd} - y_\ell(-\zeta)^{n(x_j)+n(y_\ell)}M_{ce}}$$
$$y_\ell = \frac{M_{ad} - x_k(-\zeta)^{n(x_k)}M_{bd}}{(-\zeta)^{n(y_\ell)}M_{ae} - (-\zeta)^{n(x_k)+n(y_\ell)}x_kM_{be}}$$

Combining these, we get a relation between x_j and x_k.

$$x_j = \frac{M_{bd}M_{ae} - M_{ad}M_{be}}{(-\zeta)^{n(x_j)}(M_{ae}M_{cd} - M_{ad}M_{ce}) + x_k(-\zeta)^{n(x_j)+n(x_k)}(M_{bd}M_{ce} - M_{be}M_{cd})}$$

Lemma 6.5.9. *If we know the boundary measurements of a network, then repeated substitution with the above formula to get x_j as a function of x_n will always yield a linear expression in x_n divided by another linear expression in x_n.*

Proof. We only need to check one step. Suppose we have $x_j = \frac{A+Bx_m}{C+Dx_m}$ and $x_m = \frac{E}{F+Gx_n}$, coming from the formula above. Then $x_j = \frac{(AF+BE)+AGx_n}{(CF+DE)+CGx_n}$. □

Now we prove the third part of Theorem 6.2.5.

Proof. Choose an edge on string 1 that is not set to 1. Call it x_j. Let x_k be the next edge below x_j on the left string that is not set to one. Suppose we do a transformation that preserves the boundary measurements and replaces x_j with x'_j, x_k with x'_k, and so on. Since the transformation does not change the boundary measurements, the above relation between x_j and x_k holds for x'_j and x'_k. Similarly, if x'_ℓ is the next edge weight on string 1 that is not set to 1, x'_k and x'_ℓ have the same relationship. So, substitution gives us a formula for x'_j in terms of x'_ℓ. Repeating this process all the way around the cylinder, we get an expression for x'_j in terms of itself. By Lemma 6.5.9, clearing the denominator gives a quadratic equation in x'_j. Quadratic equations have at most two solutions, so there are at most 2 possibilities for x'_j. We have identified two solutions in our involution, so we know these are the only two solutions. $\square$

Now we return to the general case of a directed cylindric k-loop plabic network. Choose $1 \leq \varkappa < k-1$ and find the $\varkappa$-expanded network. We can then find the $\varkappa+1$-expanded network of this network. Now, we can choose a face in the network and add the edges $p, -p$ between strings $\varkappa$ and $\varkappa+1$, $q, -q$ between strings $\varkappa+1$ and $\varkappa+2$, and $r, -r$ between strings $\varkappa$ and $\varkappa+1$ so that moving p around the cylinder by square moves until it is below $-p$ is equivalent to applying $T_{\varkappa,e}$, modulo gauge transformations, then moving q around the cylinder by square moves until it's below p is equivalent to applying $T_{\varkappa+1,e}$, modulo gauge transformations, and finally moving r around the cylinder by square moves until it's below q is equivalent to applying $T_{\varkappa,e}$ a second time, modulo gauge transformations (see Figure 6.6). Since gauge transformations commute with square moves (Lemma 6.5.7), we can apply all of our gauge transformations at the end, and get $T_{\varkappa,e} \circ T_{\varkappa+1,e} \circ T_{\varkappa,e}$.

Lemma 6.5.10. *Starting with a plabic network that looks like the top half of a face with $p, q,$ and r added, there is an 8-cycle of square moves. That is, there is a sequence of 8 square moves where the networks we obtain after each of the first 7 square moves are all different from each other and from the original network, but the network we obtain after the 8th square move is the same as the original network.*

Proof. Since this 8-cycle is on a portion of the cylinder isomorphic to the disk, we will use an undirected plabic network with face weights to prove this. This gives us a more general statement, as we could choose any orientations and sets of edge weights that give the plabic networks in the following figures, and the proof would hold true. Thus, we will consider that we are starting with a plabic network that looks as follows:

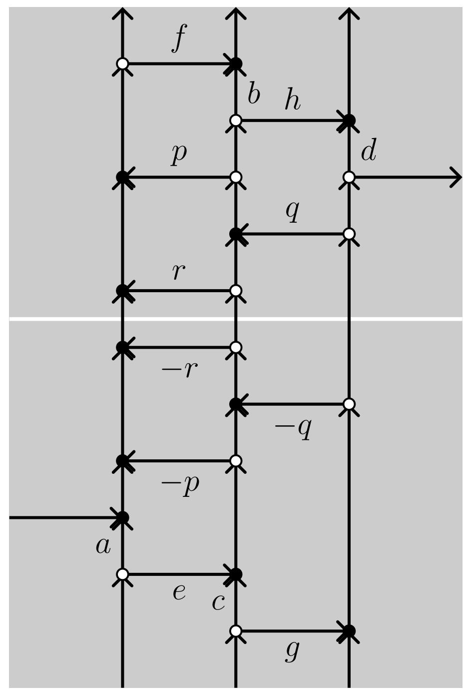

Figure 6.6: A face of a network with the edges $p, -p, q, -q, r$, and $-r$ added as described above. The area above the white line is the top half to the face, as referenced in Lemma 6.5.10.

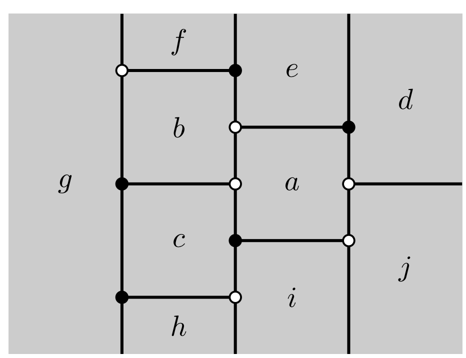

Let $A = 1 + c + ac$ and $B = 1 + b + bc + abc = 1 + bA$. Applying unicolored edge contractions shows that the above plabic network is the same as the network in the upper left corner of the following 8-cycle:

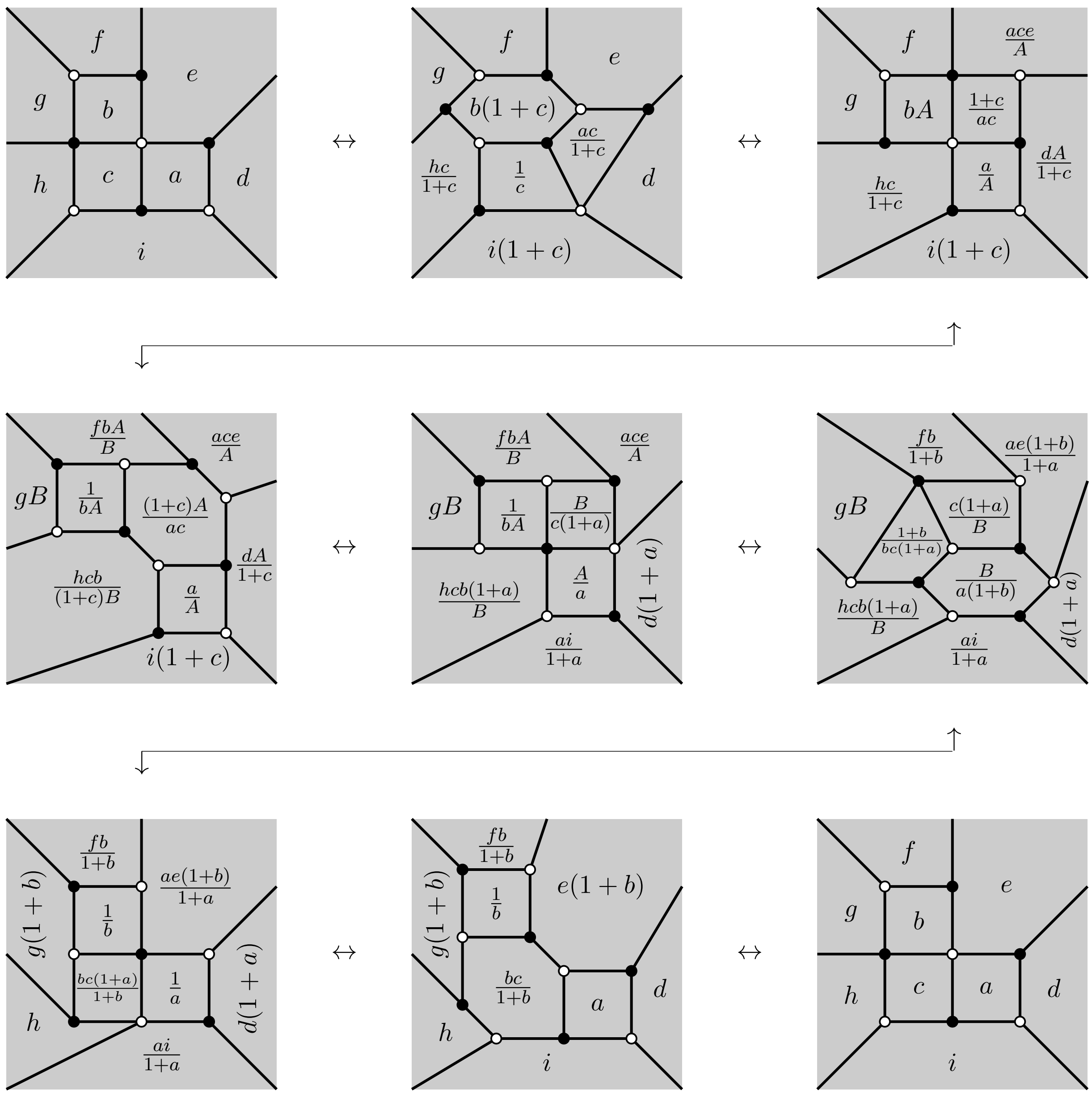

□

Finally, we can prove the last part of Theorem 6.2.5.

Proof. Consider one face in our doubly expanded plabic network. We can either add $p, -p, q, -q, r$, and $-r$ as described above, or we can add $P, -P, Q, -Q, R$, and $-R$ where $P, -P$ are between strings $\varkappa + 1$ and $\varkappa + 2$, $Q, -Q$ are between strings $\varkappa$ and $\varkappa + 1$, and $R, -R$ are between strings $\varkappa + 1$ and $\varkappa + 2$ so that moving P around the cylinder by square moves until it's below $-P$ is equivalent to applying $T_{\varkappa+1,e}$, modulo gauge transformations, then moving Q around the cylinder by square moves until it's below P is equivalent to applying $T_{\varkappa,e}$, modulo gauge transformations, and finally moving R around the cylinder by square moves until it's below Q is equivalent to applying $T_{\varkappa+1,e}$ a second time, modulo gauge transformations. If we add P, Q, R to our network, to a face, the face looks as follows:

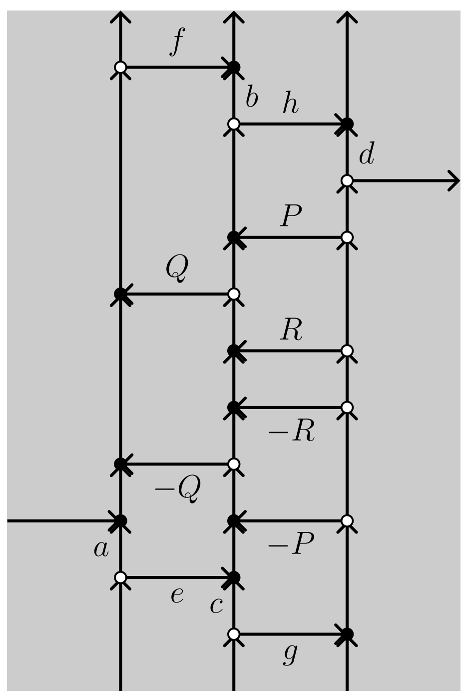

Let's look at just the upper half of this picture. Notice this is the same as the second step in the 8-cycle in Lemma 6.5.10. Starting with p, q, and r inserted into a face, the 8-cycle tells us that using a square move to change to a network where the upper half of that face looks like the one with P, Q, and R, although we do not know that the edges have the right weights, and then pushing each of those edges up one face on the cylinder, is the same as pushing p, q, and r up one face on the cylinder, and then using a square move to change to a network that looks like one with P, Q, and R pushed up one face on the cylinder.

Suppose we move p, q, and r all the way around the cylinder (performing $T_{\varkappa,e} \circ T_{\varkappa+1,e} \circ T_{\varkappa,e}$, modulo gauge transformations) and then do a square move to get to a network that looks like one with P, Q, and R pushed around the cylinder. The previous paragraph tells us that instead, we could push p, q, and r around the cylinder except for one face, then do a square move to get to a network that looks like one with P, Q, and R pushed around the cylinder except for one face, then push the three edges up the last face. We can keep doing this square move to get a face that looks like one with P, Q, and R begin pushed around the cylinder one face earlier until it's the first thing we do. Doing this move first gives us values on the edges that are the same as those after we push them around the cylinder, as the values of p, q, and r are the same before and after being pushed around the cylinder. By Lemma 6.5.2 this means that the values are the P, Q, and R defined above, and further, that $T_{\varkappa,e} \circ T_{\varkappa+1,e} \circ T_{\varkappa,e} = T_{\varkappa+1,e} \circ T_{\varkappa,e} \circ T_{\varkappa+1,e}$. □

We now turn our attention to $T_{\varkappa,f}$ and Theorem 6.3.3.

Theorem 6.5.11. *Applying $T_{\varkappa,e}$ to the edge weights defined in Lemma 6.3.1, then turning the graph back into a face weighted graph gives the following weights:*

$$
\begin{aligned}
a_i' &= \frac{\widehat{\lambda}_j(a,b,c)}{\widehat{\lambda}_p(a,b,c)\,\mathbf{b}_{\mathcal{B}_{[p,j-1]}}} \quad \textit{where } a_i \textit{ is associated to } j, a_{i-1} \textit{ is associated to } p \\
b_i' &= \frac{\widehat{\lambda}_q(a,b,c)}{\widehat{\lambda}_j(a,b,c)\,\mathbf{a}_{\mathcal{A}_{[j+1,q]}}} \quad \textit{where } b_i \textit{ is associated to } j, b_{i+1} \textit{ is associated to } q \\
c_i' &= \frac{\mathbf{a}_{\mathcal{A}_{[i,i+1]}}\,\mathbf{b}_{\mathcal{B}_{[i-1,i]}}\,c_i\widehat{\lambda}_{i-1}(a,b,c)}{\widehat{\lambda}_{i+1}(a,b,c)} \\
t' &= t
\end{aligned}
$$

Proof. The formulas for a_i', b_i', and c_i' follow from Theorem 6.5.3. Note there is no need to use the formulas for x_i', y_i', and z', as these arise from the formulas for $\widetilde{x}_i, \widetilde{y}_i$ by gauge transformations, which do not affect the face weights. Because of the way we chose our trail, none of the gauge transformations will affect the weight of the trail. Thus the trail weight remains the same. □

Now we prove Theorem 6.3.3.

Proof. By Theorem 6.5.11, these properties are inherited from Theorem 6.2.5. □

Chapter 7

Spider Web Quivers

7.1 Spider Web Quivers and a Mutation Sequence τ

Recall the cluster algebra definitions from Section 3.1.

In [ILP19], Inoue, Lam, and Pylyavskyy obtain the geometric R-matrix from a sequence of cluster mutations of a triangular grid quiver. Triangular grid quivers are exactly the dual quivers to the plabic graph associated to certain simple-crossing networks, such as the plabic graph in Example 6.2.6. In [GS18], Goncharov and Shen show that in another family of quivers, the same mutation sequence gives a Weyl group action. The rest of this chapter will explore how these cases generalize.

Definition 7.1.1. A *spider web quiver* is a quiver constructed as follows. We begin with three or more concentric circles. Place as many vertices as desired (at least 2 so as to avoid loops) on each circle. Orient the edges of each circle counter clockwise. Then add edges in the diagram between vertices on adjacent circles so that each face is oriented, contains two edges between circles, and has at least 3 sides.

For the purposes of this paper, we will assume a spider web quiver has $k+1$ circles, labeled 0 through k froum outermost to innermost. Choose $1 \leq \varkappa < k$ and label the vertices of the circle $\varkappa$ as $1, ..., n$ following the arrows around the circle. If the lowest index vertex in circle $\varkappa$ with an edge to circle $\varkappa - 1$ is i, label the vertex in circle $\varkappa - 1$ which has an arrow to i as 1^-. Continue labeling the vertices of circle $\varkappa - 1$ as $2^-, 3^-, ...$ following the arrows around the circle. If the lowest index vertex in circle $\varkappa$ with an edge to circle $\varkappa + 1$ is j, label the vertex in circle $\varkappa + 1$ which has an arrow to j as 1^+.

Continue labeling the vertices of circle $\varkappa + 1$ as $2^+, 3^+, \ldots$ following the arrows around the circle. See Figure 7.1 for examples.

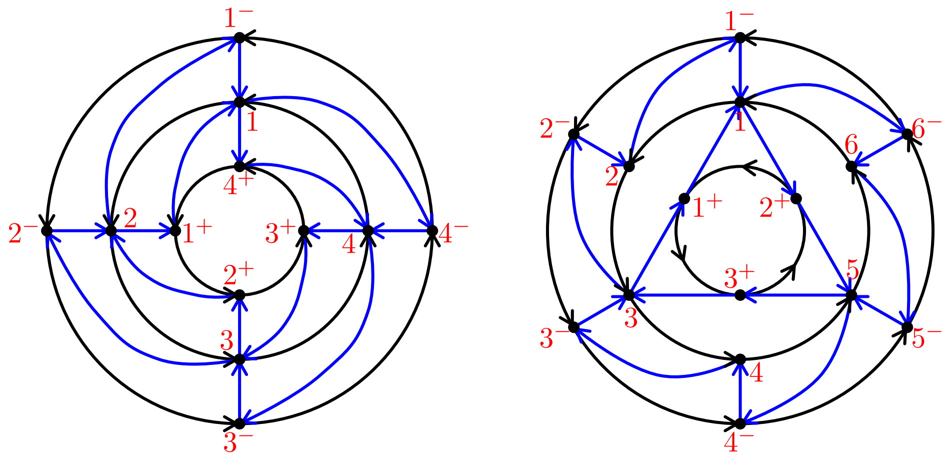

Figure 7.1: Two spider web quivers. The quiver on the left is a triangular grid quiver, as in [ILP19]. The quiver on the right is a 3-triangulation with 3 ideal triangles, as in Section 8 of [GS18].

For a choice of $\varkappa$, n will always be the number of vertices on circle $\varkappa$. We'll be considering the transformation $\tau_\varkappa := \mu_1\mu_2 \ldots \mu_{n-2} s_{n-1,n} \mu_n \mu_{n-1} \ldots \mu_1$ where $s_{n-1,n}$ is the operation that transposes vertices n and $n-1$.

Proposition 7.1.2. *If Q is a spider web quiver, then for any choice of $\varkappa$, $\tau_\varkappa(Q) = Q$.*

To prove this proposition, we first need a series of lemmas. For $1 \leq r \leq n$, define Q_r as $\mu_r \mu_{r-1} \ldots \mu_1(Q)$. Lemmas 7.1.3 through 7.1.10 may be proven by induction.

Lemma 7.1.3. *For $r < n-2$, the edges of Q_r between vertices in circle $\varkappa$ are:*

(1) a possibly empty directed path $1 \to 2 \to \ldots \to r$,

(2) a directed path $r+1 \to r+2 \to \ldots \to n$,

(3) an oriented triangle $r \to n \to r+1 \to r$.

Let A be the set of vertices in circle $\varkappa$ that have edges to circle $\varkappa - 1$ and A_s be the smallest element of A. Let $A' = \{\text{vertices } i \mid i+1 \in A\}$ and A'_s be the smallest element of A'. We will define $A_{t,[i,j]}$ to be the tth largest element of A weakly between i and j and $A'_{t,(i,j)}$ to be the tth largest element of A' strictly between i and j. We will also let $O_{t,[i,j]}$ be the tth largest element in circle $\varkappa - 1$ connected to an element of circle $\varkappa - 1$ weakly between i and j.

Lemma 7.1.4. *Suppose $1 \in A$. Then for $r < n-2$ the edges between circles $\varkappa$ and $\varkappa - 1$ in Q_r are:*

(1) $O_{1,[1,n]} \to 1 \to 1^-$,

(2) $r \to O_{1,[1,r]} \to A'_{1,(1,r)} \to O_{2,[1,r]} \to A'_{2,(1,r)} \to \ldots \to A'_{\ell,(1,r)} \to O_{\ell-1,[1,r]} \to 1$, *where $\ell \in [1,n]$ is such that $A'_{\ell,(1,r)}$ is the smallest vertex strictly between 1 and r in A',*

(3) $n \to O_{1,[1,n-1]} \to A_{1,[1,n-1]} \to O_{2,[1,n-1]} \to A_{2,[1,n-1]} \to \ldots \to A_{m,[1,n-1]} \to O_{m-1,[1,n-1]} \to r+1$, *where $m \in [1,n]$ is such that $A_{m,[1,n-1]}$ is the smallest element of A greater than $r+1$.*

Lemma 7.1.5. *Suppose $1 \notin A$. For $r < n-2$, if $r < A_s$, then the edges between circles $\varkappa$ and $\varkappa - 1$ in Q_r are:*

(1) the same edges as in the original quiver, that is, $O_{1,[1,n]} \to A_{1,[1,n]} \to O_{2,[1,n]} \to A_{2,[1,n]} \to \ldots \to O_{\ell,[1,n]} \to A_{\ell,[1,n]} \to O_{1,[1,n]}$, *where $\ell \in [1,n]$ is such that $A_{\ell,[1,n]} = A_s$.*

Otherwise the edges between circles $\varkappa$ and $\varkappa - 1$ in Q_r are:

(1) $O_{1,[1,n]} \to A_s$,

(2) $r \to O_{1,[1,r]} \to A'_{1,(1,r)} \to O_{2,[1,r]} \to A'_{2,(1,r)} \to \ldots \to A'_s$,

(3) $n \to O_{1,[1,n-1]} \to A_{1,[1,n-1]} \to O_{2,[1,n-1]} \to A_{2,[1,n-1]} \to \ldots \to A_{m,[1,n-1]} \to O_{m-1,[1,n-1]} \to r+1$, *where $m \in [1,n]$ is such that $A_{m,[1,n-1]}$ is the smallest element of A greater than $r+1$.*

Let B be the set of vertices in circle $\varkappa$ that have edges to circle $\varkappa + 1$ and B_s be the smallest element of B. Let $B' = \{\text{vertices } i \mid i+1 \in B\}$ and B'_s be the smallest element of B'. We will define $B_{t,[i,j]}$ to be the tth largest element of B weakly between i and j and $B'_{t,(i,j)}$ to be the tth largest element of B' strictly between i and j. We will also let $I_{t,[i,j]}$ be the tth largest element in circle $\varkappa+1$ connected to an element of circle $\varkappa$ weakly between i and j.

Lemma 7.1.6. *Suppose* $1 \in B$. *Then for* $r < n-2$ *the edges between circles* $\varkappa$ *and* $\varkappa+1$ *in* Q_r *are:*

(1) $I_{1,[1,n]} \to 1 \to 1^+$,

(2) $r \to I_{1,[1,r]} \to B'_{1,(1,r)} \to I_{2,[1,r]} \to B'_{2,(1,r)} \to \ldots \to B'_{\ell,(1,r)} \to I_{\ell-1,[1,r]} \to 1$, *where* $\ell \in [1,n]$ *is such that* $B'_{\ell,(1,r)}$ *is the smallest vertex strictly between 1 and* r *in* B',

(3) $n \to I_{1,[1,n-1]} \to B_{1,[1,n-1]} \to I_{2,[1,n-1]} \to B_{2,[1,n-1]} \to \ldots \to B_{m,[1,n-1]} \to I_{m-1,[1,n-1]} \to r+1$, *where* $m \in [1,n]$ *is such that* $B_{m,[1,n-1]}$ *is the largest element of* B *greater than* $r+1$.

Lemma 7.1.7. *Suppose* $1 \notin B$. *For* $r < n-2$, *if* $r < B_s$, *then the edges between circles* $\varkappa$ *and* $\varkappa+1$ *in* Q_r *are:*

(1) the same edges as in the original quiver, that is, $I_{1,[1,n]} \to B_{1,[1,n]} \to I_{2,[1,n]} \to B_{2,[1,n]} \to \ldots \to I_{\ell,[1,n]} \to B_{\ell,[1,n]} \to I_{1,[1,n]}$, *where* $\ell \in [1,n]$ *is such that* $B_{\ell,[1,n]} = B_s$.

Otherwise the edges between circles $\varkappa$ and $\varkappa+1$ in Q_r are:

(1) $I_{1,[1,n]} \to B_s$,

(2) $r \to I_{1,[1,r]} \to B'_{1,(1,r)} \to I_{2,[1,r]} \to B'_{2,(1,r)} \to ... \to B'_s$,

(3) $n \to I_{1,[1,n-1]} \to B_{1,[1,n-1]} \to I_{2,[1,n-1]} \to B_{2,[1,n-1]} \to ... \to B_{m,[1,n-1]} \to I_{m-1,[1,n-1]} \to r+1$, *where* $m \in [1,n]$ *is such that* $B_{m,[1,n-1]}$ *is the largest element of* B *greater than* $r+1$.

Lemma 7.1.8. *For $r < n-2$, the edges of Q_r between vertices in circle $\varkappa - 1$ are:*

(1) *The directed circle* $1^- \to 2^- \to ... \to n^- \to 1^-$,

(2) *The edge* $1^- \to O_{1,[1,n]}$, *if* $r \geq A_s$.

Lemma 7.1.9. *For $r < n-2$, the edges of Q_r between vertices in circle $\varkappa + 1$ are:*

(1) *The directed circle* $1^+ \to 2^+ \to ... \to n^+ \to 1^+$.

(2) *The edge* $1^+ \to I_{1,[1,n]}$, *if* $r \geq B_s$.

Lemma 7.1.10. *For $r < n-2$, the edges of Q_r between vertices between circles $\varkappa - 1$ and $\varkappa + 1$ are:*

(1) $1^- \to I_{1,[1,n]}$, *if* $A_s \leq B_s$,

(2) $1^+ \to O_{1,[1,n]}$, *if* $B_s \leq A_s$.

Lemma 7.1.11. *If $s_{n-1,n}$ transposes vertices $n-1$ and n, then $s_{n-1,n}\mu_n\mu_{n-1}(Q_{n-2}) = Q_{n-2}$.*

Proof. We can check all the cases. □

The proof of Proposition 7.1.2 follows easily.

Proof.

$$\begin{aligned}
\mu_1\mu_2...\mu_{n-2}s_{n-1,n}\mu_n\mu_{n-1}...\mu_1(Q) &= \mu_1\mu_2...\mu_{n-2}s_{n-1,n}\mu_n\mu_{n-1}(Q_{n-2}) \\
&= \mu_1\mu_2...\mu_{n-2}(Q_{n-2}) \text{ by Lemma 7.1.11} \\
&= Q \text{ as } \mu_1\mu_2...\mu_{n-2} \text{ is } (\mu_{n-2}\mu_{n-3}...\mu_1)^{-1}
\end{aligned}$$

□

7.2 x-dynamics

Given a spider web quiver Q and a choice of $\varkappa$, let α be the largest vertex on circle $\varkappa - 1$ connected to circle $\varkappa$ and β be the largest vertex on circle $\varkappa + 1$ connected to circle $\varkappa$. We can associate an x-variable to each vertex in Q. We will consider the indices for $x_1, ..., x_n$ to be modular. If $1 \leq i < j \leq n$, let $[i, j]$ denote the set $\{i, i+1, ..., j\}$. If $1 \leq j < i \leq n$ let $[i, j]$ denote the set $\{i, i+1, ..., n, 1, 2, ..., j\}$. For any set S, let $S + k := \{s - k \mid s \in S\}$. We'll define $\mathbf{x}_S := \prod_{i \in S} x_i$.

$$\text{Let } x_{[i]^-_*} := \begin{cases} x_a & \text{if there is at least one vertex on circle } \varkappa - 1 \text{ with an edge to an} \\ & \text{element of } [1, i], \text{ and the largest such vertex is } a, \\ x_\alpha & \text{otherwise.} \end{cases}$$

$$\text{Let } x_{[i]^+_*} := \begin{cases} x_b & \text{if there is at least one vertex on circle } \varkappa + 1 \text{ with an edge to an} \\ & \text{element of } [1, i], \text{ and the largest such vertex is } b, \\ x_\beta & \text{otherwise.} \end{cases}$$

Theorem 7.2.1. *For a spider web quiver Q and a choice of $\varkappa$, let*

$$\overline{x} = \frac{\sum_{j=1}^{n} \mathbf{x}_{[j+2,j-1]} \, x_{[j]^-_*} x_{[j]^+_*}}{}.$$

Then, $\tau_\varkappa(x_i) = x_i \overline{x}$.

Before proving this theorem, we will need a proposition. Recall the definitions of A and B from 7.1.

$$\text{Let } x_{i,A} := \begin{cases} x_\alpha & \text{if } i \text{ is the smallest element of } A, \\ 1 & \text{otherwise.} \end{cases}$$

$$\text{Let } x_{i,B} := \begin{cases} x_\beta & \text{if } i \text{ is the smallest element of } B, \\ 1 & \text{otherwise.} \end{cases}$$

$$\text{Let } x_{[i]^-} := \begin{cases} x_a & \text{if there is at least one vertex on circle } \varkappa - 1 \text{ with an edge to an} \\ & \text{element of } [1, i], \text{ and the largest such vertex is } a, \\ 1 & \text{otherwise.} \end{cases}$$

Let $x_{[i]^+} := \begin{cases} x_b & \text{if there is at least one vertex on circle } \varkappa+1 \text{ with an edge to an} \\ & \text{element of } [1,i], \text{ and the largest such vertex is } b, \\ 1 & \text{otherwise.} \end{cases}$

We will continue to think of the indices of variables $x_1, ..., x_n$ as modular. In particular, $x_0 = x_n$. However, we will define $x_{[0]^+} = x_{[0]^-} = 1$.

Proposition 7.2.2. *For a spider web quiver Q,*

$$\mu_{n-2}...\mu_1(x_i) = x_n x_{i+1} \sum_{j=0}^{i} \frac{x_{[j]^-} x_{[j]^+} \prod_{k=j+1}^{i} x_{k,A} x_{k,B}}{\mathbf{x}_{[j,j+1]}},$$

for $1 \leq i \leq n-2$.

Proof. Notice that $\mu_{n-2}...\mu_1(x_i) = \mu_i...\mu_1(x_i)$. Using this and Lemmas 7.1.3 through 7.1.7, we see

$$\mu_{n-2}...\mu_1(x_1) = \frac{x_n x_{[1]^-} x_{[1]^+} + x_2 x_{1,A} x_{1,B}}{x_1},$$

$$\mu_{n-2}...\mu_1(x_i) = \frac{x_n x_{[i]^-} x_{[i]^+} + \mu_{n-2}...\mu_1(x_{i-1}) x_{i+1} x_{i,A} x_{i,B}}{x_i}.$$

Then the result follows by induction. □

We now have the proof of Theorem 7.2.1.

Proof. First consider $i = n, n-1$. In this case, $\tau(x_i) = s_{n-1,n}\mu_n\mu_{n-1}...\mu_1(x_i)$. We can compute this using Lemmas 7.1.3 through 7.1.7 and Proposition 7.2.2. We have the following:

$$\tau(x_{n-1}) = \frac{x_{[n-1]^-} x_{[n-1]^+} + \mu_{n-2}...\mu_1(x_{n-2}) x_{n-1,A} x_{n-1,B}}{x_n}$$

$$\tau(x_n) = \frac{x_{[n-1]^-} x_{[n-1]^+} + \mu_{n-2}...\mu_1(x_{n-2}) x_{n-1,A} x_{n-1,B}}{x_{n-1}}$$

Notice that for any i, $x_{[i]^-_*} = x_{[i]^-} \left(\prod_{k=i+1}^{j} x_{k,A}\right)$, as long as there is an element of A in $[1,j]$. Similarly, $x_{[i]^+_*} = x_{[i]^+} \left(\prod_{k=i+1}^{j} x_{k,B}\right)$, as long as there is an element of B in $[1,j]$. Substituting for $\mu_{n-2}...\mu_1(x_{n-2})$ in each of the above cases, we have what we want.

Now consider $i < n-2$. Because mutation is an involution, we know

$$\mu_i ... \mu_1 \mu_1 \mu_2 ... \mu_{n-2} s_{n-1,n} \mu_n \mu_{n-1} ... \mu_1(x_i) = \mu_{i+1} ... \mu_{n-2} s_{n-1,n} \mu_n \mu_{n-1} ... \mu_1(x_i).$$

Since mutating at a vertex only affects the variable at that vertex, this is the same as $\mu_i \mu_{i-1} ... \mu_1(x_i)$. From Proposition 7.2.2, we know the formula for this expression. Thus, all we need to do is show, starting with the cluster variables $\widetilde{x}_i = x_i \overline{x}$, mutating at 1 through i gives us back the formulas in Proposition 7.2.2.

$$\mu_i ... \mu_1(\widetilde{x}_i) = \overline{x}^2 x_n x_{i+1} \sum_{j=0}^{i} \frac{x_{[j]^-} x_{[j]^+} \prod_{k=j+1}^{i} x_{k,A} x_{k,B}}{\overline{x}^2 \, \mathbf{x}_{[j,j+1]}} = x_n x_{i+1} \sum_{j=0}^{i} \frac{x_{[j]^-} x_{[j]^+} \prod_{k=j+1}^{i} x_{k,A} x_{k,B}}{\mathbf{x}_{[j,j+1]}}.$$

□

Example 7.2.3. Consider the quiver on the left of Figure 7.1. In this case, we have

$$\begin{aligned}\overline{x} &= \frac{\mathbf{x}_{[3,4]} \, x_{[1]^-_*} x_{[1]^+_*} + \mathbf{x}_{[4,1]} \, x_{[2]^-_*} x_{[2]^+_*} + \mathbf{x}_{[1,2]} \, x_{[3]^-_*} x_{[3]^+_*} + \mathbf{x}_{[2,3]} \, x_{[4]^-} x_{[4]^+}}{\mathbf{x}_{[1,4]}} \\ &= \frac{\mathbf{x}_{[3,4]} \, x_{1^-} x_{1^+} + \mathbf{x}_{[4,1]} \, x_{2^-} x_{2^+} + \mathbf{x}_{[1,2]} \, x_{3^-} x_{3^+} + \mathbf{x}_{[2,3]} \, x_{4^-} x_{4^+}}{\mathbf{x}_{[1,4]}}\end{aligned}$$

So, the x-variables after applying τ are as follows:

$$x_1' = \frac{\mathbf{x}_{[3,4]} \, x_{1^-} x_{1^+} + \mathbf{x}_{[4,1]} \, x_{2^-} x_{2^+} + \mathbf{x}_{[1,2]} \, x_{3^-} x_{3^+} + \mathbf{x}_{[2,3]} \, x_{4^-} x_{4^+}}{\mathbf{x}_{[2,4]}}$$

$$x_2' = \frac{\mathbf{x}_{[3,4]} \, x_{1^-} x_{1^+} + \mathbf{x}_{[4,1]} \, x_{2^-} x_{2^+} + \mathbf{x}_{[1,2]} \, x_{3^-} x_{3^+} + \mathbf{x}_{[2,3]} \, x_{4^-} x_{4^+}}{\mathbf{x}_{[3,1]}}$$

$$x_3' = \frac{\mathbf{x}_{[3,4]} \, x_{1^-} x_{1^+} + \mathbf{x}_{[4,1]} \, x_{2^-} x_{2^+} + \mathbf{x}_{[1,2]} \, x_{3^-} x_{3^+} + \mathbf{x}_{[2,3]} \, x_{4^-} x_{4^+}}{\mathbf{x}_{[4,2]}}$$

$$x_4' = \frac{\mathbf{x}_{[3,4]} \, x_{1^-} x_{1^+} + \mathbf{x}_{[4,1]} \, x_{2^-} x_{2^+} + \mathbf{x}_{[1,2]} \, x_{3^-} x_{3^+} + \mathbf{x}_{[2,3]} \, x_{4^-} x_{4^+}}{\mathbf{x}_{[1,3]}}$$

All other x-variables remain the same because there are no mutations at the corresponding vertices.

Example 7.2.4. Consider the quiver on the right of Figure 7.1. In this case, we have

$$\overline{x} = \frac{\mathbf{x}_{[3,6]} \, x_{1^-} x_{1^+} + \mathbf{x}_{[4,1]} \, x_{2^-} x_{1^+} + \mathbf{x}_{[5,2]} \, x_{3^-} x_{2^+} + \mathbf{x}_{[6,3]} \, x_{4^-} x_{2^+} + \mathbf{x}_{[1,4]} \, x_{5^-} x_{3^+} + \mathbf{x}_{[2,5]} \, x_{6^-} x_{3^+}}{\mathbf{x}_{[1,6]}}$$

So, the x-variables after applying τ are as follows:

$$x_1' = \frac{\mathbf{x}_{[3,6]}\, x_{1^-} x_{1^+} + \mathbf{x}_{[4,1]}\, x_{2^-} x_{1^+} + \mathbf{x}_{[5,2]}\, x_{3^-} x_{2^+} + \mathbf{x}_{[6,3]}\, x_{4^-} x_{2^+} + \mathbf{x}_{[1,4]}\, x_{5^-} x_{3^+} + \mathbf{x}_{[2,5]}\, x_{6^-} x_{3^+}}{\mathbf{x}_{[2,6]}}$$

$$x_2' = \frac{\mathbf{x}_{[3,6]}\, x_{1^-} x_{1^+} + \mathbf{x}_{[4,1]}\, x_{2^-} x_{1^+} + \mathbf{x}_{[5,2]}\, x_{3^-} x_{2^+} + \mathbf{x}_{[6,3]}\, x_{4^-} x_{2^+} + \mathbf{x}_{[1,4]}\, x_{5^-} x_{3^+} + \mathbf{x}_{[2,5]}\, x_{6^-} x_{3^+}}{\mathbf{x}_{[3,1]}}$$

$$x_3' = \frac{\mathbf{x}_{[3,6]}\, x_{1^-} x_{1^+} + \mathbf{x}_{[4,1]}\, x_{2^-} x_{1^+} + \mathbf{x}_{[5,2]}\, x_{3^-} x_{2^+} + \mathbf{x}_{[6,3]}\, x_{4^-} x_{2^+} + \mathbf{x}_{[1,4]}\, x_{5^-} x_{3^+} + \mathbf{x}_{[2,5]}\, x_{6^-} x_{3^+}}{\mathbf{x}_{[4,2]}}$$

$$x_4' = \frac{\mathbf{x}_{[3,6]}\, x_{1^-} x_{1^+} + \mathbf{x}_{[4,1]}\, x_{2^-} x_{1^+} + \mathbf{x}_{[5,2]}\, x_{3^-} x_{2^+} + \mathbf{x}_{[6,3]}\, x_{4^-} x_{2^+} + \mathbf{x}_{[1,4]}\, x_{5^-} x_{3^+} + \mathbf{x}_{[2,5]}\, x_{6^-} x_{3^+}}{\mathbf{x}_{[5,3]}}$$

$$x_5' = \frac{\mathbf{x}_{[3,6]}\, x_{1^-} x_{1^+} + \mathbf{x}_{[4,1]}\, x_{2^-} x_{1^+} + \mathbf{x}_{[5,2]}\, x_{3^-} x_{2^+} + \mathbf{x}_{[6,3]}\, x_{4^-} x_{2^+} + \mathbf{x}_{[1,4]}\, x_{5^-} x_{3^+} + \mathbf{x}_{[2,5]}\, x_{6^-} x_{3^+}}{\mathbf{x}_{[6,4]}}$$

$$x_6' = \frac{\mathbf{x}_{[3,6]}\, x_{1^-} x_{1^+} + \mathbf{x}_{[4,1]}\, x_{2^-} x_{1^+} + \mathbf{x}_{[5,2]}\, x_{3^-} x_{2^+} + \mathbf{x}_{[6,3]}\, x_{4^-} x_{2^+} + \mathbf{x}_{[1,4]}\, x_{5^-} x_{3^+} + \mathbf{x}_{[2,5]}\, x_{6^-} x_{3^+}}{\mathbf{x}_{[1,5]}}$$

All other x-variables remain the same because there are no mutations at the corresponding vertices.

Theorem 7.2.5. *For a spider web quiver and choice of $\varkappa$, $\tau_\varkappa$ is an involution on the x-variables.*

Proof. We know that for each k, μ_k is an involution and also $s_{n-1,n}$ is an involution. This means that for each i,

$$\mu_1\mu_2 ... \mu_n s_{n-1,n} \mu_{n-2}\mu_{n-3} ... \mu_1 \mu_1\mu_2 ... \mu_{n-2} s_{n-1,n} \mu_n \mu_{n-1} ... \mu_1(x_i) = x_i.$$

Since $\mu_n s_{n-1,n} = s_{n-1,n}\mu_{n-1}$ and $\mu_{n-1} s_{n-1,n} = s_{n-1,n}\mu_n$, we have

$$\left(\mu_1\mu_2 ... \mu_{n-2} s_{n-1,n} \mu_n \mu_{n-1} ... \mu_1\right)^2 (x_i) = x_i.$$

□

Theorem 7.2.6. *Suppose we have a spider web quiver with k of concentric circles and we choose $1 \leq \varkappa < k-1$. We obtain the same x-variables by applying the transformation $\tau_\varkappa \tau_{\varkappa+1} \tau_\varkappa$ and applying the transformation $\tau_{\varkappa+1} \tau_\varkappa \tau_{\varkappa+1}$.*

Proof. Suppose circle $\varkappa$ has vertices labeled with variables $a_1, ..., a_n$ and circle $\varkappa + 1$ has vertices labeled with $b_1, ..., b_m$. If we apply $\tau_\varkappa$, the only variables that change are $a_1, ..., a_n$, which get replaced with $\overline{a}a_1, ..., \overline{a}a_n$. We denote the new variables with primes, that is $a'_i = \overline{a}a_i$ and $b'_i = b_i$.

Next we apply $\tau_{\varkappa+1}$. This means $b'_1, ..., b'_m$ get replaced with $\overline{b'}b'_1, ..., \overline{b'}b'_m$. Let's compute $\overline{b'}$.

$$\overline{b'} = \frac{\sum_{j=1}^{m} \mathbf{b'}_{[j+2,j-1]} b'_{[j]^-_*} b'_{[j]^+_*}}{\mathbf{b'}_{[1,m]}} = \frac{\sum_{j=1}^{m-1} \mathbf{b}_{[j+2,j-1]}\, \overline{a} b_{[j]^-_*} b_{[j]^+_*}}{\mathbf{b}_{[1,m]}} = \overline{a}\overline{b}$$

So, $\overline{b'}b'_i = \overline{a}\overline{b}b_i$. We denote the new variables with additional primes, that is $a''_i = \overline{a}a_i$ and $b''_i = \overline{a}\overline{b}b_i$.

Finally, we apply $\tau_\varkappa$ again. This means $a''_1, ..., a''_n$ get replaced with $\overline{a''}a''_1, ..., \overline{a''}a''_n$. Let's compute $\overline{a''}$.

$$\overline{a''} = \frac{\sum_{j=1}^{n} \mathbf{a''}_{[j+2,j-1]} a''_{[j]^-_*} a''_{[j]^+_*}}{\mathbf{a''}_{[1,n]}} = \frac{\sum_{j=1}^{n} \overline{a}^{n-2}\, \mathbf{a}_{[j+2,j-1]}\, a_{[j]^-_*} \overline{a}\overline{b} a''_{[j]^+_*}}{\overline{a}^{n} \mathbf{a}_{[1,n]}} = \overline{b}$$

So, $\overline{a''}a''_i = \overline{a}\overline{b}a_i$.

Thus, our variables after applying the three involutions are $\overline{a}\overline{b}a_1, ..., \overline{a}\overline{b}a_n$ and $\overline{a}\overline{b}b_1, ..., \overline{a}\overline{b}b_m$. By symmetry, we can see that if we had applied $\tau_{\varkappa+1}\tau_\varkappa\tau_{\varkappa+1}$, we would have obtained the same variables. □

7.3 y-dynamics

Now we will associate a y-variable to each vertex of the quiver and discuss the y-dynamics of the quiver. Again, we will consider these indices of $y_1, ..., y_n$ to be modular.

Theorem 7.3.1. *For any vertex i^- connected to circle $\varkappa$, let d_i be the minimal j so that i^- is connected to j and e_i be the maximal j so that i^- is connected to j. Similarly, For any vertex i^+ connected to circle $\varkappa$, let f_i be the minimal j so that i^+ is connected to j and g_i be the maximal j so that i^+ is connected to j. If we apply $\tau_\varkappa$ to a spider web quiver Q, we obtain the following y-variables:*

(1) If $1 \le i \le n-1$*,* $y_i' = \dfrac{\sum_{j=i-1}^{n} \mathbf{y}_{[i-1,j]} + \mathbf{y}_{[i-1,n]} \sum_{j=1}^{i-2} \mathbf{y}_{[1,j]}}{y_{i-1}\left(\sum_{j=i+1}^{n} \mathbf{y}_{[i+1,j]} + \mathbf{y}_{[i+1,n]} \sum_{j=1}^{i} \mathbf{y}_{[1,j]}\right)}$

(2) $y_n' = \dfrac{\sum_{j=n-1}^{n} \mathbf{y}_{[n-1,j]} + \mathbf{y}_{[n-1,n]} \sum_{j=1}^{n-2} \mathbf{y}_{[1,j]}}{y_{n-1} \sum_{j=1}^{n} \mathbf{y}_{[1,j]}}$

(3) If there are no edges between i^- *and circle* $\varkappa$*, then* $y_{i^-}' = y_{i^-}$

(4) If i *is maximal so that there are edges between* i^- *and circle* $\varkappa$*, then*

$$y_{i^-}' = \frac{y_{i^-}\, \mathbf{y}_{[e_i,n]} \left(\sum_{j=d_1}^{n} \mathbf{y}_{[1,j]} + \mathbf{y}_{[1,n]} \sum_{j=1}^{d_1-1} \mathbf{y}_{[1,j]}\right)}{\sum_{j=e_i}^{n} \mathbf{y}_{[e_i,j]} + \mathbf{y}_{[e_i,n]} \sum_{j=1}^{e_i-1} \mathbf{y}_{[1,j]}}$$

(5) Otherwise, $y_{i^-}' = \dfrac{y_{i^-} \left(\sum_{j=e_i}^{n} \mathbf{y}_{[d_i,j]} + \mathbf{y}_{[d_i,n]} \sum_{j=1}^{e_i-1} \mathbf{y}_{[1,j]}\right)}{\sum_{j=d_i}^{n} \mathbf{y}_{[d_i,j]} + \mathbf{y}_{[d_i,n]} \sum_{j=1}^{d_i-1} \mathbf{y}_{[1,j]}}$

(6) If there are no edges between i^+ *and circle* $\varkappa$*, then* $y_{i^+}' = y_{i^+}$

(7) If i *is maximal so that there are edges between* i^+ *and circle* $\varkappa$*, then*

$$y_{i^+}' = \frac{y_{i^+}\, \mathbf{y}_{[g_i,n]} \left(\sum_{j=f_1}^{n} \mathbf{y}_{[1,j]} + \mathbf{y}_{[1,n]} \sum_{j=1}^{f_1-1} \mathbf{y}_{[1,j]}\right)}{\sum_{j=g_i}^{n} \mathbf{y}_{[g_i,j]} + \mathbf{y}_{[g_i,n]} \sum_{j=1}^{g_i-1} \mathbf{y}_{[1,j]}}$$

(8) Otherwise, $y_{i^+}' = \dfrac{y_{i^+} \left(\sum_{j=g_i}^{n} \mathbf{y}_{[f_i,j]} + \mathbf{y}_{[f_i,n]} \sum_{j=1}^{g_i-1} \mathbf{y}_{[1,j]}\right)}{\sum_{j=f_i}^{n} \mathbf{y}_{[f_i,j]} + \mathbf{y}_{[f_i,n]} \sum_{j=1}^{f_i-1} \quad y_{[1,j]}}$

We need several lemmas to prove this theorem.

Lemma 7.3.2. *For* $1 < m \le n-2$*, the* y*-variables for the vertices in circle* $\varkappa$ *of the quiver after* m *mutations are:*

(1) If $i < m$*, then* $y_i' = \dfrac{y_{i+1}\left(1 + \sum_{j=1}^{i-1} \mathbf{y}_{[1,j]}\right)}{1 + \sum_{j=1}^{i+1} \mathbf{y}_{[1,j]}}$

(2) $y_m' = \dfrac{1 + \sum_{j=1}^{m-1} \mathbf{y}_{[1,j]}}{\mathbf{y}_{[1,m]}}$

(3) $y_{m+1}' = \dfrac{\mathbf{y}_{[1,m+1]}}{1 + \sum_{j=1}^{m} \mathbf{y}_{[1,j]}}$

(4) If $m+1<i<n$*, then* $y_i' = y_i$

(5) $y_n' = y_n\left(1+\sum_{j=1}^{m}\mathbf{y}_{[1,j]}\right)$

Proof. This can be shown by induction. □

Lemma 7.3.3. *After mutating all* n *vertices and performing the transposition* $s_{n-1,n}$*, the* y*-variables for the vertices in circle* $\varkappa$ *of the quiver are:*

(1) If $i<n-2$*, then* $y_i' = \dfrac{y_{i+1}\left(1+\sum_{j=1}^{i-1}\mathbf{y}_{[1,j]}\right)}{1+\sum_{j=1}^{i+1}\mathbf{y}_{[1,j]}}$

(2) $y_{n-2}' = \dfrac{y_{n-1}\left(1+\sum_{j=1}^{n-3}\mathbf{y}_{[1,j]}\right)\left(1+y_n\left(1+\sum_{j=1}^{n-2}\mathbf{y}_{[1,j]}\right)\right)}{1+\sum_{j=1}^{n-1}\mathbf{y}_{[1,j]}}$

(3) $y_{n-1}' = \dfrac{1}{y_n\left(1+\sum_{j=1}^{n-2}\mathbf{y}_{[1,j]}\right)}$

(4) $y_n' = \dfrac{1+\sum_{j=1}^{n-2}\mathbf{y}_{[1,j]}}{\mathbf{y}_{[1,n-1]}}$

Proof. These values can be easily computed. □

Lemma 7.3.4. *If* $1<m\leq n-2$*, then after mutating vertex* m *for the second time, the* y*-variables in circle* $\varkappa$ *of the quiver are:*

(1) If $i<m-1$*, then* $y_i' = \dfrac{y_{i+1}\left(1+\sum_{j=1}^{i-1}\mathbf{y}_{[1,j]}\right)}{1+\sum_{j=1}^{i+1}\mathbf{y}_{[1,j]}}$

(2) $y_{m-1}' = \dfrac{\left(1+\sum_{j=1}^{m-2}\mathbf{y}_{[1,j]}\right)\left(\sum_{j=m}^{n}\mathbf{y}_{[m,j-1]}+\mathbf{y}_{[m,n]}\sum_{j=1}^{m-1}\mathbf{y}_{[1,j]}\right)}{1+\sum_{j=1}^{n-1}\mathbf{y}_{[1,j]}}$

(3) $y_m' = \dfrac{1+\sum_{j=1}^{n-1}\mathbf{y}_{[1,j]}}{\left(1+\sum_{j=1}^{m-1}\mathbf{y}_{[1,j]}\right)\left(\sum_{j=m+1}^{n}\mathbf{y}_{[m+1,j]}+\mathbf{y}_{[m+1,n]}\sum_{j=1}^{m}\mathbf{y}_{[1,j]}\right)}$

(4) If $m<i<n$*, then* $y_i' = \dfrac{\sum_{j=i-1}^{n}\mathbf{y}_{[i-1,j]}+\mathbf{y}_{[i-1,n]}\sum_{j=1}^{i-2}\mathbf{y}_{[1,j]}}{y_{i-1}\left(\sum_{j=i+1}^{n}\mathbf{y}_{[i+1,j]}+\mathbf{y}_{[i+1,n]}\sum_{j=1}^{i}\mathbf{y}_{[1,j]}\right)}$

(5) $y_n = \dfrac{\left(1+\sum_{j=1}^{m-1}\mathbf{y}_{[1,j]}\right)\left(1+y_n\left(1+\sum_{j=1}^{n-2}\mathbf{y}_{[1,j]}\right)\right)}{\sum_{j=m}^{n}\mathbf{y}_{[1,j]}+\mathbf{y}_{[1,n]}\sum_{j=1}^{m-1}\mathbf{y}_{[1,j]}}$

Proof. This can be shown by induction. □

For $1 \le i \le n-2$, let

$$\widetilde{y_i} = \frac{\mathbf{y}_{[1,i]}}{1+\sum_{j=1}^{i-1}\mathbf{y}_{[1,j]}},$$

$$\widehat{y_i} = \frac{\left(1+\sum_{j=1}^{i-1}\mathbf{y}_{[1,j]}\right)\left(\sum_{j=i+1}^{n}\mathbf{y}_{[i+1,j]}+\mathbf{y}_{[i+1,n]}\sum_{j=1}^{i}\mathbf{y}_{[1,j]}\right)}{1+\sum_{j=1}^{n-1}\mathbf{y}_{[1,j]}}.$$

That is, $\widetilde{y_i}$ is the value of y_i' before mutating at i for the first time, and $\widehat{y_i}$ is the value of y_i' before mutating at i for the second time. Let

$$y_{n-1}^* = \frac{\mathbf{y}_{[1,n-1]}}{1+\sum_{j=1}^{n-2}\mathbf{y}_{[1,j]}}, \quad y_n^* = y_n\left(1+\sum_{j=1}^{n-2}\mathbf{y}_{[1,j]}\right),$$

so y_{n-1}^* is the value of y_{n-1}' before mutating at $n-1$ and y_n^* is the value of y_n' before mutating at n.

Lemma 7.3.5. *Suppose $n \in A$. Then after completing the mutation sequence, we have the following y-variables for circle $\varkappa - 1$.*

(1) If there are no edges between i^- and circle $\varkappa$, then $y_{i^-}' = y_{i^-}$.

(2) If i is maximal so that there are edges between i^- and circle $\varkappa$, then

$$y_{i^-} = \frac{y_{i^-}\left(1+\widehat{y_{d_1}}\right)}{\left(1+\widetilde{y_{d_1}}^{-1}\right)}.$$

(3) If i is second largest so that there are edges between i^- and circle $\varkappa$, then

$$y_{i^-} = \frac{y_{i^-}(1+y_{n-1}^*)\prod_{k=d_i}^{n-2}\left(1+\widetilde{y_k}\right)}{(1+y_n^{*-1})\prod_{k=d_i}^{n-2}\left(1+\widehat{y_k}^{-1}\right)}.$$

(4) Otherwise, $y_{i^-} = \dfrac{y_{i^-}\prod_{k=d_i}^{e_i-1}\left(1+\widetilde{y_k}\right)}{\prod_{k=d_i}^{e_i-1}\left(1+\widehat{y_k}^{-1}\right)}.$

Proof. We can prove this by using Lemmas 7.1.4 and 7.1.5 to know the arrows in Q_r and applying the y-mutation rules. □

Lemma 7.3.6. *Suppose $n \notin A$. Then after completing the mutation sequence, we have the following y-variables for circle $\varkappa - 1$.*

(1) If there are no edges between i^- and circle $\varkappa$, then $y'_{i^-} = y_{i^-}$.

(2) If i is maximal so that there are edges between i^- and circle $\varkappa$, then

$$y_{i^-} = \frac{y_{i^-}(1 + y^*_{n-1})\,(1 + \widehat{y_{d_1}})\prod_{k=e_i}^{n-2}(1 + \widetilde{y_k})}{(1 + y_n^{*-1})\left(1 + \widetilde{y_{d_1}}^{-1}\right)\prod_{k=e_i}^{n-2}\left(1 + \widehat{y_k}^{-1}\right)}.$$

(3) Otherwise, $y_{i^-} = \dfrac{y_{i^-}\prod_{k=d_i}^{e_i-1}(1 + \widetilde{y_k})}{\prod_{k=d_i}^{e_i-1}\left(1 + \widehat{y_k}^{-1}\right)}.$

Proof. We can prove this by using Lemmas 7.1.4 and 7.1.5 to know the arrows in Q_r and applying the y-mutation rules. □

Lemma 7.3.7. *Suppose $n \in B$. Then after completing the mutation sequence, we have the following y-variables for circle $\varkappa + 1$.*

(1) If there are no edges between i^+ and circle $\varkappa$, then $y'_{i^+} = y_{i^+}$.

(2) If i is maximal so that there are edges between i^+ and circle $\varkappa$, then

$$y_{i^+} = \frac{y_{i^+}(1 + \widehat{y_{f_1}})}{\left(1 + \widetilde{y_{f_1}}^{-1}\right)}.$$

(3) If i is second largest so that there are edges between i^+ and circle $\varkappa$, then

$$y_{i^+} = \frac{y_{i^+}(1 + y^*_{n-1})\prod_{k=f_i}^{n-2}(1 + \widetilde{y_k})}{(1 + y_n^{*-1})\prod_{k=f_i}^{n-2}\left(1 + \widehat{y_k}^{-1}\right)}.$$

(4) Otherwise, $y_{i^+} = \dfrac{y_{i^+}\prod_{k=f_i}^{g_i-1}(1 + \widetilde{y_k})}{\prod_{k=f_i}^{g_i-1}\left(1 + \widehat{y_k}^{-1}\right)}.$

Proof. We can prove this by using Lemmas 7.1.6 and 7.1.7 to know the arrows in Q_r and applying the y-mutation rules. □

Lemma 7.3.8. *Suppose $n \notin B$. Then after completing the mutation sequence, we have the following y-variables for circle $\varkappa + 1$.*

(1) If there are no edges between i^+ and circle $\varkappa$, then $y'_{i^+} = y_{i^+}$.

(2) If i is maximal so that there are edges between i^+ and circle $\varkappa$, then

$$y_{i^+} = \frac{y_{i^+}(1 + y^*_{n-1})\,(1 + \widehat{y_{f_1}}) \prod_{k=g_i}^{n-2} (1 + \widetilde{y_k})}{(1 + y_n^{*-1})\left(1 + \widetilde{y_{f_1}}^{-1}\right) \prod_{k=g_i}^{n-2} \left(1 + \widehat{y_k}^{-1}\right)}.$$

(3) Otherwise, $y_{i^+} = \dfrac{y_{i^+} \prod_{k=f_i}^{g_i-1} (1 + \widetilde{y_k})}{\prod_{k=f_i}^{g_i-1} \left(1 + \widehat{y_k}^{-1}\right)}$.

Proof. We can prove this by using Lemmas 7.1.6 and 7.1.7 to know the arrows in Q_r and applying the y-mutation rules. □

Now we have the proof of Theorem 7.3.1.

Proof. This follows from Lemmas 7.3.4 through 7.3.8. □

Example 7.3.9. Consider the quiver on the left of Figure 7.1. In this case, we have:

$$y'_1 = \frac{1 + y_1 + \mathbf{y}_{[1,2]} + \mathbf{y}_{[1,3]}}{y_2 + \mathbf{y}_{[2,3]} + \mathbf{y}_{[2,4]} + \mathbf{y}_{[2,1]}} \qquad y'_2 = \frac{1 + y_2 + \mathbf{y}_{[2,3]} + \mathbf{y}_{[2,4]}}{y_3 + \mathbf{y}_{[3,4]} + \mathbf{y}_{[3,1]} + \mathbf{y}_{[3,2]}}$$

$$y'_3 = \frac{1 + y_3 + \mathbf{y}_{[3,4]} + \mathbf{y}_{[3,1]}}{y_4 + \mathbf{y}_{[4,1]} + \mathbf{y}_{[4,2]} + \mathbf{y}_{[4,3]}} \qquad y'_4 = \frac{1 + y_4 + \mathbf{y}_{[4,1]} + \mathbf{y}_{[4,2]}}{y_1 + \mathbf{y}_{[1,2]} + \mathbf{y}_{[1,3]} + \mathbf{y}_{[1,4]}}$$

$$y'_{1^-} = \frac{y_{1^-}(y_2 + \mathbf{y}_{[2,3]} + \mathbf{y}_{[2,4]} + \mathbf{y}_{[2,1]})}{1 + y_2 + \mathbf{y}_{[2,3]} + \mathbf{y}_{[2,4]}} \qquad y'_{2^-} = \frac{y_{2^-}(y_3 + \mathbf{y}_{[3,4]} + \mathbf{y}_{[3,1]} + \mathbf{y}_{[3,2]})}{1 + y_3 + \mathbf{y}_{[3,4]} + \mathbf{y}_{[3,1]}}$$

$$y'_{3^-} = \frac{y_{3^-}(y_4 + \mathbf{y}_{[4,1]} + \mathbf{y}_{[4,2]} + \mathbf{y}_{[4,3]})}{1 + y_4 + \mathbf{y}_{[4,1]} + \mathbf{y}_{[4,2]}} \qquad y'_{4^-} = \frac{y_{4^-}(y_1 + \mathbf{y}_{[1,2]} + \mathbf{y}_{[1,3]} + \mathbf{y}_{[1,4]})}{1 + y_1 + \mathbf{y}_{[1,2]} + \mathbf{y}_{[1,3]}}$$

$$y'_{1^+} = \frac{y_{1^+}(y_2 + \mathbf{y}_{[2,3]} + \mathbf{y}_{[2,4]} + \mathbf{y}_{[2,1]})}{1 + y_2 + \mathbf{y}_{[2,3]} + \mathbf{y}_{[2,4]}} \qquad y'_{2^+} = \frac{y_{2^+}(y_3 + \mathbf{y}_{[3,4]} + \mathbf{y}_{[3,1]} + \mathbf{y}_{[3,2]})}{1 + y_3 + \mathbf{y}_{[3,4]} + \mathbf{y}_{[3,1]}}$$

$$y'_{3^+} = \frac{y_{3^+}(y_4 + \mathbf{y}_{[4,1]} + \mathbf{y}_{[4,2]} + \mathbf{y}_{[4,3]})}{1 + y_4 + \mathbf{y}_{[4,1]} + \mathbf{y}_{[4,2]}} \qquad y'_{4^+} = \frac{y_{1^+}(y_1 + \mathbf{y}_{[1,2]} + \mathbf{y}_{[1,3]} + \mathbf{y}_{[1,4]})}{1 + y_1 + \mathbf{y}_{[1,2]} + \mathbf{y}_{[1,3]}}$$

Example 7.3.10. Consider the quiver on the right of Figure 7.1. In this case, we have:

$$y_1' = \frac{1 + y_1 + \mathbf{y}_{[1,2]} + \mathbf{y}_{[1,3]} + \mathbf{y}_{[1,4]} + \mathbf{y}_{[1,5]}}{y_2(1 + y_3 + \mathbf{y}_{[3,4]} + \mathbf{y}_{[3,5]} + \mathbf{y}_{[3,6]} + \mathbf{y}_{[3,1]})}$$

$$y_2' = \frac{1 + y_2 + \mathbf{y}_{[2,3]} + \mathbf{y}_{[2,4]} + \mathbf{y}_{[2,5]} + \mathbf{y}_{[2,6]}}{y_3(1 + y_4 + \mathbf{y}_{[4,5]} + \mathbf{y}_{[4,6]} + \mathbf{y}_{[4,1]} + \mathbf{y}_{[4,2]}}$$

$$y_3' = \frac{1 + y_3 + \mathbf{y}_{[3,4]} + \mathbf{y}_{[3,5]} + \mathbf{y}_{[3,6]} + \mathbf{y}_{[3,1]}}{y_4(1 + y_5 + \mathbf{y}_{[5,6]} + \mathbf{y}_{[5,1]} + \mathbf{y}_{[5,2]} + \mathbf{y}_{[5,3]})}$$

$$y_4' = \frac{1 + y_4 + \mathbf{y}_{[4,5]} + \mathbf{y}_{[4,6]} + \mathbf{y}_{[4,1]} + \mathbf{y}_{[4,2]}}{y_5(1 + y_6 + \mathbf{y}_{[6,1]} + \mathbf{y}_{[6,2]} + \mathbf{y}_{[6,3]} + \mathbf{y}_{[6,4]})}$$

$$y_5' = \frac{1 + y_5 + \mathbf{y}_{[5,6]} + \mathbf{y}_{[5,1]} + \mathbf{y}_{[5,2]} + \mathbf{y}_{[5,3]}}{y_6(1 + y_1 + \mathbf{y}_{[1,2]} + \mathbf{y}_{[1,3]} + \mathbf{y}_{[1,4]} + \mathbf{y}_{[1,5]})}$$

$$y_6' = \frac{1 + y_6 + \mathbf{y}_{[6,1]} + \mathbf{y}_{[6,2]} + \mathbf{y}_{[6,3]} + \mathbf{y}_{[6,4]}}{y_1(1 + y_2 + \mathbf{y}_{[2,3]} + \mathbf{y}_{[2,4]} + \mathbf{y}_{[2,5]} + \mathbf{y}_{[2,6]})}$$

$$y_{1^-}' = \frac{y_{1^-} y_2(1 + y_3 + \mathbf{y}_{[3,4]} + \mathbf{y}_{[3,5]} + \mathbf{y}_{[3,6]} + \mathbf{y}_{[3,1]})}{1 + y_2 + \mathbf{y}_{[2,3]} + \mathbf{y}_{[2,4]} + \mathbf{y}_{[2,5]} + \mathbf{y}_{[2,6]}}$$

$$y_{2^-}' = \frac{y_{2^-} y_3(1 + y_4 + \mathbf{y}_{[4,5]} + \mathbf{y}_{[4,6]} + \mathbf{y}_{[4,1]} + \mathbf{y}_{[4,2]})}{1 + y_3 + \mathbf{y}_{[3,4]} + \mathbf{y}_{[3,5]} + \mathbf{y}_{[3,6]} + \mathbf{y}_{[3,1]}}$$

$$y_{3^-}' = \frac{y_{3^-} y_4(1 + y_5 + \mathbf{y}_{[5,6]} + \mathbf{y}_{[5,1]} + \mathbf{y}_{[5,2]} + \mathbf{y}_{[5,3]})}{1 + y_4 + \mathbf{y}_{[4,5]} + \mathbf{y}_{[4,6]} + \mathbf{y}_{[4,1]} + \mathbf{y}_{[4,2]}}$$

$$y_{4^-}' = \frac{y_{4^-} y_5(1 + y_6 + \mathbf{y}_{[6,1]} + \mathbf{y}_{[6,2]} + \mathbf{y}_{[6,3]} + \mathbf{y}_{[6,4]})}{1 + y_5 + \mathbf{y}_{[5,6]} + \mathbf{y}_{[5,1]} + \mathbf{y}_{[5,2]} + \mathbf{y}_{[5,3]}}$$

$$y_{5^-}' = \frac{y_{5^-} y_6(1 + y_1 + \mathbf{y}_{[1,2]} + \mathbf{y}_{[1,3]} + \mathbf{y}_{[1,4]} + \mathbf{y}_{[1,5]})}{1 + y_6 + \mathbf{y}_{[6,1]} + \mathbf{y}_{[6,2]} + \mathbf{y}_{[6,3]} + \mathbf{y}_{[6,4]}}$$

$$y_{6^-}' = \frac{y_{6^-} y_1(1 + y_2 + \mathbf{y}_{[2,3]} + \mathbf{y}_{[2,4]} + \mathbf{y}_{[2,5]} + \mathbf{y}_{[2,6]})}{1 + y_1 + \mathbf{y}_{[1,2]} + \mathbf{y}_{[1,3]} + \mathbf{y}_{[1,4]} + \mathbf{y}_{[1,5]}}$$

$$y_{1^+}' = \frac{y_{1^+} \mathbf{y}_{[2,3]}(1 + y_4 + \mathbf{y}_{[4,5]} + \mathbf{y}_{[4,6]} + \mathbf{y}_{[4,1]} + \mathbf{y}_{[4,2]})}{1 + y_2 + \mathbf{y}_{[2,3]} + \mathbf{y}_{[2,4]} + \mathbf{y}_{[2,5]} + \mathbf{y}_{[2,6]}}$$

$$y_{2^+}' = \frac{y_{2^+} \mathbf{y}_{[4,5]}(1 + y_6 + \mathbf{y}_{[6,1]} + \mathbf{y}_{[6,2]} + \mathbf{y}_{[6,3]} + \mathbf{y}_{[6,4]})}{1 + y_4 + \mathbf{y}_{[4,5]} + \mathbf{y}_{[4,6]} + \mathbf{y}_{[4,1]} + \mathbf{y}_{[4,2]}}$$

$$y_{3^+}' = \frac{y_{3^+} \mathbf{y}_{[6,1]}(1 + y_2 + \mathbf{y}_{[2,3]} + \mathbf{y}_{[2,4]} + \mathbf{y}_{[2,5]} + \mathbf{y}_{[2,6]})}{1 + y_6 + \mathbf{y}_{[6,1]} + \mathbf{y}_{[6,2]} + \mathbf{y}_{[6,3]} + \mathbf{y}_{[6,4]}}$$

Theorem 7.3.11. *For a spider web quiver and any choice of $\varkappa$, $\tau_\varkappa$ is an involution on the y-variables.*

Proof. Theorem 5.1 of [IIK+13] and Corollary 5.5 of [IKLFP13] tell us that periodicity of x- and y-variables are equivalent. So, this follows from Theorem 7.2.5. □

Theorem 7.3.12. *Suppose we have a spider web quiver with k of concentric circles and we choose $1 \leq \varkappa < k-1$. We obtain the same y-variables by applying the transformation $\tau_{\varkappa}\tau_{\varkappa+1}\tau_{\varkappa}$ and applying the transformation $\tau_{\varkappa+1}\tau_{\varkappa}\tau_{\varkappa+1}$.*

Proof. By Theorem 5.1 of [IIK$^+$13] and Corollary 5.5 of [IKLFP13], this follows from Theorem 7.2.6. □

Chapter 8

Plabic R-matrix, Revisited

Recall in Section 6.3 that we labeled the faces to the left of string $\varkappa$ in a directed cylindric k-loop plabic network $a_1, ..., a_\ell$ starting above the trail and going up. We labeled the faces to the right of string $\varkappa + 1$ $b_1, ..., b_m$ and the faces between these two strings $c_1, ..., c_{n-1}, c_n = \frac{1}{a_1...a_\ell b_1...b_m c_1...c_{n-1}}$. For ease of notation, in this section, we will no longer consider our indices to be modular. In particular, $[i, j] = \emptyset$ if $j < i$. As $\mathbf{a}_\emptyset$ is the empty product, $\mathbf{a}_\emptyset = 1$, and similarly for $\mathbf{b}_\emptyset$ and $\mathbf{c}_\emptyset$.

Definition 8.0.1. For a plabic network, we define its *dual quiver* to be the quiver with vertices corresponding to the faces of the plabic graph and edges crossing every bicolored edge of the plabic graph. We orient the edges of the quiver so that the black vertex is always on the right and the white vertex is on the left. Notice that this orientation is the opposite of the orientation that appears in much of the literature.

We can see that the dual quiver to a cylindric k-loop plabic network is a spider web quiver where the faces between strings $\varkappa$ and $\varkappa + 1$ in the plabic network correspond to the circle $\varkappa$ in the quiver.

Proposition 8.0.2. *Let Q be the dual quiver to a cylindric k-loop plabic network. Choose $1 \leq \varkappa < k$ and label the face and trail weights of the plabic network as in Section 6.3. Recall the definitions of A and B from Section 7.1. Setting each y-variable equal to the corresponding face weight and applying $\tau_\varkappa$ yields the following y-variables:*

(1) For $i \leq n$, $y_i = \dfrac{c_i \left(\sum_{j=i-1}^{n-1} d\, \mathbf{c}_{[1,j]} + \sum_{j=0}^{i-2} \mathbf{c}_{[1,j]} \right)}{\sum_{j=i+1}^{n-1} d\, \mathbf{c}_{[1,j]} + \sum_{j=0}^{i} \mathbf{c}_{[1,j]}}$

(2) $y_n = \dfrac{d\,\mathbf{c}_{[1,n-1]} + \sum_{j=0}^{n-2} \mathbf{c}_{[1,j]}}{\mathbf{c}_{[1,n-1]} \sum_{j=1}^{n-1} d\,\mathbf{c}_{[1,j]} + \mathbf{c}_{[1,n-1]}}$

(3) If i^- *corresponds to the face with weight* a_ℓ*, then*

$$y_{i^-} = \frac{a_\ell \left(\sum_{j=d_1}^{n-1} d\,\mathbf{c}_{[1,j]} + \sum_{j=0}^{d_1-1} \mathbf{c}_{[1,j]} \right)}{\sum_{j=0}^{n-1} d\,\mathbf{c}_{[1,j]}}$$

(4) If i^- *corresponds to the face with weight* $a_{\ell-1}$*, then*

$$y_{i^-} = \frac{a_{\ell-1} \left(\sum_{j=0}^{n-1} \mathbf{c}_{[1,j]} \right)}{\sum_{j=d_i}^{n-1} d\,\mathbf{c}_{[1,j]} + \sum_{j=0}^{d_i-1} \mathbf{c}_{[1,j]}}$$

(5) If i^- *corresponds to the face with weight* a_r *for* $1 \leq r \leq \ell - 2$*, then*

$$y_{i^-} = \frac{a_r \left(\mathbf{c}_{[1,n-1]} \sum_{j=e_i}^{n-1} d\,\mathbf{c}_{[d_i+1,j]} + \mathbf{c}_{[d_i+1,n-1]} \sum_{j=0}^{e_i-1} \mathbf{c}_{[1,j]} \right)}{\mathbf{c}_{[1,n-1]} \sum_{j=d_i}^{n-1} d\,\mathbf{c}_{[d_i+1,j]} + \mathbf{c}_{[d_i+1,n-1]} \sum_{j=0}^{d_i-1} \mathbf{c}_{[d_i-1,j]}}$$

(6) If i^+ *corresponds to the face with weight* b_m *and* $n \in B$*, then*

$$y_{i^+} = \frac{b_m \left(1 + \sum_{j=1}^{n-1} d\,\mathbf{c}_{[1,j]} \right)}{\sum_{j=0}^{n-1} d\,\mathbf{c}_{[1,j]}}$$

(7) If i^+ *corresponds to the face with weight* b_{m-1} *and* $n \in B$*, then*

$$y_{i^+} = \frac{b_{m-1} \left(\sum_{j=0}^{n-1} \mathbf{c}_{[1,j]} \right)}{\sum_{j=f_i}^{n-1} d\,\mathbf{c}_{[1,j]} + \sum_{j=0}^{f_i-1} \mathbf{c}_{[1,j]}}$$

(8) If i^+ *corresponds to the face with weight* b_m *and* $n \notin B$*, then*

$$y_{i^+} = \frac{b_m \left(1 + \sum_{j=1}^{n-1} d\,\mathbf{c}_{[1,j]} \right)}{d \left(\sum_{j=g_i}^{n-1} d\,\mathbf{c}_{[1,j]} + \sum_{j=0}^{g_i-1} \mathbf{c}_{[1,j]} \right)}$$

(9) If i^+ corresponds to the face with weight b_{m-1} and $n \notin B$, then

$$y_{i^+} = \frac{b_{m-1}\left(\mathbf{c}_{[1,n-1]}\sum_{j=g_i}^{n-1} d\,\mathbf{c}_{[f_i+1,j]} + \mathbf{c}_{[f_i+1,n-1]}\sum_{j=0}^{g_i-1}\mathbf{c}_{[1,j]}\right)}{\mathbf{c}_{[1,n-1]}\sum_{j=f_i}^{n-1} d\,\mathbf{c}_{[f_i+1,j]} + \mathbf{c}_{[f_i+1,n-1]}\sum_{j=0}^{n}\mathbf{c}_{[f_i-1,j]}}$$

(10) If i^+ corresponds to the face with weight b_r for $1 \le r \le m-2$, then

$$y_{i^+} = \frac{b_r\left(\mathbf{c}_{[1,n-1]}\sum_{j=g_i}^{n-1} d\,\mathbf{c}_{[f_i+1,j]} + \mathbf{c}_{[f_i+1,n-1]}\sum_{j=0}^{g_i-1}\mathbf{c}_{[1,j]}\right)}{\mathbf{c}_{[1,n-1]}\sum_{j=f_i}^{n-1} d\,\mathbf{c}_{[f_i+1,j]} + \mathbf{c}_{[f_i+1,n-1]}\sum_{j=0}^{n}\mathbf{c}_{[f_i-1,j]}}$$

(11) All other y-variables are equal to the weights of the corresponding faces in the network.

Proof. Notice that because of the way the faces were numbered, $n \in A$ and $f_1 = 1$ for any such quiver. Then we can find the formulas for the y-variables by computation and Theorem 7.3.1. □

Theorem 8.0.3. *Let Q be the dual quiver to a cylindric k-loop plabic network. Choose $1 \le \varkappa < k$ and label the face and trail weights of the plabic network as in Section 6.3. If we set each y-variable equal to the corresponding face weight and apply $\tau_\varkappa$, the y-variables we obtain are the same as the face variables we obtain when we apply $T_{\varkappa,f}$ to the network.*

Proof. Let's investigate $\widehat{\lambda}_i(a,b,c)$. There are n terms in this sum; each one crosses from the left string to the right string at a different edge. If we first calculate the term where we go across as soon as possible, then our first term is

$$\mathbf{c}_{[1,i]}\,\mathbf{b}_{[1,m]}\,\mathbf{b}_{\mathcal{B}_{[1,i-1]}}\,\mathbf{a}_{\mathcal{A}_{[1,i]}}\,.$$

If we compute the rest of our terms, each time crossing one slanted edge later, then each time we pick up one additional face variable. First we pick up c_{i+1}, then c_{i+2}, all the way throughout c_n, and then we cycle back to the beginning and pick up c_1, then c_2, up to c_{i-1}. Since multiplying by c_n is the same as dividing by $a_1...a_\ell b_1...b_m c_1...c_{n-1}$, we get the following expression for $\widehat{\lambda}_i(a,b,c)$:

$$\mathbf{c}_{[1,i]}\,\mathbf{b}_{[1,m]}\,\mathbf{b}_{\mathcal{B}_{[1,i-1]}}\,\mathbf{a}_{\mathcal{A}_{[1,i]}}\sum_{j=i}^{n-1}\mathbf{c}_{[i+1,j]}+\frac{\mathbf{b}_{\mathcal{B}_{[1,i-1]}}\sum_{j=0}^{i-1}\mathbf{c}_{[1,j]}}{\mathbf{a}_{\mathcal{A}_{[i+1,n]}}}$$

Substituting this into our expressions for the face variables under $T_{\varkappa,f}$ and using the previous proposition proves the theorem. □

Example 8.0.4. Notice that the quiver in Example 7.3.9 is dual to the plabic graph in Example 6.3.4. We can see that the formulas we have calculated are the same if we make the following substitutions:

$y_1 = c_1$, $y_2 = c_2$, $y_3 = c_3$, $y_4 = \frac{1}{a_1a_2a_3a_4b_1b_2b_3b_4c_1c_2c_3}$

$y_{1^-} = a_2$, $y_{2^-} = a_3$, $y_{3^-} = a_4$, $y_{4^-} = a_1$

$y_{1^+} = b_1$, $y_{2^+} = b_2$, $y_{3^+} = b_3$, $y_{4^+} = b_4$

Example 8.0.5. Notice that the quiver in Example 7.3.10 is dual to the plabic graph in Example 6.3.5. We can see that the formulas we have calculated are the same if we make the following substitutions:

$y_1 = c_1$, $y_2 = c_2$, $y_3 = c_3$, $y_4 = c_4$, $y_5 = c_5$, $y_6 = \frac{1}{a_1a_2a_3a_4a_5a_6b_1b_2b_3c_1c_2c_3c_4c_5}$

$y_{1^-} = a_2$, $y_{2^-} = a_3$, $y_{3^-} = a_4$, $y_{4^-} = a_5$, $y_{5^-} = a_6$, $y_{6^-} = a_1$

$y_{1^+} = b_1$, $y_{2^+} = b_2$, $y_{3^+} = b_3$

References

[BB06] Anders Bjorner and Francesco Brenti. *Combinatorics of Coxeter groups*, volume 231. Springer Science & Business Media, 2006.

[BCM20] Anna Brosowsky, Sunita Chepuri, and Alex Mason. Parametrizations of k-nonnegative matrices: Cluster algebras and k-positivity tests. *J. Combin. Theory Ser. A*, 174, 2020.

[Bre95] Francesco Brenti. Combinatorics and total positivity. *J. Combin. Theory Ser. A*, 71:175–218, 1995.

[BW01] Sara C Billey and Gregory S Warrington. Kazhdan-lusztig polynomials for 321-hexagon-avoiding permutations. *Journal of Algebraic Combinatorics*, 13(2):111–136, 2001.

[Che20] Sunita Chepuri. Plabic r-matrices. *Publications of the Research Institute for Mathematical Sciences*, 56, 2020.

[CIM98] E.B. Curtis, D. Ingerman, and J.A. Morrow. Circular planar graphs and resistor networks. *Linear Algebra Appl.*, 283:115–150, 1998.

[CJS15] Michael Chmutov, Pakawut Jiradilok, and James Stevens. Double rim hook cluster algebras. *REU Report*, 2015.

[CKST17] Sunita Chepuri, Neeraja Kulkarni, Joe Suk, and Ewin Tang. Factorizations of k-nonnegative matrices. *preprint*, 2017. arXiv:1710.10867.

[CSB20] Sunita Chepuri and Melissa Sherman-Bennett. 1324-and 2143-avoiding kazhdan-lusztig immanants and k-positivity. *preprint*, 2020. arXiv:2002.07851.

[Edr52] Albert Edrei. On the generating function of totally positive sequences, ii. *J. d'Anal. Math*, 2:104–109, 1952.

[FGPW15] Sebastián Franco, Daniele Galloni, Brenda Penante, and Congkao Wen. Non-planar on-shell diagrams. *Journal of High Energy Physics*, 2015(6):199, 2015.

[FJ11] Shaun M. Fallat and Charles R. Johnson. *Totally Nonnegative Matrices.* Princeton University Press, 2011.

[FJS17] Shaun Fallat, Charles R. Johnson, and Alan D. Sokal. Total positivity of sums, hadamard products and hadamard powers: Results and counterexamples. *Linear Algebra and its Applications*, 520:242 – 259, 2017.

[Fom10] Sergey Fomin. Total positivity and cluster algebras. In *Proceedings of the International Congress of Mathematicians 2010 (ICM 2010) (In 4 Volumes) Vol. I: Plenary Lectures and Ceremonies Vols. II–IV: Invited Lectures*, pages 125–145, 2010.

[FWZ16] S Fomin, L Williams, and A Zelevinsky. Introduction to cluster algebras. chapters 1-3. *preprint*, 2016. arXiv:1608.05735.

[FZ99] Sergey Fomin and Andrei Zelevinsky. Double bruhat cells and total positivity. *Journal of the American Mathematical Society*, 12(2):335–380, 1999.

[FZ00a] Sergey Fomin and Andrei Zelevinsky. Total positivity: tests and parametrizations. *The Mathematical Intelligencer*, 22(1):23–33, 2000.

[FZ00b] Sergey Fomin and Andrei Zelevinsky. Totally nonnegative and oscillatory elements in semisimple groups. *Proceedings of the American Mathematical Society*, 128(12):3749–3759, 2000.

[GJ92] IP Goulden and David Jackson. Immanants of combinatorial matrices. *Journal of Algebra*, 148(2):305–324, 1992.

[GK37] Felix Gantmacher and Mark Krein. Sur les matrices completement nonnegatives at oscillatoires. *Compositio Math.*, 4:445–476, 1937.

[GK60] Felix Gantmacher and Mark Krein. *Oszillationsmatrizen, Oszillationskerne und Kleine Schwingungen Mechanischer Systeme*. Akademie-Verlag, Berlin, 1960.

[GKL17] Pavel Galashin, Steven N Karp, and Thomas Lam. The totally nonnegative grassmannian is a ball. *preprint*, 2017. arXiv:1707.02010.

[GM96] Mariano Gasca and Charles Micchelli, editors. *Total positivity and its applications*, volume 359. Kluwer Academic Publishers, Boston, MA, 1996.

[Gre92] Curtis Greene. Proof of a conjecture on immanants of the jacobi-trudi matrix. *Linear algebra and its applications*, 171:65–79, 1992.

[GS18] Alexander Goncharov and Linhui Shen. Donaldson-thomas transformations of moduli spaces of g-local systems. *Adv. Math.*, 327:225–348, 2018.

[GSV08] Michael Gekhtman, Michael Shapiro, and Alek Vainshtein. Poisson geometry of directed networks in an annulus. *preprint*, 2008. arXiv:0901.0020.

[GV85] Ira Gessel and Gérard Viennot. Binomial determinants, paths, and hook length formulae. *Advances in mathematics*, 58(3):300–321, 1985.

[GV89] Ira M Gessel and Xavier Viennot. Determinants, paths, and plane partitions. *preprint*, 1989.

[Hai93] Mark Haiman. Hecke algebra characters and immanant conjectures. *Journal of the American Mathematical Society*, 6(3):569–595, 1993.

[IIK+13] Rei Inoue, Osamu Iyama, Bernhard Keller, Atsuo Kuniba, and Tomoki Nakanishi. Periodicities of t and y-systems, dilogarithm identities, and cluster algebras i: Type b_r. *Publ. RIMS*, (49):1–42, 2013.

[IKLFP13] Giovanni Cerulli Irelli, Bernhard Keller, Daniel Labardini-Fragoso, and Pierre-Guy Plamondon. Linear independence of cluster monomials for skew-symmetric cluster algebras. *Compositio Mathematica*, 149(10):1753–1764, 2013.

[ILP19] Rei Inoue, Thomas Lam, and Pavlo Pylyavskyy. On the cluster nature and quantization of geometric r-matrices. *Publ. Res. Inst. Math. Sci.*, 55(1):25–78, 2019.

[Kar68] Samuel Karlin. *Total positivity*. Stanford University Press, 1968.

[Kaz80] David Kazhdan. Schubert varieties and poincaré duality. In *Proc. Symp. in Pure Math.*, volume 36, pages 185–203, 1980.

[KW09] Richard Kenyon and David Wilson. Combinatorics of tripartite boundary connections for trees and dimers. *Electron. J. Combin.*, 16(1), 2009.

[KW11] Richard Kenyon and David Wilson. Boundary partitions in trees and dimers. *Trans. Amer. Math. Soc.*, 363(3):1325–1364, 2011.

[Lin73] Bernt Lindström. On the vector representations of induced matroids. *Bull. London Math. Soc.*, 5:85–90, 1973.

[Loe55] Charles Loewner. On totally positive matrices. *Mathematische Zeitschrift*, 63(1):338–340, 1955.

[LP12] Thomas Lam and Pavlo Pylyavskyy. Total positivity in loop groups, i: Whirls and curls. *Advances in Mathematics*, 230(3):1222–1271, 2012.

[LS90] Venkatramani Lakshmibai and B Sandhya. Criterion for smoothness of schubert varieties in $sl(n)/b$. In *Proceedings of the Indian Academy of Sciences-Mathematical Sciences*, volume 100, page 45, 1990.

[Lus94] George Lusztig. Total positivity in reductive groups. In *Lie theory and geometry*, pages 531–568. 1994.

[Mac18] John Machacek. Boundary measurement matrices for directed networks on surfaces. *Advances in Applied Mathematics*, 93:69–92, 2018.

[Mac19] John Machacek. Boundary measurement and sign variation in real projective space. *preprint*, 2019. arXiv:1909.04640.

[Pos06] Alex Postnikov. Total positivity, grassmannians, and networks. *preprint*, 2006. arXiv:math/0609764.

[Pyl18] Pavlo Pylyavskyy. personal communication, 2018.

[RS06] Brendon Rhoades and Mark Skandera. Kazhdan–lusztig immanants and products of matrix minors. *Journal of Algebra*, 304(2):793–811, 2006.

[Sch30] Isaac Schoenberg. Uber variationsverminderende lineare transformationen. *Math. Z.*, 32:321–328, 1930.

[Sjö07] Jonas Sjöstrand. Bruhat intervals as rooks on skew ferrers boards. *Journal of Combinatorial Theory, Series A*, 114(7):1182–1198, 2007.

[Ska08] Mark Skandera. On the dual canonical and kazhdan–lusztig bases and 3412-, 4231-avoiding permutations. *Journal of Pure and Applied Algebra*, 212(5):1086–1104, 2008.

[Sta89] Richard Stanley. Log-concave and unimodal sequences in algebra, combinatorics, and geometry. *Ann. New York Acad. Sci*, 576(1):500–535, 1989.

[Ste91] John Stembridge. Immanants of totally positive matrices are nonnegative. *Bull. London Math. Soc.*, 23:422–428, 1991.

[Ste92] John Stembridge. Some conjectures for immanants. *Canadian journal of mathematics*, 44(5):1079–1099, 1992.

[Ten07] Bridget Tenner. Pattern avoidance and the bruhat order. *Journal of Combinatorial Theory, Series A*, 114(5):888–905, 2007.

[Tho64] Elmar Thoma. Die unzerlegbaren, positiv-definiten klassenfunktionen der abzählbar unendlichen symmetrischen gruppe. *Math. Zeit.*, 85:40–61, 1964.

[Whi52] Anne Whitney. A reduction theorem for totally positive matrices. *Journal d'Analyse Mathématique*, 2(1):88–92, 1952.